Prepared for:

Rijkswaterstaat
Dienst Noord-Holland

Evaluation of SPM measurements in the North Sea

Research in the framework of the EIA sand extraction North Sea 2008-2012

Report

Vrije Universiteit amsterdam
Institute for Environmental Studies

A2273

April 2010

Client **Rijkswaterstaat Dienst Noord-Holland**

Title **Evaluation of SPM measurements in the North Sea;**

Research in the framework of the EIA sand extraction North Sea 2008 – 2012; Report 1

Abstract This report presents the evaluation of existing results of SPM measurements in the North Sea in the framework of the evaluation program of the EIA for sand extraction in the North Sea 2008-2012 for the purpose of coastline nourishments.

We present results of the analysis of in-situ data and remote sensing data and model results.

References Rijkswaterstaat Contract 311011214 dd December 2008

Rev.	Originator		Date	Remarks	Checked by		Approved by	
0	B.T. Grasmeijer		Dec 2009		G. van Banning			
1	B.T. Grasmeijer M.A. Eleveld		Apr 2010		G. van Banning		B.T. Grasmeijer	

Document Control	Contents	Status
Report number: A2273R2r1 Keywords: silt concentration, total suspended solids, suspended particle matter, measurements, evaluation Project number: A2273 File location: A2273R2r1_T0T1	text pages : 44 tables : 8 figures : 184 appendices : 2	☐ preliminary ☐ draft ☑ final

Alkyon
Hydraulic Consultancy & Research

postal address
PO Box 248
8300 AE, Emmeloord
The Netherlands

visiting address
Voorsterweg 28, Marknesse
tel : 0527 24 81 00
fax: 0527 24 81 11

e-mail
info@alkyon.nl
internet
http://www.alkyon.nl

Executive summary

Large amounts of sand are annually extracted from the North Sea for nourishments to protect the Dutch sandy coast against flooding. The existing coastline is in this way maintained and the coastal foundation, defined as the area between NAP-20 m and the dunes, preserved.

An Environmental Impact Assessment (EIA) has to be made to assure that environmental aspects are taken into account in the decision on sand extraction permits. Van Duin *et al.* (2007) performed the EIA for sand extraction in the North Sea 2008-2012 for the purpose of coastline nourishments.

The final part of the assessment procedure is an evaluation. The EIA by Van Duin *et al.* (2007) presents an onset for an evaluation program (EP). Ellerbroek *et al.* (2008) present a more detailed EP. An important part of the EP for the EIA 2008-2012 concerns the evaluation of existing results of SPM measurements in the North Sea. *Rijkswaterstaat Dienst Noord-Holland* has asked Alkyon to make this evaluation. This report presents the research results.

Firstly, we report on the concentration time series available in Waterbase that have been measured along different transects in the framework of the so-called MWTL programme (Monitoring Programme of the National Water Systems). We compare suspended matter concentrations measured in the period 1975-1983 with the period 1984-2008 and discuss statistical parameters and significance of trends. Conclusions are summarized as follows:

- Generally, no significant (within the 95% confidence bandwidth) trends are observed in the suspended matter concentrations between 1975 and 2008. For nearly all analyzed stations (80%), the concentrations are neither significantly increasing nor significantly decreasing.
- Based on t-tests, we found the difference between the mean values for 1975-1983 and those for 1985-2008 not to be significant at the 5% significance level for most stations. This accounts also for the trimmed mean and the geometric mean.
- Two stations show a statistically significant decreasing trend, i.e. Terschelling 4 and Noordwijk 2 and two show a statistically significant increasing trend, i.e. Goeree 10 and 20.

- The statistical insignificance of trends or difference in means between two periods may have two causes. The first is that the SPM concentrations behave similarly throughout the measurement periods. The second is that the number of samples is insufficient to determine a significant change. We tested the latter by making a power analysis on the data from Noordwijk 10.
- For the Noordwijk 10 observations, the number of samples should have been 1940 to be able to differentiate between a mean of 5.46 mg/l and 5.77 mg/l (either increasing or decreasing). This would require a sampling interval of 1 day (365 samples per year) for a period of 6 years (rounded off) or a sampling interval of 1 week (52 samples per year) for a period of 38 years (rounded off). The real number of samples in the period 1984-2008 was 782.
- To be able to measure a statistically significant increase or decrease in the mean of 1 mg/l at Noordwijk 10 since the period 1975-1983 requires 190 samples. This would require a sampling interval of 1 week (52 samples per year) for a period of

4 years (rounded off) or a sampling interval of 2 weeks (26 samples per year) for a period of 8 years (rounded off).

- Increasing the number of samples by smartly combining data from different stations or synthetic data generation (e.g. with a neural network) may also improve the power of the statistical tests.

- As the present data suggest that trends for most stations are not significantly increasing or decreasing, comparisons are justified between recent observations and interpolated maps based on 1975-1983 MWTL data.
- Mean suspended matter concentration contours show values between 30 and 300 mg/l in the nearshore regions. This reduces to 3-5 mg/l further offshore.
- Trimmed mean values (excluding outliers) are on average about 5% smaller than the mean values.
- Geometric mean values are on average 32 % smaller than the mean values.
- The median (50^{th} percentile) values are 68% smaller to 6% larger than the mean values (on average 28% smaller).
- The standard deviation of the suspended matter concentrations along the Dutch coast is of the same order as the mean.
- The suspended matter concentrations are on average 83% higher in winter than in summer.

- Power spectral density estimates of the suspended matter concentration observed at 6 different stations showed a clear peak at a frequency corresponding to a periodicity of 1 year. This agrees with the seasonal variation in wave conditions with higher waves each year in winter and smaller waves in summer.
- The Terschelling 4 km offshore station and the Walcheren 2 km offshore station suggest a small spectral peak around 8 years (Terschelling) or 4 years (Walcheren) that just peaks above the 95% confidence band of surrounding frequencies. However, the measurement period and temporal resolution of the data is insufficient to draw firm conclusions on the significance of this peak. Other power spectral density functions do not show clear peaks at these frequencies, or a clear increase of the power spectral density for periods longer than 4 years.
- No other important peaks were found in the spectrum
- Time series of the moving average with a two-year window of the concentration observed at 6 stations showed intermittent high-concentration events. It is difficult to recognize a distinct periodicity.

Secondly, we present an analysis of the CEFAS Minipod and Smartbuoy measurements at 2 and 5 km off the coast of Noordwijk aan Zee. We compare observed concentrations with predictions using a process-based 1DV model and using a neural network. Conclusions are summarized as follows:

- Suspended matter concentrations at 2 and 5 km off the coast of Noordwijk aan Zee could rather accurately (R^2>0.8) be simulated using a neural network with 9 neurons, using wave height, wave period and water depth time series as an input and near-bed suspended matter concentration as a target.
- The suspended matter concentration at aforementioned stations could be predicted with reasonable accuracy using the Van Rijn (2005) tidal mud transport model. These results were less accurate then those of the neural network.

Thirdly, we present an analysis of the silt profiler T0 measurement campaign made in 22-24 May 2007 off the coast of Vlieland, Texel and Noord-Holland. We compare concentrations measured during this campaign with MWTL observations. The conclusion is as follows:

- The suspended matter concentrations measured during the T0 campaign in May 2007 off the coast of Vlieland, Texel and Noord-Holland are much smaller (factor 2 to 5) than MWTL mean and MWTL summer-mean concentrations may therefore not be representative.

Fourthly, we present an analysis of remote sensing MERIS-RR data for 2003-2006 as processed in the Ovatie project. We discuss SPM distributions, outliers possibly due to sand extraction and dredge disposal. We report on time series for a location near Huisduinen and Callantsoog.

- Time series of SPM concentrations extracted at the middle points of the sand extraction areas near Huisduinen (Q2J and Q2L) from 2003-2006 showed mean T0 concentrations of 2.7 and 2.3 mg/l respectively.
- The T0 concentrations from remote sensing images are similar to the MWTL mean concentrations and about 2-4 times larger than the in-situ siltprofiler T0 concentrations close to Q2J and Q2L (0.6-1.5 mg/l).

Conclusions from remote sensing tests for T1 conditions

- The H0 hypothesis, that extra SPM from sand extraction cannot be seen on the SPM concentrations derived from remote sensing data, can be rejected.

- The H0 hypothesis that the SPM concentrations at the sand extraction (impact) site do not cause near-surface outliers may be true. Nonetheless, outliers in SPM concentrations near a dredge dump and sand extraction location were found.

- The H0 hypothesis to be tested is that the SPM concentrations at the sand extraction (impact) site are not significantly higher than at the control locations. This hypothesis may be true for the tested sampling locations.

Finally, we studied the effect of dredging on the suspended matter concentrations in the North Sea based on 3D numerical model simulations.

Conclusions from 3D numerical simulations:

- The extra mean (averaged over 15.5 days) near-surface concentrations (more than background) amounts to 0.5-1 mg/l over an area of about 6 km^2 for a realistic scenario.

- The extra mean (averaged over 15.5 days) near-surface concentrations (more than background) amounts to 0.5-2 mg/l over an area of about 75 km^2 for an "extensive dredging" scenario 2. The area over which the extra mean concentration is 1-2 mg/l for scenario 2 is about 9 km^2.

- The effect of dredging is temporary (disappears a few days after dredging has stopped) and is a factor 2-8 smaller than the observed mean background concentration also a factor 2-8 smaller than the standard deviation of the observed natural background concentration.

- The dredging activity studied here takes place in an area where the mean SPM concentration is relatively low and also the variation in SPM concentration is relatively low.

- This means that we may generalize the conclusion that the effect of overflow by dredging on the SPM concentrations in the North Sea is not only much smaller than the natural mean but also much smaller than the natural variation around the mean.

The investigations presented in this report reveal the suspended matter concentrations in the North Sea to be strongly variable in space and particularly in time. The variation in wave conditions produces part of this variability in SPM concentrations. The high cross-correlations between wave height and SPM concentration found in the CEFAS dataset illustrate this dependency. However, more factors play a role. We have summarized the most important aspects in an incomplete list below.

- Waves stirring up material from the sea bed
- Currents stirring up material from the bed and transporting it from other source terms
- Shipping (merchant shipping, dredging, fishery etc)
- Rivers discharge
- Oil or gas platforms
- Wind farms
- Land reclamation
- Cables and pipelines

It is difficult to asses the relative effect of the above mentioned aspects on the SPM concentrations and to discern between the different effects. For example, fishing vessels such as outrigger trawlers are likely to stir up material from the bed. However, the degree to which this affects the mean and variation of the SPM concentrations in the North Sea has never been investigated. What is more, both vessel types and fishing gears have changed over time (Rijnsdorp et al, 2008). Also sand extraction activities have increased significantly since the 1990's (ICES, 2001). In addition, shipping traffic is growing and the number of offshore wind farms increases. This makes assessing the effect on the SPM concentrations at different moments in time to a challenge.

Most important step in handling this challenge is improving our present partial understanding of the physics and the natural behaviour of suspended particle matter in the North Sea. In this respect, making observations with a high temporal and spatial resolution are essential, illustrated by the results presented here. In addition, both statistical and physical modelling is required to interpolate and extrapolate this and to asses the effects of human interference relative to the natural behaviour of the system.

Based on this we recommend expanding the present MWTL program by increasing the number of stations and the temporal resolution most preferably back to or close to the situation in 1975-1984.

Secondly, we recommend making observations of the SPM values not only in the upper part of the water column but also at mid depth and close to the sea bed.

Finally, we recommend processing remote sensing data on a 300 m grid and making these available as monitoring data.

Contents

List of Tables

List of Figures

1 Introduction

1.1 Background

Large amounts of sand are annually extracted from the North Sea for nourishments to protect the Dutch sandy coast against flooding. The existing coastline is in this way maintained and the coastal foundation, defined as the area between NAP-20 m and the dunes, preserved. The *Tweede Regionaal Ontgrondingenplan Noordzee (RON2)* describes the policy for extracting minerals from the Dutch part of the North Sea. Extracting sand from the North Sea requires permission according to the *Ontgrondingen-wet*. The accredited authority (*bevoegd gezag*) for the ontgrondingen-wet is the Assistant Secretary of State of the Ministry of Public Works in the Netherlands (*Staatssecretaris van Verkeer en Waterstaat*). In addition, it requires permission according to the *Natuurbeschermingswet* for which the accredited authority is the Minister of Agriculture, Nature and Food quality (*Minister van Landbouw, Natuur en Voedselkwaliteit*).

An Environmental Impact Assessment (EIA) has to be made to assure that environmental aspects are taken into account in the decision on sand extraction permits. Granting a permit in the framework of the *Ontgrondingenwet* requires an EIA as the extraction area is larger than 500 ha or the amount of sand extracted is 10.000.000 m^3 or more (*Besluit Milieueffectrapportage 1994*, as revised on 16 augustus 2006).

The initiator of extracting sand for the purpose of nourishments for 2008-2012 is the *Hoofdingenieur Directeur (HID)* of the *Regionale Dienst Noord-Holland* of *Rijkswaterstaat*. The initiator for sand extraction for other (commercial) use is *Stichting LaMer*.

Van Duin *et al.* (2007) performed the EIA for sand extraction in the North Sea 2008-2012 for the purpose of coastline nourishments. Also an EIA for commercial sand extraction was performed (Van Duin e.a., 2008). *Rijkswaterstaat* and *Stichting LaMer* are partners in these EIA's.

The final part of the assessment procedure is an evaluation. The initiator has to carry out the required research on the basis of which the accredited authority can make the evaluation. The EIA by Van Duin *et al.* (2007, 2008) presents an onset for an evaluation program (EP). Ellerbroek *et al.* (2008) present a more detailed EP.

An important part of the EP for the EIA 2008-2012 concerns the evaluation of SPM measurements in the North Sea. *Rijkswaterstaat Dienst Noord-Holland* has asked Alkyon to make this evaluation. This report presents the research results.

1.2 Report overview

Section 2.2 reports on the concentration time series available in Waterbase (www.waterbase.nl) that have been measured along different transects in the framework of the so-called MWTL programme (Monitoring Programme of the National Water Systems). It compares suspended matter concentrations measured in the period 1975-1983 with the period 1984-2008, discusses statistical parameters and significance of trends.

Section 2.3 presents an analysis of the CEFAS Minipod and Smartbuoy measurements at 2 and 5 km off the coast of Noordwijk aan Zee. It compares observed concentrations with predictions using a process-based 1DV model and using a neural network.

Section 2.4 presents an analysis of the silt profiler T0 measurement campaign made on 22-24 May 2007 off the coast of Vlieland, Texel and Noord-Holland and T1 measurements made on 17 September and 1 and 2 October 2007. It compares concentrations measured during this campaign with MWTL observations.

Chapter 3 analyses remote sensing MERIS-RR data for 2003-2006 as processed in the Ovatie project. It discusses SPM distributions, outliers possibly due to sand extraction and dredge spoil disposal and reports on time series for a location near Huisduinen and Callantsoog.

Chapter 4 describe the results from a 3D model to simulate the suspended sediment concentrations of a silt fraction and a sand fraction in part of the Wadden Sea and part of the North Sea and to simulate the effects of overflow from dredging activities on these concentrations offshore Den Helder on three different days in 2007. The 3D model includes effects of a temporally and spatially varying wind field, waves and salinity.

Chapter 5 summarizes the conclusions of this study.

2 Analysis and evaluation of in-situ measurements

2.1 Introduction

The spatial and temporal behaviour of suspended matter concentrations along the Dutch coast has been described by Suijlen & Duin (2002) who based their analysis of data measured between 1975 and 1983 in the framework of the so-called MWTL programme (Monitoring Programme of the National Water Systems). These measurements have been continued to a lesser extent in later years. Besides this, SeaWIFS observations are available that provide spatial and temporal information of the suspended matter concentrations in the upper part of the water columns between 1999 and 2003.

Aforementioned information is limited to the upper part of the water column. The so-called CEFAS dataset contains measurements of the sediment concentrations at different heights above the bed for several months in the years 2000 and 2001. The measurements were made using a Smartbuoy for the upper part of the water columns and a Minipod for the region closer to the seabed.

In the framework of the EIA for sand extraction in the North Sea a T0 measurement campaign has been set-up to measure the background SPM concentrations and related parameters under conditions without dredging in the period 22-24 May 2007. Commissioned by Rijkswaterstaat, Havenbedrijf Rotterdam (HBR) performed measurements at 46 locations with a so-called silt profiler in this period off the coasts of Noord-Holland, Texel and Vlieland.

The present study evaluates the aforementioned in-situ measurements. Analysis of the available remote sensing images is made in Chapter 3 of this report.

2.2 MWTL 1975-2008

2.2.1 Introduction

We analysed concentration time series available in Waterbase that have been measured along different transects in the framework of the so-called MWTL programme (Monitoring Programme of the National Water Systems). Some stations and transects were discontinued after 1983. We will compare suspended matter concentrations measured in the period 1975-1983 with values from stations that were continued after 1983. This concerns stations in the Terschelling (TS), Noordwijk (NW), Goeree (GO) and Walcheren (WA) transects.

The analysis presented here is in some aspects similar to that by Suijlen & Duin (2002). Unfortunately, their interpolated charts are not available digitally. Therefore, we re-examined the available dataset, including nearshore stations that were not included by Suijlen & Duin (2002). In addition, we determined statistical parameters not only for the earlier observations (1975-1983) but also for more recent observations (1984-2008) and investigated linear trends and their confidence interval. Suijlen & Duin (2002) hypothesized on a periodicity of 3-8 years in the total suspended matter concentrations along the Dutch coast that possibly corresponds with the so-called North Atlantic Oscillation. We analysed relatively long MWTL time series (1975-2008) from 6 stations in detail to investigate this long-term variability.

2.2.2 Statistical parameters

Statistical parameters are useful in analysing, interpreting and presenting data. We adopted the following statistical parameters to summarize and describe the MWTL suspended matter concentrations:

- mean (arithmetic)
- trimmed mean
- geometric mean
- standard deviation
- 10th percentile
- 50th percentile (median)
- 90th percentile
- winter mean (December-March)
- summer mean (May-October)
- linear trend and 95% confidence interval

The trimmed mean is the mean excluding outliers. We adopted the highest and lowest 2% for this. The geometric mean is similar to the arithmetic mean, except that instead of adding the set of numbers and then dividing the sum by the count of numbers n in the set, the numbers are multiplied and then the n^{th} root of the resulting product is taken. This procedure is similar to taking the mean of the logarithm of concentrations. The geometric mean is always smaller than or equal to the arithmetic mean and is often used for a set of numbers whose values are exponential in nature, like suspended matter concentration.

The standard deviation is a measure of the variability of the MWTL concentrations. A low standard deviation indicates that the data points tend to be very close to the same value (the mean) while high standard deviation indicates that the data are “spread out” over a large range of values. The latter may be expected for the total suspended matter concentrations in the Dutch coastal zone of the North Sea.
A percentile is the value of a variable below which a certain percentage of the observations fall. So the 10th percentile is the value below which 10 percent of the observations are found and the 90th percentile the value below which 90 percent is found. These two values give an impression of the lower and upper concentration limits along the Dutch coast. The 50th percentile is the median of the observations.

Waves have an important effect on resuspension processes in the shallow waters of the North Sea. Therefore, we clustered the total suspended matter concentrations in two subsets that correspond with the two seasons of the wave climate, following Suijlen & Duin (2002). Monthly-averaged wave heights show a typical seasonal trend with relatively calm conditions during the summer months from May to October and more energetic conditions during the winter months from December to March. We adopted these periods to determine the typical summer and winter mean suspended matter concentrations. The selection of the months per season is the same as by Suijlen & Duin (2002).

Mean (arithmetic mean)

Figure 2.1 presents the mean values of 96 stations along the Dutch coast for the period 1975-1983. Figure 2.2 shows the interpolated filled contours for this period. Suspended matter concentrations between 15 and 240 mg/l are found in the nearshore regions (≤ 2 km). This reduces to 3-5 mg/l further offshore. The coloured symbols in Figure 2.2 indicate the mean values determined from the 1984-2008 MWTL data. Comparison between the filled contours (1975-1983) and the coloured symbols (1984-2008) shows some differences between the two periods. On average, the 1984-2008 values are 9% larger than those from 1975-1983. However, based on a *t*-test, we found this difference not to be significant at the 5% significance level. The range of values is wide. The recent mean values are sometimes smaller (up to 40%) and sometimes larger (up to 70%) than those in 1975-1983.

Later in this chapter we will discuss observed trends and their significance per station. This will clarify whether the differences are the result of a trend or related to natural variations.

Trimmed mean (i.e. excluding outliers)

The trimmed mean values for 1975-1983 shown in Figure 2.3 are on average about 5% smaller than the mean values. For the biggest difference, the trimmed value is 45% smaller. As for the arithmetic mean, the comparison between the filled contours of the trimmed mean values for the period 1975-1983 and the coloured symbols for the period 1984-2008 shows some differences (Figure 2.4). The more recent trimmed mean values are on average 5% larger than those in 1975-1983 but the range is wide. Based on a *t*-test we found this difference not to be significant at the 5% significance level. The 1984-2008 values are sometimes smaller (up to 49%) and sometimes larger (up to 75%) than those from 1975-1983. We will discuss the significance of these differences later in this report.

Geometric mean

The geometric mean values for 1975-1983 shown in Figure 2.5 are 10 to 60% smaller than the mean values (on average 32% smaller). This is because the geometric mean tends to dampen the effect of very high or low values, which biases the arithmetic mean. The geometric mean may be more appropriate description of the mean concentration as the levels may vary anywhere from 1 mg/l to 300 fold over a given period.

Figure 2.6 shows the interpolated filled contours of the geometric mean for 1975-1983. The coloured symbols in Figure 2.6 indicate the mean values determined from the 1984-2008 MWTL data. The geometric means of the observations between 1984 and 2008 are on average 14% larger than the earlier observations between 1975 and 1983. However, based on a *t*-test, we found this difference not to be significant at the 5% significance level. The range of values is again wide. The 1984-2008 values are sometimes smaller (up to 53% smaller) and sometimes larger (up to 99% larger) than the earlier observations.

Standard deviation

Figure 2.7 presents the standard deviation of the suspended solid concentrations observed between 1975 and 1983 at 96 stations along the Dutch coast. Figure 2.8 shows the standard deviations in filled contours for 1975-1983. The coloured symbols in Figure 2.8 show the standard deviations determined from the 1984-2008 data. The standard deviation is of the same order as the mean, indicating a wide scatter of the concentration values. Therefore, one individual survey may differ significantly from the mean distributions shown here.

The standard deviations of the observations between 1984 and 2008 are on average 10% larger than the earlier observations between 1975 and 1983 but the range is again wide. The 1984-2008 values are sometimes smaller (up to 39% smaller) and sometimes larger (up to 125% larger) than the earlier observations.

10th percentile

The 10th percentile of the total suspended solids concentration along the Dutch coast roughly varies between 3-40 mg/l near the shore (≤ 2 km) to less than 1 mg/l offshore (Figure 2.9 and 2.10). The average increase at 20 stations along the coast is about 46% since 1975-1983 but it ranges per station between 47% smaller and 200% larger than the earlier observations.

50th percentile

The 50th percentile (median) of the total suspended solids concentration roughly varies between 10 and 120 mg/l in the nearshore regions. This reduces to 2-3 mg/l further offshore (Figure 2.10a and 2.10b). The 50th percentile values are 68% smaller to 6% larger than the mean values (on average 28% smaller). The average increase at 20 stations along the coast is about 5% since 1975-1983 but it ranges per station between 57% smaller and 78% larger than the earlier observations.

90th percentile

The 90th percentile of the total suspended solids concentration roughly varies between 30-470 mg/l near the shore to 5-10 mg/l offshore (Figure 2.11 and 2.12). The average increase at 20 stations along the coast is about 2% since 1975-1983 but it ranges per station between 59% smaller and 89% larger than the earlier observations.

Summer mean

The summer-mean suspended solids concentration (May-October) roughly varies between 10-200 mg/l near the shore (≤ 2 km) to 3-4 mg/l offshore (Figures 2.13 and 2.14). The summer-mean concentrations have increased with about 4% on average since 1975-1983 but this varies per station between 40% smaller to 59% larger (Figure 2.14).

Winter mean

The winter-mean suspended solids concentration (December-March) roughly varies between 17-275 mg/l near the shore (≤ 2 km) to 4-5 mg/l offshore (Figures 2.15 and 2.16). On average, the suspended matter concentrations are 83% higher in winter than in summer (compare Figure 2.14 and 2.16). This ranges per station between 37% smaller and 475% higher concentrations than in summer.

The winter-mean concentrations have increased with about 19% on average since 1975-1983 but this varies per station between 32% smaller and 134% larger (Figure 2.16).

2.2.3 Cross-shore distribution and trends in selected transects

To investigate the cross-shore distribution and trends in the suspended matter concentrations along the Dutch coast we analysed observed concentration in transects that contain data from 1975 to 2008. This concerns stations in the Terschelling (TS), Noordwijk (NW), Goeree (GO) and Walcheren (WA) transects (Figure 2.17).

Terschelling

Figure 2.18 presents time series of the total suspended matter concentration measured in the Terschelling transect at 4, 10, 20, 30, 50 and 70 km offshore. The blue lines denote linear trends. The table presents the following statistical parameters: mean, geometric mean, trimmed mean, standard deviation, linear trend and the 95% confidence interval for the trend.

The mean concentration decreases from about 13 mg/l to 3 mg/l when moving from 4 to 70 km offshore. The geometric mean decreases from about 8 mg/l to 2 mg/l and the trimmed mean from about 12 mg/l to 2 mg/l when moving over the same distance offshore. The standard deviation is of the same order of magnitude as the mean values.

There is one Terschelling station showing a decreasing trend that is significant within the 95% confidence interval, i.e. at 4 km offshore. The concentrations decrease per year with about 0.29 mg/l at this location where the mean is 13 mg/l. According to the 95% confidence bandwidth this decrease may range between 0.15 to 0.44 mg/l per year. The trends are not significant at the other locations.

Noordwijk

Figure 2.19 presents time series of the total suspended matter concentration measured in the Noordwijk transect at 1, 2, 4, 10, 20, 30, 50 and 70 km offshore. This figure also presents the accompanying statistical parameters for these stations.

The mean Noordwijk concentrations are on average 16% higher than the Terschelling values at the same distance offshore. The mean concentration decreases from about 30 mg/l to 4 mg/l when moving from 1 to 70 km offshore in the Noordwijk transect. The geometric mean decreases from about 21 mg/l to 3 mg/l and the trimmed mean from about 20 mg/l to 3 mg/l when moving over the same distance offshore. The standard deviation is of the same order of magnitude as the mean values.

There is one Noordwijk station showing a decreasing trend that is just significant within the 95% confidence interval, i.e. at 2 km offshore. The concentrations decrease per year with about 0.11 mg/l at this location where the mean is 14 mg/l. According to the 95% confidence bandwidth this decrease may range between 0 to 0.26 mg/l per year. The trends are not significant at the other locations.

Goeree

Four stations in the Goeree transect have been discontinued since 1983 and one since 1996. The station at 6 km offshore is the only one providing continuous data from 1975 to 2008. Nonetheless, Figure 2.20 presents time series of the total suspended matter concentration measured in this transect at 2, 6, 10, 20, 30, 50 and 70 km offshore and also presents the accompanying statistical parameters.

The mean Goeree concentrations are on average 82% higher than the Terschelling values at the same distance offshore. The mean concentration decreases from about 27 mg/l to 5 mg/l when moving from 2 to 70 km offshore in the Goeree transect. The geometric mean decreases from about 16 mg/l to 3 mg/l and the trimmed mean from about 27 mg/l to 4 mg/l when moving over the same distance offshore. The standard deviation is of the same order of magnitude as the mean values.

There are two Goeree stations showing an increasing trend that is significant within the 95% confidence interval, i.e. at 10 and 20 km offshore. The concentrations increase per year with about 0.67 mg/l at 10 km offshore and 0.15 mg/l at 20 km offshore. However, the 95% confidence bandwidth is rather wide due to the limited lengths of the time series. At 10 km offshore the increasing trend may range between 0.07 and 1.28 mg/l per year and at 20 km offshore it may range between 0.01 and 0.28 mg/l per year. The trends are not significant at the other locations.

Walcheren

Three stations in the Walcheren transect have been discontinued since 1983 and two since 1996. The stations at 2, 20 and 70 km offshore provide data from 1975 to 2008. Figure 2.21 presents time series of the total suspended matter concentration measured in this transect at 1, 2, 4, 10, 20, 30 and 50 km offshore and also presents the accompanying statistical parameters.

The mean Walcheren concentrations are on average 193% higher than the Terschelling values at the same distance offshore. The mean concentration is about 27 mg/l at 1 km offshore. It increases towards 40 mg/l at 4 km offshore and decreases to about 5 mg/l when moving to 50 km offshore. The geometric mean and the trimmed mean show a similar tendency but with 30% and 4% lower values, respectively. Also here is the standard deviation of the same order as the mean values.

None of the Walcheren stations shows a significant increasing or decreasing trend within the 95% confidence bandwidth.

Summary

Figure 2.22 shows the cross-shore distribution of statistical parameters determined from total suspended matter concentrations in the Terschelling, Noordwijk, Goeree and Walcheren transects, summarizing the descriptions above.

Section 2.2.2 compares statistical parameters from the period 1975-1983 with the period 1984-2008 for 20 stations along the coast. From this comparison the impression may arise that the suspended matter concentrations along the Dutch coast have increased in the past decades. However, this conclusion may not be drawn as the dataset for 1984-2008 is not complete and the suggested increase therefore often not statistically significant. For example, the stations at 2, 10 20 and 70 km off the coast of Noordwijk contain data from 1975 till 2008, although sometimes with a gap of a few years. In contrast, the stations at 4, 30 and 50 km off the coast of Noordwijk contain data only for the period 1988-1995.

Two stations show a statistically significant decreasing trend, i.e. Terschelling 4 and Noordwijk 2 and two show a statistically significant increasing trend, i.e. Goeree 10 and 20. Other trends are statistically not significant.

The statistical insignificance of trends or difference in means between two periods may have two causes. The first is that the SPM concentrations behave similarly throughout the measurement periods. The second is that the number of samples is insufficient to determine a significant change. We tested the latter by making a power analysis on the data from the Noordwijk locations at 2 km and 10 km offshore. The first shows a statistically significant decreasing trend; the trend from the second is not statistically significant.

At 2 km offshore, the mean in the period 1975-1983 was 15.19 mg/l and the standard deviation 12.97 mg/l. The mean in the period 1984-2008 was 13.05 mg/l. Based on a power analysis the required number of samples to differentiate between the means is 387. The real number of samples was 520, which is more than required for statistical significance. We may conclude from this that the difference between the means (decreasing) is statistically significant.

At 10 km offshore, the mean in the period 1975-1983 was 5.46 mg/l and the standard deviation 4.21 mg/l. The mean in the period 1984-2008 was 5.77 mg/l. Based on a power analysis the required number of samples to differentiate between the means is 1940. Unfortunately, the real number of samples was 782, which is less than required to determine a statistical significant change. We may conclude from this that the difference between the means is statistically not significant.

For the 10 km offshore observations, the number of samples should have been 1940 to be able to differentiate between a mean of 5.46 mg/l and 5.77 mg/l (either increasing or decreasing). This would require a sampling interval of 1 day (365 samples per year) for a period of 6 years (rounded off) or a sampling interval of 1 week (52 samples per year) for a period of 38 years (rounded off).

Another interesting test case is to see how many samples are required to be able to measure a statistically significant increase or decrease in the mean of 1 mg/l at Noordwijk 10 km offshore since the period 1975-1983. Based on a power analysis we estimated this at 190 samples. This would require a sampling interval of 1 week (52 samples per year) for a period of 4 years (rounded off) or a sampling interval of 2 weeks (26 samples per year) for a period of 8 years (rounded off).

2.2.4 Long term variability

Suijlen & Duin (2002) hypothesized on a periodicity of 3-8 years in the total suspended matter concentrations along the Dutch coast that possibly corresponds with the so-called North Atlantic Oscillation. We analysed relatively long MWTL time series (1975-2008) from 6 stations in detail to investigate this long-term variability. The time series adopted here are 9 years longer than those used by Suijlen & Duin (2002).

Figure 2.23 presents power spectral density of the suspended matter concentrations for the following 6 stations:

- Terschelling 4 km offshore
- Noordwijk 2 km offshore
- Noordwijk 20 km offshore
- Goeree 6 km offshore
- Walcheren 2 km offshore
- Walcheren 20 km offshore

Concentration time series for these stations are shown in Figures 2.18 to 2.21. The sampling interval for these observations was not equidistant but often close to 14 days. Therefore, we created new interpolated time series adopting this interval. We estimated the power spectral density using the Welch (1967) averaged modified periodogram method of spectral estimation. The time series were segmented into sections of equal length (128 samples), each with 50% overlap. Each segment was windowed with a Hamming window of the same length as the segment.

The spectra show a clear peak at a frequency that corresponds to a periodicity of 1 year. This agrees with the seasonal variation in wave conditions with higher waves each year in winter and smaller waves in summer. Figure 2.23 also denotes the 95% confidence interval and the 3 months, 2 year and 4 year periodicity in the spectral density plots. The Terschelling 4 km offshore station and the Walcheren 2 km offshore station suggest a small spectral peak around 8 years (Terschelling) or 4 years (Walcheren) that just peaks above the 95% confidence band of surrounding frequencies. The 8 year peak for Terschelling might be related to the North Atlantic Oscillation. However, the measurement period and temporal resolution of the data is insufficient to draw firm conclusions on the significance of this peak. The other power spectral density functions do not show clear peaks at these frequencies, or a clear increase of the power spectral density for periods longer than 4 years.

Figure 2.24 presents the moving average with a two-year window of the concentration time series observed at the 6 aforementioned stations. The high-concentration events are intermittent. It is difficult to recognize a distinct periodicity.

2.3 CEFAS Minipod en Smartbuoy

2.3.1 General

In the framework of a joint research program, Rijkswaterstaat-RIKZ and the Centre for Environment, Fisheries and Aquaculture Science (CEFAS) in the UK made measurements with a Minipod and a Smartbuoy in 2001 and 2002 at different locations offshore of the coast of Noordwijk aan Zee, The Netherlands (CEFAS, 2003). Aim was to increase understanding of the horizontal en vertical transport of fine sediment in suspension at these locations.

Table 2.1 Time schedule of CEFAS Minipod and Smartbuoy measurements

Location	Deployment	First good observation (GMT)	Last good observation (GMT)
Noordwijk 2-1	180	20/Nov/01 12:00	18/Dec/01 09:00
Noordwijk 2-2	181	18/Dec/01 12:00	02/Jan/02 18:00
Noordwijk 5-1	182	05/Mar/02 10:00	21/Mar/02 08:00
Noordwijk 5-1	183	21/Mar/02 12:00	22/Apr/02 11:00
Noordwijk 10-1		10/Apr/00 20:00	01/Jun/00 23:00
Noordwijk 10-2		07/Nov/00 09:00	14/Mar/01 23:00
Noordwijk 10-3		20/Mar/01 10:00	05/Jul/01 23:00
Noordwijk 10-4		21/Aug/01 10:00	18/Sep/01 08:00

The CEFAS Smartbuoy and Minipod were deployed at three different locations, i.e. Noordwijk 2 (2 km offshore at 52°15'.28N 004°24'.28E), Noordwijk 5 (5 km offshore at

52°16'.55N 004°22'.01E) from 20 November 2001 till 22 April 2002 and Noordwijk 10 (10 km offshore). The data report by CEFAS (2003) presents a basic analysis of the measurements.

2.3.2 Noordwijk 2-1 en 2-2

Wind, wave and current conditions and concentrations

Figure 2.23 shows the wind speed and direction observed at 10 km offshore at Meetpost Noordwijk and the wave height, wave period, water depth, flow velocity and suspended sediment concentrations measured with the MiniPod during Noordwijk 2-1 period (deployment 180). The red lines in this figure illustrate the slow-varying components of the measured signals. These were obtained by low-pass-filtering the signals using a low-pass frequency of 1/(2 x tidal period).

The windspeed is near gale force twice during the Noordwijk 2-1 measurement campaign, i.e. around 22 November and around 5 December 2001. The significant wave height at 2 km offshore just exceeds 3 m during these conditions and the wind direction is northwest. The wave height decreases due to the wind direction turning eastward. The wave spectrum peak period ranges between 5 and 13 seconds during the measurement campaign. During near-gale conditions, the wave period ranges between 7 and 9 seconds. Longer swell waves occur afterwards. The water depth ranges between 11.6 and 13.6 m. The maximum current velocity is 0.7 m/s.

The observed suspended sediment concentration at ± 0.86 m above the seabed varies about 0.2 kg/m^3 during the near-gale conditions and decreases to about 0.1 kg/m^3 afterwards. The OBS-concentrations agree well with concentrations determined from water samples. The concentrations near the water surface (from the Smartbuoy) amount to 4 to 77% of the concentrations measured at 0.86 m above the bed.

Figure 2.26 shows the basic parameters measured during the Noordwijk 2-2 campaign. The windspeed is near-gale force (> 13.8 m/s) around 21 and 24 December 2001 and gale force around 28 December (> 17.1 m/s). The wind direction is west-northwest most of the time except around 22 and 30 December. The significant wave height follows the development of the wind speed. Around 21 and 24 December, the significant wave height is about 1.8 m and on 28 December it is about 3.0 m. The wave period ranges between 6 and 11 seconds. The water depth ranges between 9.6 and 12.6 m and the maximum current velocity is 0.7 m/s.

The sediment concentration at 0.86 m above the seabed is about 0.25 kg/m^3 during periods with near-gale force winds and varies roughly between 0.06 and 0.20 kg/m^3 afterwards. The OBS-concentrations agree well with concentrations determined from water samples also for this campaign. The concentrations near the water surface (from the Smartbuoy) amount to 8 to 100% of the concentrations measured at 0.86 m above the bed.

Cross-correlation between wave height and concentration

Cross-correlation is a measure of similarity of two waveforms as a function of a time-lag applied to one of them. Figure 2.27 shows the cross-correlation as a function of time lag between wave height and concentration measured at 0.86 above the seabed (Minipod) and between wave height and the concentration measured near the water surface (Smartbuoy) for Noordwijk 2-1 and 2-2 campaigns.

The cross-correlation between wave height and concentration is relatively high (0.8-0.9) near time lag zero both for the Minipod data as for the Smartbuoy data and for both deployments. This may be expected as waves play an important role in stirring sediment from the seabed and keeping it in suspension. The concentration signal measured near the seabed lags a few hours (roughly 6-12 hours) behind the wave height signal. This is not the case for the concentrations near the water surface for which the cross-correlation is maximum at zero time lag. The lagging of the near-bed concentration signal is caused by sediment higher up in the water column settling from suspension after the wave height has decreased. The near-bed layers receive sediment from the upper layers.

2.3.3 Noordwijk 5-1 and 5-2

Wind, wave and current conditions and concentrations

Figure 2.28 presents the wind speed and direction observed at 10 km offshore at Meetpost Noordwijk and the wave height, wave period, water depth, flow velocity and suspended sediment concentrations measured with the Minipod and the Smartbuoy during Noordwijk 5-1 period (deployment 182). The red lines in this figure illustrate the slow-varying components of the measured signals. These were obtained by low-pass-filtering the signals using a low-pass frequency of 1/(2 x tidal period).

The wind speed plot shows periods of a strong breeze (>10.8 m/s), a gentle breeze (>3.4 m/s) and near-gale force (> 13.8 m/s) winds from 6 to 11 March. Wind direction is southwest to west during this period and significant wave heights are about 2 m during strong breeze conditions and more than 4 m during near-gale force winds. The wind speed drops between 11 and 12 March and the wave height decreases subsequently. Wind direction changes from southwest to northeast between the 12 and 13 March. Wave heights remain relatively low from 13 to 17 March. The short period of westerly near-gale force winds on the 18th of March generate waves of up to 2.5 m. During near-gale conditions, the wave period ranges between 7 and 9 seconds. Longer swell waves occur afterwards. The water depth ranges between 17.0 and 19.5 m and the maximum current velocity is 0.6 m/s.

The concentration plot in Figure 2.28 shows two distinct periods in the Noordwijk 5-1 campaign. The first period is from 6 to 11 March with concentrations between 0.03 and 0.3 kg/m^3 at 0.86 m above the bed. The second period is from 12 to 20 March with much lower concentrations (about 0.02 kg/m^3). The concentrations near the water surface (from the Smartbuoy) amount to 3 to 100% of the concentrations measured at 0.86 m above the bed. There is a strong relation with the wave height variation.

Figure 2.29 shows the wind, wave, current and concentration parameters for the Noordwijk 5-2 campaign. The conditions are relatively calm during this period. The significant wave height is less than 0.5 m for most of the time. The wave period ranges between 7 and 14 seconds, water depth between 16.9 and 19.2 m and the maximum current velocity is 0.7 m/s. Maximum concentration at 0.86 m above the bed is 0.04 kg/m^3. The concentrations near the water surface (from the Smartbuoy) amount to 10 to 100% of the concentrations measured at 0.86 m above the bed.

Cross-correlation between wave height and concentration

Figure 2.30 shows the cross-correlation as a function of time lag between wave height and concentration measured at 0.86 above the seabed (Minipod) and between wave height and the concentration measured near the water surface (Smartbuoy) for Noordwijk 5-1 and 5-2 campaigns.

The cross-correlation between wave height and concentration for Noordwijk 5-1 is at zero time lag about 0.7 for the near-bed concentrations (Minipod) and about 0.8 for the near-surface concentrations (Smartbuoy). For Noordwijk 5-2 this is about 0.8 and 0.9, respectively. It is interesting to see that the cross-correlation with wave height is higher for the near-surface concentration than for the near-bed concentrations. This is consistent with the cross-correlations determined for the Noordwijk 2-1 and 2-2 observations (Figure 2.27).

2.3.4 Simulations with Van Rijn (2005) tidal mud transport model

This section compares suspended sediment concentrations measured during the Noordwijk 2-1, 2-2, 5-1 and 5-2 campaigns with simulations using the Van Rijn (2005) tidal mud transport model.

Model description

The Van Rijn (2005) tidal mud transport model computes the mud concentrations and mud transport rates in tidal conditions, including the effect of waves. Although the name suggests something differently, the model also computes the sand transport rates. The velocities and mud and sand concentrations are computed as a function of the height above the bed and as a function of time. Alkyon developed the MATLAB code.

The vertical grid points (default is 50 but it is a user defined model setting) are distributed exponentially as follows:

$$z = a\left(\frac{h}{a}\right)^{\frac{k-1}{N-1}} \tag{1}$$

where *a* is the reference height above the bed, $h = h_0 + \eta$ is the water depth, *k* is the index number of point k and *N* is the total number of grid points.

The model requires time series of the following parameters as an input:

- water depth $h = h_0 + \eta$ (m)
- depth-averaged velocity in x direction u_x (m/s)
- depth-averaged velocity in y direction u_y (m/s)
- significant wave height H_s (m)
- wave spectrum peak period T_p (s)

These boundary conditions can be obtained from measurements but artificial time series like simple sine functions may also be used. We used the data from the Noordwijk 2-1, 2-2, 5-1 and 5-2 campaigns.

Important free model parameters include the following:

- fraction of mud in the bed material p_{mud} (-)
- background concentration mud $c_{mud,o}$ (-)
- maximum mud settling velocity $w_{mud,max}$ (m/s)

- calibration parameter α_d in the turbulence damping function (-), see Equation (8)

The mud concentration profile at each time *t* is represented as follows:

$$c w_{mud} + \varepsilon_s \frac{dc}{dz} = 0 \tag{2}$$

where *c* is the volume concentration (-), w_{mud} the mud settling velocity in m/s, which is a function of concentration, ε_s is the sediment mixing coefficient in m^2/s, which also is a function of concentration

The settling velocity and the sediment mixing coefficient both depend on the concentration. Therefore, Equation (2) cannot be solved analytically but has to be solved numerically. This is done by first predicting the near-bed reference concentration and subsequently diffusing the sediment upward.

The near-bed reference concentration is represented as follows:

$$c_{a,mud} = p_{mud}\left[c_{a,mud,o} + \alpha\left(\frac{\tau_b - \tau_{b,cr,e}}{\tau_{b,cr,e}}\right)^{1.5}\right] \tag{3}$$

where α_{mud} is an erosion coefficient (0.0001-0.1), p_{mud} is the fraction of mud, $c_{a,mud,0}$ is a constant background concentration near the bed (10-200 kg/m^3), $\tau_{b,cr,e}$ is the critical bed shear stress for erosion, τ_b is the combined shear stress due to currents and waves.

The effect of a time lag on the mud concentrations is represented by applying an exponential approach with

$$\frac{dc_{a,mud}}{dt} = -A\left(c_{a,mud,t} - c_{a,mud,t,eq}\right) \tag{4}$$

where $c_{a,mud,t,eq}$ is the equilibrium concentration at time *t* and A is an adjustment parameter defined as follows:

$$A = \gamma_c \frac{1}{h}\frac{w_{mud}}{u_{*,cw}}\left(1 + 2\frac{w_{mud}}{u_{*,cw}}\right)\left(1 + \frac{H_s}{h}\right)^2 \tag{5}$$

where γ_c is a coefficient is the range between 0.01 and 0.1.

The concentration dependent settling velocity is represented as follows:

$$\begin{aligned} w_{mud} &= \exp\left[\left(0.182\ln\left(\frac{w_{mud,\max}}{w_{mud,\min}}\right)\right)\ln(c) + 2.09\ln(w_{mud,\max}) - 1.09\ln(w_{mud,\min})\right] & c \le 0.0025 \\ w_{mud} &= w_{mud,\max}(1-c)^4 & c > 0.0025 \end{aligned} \tag{6}$$

where $w_{mud,\max}$ is the maximum settling velocity at *c* = 0.0025, ranging between 0.5 and 3 mm/s, $w_{mud,\min}$ is the minimum settling velocity at c = 0.00001, ranging between 0.05 to 0.1 mm/s.

The sediment mixing coefficient is represented by a parabolic distribution as follows:

$$\varepsilon_s = \gamma_d \varepsilon_{s,\max} \left[1 - \left(1 - 2\frac{z}{h} \right)^2 \right] \tag{7}$$

where $\varepsilon_{s,\max}$ is the sediment mixing at mid depth and γ_d is a turbulence damping coefficient that depends on the Richardson number as follows:

$$\gamma_d = \left(1 + \alpha_d \sqrt{Ri} \right)^{-1} \tag{8}$$

where α_d is a calibration parameter (10-20) and *Ri* is the Richardson number.

The Richardson number can be written as follows:

$$Ri = -\frac{g}{\rho} \frac{\frac{d\rho}{dz}}{\left(\frac{du}{dz} \right)^2} \tag{9}$$

Consequently, the Richardson number depends on the suspended sediment concentration through the density.

Comparison of measured and computed sediment concentrations

We calibrated the Van Rijn (2005) tidal mud transport model on the measured concentration time series using the Nelder & Mead (1965) simplex algorithm. This is a direct search method for multidimensional unconstrained minimization. Lagarias *et al* (1998) present its convergence properties. We adopted this algorithm to minimize the sum of squares prediction error F_p by varying 4 of the most important free model parameters.

$$F_p = \sum_{x,t} \varepsilon_p^2 \tag{10}$$

where ε_p is the mismatch between the model value and an observation.

We used the above mentioned free model parameters for model calibration and limited the simplex search to 100 function evaluations. The model was calibrated on all four measurement campaigns. The resulting values of the free model parameters are shown in Table 2.2. Figures 2.31 to 2.34 compare measured and predicted concentrations.

The optimization runs consistently resulted in a small fraction of mud in the bed material (about 0.7%), a critical erosion shear stress of about 0.18 N/m^2, a settling velocity of about 0.2 mm/s and a relatively high near-bed background volume concentration of 0.3. We should note here that the latter is multiplied by a relatively small mud fraction of 0.7% (see Equation (3)) resulting in a 'real' near-bed concentration of 0.002 m^3/m^3. The small mud fraction is consistent with maps produced by Deltares / TNO Built Environment and Geosciences - Geological Survey of the Netherlands (Figure 2.34b).

Table 2.2 Values of free model parameters in Van Rijn (2005) tidal mud transport model

parameter	value
p_{mud}	0.0007
$c_{mud,o}$	0.3 m^3/m^3
$\tau_{b,cr}$	0.18 N/m^2
$w_{s,mud,max}$	0.2 mm/s

The model results (low-pass filtered) reasonably agree with general trends in the data (low-pass filtered). During energetic conditions, the model predicts the suspension events with concentrations of the same order of magnitude as observed, both near the bed (Minipod) as near the water surface (Smartbuoy). However, the predicted near-bed concentrations drop back to near-zero more often than observed in the measurements.

2.3.5 Simulations with artificial neural network

Introduction

Neural networks are composed of simple elements operating in parallel. These elements are inspired by biological nervous systems. As in nature, the connections between elements largely determine the network function. A neural network can be trained to perform a particular function by adjusting the values of the connections (weights) between elements.

Neural network set-up

We use a feed-forward network with a tan-sigmoid transfer function in the hidden layer and linear transfer function in the output layer. This structure is useful for function approximation (or regression) problems. We use 9 neurons (somewhat arbitrary) in one hidden layer. The network has one output neuron, because there is only one target value associated with each input vector. The network uses the default Levenberg-Marquardt algorithm for training.

We randomly divided input vectors and the target vector into three sets as follows:

- 70% were used for training
- 15% were used to validate that the network is generalizing and to stop training before overfitting
- 15% were used as a completely independent test of network generalization

We adopted the following low-frequency time series (hourly data) from the Noordwijk 2-1, 2-2, 5-1 and 5-2 as an input:

- significant wave height
- wave spectrum peak period
- water depth

Current velocity measurements are not as often available as wave observations. Using the current velocities as an input vector would limit the applicability of the neural network. Therefore, we used time series of wave parameters and water depth only. For the same reason we did not include the effect of a time lag between the input and output vectors.

Observed time series of the low-frequency near-bed concentrations (Minipod) were used as the training target.

Results

Figure 2.35 compares observed and neural-network-predicted concentrations for the Noordwijk 2-1 and 2-2 campaigns. The predictions show encouraging agreement with the low-pass filtered observations ($R^2 > 0.85$). Figure 2.36 shows observed and predicted concentrations for the Noordwijk 5-1 and 5-2 campaigns. Also for these campaigns, the neural network predictions agree well with the observations ($R^2 > 0.86$).

Why use neural networks

We should note here that a neural network is only an "input-output model" or "black box model". It gives no insight in the working of the modelled system but only simulates the input-output relationship. As we want to understand the physics behind the suspended matter concentrations in the North Sea, developing a neural network is not an objective in itself. A neural network is however useful to generate boundary condition to force a process-based model or to generate time-series for calibration and validation purposes. In addition, it might be used to make predictions for other locations with conditions similar to those the network was trained on.

For example, a neural network can be used for the generation of long time series of SPM concentrations using time series of observed wave parameters. This shows us among other things the long term variability of SPM concentrations due to the wave climate.

2.4 Siltprofiler T0 campaign 22-24 May 2007

2.4.1 Introduction

The T0 campaign concerns measurements of background SPM concentrations and related parameters under conditions without dredging. Talmon (2007) describes the measurements. A summary follows below.

Commissioned by Rijkswaterstaat, Havenbedrijf Rotterdam (HBR) performed measurements at 46 locations with a so-called silt profiler in the period 22-24 May 2007 offshore the coasts of Noord-Holland, Texel and Vlieland with survey vessel Spirit. Vertical profiles of the following parameters were measured (Talmon, 2007):

- Temperature
- Pressure (= depth of the instrument)
- Conductivity
- Suspended matter concentration
- Chlorophyl-A (fluorescence)
- Secchi depth
- Current velocity and direction

Figure 2.37 shows the measurement locations. Vertical profiles of current velocity and direction were measured with an Acoustic Doppler Current Profiler (ADCP) during the silt profiler casts. The depth at each location was measured with a single beam echosounder. De suspended matter concentration were measured with two Seapoint Optical Backscatter Sensors (OBS) and an extinction meter.

For calibration purposes water samples were taken with Niskin Bottles (1,7 L) at 15 of the 46 locations. At each of the 15 locations, a sample was taken 1 m below the water surface, one at mid depth and one close to the seabed. This comes down to 45 samples in total. In addition, 5-litre water samples were taken at 1 m below the water surface to determine the sediment grain size distribution at each of the 15 locations.

Figure 2.38 shows the date and time of the T0 measurements in a plot of observed water levels at Den Helder on the three measurement days. The measurement were made approximately from the moment of high tide to the moment of low tide, so during high tide or the ebbing phase.

Dates, times and positions of the observations are presented by Talmon (2007) and on the DVD's with this report.

2.4.2 T0 silt profiler data 2007 compared to MWTL 1975-1983

Based on analysis of the MWTL observations from 1975 to 2008 we concluded in Section 2.2.3 that generally the suspended matter concentrations along the Dutch coast show no significant increasing or decreasing trends. This means that observations from 2007 may be compared to interpolated maps based on MWTL data from 1975-1983.

Figure 2.39 plots the T0 silt profiler concentrations from May 2007 measured at 1 m below the water surface as coloured symbols in the filled contours representing the mean of the MWTL 1975-1983 data (see also Section 2.2.2). This figure clearly shows that the T0 silt profiler concentrations are a factor 2 to 5 smaller than the mean MWTL suspended matter concentrations. For example, near the Marsdiep inlet south of Texel, the MWTL mean filled contours shows colours in the range between 30-200 mg/l whereas the T0 silt profiler observations have colours in the range between 5-10 or 10-20 mg/l. The same holds for the MWTL trimmed mean contours that are on average about 5% smaller than the mean (Figure 2.40).

The MWTL geometric mean is on average 32 % smaller than the mean. Still the T0 silt profiler concentrations are smaller than this geometric mean (Figure 2.41). The difference is about a factor 2 offshore and about a factor 3 closer to the shore.

It is interesting to see in Figure 2.42 that the T0 silt profiler concentrations compare rather well with the 10th percentile of the MWTL 1975-1983 observations. This means that the T0 measurements fall in the low range of suspended matter concentrations observed in this coastal region of Noord-Holland, Texel and Vlieland.

Monthly-averaged wave heights show a typical seasonal trend with relatively calm conditions during the summer months from May to October and more energetic conditions during the winter months from December to March. In Section 2.2.2 we adopted these periods to determine the typical summer and winter mean suspended matter concentrations. The T0 measurement campaign (May 2007) falls in the summer season. Figure 2.43 plots the T0 silt profiler concentrations measured in May 2007 at 1 m below the water surface in the MWTL 1975-1983 summer-mean concentration contours. The figure clearly illustrates that the concentrations measured during the T0 campaign in May 2007 are much smaller and therefore not representative for an average summer period.

2.5 Siltprofiler T1 campaign 17 Sept, 1-2 Oct 2007

2.5.1 Introduction

The T1 campaign concerns measurements of SPM concentrations and related parameters under conditions with dredging activities. Talmon (2008) describes the measurements. The measurement parameters and the procedures were similar to those of the T0 measurements.

Commissioned by Rijkswaterstaat, Havenbedrijf Rotterdam (HBR) performed measurements at 16 locations with a so-called silt profiler on 17 September and 1 and 2 October 2007 offshore the coast of Den Helder with survey vessel Spirit.

Figure 2.44 shows the measurement locations. Figure 2.45 shows the date and time of the T1 measurements in a plot of observed water levels at Den Helder on the three measurement days. The measurements on 17 September 2007 were made approximately from the moment of high tide to the moment of low tide, so during high tide or the ebbing phase. The measurements on 1 October 2007 were made also during the ebbing phase and on 2 October 2007 mainly during the flooding phase of the tide.

2.5.2 T1 silt profiler data 2007 compared to MWTL 1975-1983

Mean

Figure 2.46 shows the interpolated filled contours for the period 1975-1983. Highest suspended matter concentrations between 15 and 240 mg/l are found in the nearshore regions ($\leq$ 2 km). This reduces to 3-5 mg/l further offshore.

The coloured symbols in Figure 2.46 denote the T1 observations near the surface on 17 September 2007. The observed T1 values at the most offshore location range between 1 and 2 mg/l. The observed values closer to the shore are 3-4 mg/l. The 1975-1983 concentrations are a factor 2-3 higher, with 3-4 mg/l for the most offshore locations to 5-10 mg/l closer to the shore.

Figure 2.47 shows the same interpolated contours as Figure 3.1 but the coloured symbols now denote T1 observations on 1 October 2007. The concentrations measured on 1 October are higher than those observed on 17 September.

The observed T1 values at the most offshore locations range between 4 and 10 mg/l. This is generally of the same order of magnitude as the 1975-1983 data. For some locations the T1 observations are a factor 2 higher. Closer to the shore the T1 values range between 5 and 40 mg/l. The 1975-1983 filled contours show values of 5-10 mg/l here, which means that the T1 observations are a factor 4 higher for some locations.

Figure 2.48 shows the 1975-1983 filled contours together with the T1 observations made on 2 October 2007. As for the 1 October data, the concentrations measured on 2 October are generally higher than those measured on 17 September.

The observed T1 values at the most offshore locations range on 2 October between 1 and 8 mg/l. For some stations it is a factor 4 smaller than the 1975-1983 values, for others it is a factor 4 larger. Closer to the shore the observed T1 values range between 5-20 mg/l, which is of the same order or a factor 2 higher than the 1975-1983 data.

Trimmed mean

The trimmed mean is the mean excluding outliers. We adopted the highest and lowest 2% for this. The trimmed mean values for 1975-1983 shown in Figure 2.49 are on average about 5% smaller than the mean values in Figure 3.1. For the biggest difference, the trimmed value is 45% smaller. Figure 2.49 also presents the T1 observations made on 17 September 2007. The observed T1 values at the most offshore location range between 1 and 2 mg/l. The observed values closer to the shore are 3-4 mg/l. The 1975-1983 trimmed mean concentrations are a factor 2-3 higher, with 3-4 mg/l for the most offshore locations to 5-10 mg/l closer to the shore.

Figure 2.50 presents the T1 values observed on 1 October 2007 together with the 1975-1983 filled contours. The T1 values at the most offshore locations range between 4 and 10 mg/l. This is generally of the same order of magnitude as the 1975-1983 trimmed mean. For some locations the T1 observations are a factor 2 higher. Closer to the shore the T1 values range between 5 and 40 mg/l. The 1975-1983 trimmed means shows values of 5-10 mg/l here, which indicates that the T1 observations are a factor 4 higher for some locations.

Figure 2.51 shows the T1 concentrations measured on 2 October 2007 together with the 1975-1983 data. The observed T1 values at the most offshore locations range on 2 October between 1 and 8 mg/l. For some stations it is a factor 4 smaller than the 1975-1983 trimmed means, for others it is a factor 4 larger. Closer to the shore the observed T1 values range between 5-20 mg/l, which is of the same order or a factor 2 higher than the 1975-1983 trimmed mean.

Geometric mean

The geometric mean is similar to the arithmetic mean, except that instead of adding the set of numbers and then dividing the sum by the count of numbers n in the set, the numbers are multiplied and then the n^{th} root of the resulting product is taken. This procedure is similar to taking the mean of the logarithm of concentrations. The geometric mean is always smaller than or equal to the arithmetic mean and is often used for a set of numbers whose values are exponential in nature, like suspended matter concentration.

The geometric mean values for 1975-1983 shown in Figure 2.52 are 10 to 60% smaller than the mean values (on average 32% smaller). This is because the geometric mean tends to dampen the effect of very high or low values, which biases the arithmetic mean. The geometric mean may be more appropriate description of the mean concentration as the levels may vary anywhere from 1 mg/l to 300 fold over a given period.

Figure 2.52 also shows the T1 observations made on 17 September 2007. The observed T1 values at the most offshore location range between 1 and 2 mg/l. The observed values closer to the shore are 3-4 mg/l. The 1975-1983 geometric means are of the same order of magnitude or a factor 2 higher, with 3-4 mg/l for the most offshore locations to 3-5 mg/l closer to the shore.

Figure 2.53 presents the T1 values observed on 1 October together with the 1975-1983 geometric means. The observed T1 values at the most offshore locations range between 4 and 10 mg/l. This is generally a factor 2 higher than the 1975-1983 geometric means. Closer to the shore the T1 values range between 5 and 40 mg/l. The 1975-1983 geometric means show values of 3-5 mg/l here, which means that the T1 observations are a factor 8 higher for some locations.

Figure 2.54 shows the T1 concentrations measured on 2 October 2007 and compares these with the geometric means from 1975-1983. The observed T1 values at the most offshore locations range on 2 October between 1 and 8 mg/l. The geometric mean is about 2-3 mg/l here, which means that for some stations it is a factor 2 smaller than the 1975-1983 geometric means, for others it is about a factor 3 larger. Closer to the shore the observed T1 values range between 5-20 mg/l, which is of the same order or a factor 2 higher than the 1975-1983 geometric means.

Standard deviation

Figure 2.55 presents the standard deviation of the suspended solid concentrations observed between 1975 and 1983. The x-marks denote the locations of the T1 observations. The standard deviation is of the same order as the mean (compare Figure 2.46 and 2.55), indicating a wide scatter of the concentration values. Therefore, one individual survey may differ significantly from the mean distributions shown here.

The 1975-1983 standard deviation for the most offshore T1 locations ranges between 3 and 4 mg/l, while closer to the shore this becomes 4-10 mg/l.

10th percentile

The T1 concentrations measured on 17 September are with 1-2 mg/l generally slightly larger than the 1975-1983 10th percentile with values < 1.0 mg/l (Figure 2.56). The T1-value closest to Marsdiep is 3-4 mg/l where the 1975-1983 contour lines show 1-2 mg/l.

The T1 values measured on 1 October are generally more than a factor 5 larger than the 1975-1983 10th percentile (Figure 2.57).

The most offshore T1 value measured on 2 October 2007 is the same as the 10th percentile from the 1975-1983 MWTL data but the values from other stations are about a factor 2-5 larger (Figure 2.58).

50th percentile (median)

The T1 concentrations measured on 17 September are with 1-2 mg/l generally smaller than the 1975-1983 50th percentile with values 5-20 mg/l (Figure 2.59). The T1-value closest to Marsdiep are 3-4 mg/l where the 1975-1983 contour lines show 10-20 mg/l.

The T1 values measured on 1 October are generally of the same order or a factor 2 smaller than the 1975-1983 50th percentile (Figure 2.60), except for the T1 value closest to Marsdiep, which is about a factor 2 larger.

The T1 values measured on 2 October are generally of the same order as the 50th percentile, except for the most offshore T1 value that is smaller than the 50th percentile from the 1975-1983 MWTL data (Figure 2.61).

90th percentile

The T1 values measured on 17 September are about a factor 5 smaller than the 1975-1983 10th percentiles (Figure 2.62).

The T1 values observed on 1 October are of the same order as the 90th percentiles for some stations (Figure 2.63). The most offshore T1 stations show values that are about a factor 5 smaller and the T1 station closest to Marsdiep shows a value that is a factor 2 larger.

The T1 concentrations measured on 2 October are of the same order as the 90th percentile for 9 out of the 15 T1 observations made on this day and about a factor 2-5 smaller for the others (Figure 2.64).

Summer mean

The T1 concentrations measured on 17 September 2007 are slightly smaller than the summer mean concentrations from the 1975-1983 data. The T1 values at the most offshore location range between 1 and 2 mg/l, where the 1975-1983 summer-mean is 3-4 mg/l. The observed T1 values closer to the shore are 3-4 mg/l where the summer-mean is 4-5 mg/l.

The T1 concentrations measured on 1 October 2007 are generally slightly larger than the 1975-1983 summer-mean concentrations. For some stations this is up to a factor 2 larger (T1-values 4-10 mg/l where 1975-1983 data show 3-5 mg/l). In contrast, the T1 observation closest to the Marsdiep inlet shows a value of 40 mg/l where the summer-mean 1975-1983 contour lines show values of 5-10 mg/l. We should note however that the uncertainty of the 1975-1983 contour lines close to Marsdiep is large due to a relatively low spatial resolution of the MWTL data on the North Sea near Marsdiep.

The T1 concentrations measured on 2 October 2007 are generally 5-10 mg/l where the 1975-1983 data shows values from 3-4 mg/l. Some offshore T1-stations show smaller values. The T1-value closest to Marsdiep is 10-20 mg/l where the summer-mean 1975-1983 contour lines show values of 5-10 mg/l.

Winter mean

The T1 concentrations measured on 17 September 2007 are a factor 2 to 5 smaller than the winter-mean concentrations from the 1975-1983 data. The T1 values at the most offshore location range between 1 and 2 mg/l, where the 1975-1983 winter-mean is 3-5 mg/l. The observed T1 values closer to the shore are 3-4 mg/l where the winter-mean is 10-20 mg/l.

The T1 concentrations measured on 1 October 2007 compare well with the 1975-1983 winter-mean concentrations. The difference is largest for the T1 observation closest to the Marsdiep inlet that shows a value of 40 mg/l where the winter-mean 1975-1983 contour lines show values of 10-20 mg/l.

The T1 concentrations measured on 2 October 2007 closest to Marsdiep show good agreement with the winter-mean 1975-1983 data. Some T1-stations further offshore show larger values (5-10 mg/l where the 1975-1983 winter-mean shows 4-5 mg/l). The T1-sation furthest offshore is relatively small (< 1 mg/l), where the 1975-1983 winter-mean shows 3-4 mg/l

3 Analysis and evaluation of remote sensing data

3.1 Introduction

The colour of North Sea waters is determined by its components, and from this colour, subsequently concentrations of its optical components can be derived. Ocean colour satellite sensors measure this colour regularly at carefully chosen small wavelength intervals, but have relatively large pixels (raster cells) (Rast et al., 1999). The optically active substances are Suspended Particulate Matter (SPM), Chlorophyll-a (CHL), and Coloured Dissolved Organic Matter (CDOM).

SPM derived from remote sensing is by definition closely linked to in situ data (such as MWTL), as both comprise all residue that remains on a filter. Remote sensing data is averaged over 1 km^2 or at MERIS Full resolution over 300 m^2. Highest concentrations occur far below surface, and the satellite sensor does not sample their signal if light extinction in the overlying water column is more than 90%. Therefore, one could argue that increased SPM concentrations from sand extraction cannot be detected from remote sensing data, even when direct near-field effects would be observed from a ship plume with distinctly higher concentrations.

This chapter is mainly concerned with the sand extraction activity off the coast of Huisduinen (Fig 3.1). Talmon (2007, 2008a, 2008b) describes the silt concentration measurements made before and during these activities.

Two scenarios are possible:

1) Mid-field effects. The Huisduinen sand extraction comprises 7×10^6 m^3 sand with 2 percent (1.4×10^5 m^3) mud, mostly in the form of thin layers. This equals 2.24×10^{11} g mud if the same porosity as for sand is assumed (40%, density of 1600 kg/m^3). The extraction took some 100 days, which is 193 tidal periods, with an assumed averaged mud release of 1.16×10^9 g per tide. This amount is dispersed in one tidal period over an estimated volume of 5×10^8 m^3 (5 km × 5 km, average depth 20 m). This means an average increase of SPM concentration of 2.3 mg/l, assuming that the residence time in this area is one tidal period, which is reasonable, considered the residual current speed between 5 and 10 cm/s in this area.
2) Far-field lag effects. At distances of a few km downstream of the dredging vessel much higher concentration increases could be encountered, but not near the surface. Probably it needs strong tidal currents and wave action to bring this material to the surface. Most of the mud discharging at the bottom of the ship immediately sinks to the bottom to form a mobile High Concentrated Benthic Suspension (HCBS) layer. From this extra SPM source on or near the sea bottom, some will consolidate at the bottom, but most will move with bottom currents (Hitchcock and Bell, 2004) and can be mixed up under the influence of waves, and become subsequently visible. Such an indirect mid-field response might be extracted from the remote sensing products using a spatial statistical analysis on a larger time scale in addition to a time series extracted at certain locations.

We note here that the fraction of fine sediment in the top 30 cm of the seabed is below 10 % and generally only a few percent. Nonetheless, this pool of fine sediment in the seabed top layer is more than 10 times larger than the pool of sediment in suspension

(De Kok, 2004), and constitutes an important source of fine sediment in periods of high wave activity (in particular during strong swell). The time scale for renewal of the fine sediment pool in the seabed top layer (upper 30 cm) is estimated at ca. 2 years, as derived by Laane et al. (1999) from the time lag of seabed decontamination relative to the reduction of contaminant concentrations in the water column. Therefore the increased mud content from sand extraction in the HCBS layer and at the seabed seems an important extra source.

However, dredge spoil dump at Loswal Noord-West (10 km West of Scheveningen) and at the Verdiepte Loswal (10 km West of Hoek van Holland) together averages about 4 $\times 10^9$ kg mud year^{-1}; at Loswal IJmuiden about 1 $\times 10^9$ kg. This is in the same order as 1.1 to 1.4 $\times$ 10^9 kg mud that becomes available with an extraction of 35 $\times$ 10^9 m^3 sand per year. Note that this mud might have been deposited long-time ago and is therefore “new in the system”. Therefore both dredge spoil dump and sand extraction were studied.

The H0 hypothesis is that extra SPM from sand extraction cannot be seen on the SPM concentrations derived from remote sensing data. The alternative hypothesis is that extra SPM from sand extraction can be seen on this data.

This chapter is mainly concerned with the sand extraction activity off the coast of Huisduinen (Fig 3.1). Talmon (2007, 2008a, 2008b) describes the silt concentration measurements made before and during these activities.

3.2 Material

3.2.1 Remote sensing datasets

For T0, water quality data from MERIS-RR for 2003-2006 as processed in the Ovatie project (Peters et al., in prep) were used (with DID permission).

Table 3.1 Number of processed MERIS-RR files

		2003	2004	2005	2006	Total
Annual		577	597	590	585	2349
Seasonal	Summer	312	265	304	306	1229
	Winter1	265	290	286	276	1120
	Winter2	291	284	285		
Monthly	Jan	46	46	43	43	178
	Feb	34	51	48	47	180
	Mar	44	53	53	53	203
	Apr	72	49	53	45	219
	May	51	54	50	55	195
	Jun	43	47	52	53	210
	Jul	52	53	49	51	205
	Aug	50	53	54	55	212
	Sept	44	51	46	47	188
	Okt	53	53	54	54	214
	Nov	47	45	47	42	181
	Dec	41	42	41	40	164

Winter1 Jan-Mar & Oct-Dec; Winter2 Oct-Dec (year) & Winter Jan-Mar (year +1).

Table 3.1 characterises the data set by listing the number of files. These are all files that cover some part of the North Sea. The collected data therefore does not necessarily cover the Dutch coastal zone. When information within the Dutch coastal zone was collected, clouds might have occurred. (Appendix A presents quality assurance information.)

3.2.2 List of sand extraction activities

Although this report aims to characterise T0 for the 2007 Huisduinen sand extraction works, also additional historic activities, possibly favourable for detection of disturbance were studied. A list of beach nourishments and selection on quantity (top 10), location (Kustvak Noord-Holland), and period (2003 - 2006) caused additional research on the Callandsoog-Zwanewater nourishment (Table 3.2). Sand extraction occurred from 17 February until end May 2003 at mining locations Q2C andQ2E (information from DNZ). Note that dredge spoil dumping on the Loswallen might also be visible. Figure 3.1 presents the locations of the sand extractions sites.

Table 3.2 Nourishments and their extraction locations

Start Date	End Date	Location	Begin transect	End transect	Amount (m^3)	Extraction locations
02/2003	05/2003	Callantsoog-Zwanenwater	10	16	2.572.642	Q2C, Q2E
08/2007	12/2007	Den Helder-Julianadorp	0	7.1	5.000.000	Q2J, Q2L

3.2.3 Restructuring individual datasets: inventory and some examples

The Ovatie-2 Hydropt water quality products (Peters et al., in prep.) were compiled into comprehensive .mat files (Table 3.3) accompanied by SPM quicklooks (as jpgs). The data are in satellite scene (row, column) coordinates: files are projected to the same grid, but are annotated with lat-lon as an attribute. The comprehensive file structure facilitates intercomparison of water quality parameters SPM, CHL, CDOM plus retrieval error products, K_D at several MERIS wavelengths, and some additional info (if needed).

Table 3.3 Parameters in the (restructured) Ovatie-2 Hydropt water quality products dataset

Parameters in files	Explanation of abbreviations
Location/metadata/wind: lat, lon, msk, metaData, windu, windv, wspeed	Msk indicates area, MetaData, and wind from ECMWF
Light: Kd, phi0, phiv, theta0, thetav	K_D diffuse attenuation ((per MERIS band) Phi and theta are solar (0) and view (v) angles
Water quality parameters: c (CHL, SPM, CDOM)	C indicates concentrations retrieved with Hydropt (water, CHL, SPM, CDOM)
Errors products: l2_flags, chisq, P, dc (CHL, SPM, CDOM)	L2_flags indicate MERIS l2_flags Chisq matching of predicted and measured reflectances P is the cumulative distribution function of chisq Dc derived errors with concentrations

Plotting the SPM and land, cloud quality flags information from these files (Figure 3.2) generates similar info as the SPM atlases (Pasterkamp et al., 2002, 2003).

The cross-shore SPM distribution (the width of the region of high SPM concentrations along the coast) varies with wind induced waves, and water depth (local topography). Patterns in the form of bulges might be caused by high discharge, effect of the Verdiepte Loswal, tide barocline meandering in a stratified Rhine ROFI. A spot offshore from Den Haag in the lower panel in Figure 3.2 could indicate dredge spoil dumping. Discharge can mask ambient marine sediment concentrations, but can also cause high SPM bulges near river outlets (cf. Eleveld et al., 2008). A more regular pattern of bulges could be related to tide. A sand extraction or dredge spoil dumping activity (Figure 3.2 lowest panel) could be detected as an offshore (of -20 m) point source, which should then be checked against additional data.

3.3 Methods

3.3.1 Study area

The MER maps (Van Duin et al., 2007) show sand extraction activities in a zone deeper than -20 m NAP and inshore of the 12 miles line. This means that the analysis should be performed on an area smaller than the Dutch EEZ (NCP) by projecting all SPM to this smaller area and subsequently calculating SPM statistics.

3.3.2 Characterising T0 SPM distribution

The NL20 area was defined in UTM projection and extending from lat 51..54 to lon 3..7 (Figure 3.3). Subsequently, the data were projected for the individual parameters CHL, SPM, CDOM and K_{D560}. SPM files contain only the grid of lat, lon and SPM concentrations, making file size indicative of coverage (the number of good SPM pixels). For 2003-2006 this resulted in a list of 864 images with more than 10 % coverage in the NL20 area.

Earlier works by Eleveld et al. (2008) have shown that statistics might generate additional information on processes such as seasonal stratification: composites highlighted wind induced wave action and mixing causing high surface SPM concentrations in winter, whereas summer stratification in the deeper North Sea led to a lower average SPM surface signal and higher variability due to occasional reduced mixing.

Table 3.4 Parameters in MERIS-RR dataset

Parameters in files	Explanation of abbreviations
Location: X, Y	Lat-lon grid, similar for all files
Number of observations: N, mapmatlist	N indicates the number of grid cells List of files used to generate the statistics
Measures of central tendency: Z, Z_median, (Z_50)	Z indicates mean Z-median = Z_50 (50 percentile) indicates median of the normal distribution and approaches the geometric mean
Measures of spread: Z_sd, Z_var, Z_10, Z_90, Z_95,	Standard deviation = square root of variance 10 and 90 percentile as indicators of min and max 95 percentile also indicating 2 times standard deviation

Because sand extraction activities typically take a few months, monthly timescales seemed suitable here. Table 3.4 presents the statistics calculated for every grid cell of all SPM maps. Log transformation allows calculation of geometric mean and geometric variance (and standard deviation), but geometric mean was already approached by the median of the normal distribution.

3.3.3 Outlier algorithm development

We assumed the sand extraction activities to be outliers in the MERIS-RR images. Outliers can be statistically defined as values higher than a 95 percentile (which equals one-sided twice standard deviation). Because of the large spatial gradients such a distribution can best be calculated for each cell. Because of the seasonal variation plus additional wind wave-related variability, the baseline P95 level can best be defined per month over the 2003-2006 period (e.g. P95 for all 2003 - 2006 January months). In this case, the monthly timescale was based on environmental conditions influencing water quality products (particularly SPM). High winds and storms occur more frequently in certain winter months, which subsequently influences wave heights and resuspension. Many tidal components contributing to shear stress and transport average out when monthly composites are used, whereas the transport from residual current remains. Four years of data also provide enough observations for the statistics. For every month the outlier detection for individual maps is defined as:

$$\text{Outlier} = SPM_{rs} - P95_{2003 \ldots 2006} \text{ (positive values)}$$

Sand extraction often occurs for longer periods. Outlier detection for individual months is defined as:

$$\text{Outlier} = P95_{year} - P95_{2003 \ldots 2006} \text{ (positive values)}$$

$P95_{year}$ is first $P95_{2003}$ Callantsoog, later $P95_{2007}$ Huisduinen.

Note that outliers will result from high scattering. This will primarily be caused by high SPM concentrations high in the water column as a direct impact from sand extraction, or resuspension of the extra mining-related SPM from the bottom or resuspension of ambient (non-mining related) mud by storm.

The H0 hypothesis is that the SPM concentrations at the sand extraction (impact) site do not contain near-surface outliers. The alternative hypothesis is that extra SPM concentrations are visible as outliers at the impact site.

Section 3.4 presents our first results and compares them with sand extraction activities.

3.3.4 Time series: statistical analysis on points or along lines

To further characterise T0 for Huisduinen, time series at the middle points of Q2J and Q2L (mining locations for the Huisduinen 2007 nourishment) were extracted from the compiled files for 2003-2006 (Table 3.5). Zooming into one additional T0 sand extraction activity along the Holland coast that was relatively large (for 2003-2006), not too much influenced by the Rhine ROFI, and occurred in spring and summer when there are relatively many unclouded images available also resulted in further study of the Callandsoog-Zwanenwater nourishment, with mining areas Q2C and Q2E.

Table 3.5 Centre points of extraction locations

Start Date	End Date	Location	Amount (m^3)	Win locations	X, Y (UTM, ED 50 in m)	Lat, lon (in dec degr)
02/2003	05/2003	Callantsoog-Zwanenwater	2.572.642	Q2C Q2E	604615, 5859290 603586, 5855658	52.8720, 4.5542 52.8396, 4.5378
08/2007	12/2007	Den Helder-Julianadorp	5.000.000	Q2J Q2L	601700, 5867931 598876, 5869060	52.9502, 4.5136 52.9609, 4.4720

Cross-shore lines were drawn to sample (perturbation with respect to) the natural cross-shore SPM gradient. A transect ca 10 to the North was considered to be potentially perturbed (impacted) because of its downstream location with respect to residual flux, and can serve to estimate the extent of the impact. The transect located ca. 5-10 km to the South and outside the range of direct tidal advection was considered as control location. The outer ends of the transects serve to assess autonomous variation, which proved to be considerable.

In preparation for the Huisduinen impact control testing, additional points were extracted surrounding the sand extraction areas and at the location of active Loswallen (Figure 3.4-3.6). First, the data were plotted in Matlab, and then the more-or-less normally distributed log transformed data were tested in Excel. Note however, that the method might be sensitive to the location of the points and transects in relation to bathymetry.

First F-tests were performed to test if equal variances of the impact locations Q2C and Q2E and control locations to the south can be assumed, followed by t-tests to test if the geometric means of the impact locations Q2C and Q2E are significantly higher than the mean of the control locations to the south. Finally a paired t-test and regression analysis served to compare simultaneous impact and control concentrations.

The H0 hypothesis to be tested is that the SPM concentrations at the sand extraction (impact) site are not significantly higher than at the control locations. The alternative hypothesis is that extra SPM concentrations are significantly higher at the impact site.

3.3.5 Optics for interpretation of plume characteristics

SPM and vertical diffuse attenuation coefficient (K_D) values were combined to make a first estimate of concentrations of a plume (in mg l^{-1} and kg mud). Usually vertical diffuse attenuation is least and reflection is greatest in the green channel (560 nm). K_D values at 560 nm were used as a first approximation of optical depth, $\varsigma = 1/K_{D560}$ (Gordon and McCluney, 1975).

3.4 Results

3.4.1 SPM distributions

Figure 3.6 shows statistics of all measurements in the period 2003-2006 binned per month for 2 contrasting months: February on the left hand side, July on the right hand side. The top panels present the median, the middle panels the number of observations and the lower panels the 95 percentiles. The figures clearly illustrate a large seasonal variation in the cross-shore gradient of SPM concentrations.

3.4.2 Outliers, sand extraction and dredge spoil disposal

The upper panel in Figure 3.7 shows the composite April 2003 anomaly with high values (outliers) near sand extraction sites Q2C and Q2E and Loswal Noordwest. The outliers are caused by one individual map of 7 April 2003 shown in the lower panel of Figure 3.7. Another striking feature is the spot close to Loswal Noordwest. This could also be traced back to 7 April 2003.

Figure 3.8 presents an SPM quicklook with quality flags, confirming that the signal near Loswal Noordwest occurs in the water, and not in the atmosphere.

Figure 3.9 shows all optical water quality parameters and their estimated retrieval error products. This figure confirms that the signal is truly caused by SPM, and not caused by a scattering algal bloom. Note that the CDOM product still needs validation.

3.4.3 Time series: T0 at Huisduinen and Callantsoog T0-T1 statistics

Figures 3.10 to 3.11 present different aspects of T0 time-series for the Huisduinen site.

Figure 3.10 shows examples of extracted SPM values along transects I10, I0 and C10 for Jan-Feb 2003 (left) and Jul-Aug 2003 (right) for the Huisduinen site (x-axis in km); see Figure 3.4 for sample design. Figure 3.10 confirms a large autonomous (T0) spatial and seasonal variation in the cross-shore gradient of SPM concentrations.

Figure 3.11 presents T0 time series at the centre points of the Q2J and Q2L Huisduinen sand extraction sites. Mean SPM values are ca 1.6 and 1.7 g m^{-3}, respectively. The (span) moving averages illustrate seasonality and inter-annual variation.

Figure 3.12 shows T0 time series at the centre points of the Q2C and Q2E Callantsoog sand extraction sites. Sand was extracted between 17 Feb and end May 2003. High values occur for the period between mid and end February 2003 suggesting effects of sand extraction on the SPM concentrations. However, the relatively high values also occur at the centre points of Q2J and Q2L near Huisduinen where no sand was extracted at that time (Figure 3.11).

Figure 3.13 presents time series from Loswal Noordwest revealing relatively high values in April 2003 but not exceptionally high as compared to other years.

A preliminary study of both T0 and T1 at Callantsoog showed no significant impact of sand mining (Figure 3.14). F-tests showed no significant differences in variances of the impact locations Q2C and Q2E and control locations to the south. T-Tests showed no significant differences in the geometric means of the impact locations Q2C and Q2E from control locations to the south. Finally a paired t-test showed no significant differences in simultaneous impact and control concentrations, and regression analysis even showed that they are significantly correlated, probably indicating similar SPM response to natural variability.

However, note that this method is sensitive to the exact locations of the points (because of sensitivity to east-west gradients, cf. fig 3.10), but the conclusion is supported by clear absence of a signal (outlier) on the SPM maps from remote sensing data.

3.4.4 Interpretation of plume characteristics

Optics can be used to estimate top of plume characteristics for the detected plume near the Loswal Noordwest dredge disposal location of 7 April 2003 (Figures 3.7 - 3.9).

The detected plume area is ca 144 $\times 10^6$ m^2 (Figure 3.7). Average K_{D560} was 0.7, which roughly corresponds with an optical depth of 1.40 m. The total volume for which this higher concentration was detected is 2 $\times 10^8$ m^3. Average concentrations for this plume were 12 g m^{-3}. This gives an estimate of 2400 tonnes SPM in the top layer. A medium size dredging vessel can contain ca. 3000 tonnes (dry weight) of mud.

In two days, concentrations dropped from 12 to 6 g m^{-3}. The other 6 g m^{-3} disperses and settled out of the 1.4 m deep surface layer, which would require a settling velocity of about 0.7 m day^{-1}.

Average concentrations were 12 g m^{-3}. Giving an estimate of 6 kg SPM in the top layer.

3.5 Mean and standard deviation 2003-2006

Figure 3.15 presents the mean SPM concentrations for the period 2003-2006 as derived from HYDROPT MERIS observations. Highest suspended matter concentrations between 30 and 200 mg/l are found in the nearshore regions. This reduces to 2-3 mg/l further offshore. These concentrations are consistent with those interpolated from the in-situ MWTL observations shown in Figure 2.2 and discussed in Section 2.2.2 of this report.

Figure 3.16 shows the standard deviations of SPM concentrations for the period 2003-2006 as derived from HYDROPT MERIS observations. The standard deviation is of the same order as the mean, indicating a wide scatter of the concentration values. The variation in concentrations derived from HYDROPT MERIS observations is consistent with that from MWTL observations shows in Figure 2.7 and discussed in Section 2.2.2 of this report.

3.6 Comparison remote sensing SPM with MWTL SPM

Figure 3.17 compares annual geometric mean values of SPM as observed in-situ on MWTL monitoring stations with those derived from HYDROPT MERIS observations at MWTL locations for 2003-2006 (Peters et al., in prep.). The correlation between the two methods is good with $r^2 > 0.9$ and a root-mean-square error between 20 and 30%. The SPM slope slightly deviates from the 1:1 line leading to small underestimations of high SPM values and small overestimations of low SPM values.

3.7 Effect of sand mining

Mining activities during observations

Sand extraction activities occurred between 3 August and 23 December with max 5 vessels and works prolonged almost continuously. Dredging and filling of a single vessel takes about 4 hrs. Table 3.6 lists the file in Annex 1 in which was confirmed that the image was acquired during winnowing (by Lelystad, or Geopotes 14 or 15, and provided time-registration in MARS files was in UTC.)

Table 3.6 Confirmed mining activities during image acquisition

Nr	Image	Lelystad	G15	G14
1	IVM_MER_RR__2CNACR_20070501T103111_prod_tsm_area_2_300.jpg			
2	IVM_MER_RR__2CNACR_20070504T104410_prod_tsm_area_2_300.jpg			
3	IVM_MER_RR__2CNACR_20070515T095242_prod_tsm_area_2_300.jpg			
4	IVM_MER_RR__2CNACR_20070530T102044_prod_tsm_area_2_300.jpg			
5	IVM_MER_RR__2CNACR_20070805T101548_prod_tsm_area_2_300.jpg		X	
6	IVM_MER_RR__2CNACR_20070811T102712_prod_tsm_area_2_300.jpg			
7	IVM_MER_RR__2CNACR_20070817T103804_prod_tsm_area_2_300.jpg			
8	IVM_MER_RR__2CNACR_20070821T101242_prod_tsm_area_2_300.jpg		X	
9	IVM_MER_RR__2CNACR_20070824T101723_prod_tsm_area_2_300.jpg		X	
10	IVM_MER_RR__2CNACR_20070915T102641_prod_tsm_area_2_300.jpg	X		
11	IVM_MER_RR__2CNACR_20070916T095523_prod_tsm_area_2_300.jpg	X		
12	IVM_MER_RR__2CNACR_20071002T095239_prod_tsm_area_2_300.jpg	X		X
13	IVM_MER_RR__2CNACR_20071007T103529_prod_tsm_area_2_300.jpg		X	X
14	IVM_MER_RR__2CNACR_20071013T104743_prod_tsm_area_2_300.jpg			
15	IVM_MER_RR__2CNACR_20071014T101613_prod_tsm_area_2_300.jpg			
16	IVM_MER_RR__2CNACR_20071020T102824_prod_tsm_area_2_300.jpg			
17	IVM_MER_RR__2CNACR_20071023T103429_prod_tsm_area_2_300.jpg			
18	IVM_MER_RR__2CNACR_20071101T105241_prod_tsm_area_2_300.jpg			
19	IVM_MER_RR__2CNACR_20071115T101342_prod_tsm_area_2_300.jpg		X	X
20	IVM_MER_RR__2CNACR_20071118T101941_prod_tsm_area_2_300.jpg			
21	IVM_MER_RR__2CNACR_20071201T101153_prod_tsm_area_2_300.jpg	X	X	X
22	IVM_MER_RR__2CNACR_20071216T104112_prod_tsm_area_2_300.jpg			
23	IVM_MER_RR__2CNACR_20071229T103239_prod_tsm_area_2_300.jpg			
1	MER_FR__2PNEPA20070520_104107_000000982058_00180_27288_0587			
2	MER_FR__2PNEPA20070523_104648_000000982058_00223_27331_0593	X	X	
3	MER_FR__2PNEPA20070805_102115_000000982060_00280_28390_0589	X		
4	MER_FR__2PNEPA20070919_100658_000000982061_00423_29034_0586		X	X
5	MER_FR__2PNEPA20071007_104102_000000982062_00180_29292_0592			
6	MER_FR__2PNEPA20071014_102112_000000982062_00280_29392_0590			
7	MER_FR__2PNEPA20071020_103234_000000982062_00366_29478_0591			
8	MER_FR__2PNEPA20071023_103815_000000982062_00409_29521_0585			

Interpretation of plots of corresponding remote sensing datasets

Figures 3.18 to 3.41 (MERIS-RR) and Figures 3.42 to 3.45 (MERIS-FR) show examples of SPM quicklooks. As expected, no elevated concentrations compared to surroundings were found for images acquired close to date when control measurements (T0 conditions at 22-24 May) were made for the Huisduinen sand extraction locations.

Although Table 3.6 shows that active sand mining occurred on 5 August, no plume was visible, neither on the MERIS-RR nor on detailed FR quicklooks. On 2 Oct. a small turquoise patch is visible near the mining locations and a larger one to the North, but this part of the image is also influenced by nearby clouds. On 7 Oct. no elevated concentrations show on the RR data, but (with the improved resolution and colour scaling) minor increase could be visible in the FR data. On 20 Oct. no activities were logged (Table 3.6), but there is still a patchy signal close to the mining locations. 23 Oct. gives a clear image without elevated surface concentrations near the mining locations. This also seems the case for the Nov. and Dec. images.

Time series: T0 and T1 at Huisduinen

Figure 3.47 shows that derived SPM concentrations often vary similarly for the nearby locations Q2J and Q2L. However, they also frequently deviate, but this occurs both before mining commenced and during mining.

Figure 3.48 shows that SPM is occasionally high in 2007 (from medio September - medio October, and in December for 2QL); note that 2004 (when no mining occurred) shows even more high autumn and winter values.

Figure 3.49 was made to allow control-impact checks along transects. It shows similar Control (C10) and Impact (I0 and I10) signals for both Sept.-Oct. as Nov.-Dec. Note that Imp 0 crosses Q2L at about 3 km and Q2J at about 6 km on the X-axes. Relatively high values occur in Nov.-Dec.

Figure 3.50 serves as a C I reference: situation in May.-Jun. before mining.

Potentially detected plumes

Figures 3.51 to 3.70 shows some examples of results from Eleveld's outlier detection algorithm (Grasmeijer and Eleveld., 2009) for in individual control (May) and impact (Aug-Dec) images.

Provided exceptions for 11 and 24 Aug., and possibly on 2 and 7 Oct. (in the N), this confirmed that here was no plume visible at the mining locations in individual control (May) images, nor in the impact (Aug-Dec) images.

This does not invalidate the outlier detection algorithm though. Again (cf. Figs. 3.6-3.9) Grasmeijer and Eleveld., 2009) outliers, possibly related to dredge dumping near Loswal could be visible (cf. 4 May, 4, 21 & 24 Aug, 15 Nov). High concentrations are also frequently visible near the mining sites but closer to shore, particularly over the ebb tidal delta of the Marsdiep tidal inlet/outlet. These concentrations can be associated with outflowing Wadden Sea water, normally with higher SPM concentrations than in the North Sea (Alkyon, 2010).

For all these potential plumes all water quality parameters were plotted. Four potential plumes resulted: 11 Aug. (plume near mining), 2 & 7 Oct. (plume north of mining), and 15 Nov. (plume near Loswal). For the rest the areas of interest were flagged as 'bad input' (PCD_1_13).

Figures 3.71 to 3.74 show plots of all water quality parameters and products, which were not masked by confidence flags. The plume of 11 Aug. (near mining) might be somewhat influenced by CHL (living phytoplankton). CDOM is high as well. On 2 and 7 Oct. a possible SPM plume to the south of the mining location was detected. CHL is less important. Again a possible SPM plume was detected near Loswal on15 Nov. CHL is less important.

Discussion

If an extra source is introduced a new distribution with (relatively) more high values (and less low values) can be expected. The mapped perturbation detection algorithm acknowledges this and takes background concentrations (for all locations) and overall conditions (simplified by the chosen monthly timescale) into account.

To visualize the approach for a direct (local) effect, the concentrations were extracted from the regridded data at the mining locations (Q2J and Q2L) for the whole mining period (Aug-Dec 2007) and the reference climatology (Aug-Dec 2003 … 2006). The results were plotted as histograms (Fig. 3.75).

Taking the whole sand mining period (Aug-Dec 2007) into account results in more samples. Note also, that with this local approach no attention is paid to advection (local versus a map) and less attention is paid to seasonality (Aug-Dec instead of per month) than present in earlier presented mapped results. Finally, note that the results are influenced (flawed) by the difference in number of samples between 2007 and 2003 .. 2006. The latter concern is also valid for the mapped perturbation detection algorithm results.

This exercise shows real distributions, with many values in the first bin (perhaps a hidden trait in the output from the algorithm), and a few (occasional) outliers (for both impact and control) that might considerably influence the P95.

The new distribution with more high values (from an extra source, as mentioned before) isn't immediately obvious in Figure 3.75, but tests for this are recommended. Pending the outcomes, additional visual inspection is still needed.

Likely causes for the new distribution with more high values (from an extra source) not being immediately apparent could be, that: the source is relatively small, the impact of the source on the surface is small, the impact of the source on the surface consists of pulses and settling speed is higher than sampling frequency so only few events are captured.

Conclusions from remote sensing tests for T1 conditions

- The H0 hypothesis, that extra SPM from sand extraction cannot be seen on the SPM concentrations derived from remote sensing data, can be rejected.

- The H0 hypothesis that the SPM concentrations at the sand extraction (impact) site do not cause near-surface outliers may be true. Nonetheless, outliers in SPM concentrations near a dredge dump and sand mining locations were found.

- The H0 hypothesis to be tested is that the SPM concentrations at the sand extraction (impact) site are not significantly higher than at the control locations. This hypothesis may be true for the tested sampling locations.

4 Results from 3D model simulations

4.1 Introduction

Alkyon (2010) describe the set-up and the results from a 3D model to simulate the suspended sediment concentrations of a silt fraction and a sand fraction in part of the Wadden Sea and part of the North Sea and to simulate the effects of overflow from dredging activities on these concentrations offshore Den Helder on three different days in 2007. The 3D model includes effects of a temporally and spatially varying wind field, waves and salinity.

Alkyon (2010) schematized the sediment release rate from overflow by adopting two different scenarios. In scenario 1 a release rate from the dynamic overflow plume of 130 kg/s and from the passive flume of 20 kg/s was adopted. In scenario 2 the release rates were a factor 2 higher, i.e. 260 kg/s from the dynamic plume and 40 kg/s from the passive plume.

The release rate from the dynamic plume in the first scenario (130 kg/s) is based on observed concentrations and flow velocities in the dredger's suction pipes and the observed tons of dry weight in the dredger. The amount of sediment in the overflow is the difference between the amount of material that went through the suction pipes and the tons of dry weight that remains in the dredger. The release rate from the passive plume in the first scenario (20 kg/s) is based on the upper limit of values reported by Van Maren et al. (2008).

The release rates in the second scenario were made a factor 2 higher than those in scenario 1. Simulations with scenario 2 were made to illustrate the sensitivity of the model results for other release rates. We should note here that the release rates adopted in scenario 2 are relatively high as compared to release rates observed during dredging in the North Sea (see Van Maren et al., 2008).

The dynamic overflow plume settles relatively quickly to the bed and was therefore schematized as being released in the lowest computational layer. The passive plume was released over the entire water column.

Alkyon (2010) adopted the Van Rijn (2007) sediment transport module in Delft3D and used a single sediment grain size of 30 μm for silt (mean of values presented by Talmon, 2008) and 200 μm for sand. The resulting sediment fall velocity varies with salinity and concentration for silt but amounts to about 0.07 cm/s for silt and to 2.3 cm/s for sand. Smaller grain sizes and thus fall velocities will result in higher concentrations. To give an impression, based on rough estimates with a 1-DV sediment transport model we found an increase of the background near-surface concentrations of about 25% with a sediment fall velocity of 0.05 cm/s for silt instead of 0.07 cm/s (increase from 8 mg/l to 10 mg/l).

Alkyon (2010) generated an equilibrium bed composition (distribution of sediment fractions in the bed) by restarting the model 10 times, each time using the bed composition resulting from the previous run as an input for the next. The resulting percentage of silt ranged between about 0.5% on the North Sea to more than 50% on the shoals in the Wadden Sea.

We refer to Alkyon (2010) for a discussion on other parameter settings and their effects. Default values we used for most model parameters.

Alkyon (2010) used a dredging period of 1 hour with a return period of 3.4 hours. Dredging took place during the entire simulation period.

In this report we illustrate the effect of dredging on the suspended sediment concentrations by subtracting results from 2 simulations as follows:

$$c_{effect} = c_{with\ dredging} - c_{without\ dredging}$$

We will show the spatial variation of c_{effect} near the water surface.

4.2 Results (effect of dredging)

17 September 2007 10:09 h -13:59 h

Figures 4.1 to 4.12 present the simulated effect of overflow from a dredger on the suspended sediment concentrations for 12 different time steps in a tidal cycle on 17 September 2007. The upper panels show the effect for dredging scenario 1, the lower panels for dredging scenario 2.

It can be seen from these figures that a relatively small sediment plume occurs near the dredging location (2 km south of the measurement area) during the flooding phase of the tide (Figure 4.1). Maximum added near-surface concentrations are 0.5-1.0 mg/l for scenario 1 and 1-2 mg/l for scenario 2.

The plume is advected northward during the flooding phase and maximum concentrations increase to 2-4 mg/l at high tide for scenario 1 and about 9 mg/l for scenario 2 (Figures 4.2-4.4). A second plume from a previous dredging activity shows up at about 10 km north of the measurement area in these plots. This is 20 km north of the dredging location. Maximum concentrations in this old plume amount to 0.5 mg/l both for scenario 1 and 2.

The second plume is likely caused by previous dredging activities and northward advection of the associated overflow plume during a tidal cycle on 16 September or earlier and resuspension of the overflow sediments during the flooding phase on 17 September. The second plume disappears from the plots just after high tide.

The original plume is advected back southward during the ebbing phase (Figures 4.5-4.12). Maximum near-surface concentrations amount to about 1-2 mg/l for the first scenario and 2-4 mg/l for the second. Concentrations decrease gradually to 0.5-1.0 mg/l at low tide for the first scenario and 1-2 mg/l for the second.

1 October 2007 09:36 h – 15:53 h

Figures 4.13 to 4.24 show the simulated effect of overflow on the suspended sediment concentrations for different time steps in a tidal cycle on 1 October 2007. On this day, the effect of dredging is more pronounced than on 17 September. The area affected is larger and the added concentrations are higher.

On 1 October 2007 during the flooding phase of the tide a small plume is visible at the most southward measurement location (Figure 4.13). Maximum near-surface concentrations amount to 0.5-1.0 mg/l for the first dredging scenario and 2-4 mg/l for the second but the area of influence is relatively small (about 1 km).

A larger area affected by overflow from dredging shows up in the plots just before high tide (Figures 4.14-4.15). This is likely due to previous dredging activities from which the plume has been advected north and south of the dredging location. The sediments from these plumes that have settled to the bed are resuspended by the flood velocities on 1 October 2007 around 07:30 h and 08:30 h (presented by Alkyon, 2010). Added near-surface concentrations generally amount to 0.5-1.0 mg/l for both dredging scenarios. Maxima of 1-2 mg/l occur locally.

It is interesting the see a difference between scenario 1 and 2. The added near-surface concentrations tend to show up more south of the measurement area for the first scenario and mainly north for the second scenario. This is likely related to the behaviour of the fall velocity formulations in the Van Rijn (2007) model. Increasing the concentrations e.g. by overflow increases the fall velocity in the model. This causes the sediments to settle to the bed more rapidly than without the extra concentration.

Added near-surface concentrations decrease during the ebbing phase of the tide (Figure 4.16-4.24).

The affected area stretches from about 20 km south of the dredging area to 40 km north on 1 October 2007. This is much larger than on 17 September.

2 October 2007 05:57 h – 17:08 h

Figures 4.25 to 4.36 show the simulated effect of overflow on the suspended sediment concentrations on 2 October 2007.

Maximum added near-surface concentrations due to overflow amount to about 0.5-1 mg/l during the flooding phase for the first scenario and 1-2 mg/l for the second scenario (Figures 4.25-4.30). It is interesting to see that the effect on 2 October is smaller than that on 1 October, which is likely due to the smaller wave heights in the area (Alkyon, 2010).

Added near-surface concentrations decrease just after high tide (Figures 4.31-4.33) and increase slightly during the ebbing phase to maximum values of 1-2 mg/l just before low tide for both scenarios (Figures 4.34-4.36). The affected area stretches from about 10 km south of the dredging location to about 40 km north.

Effect of dredging on mean concentrations (2 week period)

Figure 4.37 shows the simulated effect of dredging on the mean SPM concentrations for a period of more than 2 weeks (15.5 days: 17 September 06:00 h to 2 October 18:00 h). As for all simulations shown before, the dredging period was 1 hour with a return period of 3.4 hours. Dredging took place during the entire simulation period.

We have changed the colour scale to half the values used for the MWTL data to make the effect of dredging better visible.

Figure 4.37 shows that for dredging scenario 1, the extra mean (averaged over 15.5 days) near-surface concentrations (more than background) amounts to 0.5-1 mg/l over an area of about 6 km^2.

The extra mean near-surface concentrations amounts to 0.5-2 mg/l over an area of about 75 km^2 for scenario 2. The area over which the extra mean concentration is 1-2 mg/l for scenario 2 is about 9 km^2.

The effect of dredging is temporary (disappears a few days after dredging has stopped) and is a factor 2-8 smaller than the observed mean (1975-1983) background concentration (see for example Figure 2.47) and also a factor 2-8 smaller than the standard deviation of the observed natural background concentration (see for example Figure 2.55).

We should note here that the dredging activity studied here takes place in an area where the mean SPM concentration is relatively low (see e.g. Figure 2.2) and also the variation in SPM concentration is relatively low (see e.g. Figure 2.8).

This means that we may generalize the conclusion that the effect of overflow by dredging on the SPM concentrations in the North Sea is not only much smaller than the natural mean but also much smaller than the natural variation around the mean.

5 Conclusions

The conclusions of this study are summarized as follows:

- Generally, no significant (within the 95% confidence bandwidth) trends are observed in the suspended matter concentrations between 1975 and 2008. For nearly all analyzed stations (80%), the concentrations are neither significantly increasing nor significantly decreasing.
- Based on t-tests, we found the difference between the mean values for 1975-1983 and those for 1985-2008 not to be significant at the 5% significance level for most stations. This accounts also for the trimmed mean and the geometric mean.
- Two stations show a statistically significant decreasing trend, i.e. Terschelling 4 and Noordwijk 2 and two show a statistically significant increasing trend, i.e. Goeree 10 and 20.

- The statistical insignificance of trends or difference in means between two periods may have two causes. The first is that the SPM concentrations behave similarly throughout the measurement periods. The second is that the number of samples is insufficient to determine a significant change. We tested the latter by making a power analysis on the data from Noordwijk 10.
- For the Noordwijk 10 observations, the number of samples should have been 1940 to be able to differentiate between a mean of 5.46 mg/l and 5.77 mg/l (either increasing or decreasing). This would require a sampling interval of 1 day (365 samples per year) for a period of 6 years (rounded off) or a sampling interval of 1 week (52 samples per year) for a period of 38 years (rounded off). The real number of samples in the period 1984-2008 was 782.
- To be able to measure a statistically significant increase or decrease in the mean of 1 mg/l at Noordwijk 10 since the period 1975-1983 requires 190 samples. This would require a sampling interval of 1 week (52 samples per year) for a period of 4 years (rounded off) or a sampling interval of 2 weeks (26 samples per year) for a period of 8 years (rounded off).
- Increasing the number of samples by smartly combining data from different stations or synthetic data generation (e.g. with a neural network) may also improve the power of the statistical tests.

- As the present data suggest that trends for most stations are not significantly increasing or decreasing, comparisons are justified between recent observations and interpolated maps based on 1975-1983 MWTL data.
- Mean suspended matter concentration contours show values between 30 and 300 mg/l in the nearshore regions. This reduces to 3-5 mg/l further offshore.
- Trimmed mean values (excluding outliers) are on average about 5% smaller than the mean values.
- Geometric mean values are on average 32 % smaller than the mean values.
- The median (50^{th} percentile) values are 68% smaller to 6% larger than the mean values (on average 28% smaller).
- The standard deviation of the suspended matter concentrations along the Dutch coast is of the same order as the mean.
- The suspended matter concentrations are on average 83% higher in winter than in summer.

- Power spectral density estimates of the suspended matter concentration observed at 6 different stations showed a clear peak at a frequency corresponding to a periodicity of 1 year. This agrees with the seasonal variation in wave conditions with higher waves each year in winter and smaller waves in summer.
- The Terschelling 4 km offshore station and the Walcheren 2 km offshore station suggest a small spectral peak around 8 years (Terschelling) or 4 years (Walcheren) that just peaks above the 95% confidence band of surrounding frequencies. However, the measurement period and temporal resolution of the data is insufficient to draw firm conclusions on the significance of this peak. Other power spectral density functions do not show clear peaks at these frequencies, or a clear increase of the power spectral density for periods longer than 4 years.
- No other important peaks were found in the spectrum
- Time series of the moving average with a two-year window of the concentration observed at 6 stations showed intermittent high-concentration events. It is difficult to recognize a distinct periodicity.

Secondly, we present an analysis of the CEFAS Minipod and Smartbuoy measurements at 2 and 5 km off the coast of Noordwijk aan Zee. We compare observed concentrations with predictions using a process-based 1DV model and using a neural network. Conclusions are summarized as follows:

- Suspended matter concentrations at 2 and 5 km off the coast of Noordwijk aan Zee could rather accurately (R^2>0.8) be simulated using a neural network with 9 neurons, using wave height, wave period and water depth time series as an input and near-bed suspended matter concentration as a target.
- The suspended matter concentration at aforementioned stations could be predicted with reasonable accuracy using the Van Rijn (2005) tidal mud transport model. These results were less accurate then those of the neural network.

Thirdly, we present an analysis of the silt profiler T0 measurement campaign made in 22-24 May 2007 off the coast of Vlieland, Texel and Noord-Holland. We compare concentrations measured during this campaign with MWTL observations. The conclusion is as follows:

- The suspended matter concentrations measured during the T0 campaign in May 2007 off the coast of Vlieland, Texel and Noord-Holland are much smaller (factor 2 to 5) than MWTL mean and MWTL summer-mean concentrations..

Fourthly, we present an analysis of remote sensing MERIS-RR data for 2003-2006 as processed in the Ovatie project. We discuss SPM distributions, outliers possibly due to sand extraction and dredge disposal. We report on time series for a location near Huisduinen and Callantsoog.

- Time series of SPM concentrations extracted at the middle points of the sand extraction areas near Huisduinen (Q2J and Q2L) from 2003-2006 showed mean T0 concentrations of 2.7 and 2.3 mg/l respectively.

Conclusions from remote sensing tests for T1 conditions

- The H0 hypothesis, that extra SPM from sand extraction cannot be seen on the SPM concentrations derived from remote sensing data, can be rejected.

- The H0 hypothesis that the SPM concentrations at the sand extraction (impact) site do not cause near-surface outliers may be true. Nonetheless, outliers in SPM concentrations near a dredge dump and sand extraction location were found.

- The H0 hypothesis to be tested is that the SPM concentrations at the sand extraction (impact) site are not significantly higher than at the control locations. This hypothesis may be true for the tested sampling locations.

Conclusions from simulations with a 3D numerical model (effect of dredging of SPM concentrations).

- The extra mean (averaged over 15.5 days) near-surface concentrations (more than background) amounts to 0.5-1 mg/l over an area of about 6 km^2 for a realistic scenario.

- The extra mean (averaged over 15.5 days) near-surface concentrations (more than background) amounts to 0.5-2 mg/l over an area of about 75 km^2 for an "extensive dredging" scenario 2. The area over which the extra mean concentration is 1-2 mg/l for scenario 2 is about 9 km^2.

- The effect of dredging is temporary (disappears a few days after dredging has stopped) and is a factor 2-8 smaller than the observed mean background concentration also a factor 2-8 smaller than the standard deviation of the observed natural background concentration.

- The dredging activity studied here takes place in an area where the mean SPM concentration is relatively low and also the variation in SPM concentration is relatively low.

- This means that we may generalize the conclusion that the effect of overflow by dredging on the SPM concentrations in the North Sea is not only much smaller than the natural mean but also much smaller than the natural variation around the mean.

Causes for relatively small effect of dredging on the SPM concentrations in the North Sea are likely the relatively small fractions of fine material in the seabed and the fact that the sediment from the overflow settles relatively quickly to the bed as a density current (van Maren et al, 2008).

The investigations presented in this report reveal the suspended matter concentrations in the North Sea to be strongly variable in space and particularly in time. The variation in wave conditions produces part of this variability in SPM concentrations. The high cross-correlations between wave height and SPM concentration found in the CEFAS dataset illustrate this dependency. However, more factors play a role. We have summarized the most important aspects in an incomplete list below.

- Waves stirring up material from the sea bed
- Currents stirring up material from the bed and transporting it from other source terms
- Shipping (merchant shipping, dredging, fishery etc)
- Rivers discharge

- Oil or gas platforms
- Wind farms
- Land reclamation
- Cables and pipelines

It is difficult to asses the relative effect of the above mentioned aspects on the SPM concentrations and to discern between the different effects. For example, fishing vessels such as outrigger trawlers are likely to stir up material from the bed. However, the degree to which this affects the mean and variation of the SPM concentrations in the North Sea has never been investigated. What is more, both vessel types and fishing gears have changed over time (Rijnsdorp et al, 2008). Also sand extraction activities have increased significantly since the 1990's (ICES, 2001). In addition, shipping traffic is growing and the number of offshore wind farms increases. This makes assessing the effect on the SPM concentrations at different moments in time to a challenge.

Most important step in handling this challenge is improving our present partial understanding of the physics and the natural behaviour of suspended particle matter in the North Sea. In this respect, making observations with a high temporal and spatial resolution are essential, illustrated by the results presented here. In addition, both statistical and physical modelling is required to interpolate and extrapolate this and to asses the effects of human interference relative to the natural behaviour of the system.

Based on this we recommend expanding the present MWTL program by increasing the number of stations and the temporal resolution most preferably back to or close to the situation in 1975-1984.

Secondly, we recommend making observations of the SPM values not only in the upper part of the water column but also at mid depth and close to the sea bed.

Finally, we recommend processing remote sensing data on a 300 m grid and making these available as monitoring data.

References

CEFAS, 2003. RIKZ/CEFAS Minipod deployments at Noordwijk 2 and 5. Final Report, May 2003. CEFAS, Lowesoft, Suffolk, United Kingdom.

De Kok, J.M. 2004. Slibtransport langs de Nederlandse kust: bronnen, fluxen en concentraties. Report RIKZ/OS/2004.148w

Eleveld, M.A., 2008. Eleveld, M.A., Pasterkamp, R. & van der Woerd, H.J., & Pietrzak, J.D. (2008). Remotely sensed seasonality in the spatial distribution of sea-surface suspended particulate matter in the southern North Sea. Est. Coast. Shelf Sci. 80(1), 103-113.

Ellerbroek, G., Rozemeijer, M.J.C., De Kok, J.M. , De Ronde, J., 2008. Evaluatieprogramma MER winning suppletiezand Noordzee 2008-2012. Rijkswaterstaat Noord-Holland. 16-jul-2008. 26 pagina's.

Gordon, H.R., W. R. McCluney (1975) Estimation of the depth of sunlight penetration in the sea for remote sensing. Applied Optics, 14, 413-416.

Grasmeijer, B.T., Eleveld, M.A., 2009. Evaluation of SPM measurements in the North Sea. Research in the framework of the EIA sand extraction North Sea 2008-2012. Report I (T0). Alkyon & VU-IVM, Emmeloord, A2273, 32 pp. + Figs. + Appendix

Hitchcock, D.H., Bell, S., 2004. Physical impacts of marine aggregate dredging on seabed resources in coastal deposits. Journal of Coastal Research 20(1): 101-114.

ICES (2001). Report of the Working Group on the Effects of Extraction of Marine Sediments on the Ecosystem (ICES CM 2001/E:06), Scotland.

Kraaijeveld, M., Fioole, A., 2005. Vertroebeling tijdens en na baggeren met sleephopperzuiger in het Noordzeekanaal. RIZA rapport 2005.006 (jan. 2005).

Laane, R.W.P.M., Sonneveldt, H.L.A., Van der Weyden, H.J., Loch, J.P.G. and Groeneveld, G. 1999. Trends in the spatial and temporal distribution of metals (Cd, Cu, Zn and Pb) and organic compounds (PCBs and PAHs) in Dutch coastal zone sediments from 1981 to 1996: a model case study for Cd and PCBs. J. Sea Res. 41:1-17

Lagarias, J.C., Reeds, J.A., Wright, M.H., and Wright, P.E., 1998. Convergence properties of the Nelder-Mead simplex method in low dimensions. SIAM Journal of Optimization, 9(1): 112-147.

Nelder, J.A. and Mead, R., 1965. A simplex method for function minimization, Computer Journal 7 (1965), 308{313.

Pasterkamp, R., Eleveld, M., Van der Woerd, H. & Van Drunen, M., 2003. Noordzee-atlas voor zwevend stof op basis van satellietbeelden in 2001. RWS AGI Report AGI-GAR-2003-38, Delft, 44 pp., in press.

Pasterkamp, R., Van Drunen, M., Eleveld, M & Gilbert, A., 2002. Atlas of suspended sediment transport for the North Sea: Based on satellite imagery of 2000. RWS RIKZ Report RIKZ/IT/2002.102. Den Haag, 34 pp.,

Peters, SW.M.., van der Woerd, H.J., Eleveld, M.A., in prep. Ovatie-2 Final report. IVM report.

Rast, M.,. Bezy, J.L., S. Bruzzi S., 1999. The ESA Medium Resolution Imaging Spectrometer MERIS – a review of the instrument and its mission. Int. j. remote sensing 20 (9), 1681-1702.

Rijnsdorp, A.D. et al., 2008. Journal of Sea Research 60 (2008) 126–138.

Suijlen, J.M., Duin, R.N.M., 2002. Atlas of near-surface total suspended matter concentrations in the Dutch coastal zone of the North Sea. Rijkswaterstaat Rijksinstituut voor Kust en Zee (RIKZ). Rapport RIKZ/2002.059. 10-dec-2002. 46 pagina's.

Talmon, A.M., 2007. Meetrapport SiltProfilermetingen 22-24 mei 2007 voor de Noord-Hollandse kust. WL|Delft Hydraulics (Deltares), Rapport Z4426, december 2007, 221 pagina's (inclusief bijlagen).

Talmon, A.M., 2008a. Meetrapport SiltProfilermetingen 17 september, 1 en 2 oktober 2007 voor de Noord-Hollandse kust. Deltares rapport Z4481 (juni 2008).
Talmon, A.M., 2008b. Meetrapport suspensiemetingen Ms. Zirfea bij zandwinning 17, 18 en 19 september voor de Noord-Hollandse kust. Deltares rapport Z4521 (sept.008)
Van Duin, C.F., Gotjé, W. Jaspers, C.J., Kreft, M., 2007. MER winning suppletiezand Noordzee 2008 t/m 2012. Grontmij, Rapport 13/99080995/CD, 1-nov-2007. 242 pagina's.
Van Prooijen, B., Bliek, B., Los, H., Desmit, X., 2007. Winning ophoogzand Noordzee 2008-2017. Slibtransport, nutriëntentransport en primaire productie. Rapport Svasek voor Stichting La Mer (nov 2007)
Van Rijn, L.C., 2005. Principles of sedimentation and erosion engineering in rivers estuaries and coastal seas. Aqua Publications, The Netherlands
Welch, P.D, 1967. The Use of Fast Fourier Transform for the Estimation of Power Spectra: A Method Based on Time Averaging Over Short, Modified Periodograms,IEEE Trans. Audio Electroacoustics, Vol. AU-15 (June 1967), pp.70-73.

Appendix A

Quality insurance of RS products

Original data are reflectances measured with an imaging spectrometer mounted on a satellite (Rast et al, 1999). To derive water quality parameters (SPM, CHL and CDOM), the Hydropt algorithm (Pasterkamp et al., 2005; Van der Woerd & Pasterkamp, 2008) was used to compare these reflectance data with simulated reflectances from a radiative transfer model. The modelled spectrum had been calculated by ***parameterising*** a forward model with an sIOP model, absoption and scattering properties for realistic REVAMP IOPs (Tilstone et al., in prep). The result is a lookup table (LUT) with reflectances (modelled spectra) for every possible combination of a, b, and solar and sensor view angles (SZA, VNA, phi). As a ***calibration*** step the images are processed (using the inverse model) with an optimised SIOP set, using yearly average of 2006 concentrations at MWTL stations, because this gives more weight to Dutch IOPs and it compensates for errors in SIOPs and in atmospheric correction. The settings during processing were that ESA's quality flag (PCD_1_13) had initially been ignored, but remote sensing reflectances <=0 and > 0.3 were not processed. Bands 1 to 7 and 9 were used. The results have been validated with time series plots of CHL and SPM concentrations for in situ and remote sensing data (Peters et al., in prep.).

A chronological inventory of additional quality insurance reported in grey literature:
- Pasterkamp et al., 2002-2005. ESA MAVT papers.
- Dury et al., 2004. AGI report 0406GAR001. (External)
- Peters et al,. 2005. REVAMP atlas.
- Pasterkamp et al., 2005. Rem. Sens. Mar. Coast. Env. Conf. paper
- Duin et al., 2006. Conference papers. (External)
- Dury and Zeeberg, 2007. AGI report AGI-2007-GPMP-017 (Team effort)
- Uhlich et al., 2008. Quo data report. (External)

Figures

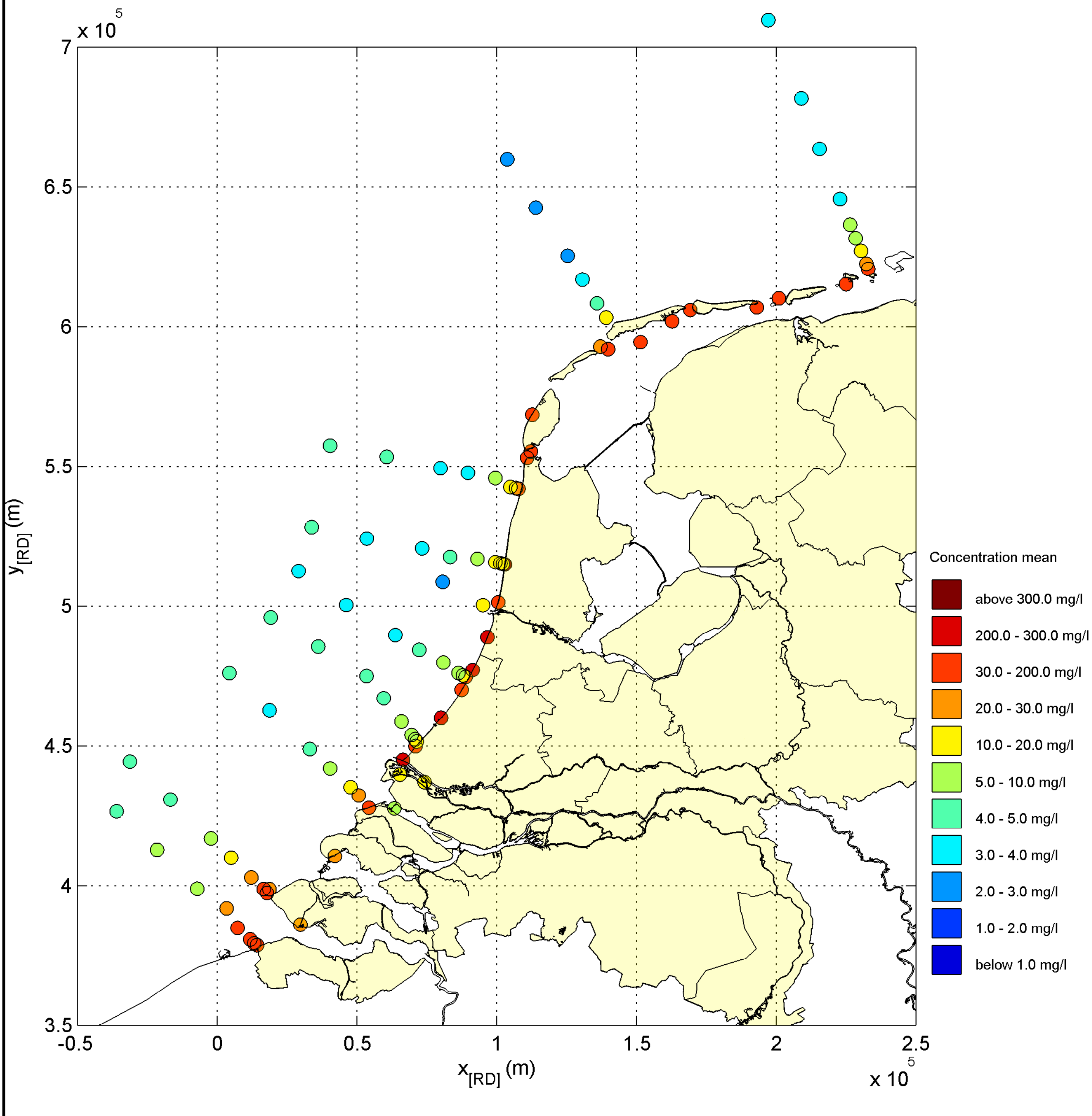

Mean of total suspended solids concentration (mg/l) for 96 stations along the Dutch coast based on waterbase data between 1975 and 1983	Waterbase 1975-1983	
Alkyon Hydraulic Consultancy & Research	A2273	Fig.2.1

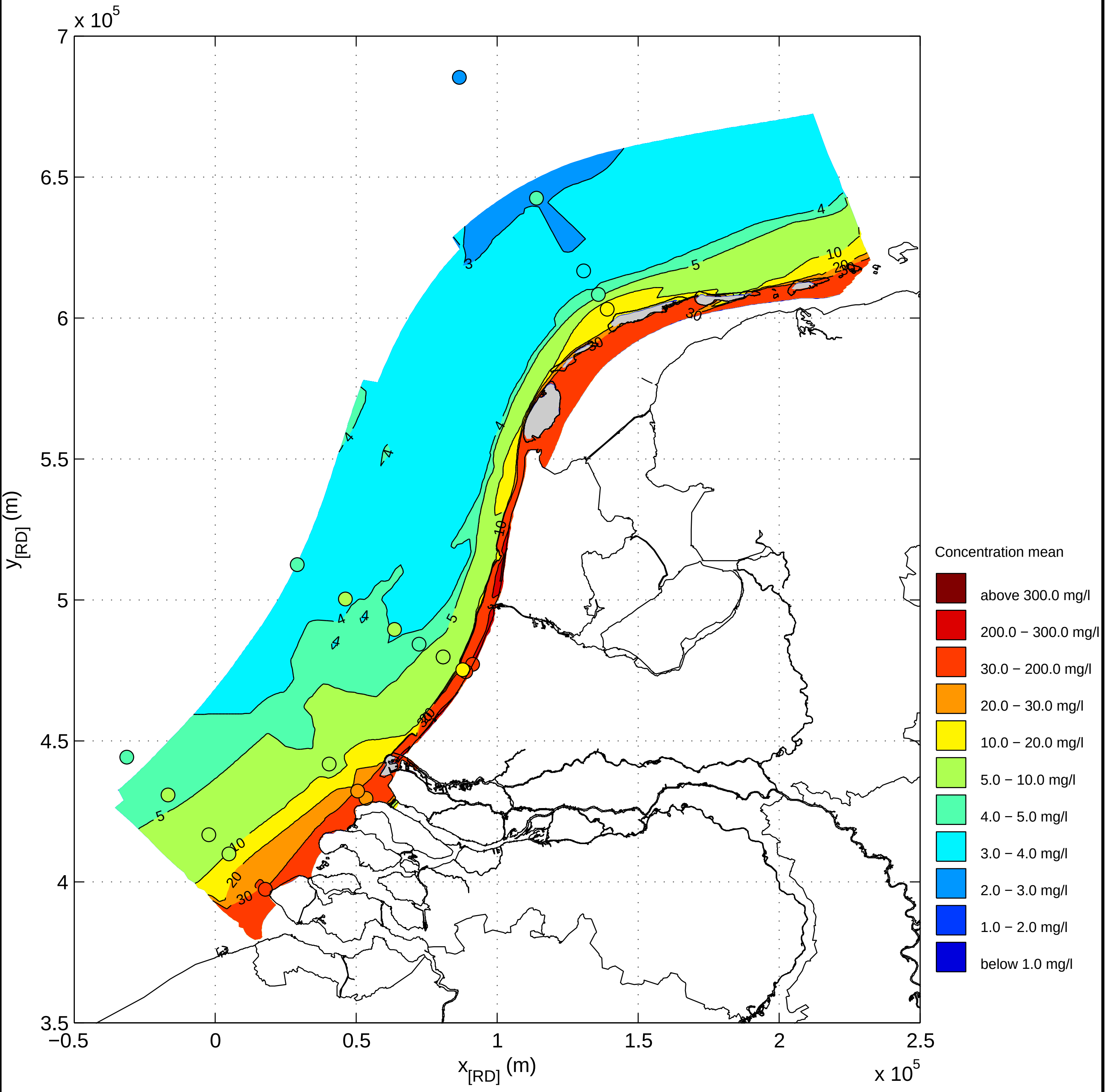

Mean of total suspended solids concentration (mg/l) filled contours present the interpolated 1975−1983 waterbase data coloured symbols present the 1984−2008 waterbase data	1975−1983 and 1984−2008	
Alkyon Hydraulic Consultancy & Research	A2273	Fig.2.2

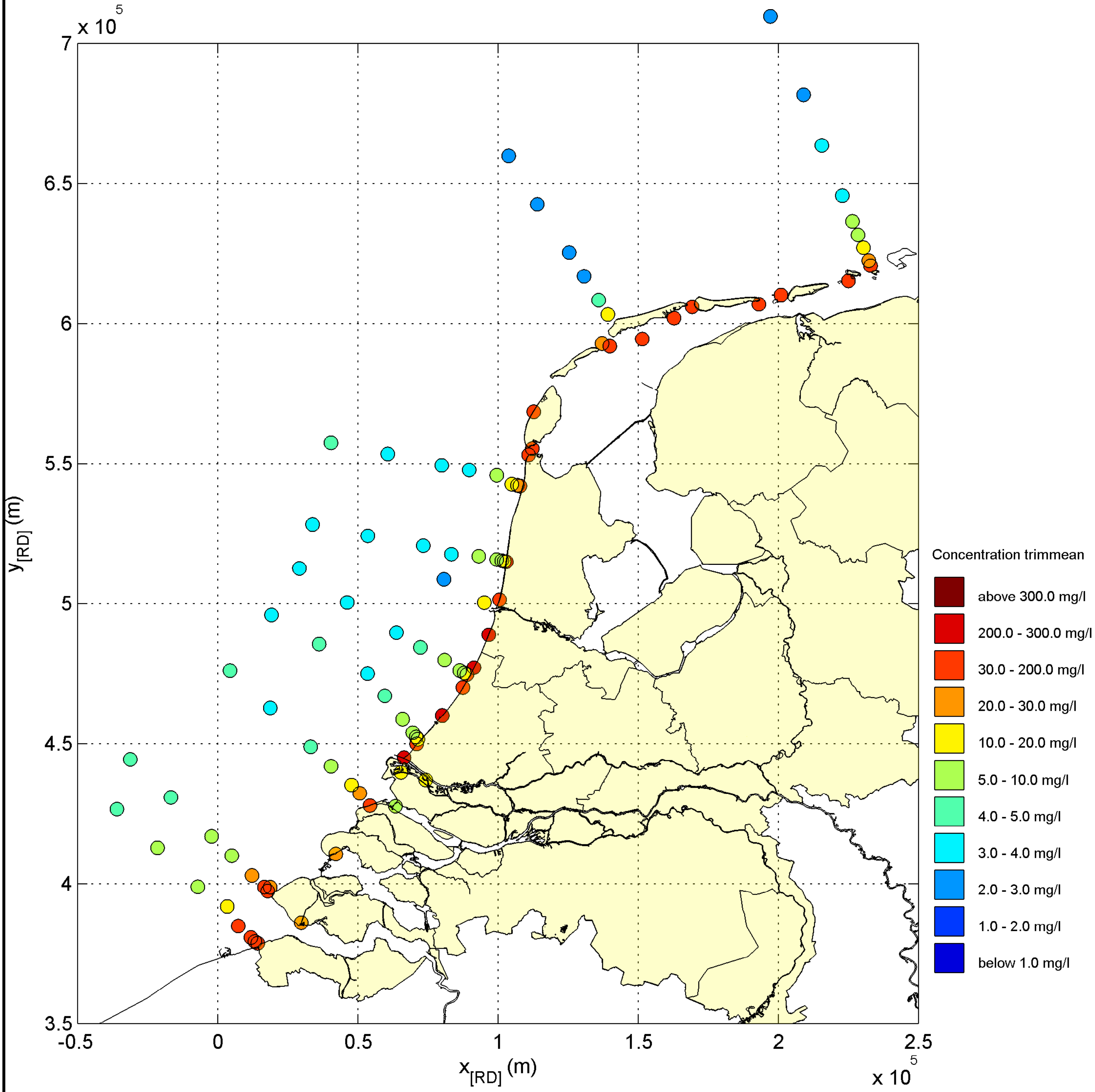

Trimmed mean of total suspended solids concentration (mg/l) for 96 stations along the Dutch coast based on waterbase data between 1975 and 1983	Waterbase 1975-1983	
Alkyon Hydraulic Consultancy & Research	A2273	Fig.2.3

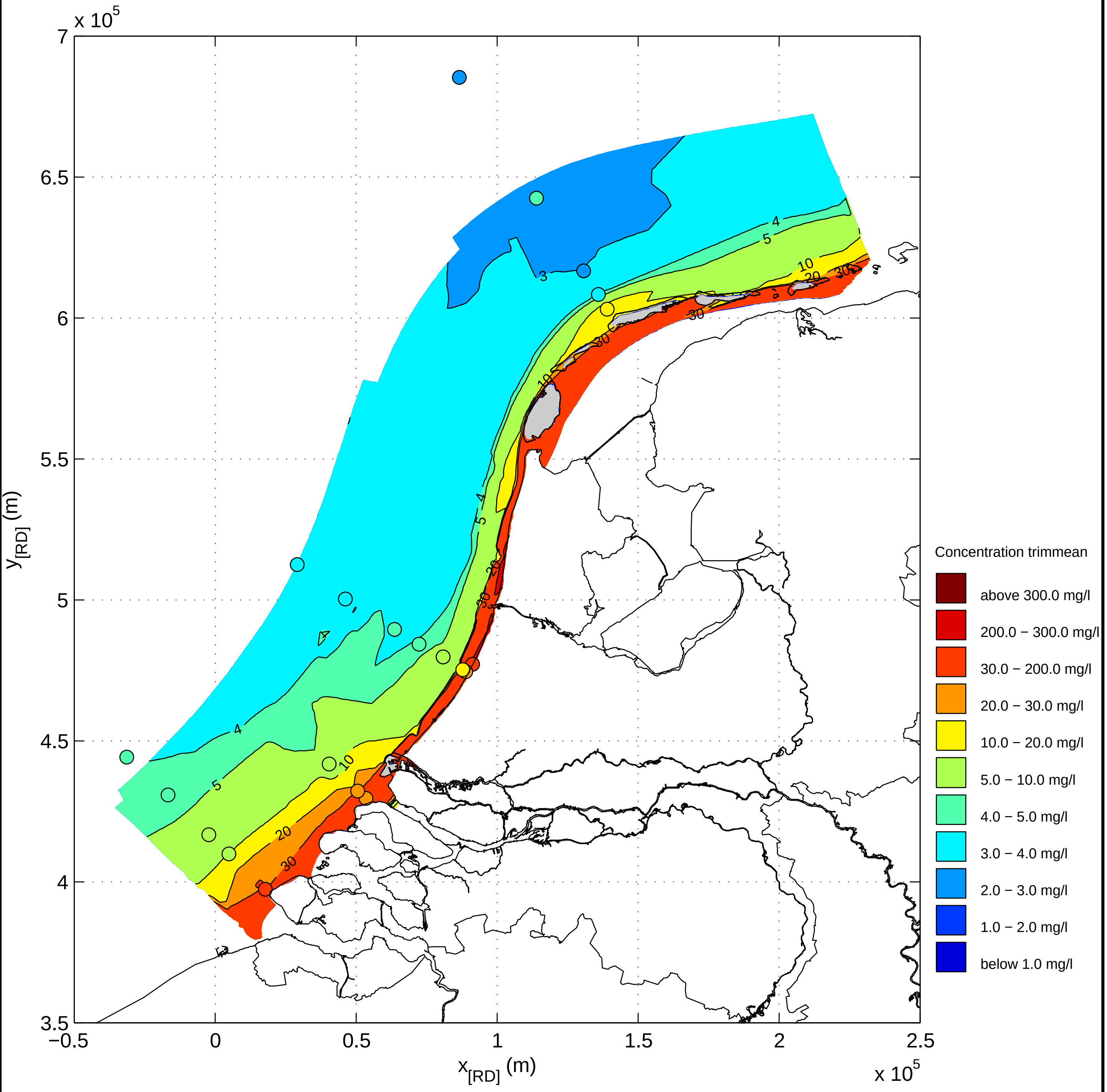

Trimmed mean of total suspended solids concentration (mg/l) filled contours present the interpolated 1975−1983 waterbase data coloured symbols present the 1984−2008 waterbase data	1975−1983 and 1984−2008	
Alkyon Hydraulic Consultancy & Research	A2273	Fig.2.4

A2273_MWTL_1975_1983_geomean

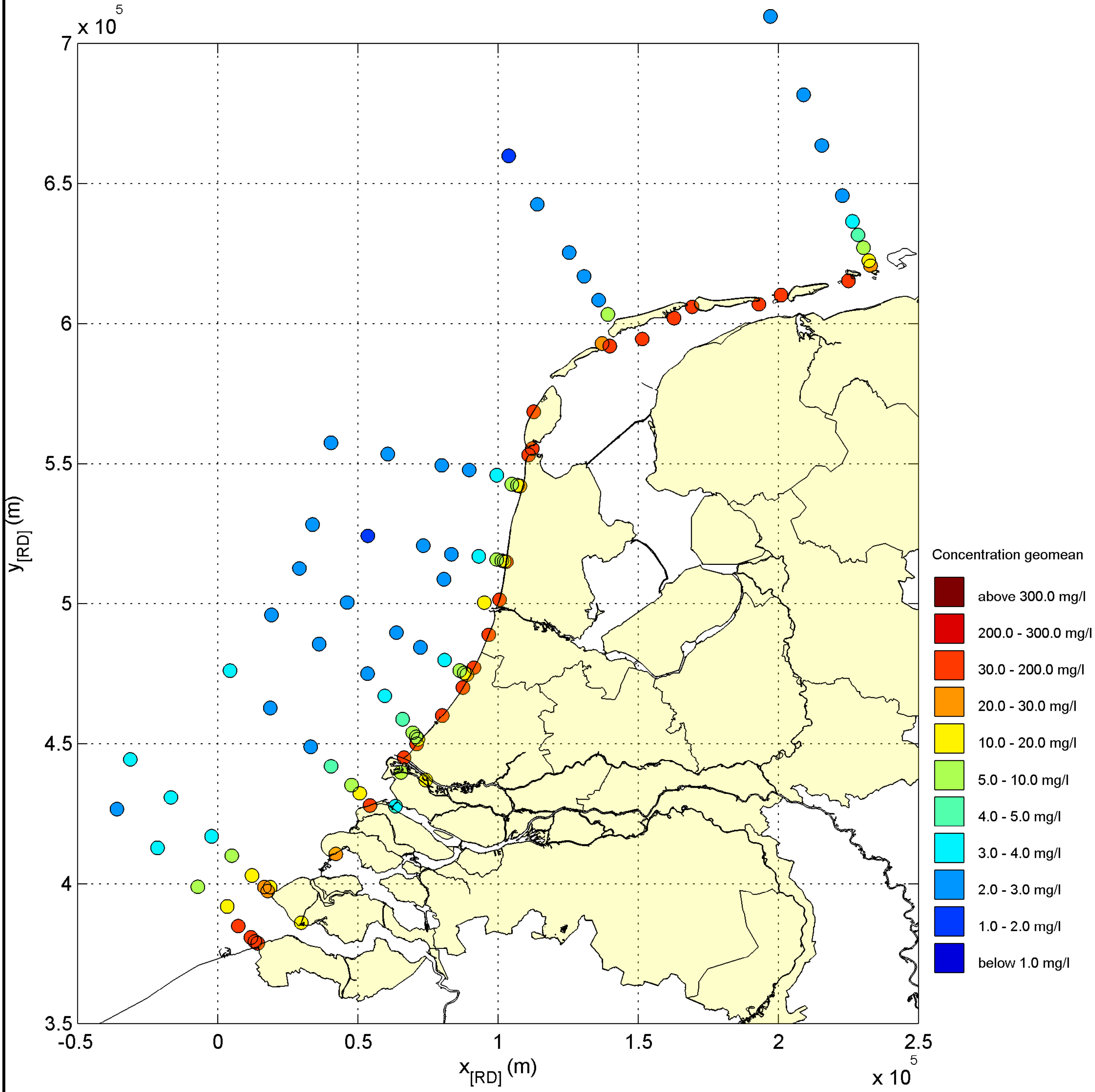

Geometric mean of total suspended solids concentration (mg/l) for 96 stations along the Dutch coast based on waterbase data between 1975 and 1983		
	Waterbase 1975-1983	
Alkyon Hydraulic Consultancy & Research	A2273	Fig.2.5

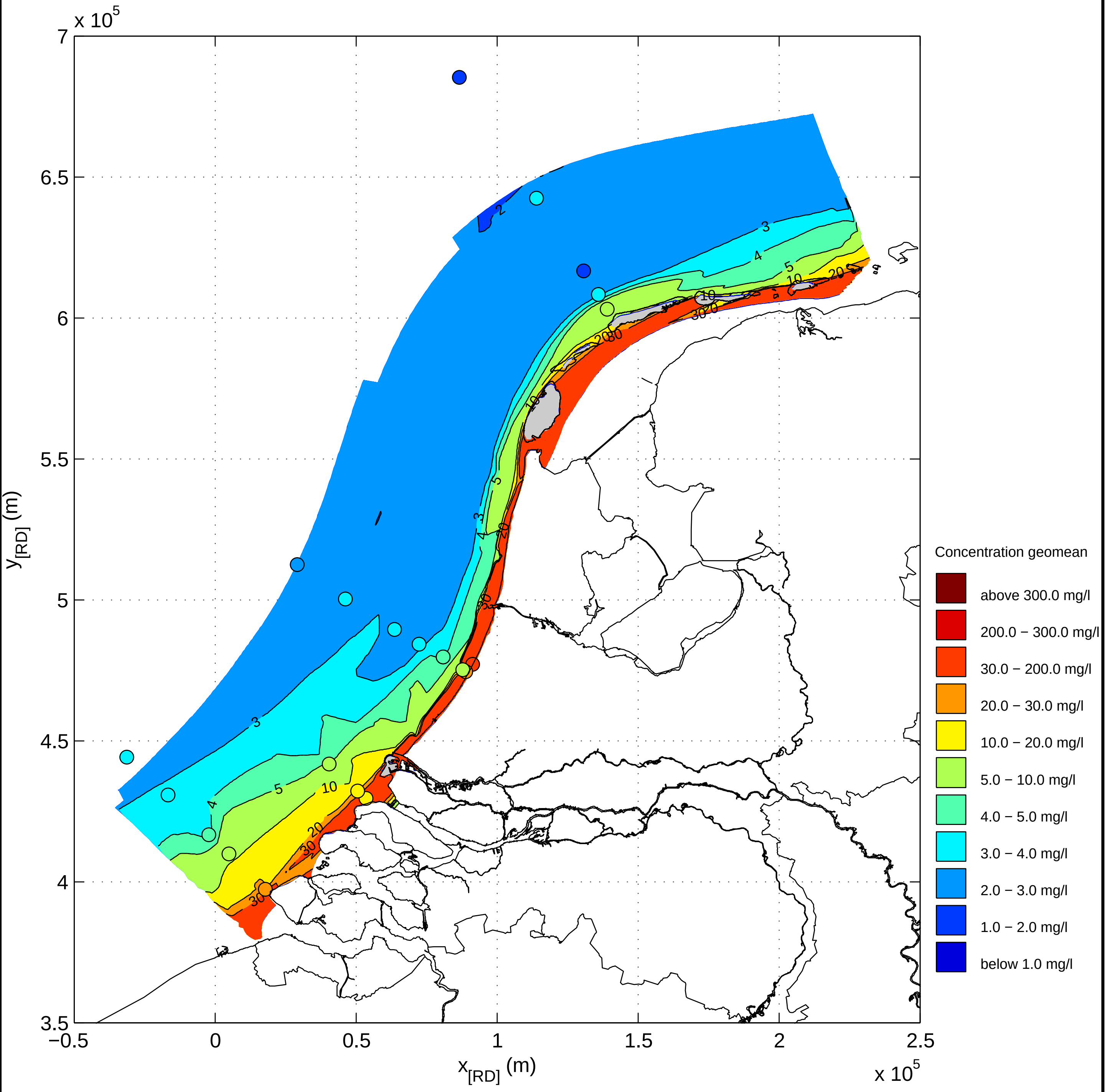

Geometric mean of total suspended solids concentration (mg/l) filled contours present the interpolated 1975−1983 waterbase data coloured symbols present the 1984−2008 waterbase data	1975−1983 and 1984−2008	
Alkyon Hydraulic Consultancy & Research	A2273	Fig.2.6

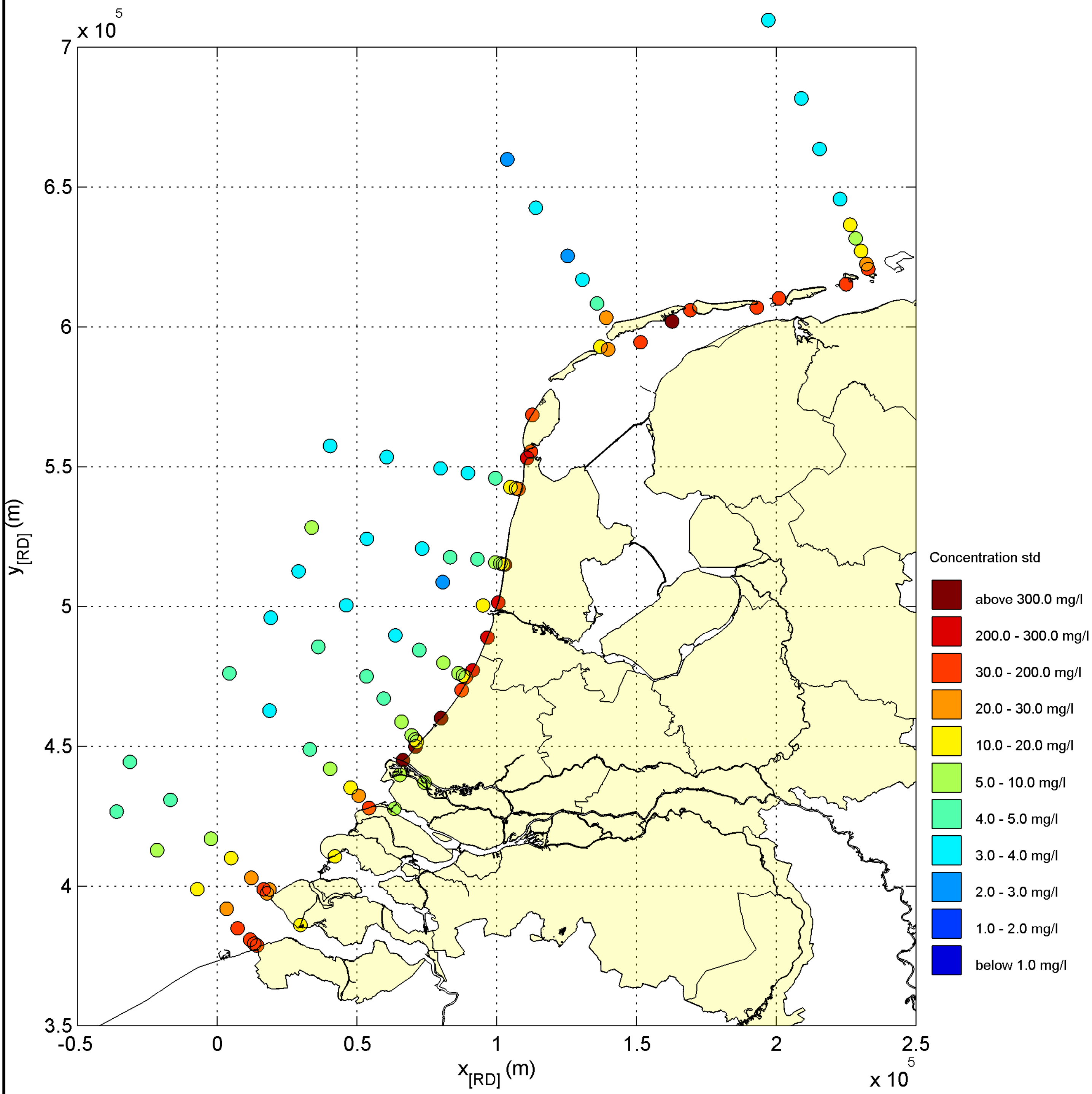

Standard deviation of total suspended solids concentration (mg/l) for 96 stations along the Dutch coast based on waterbase data between 1975 and 1983	Waterbase 1975-1983	
Alkyon Hydraulic Consultancy & Research	A2273	Fig.2.7

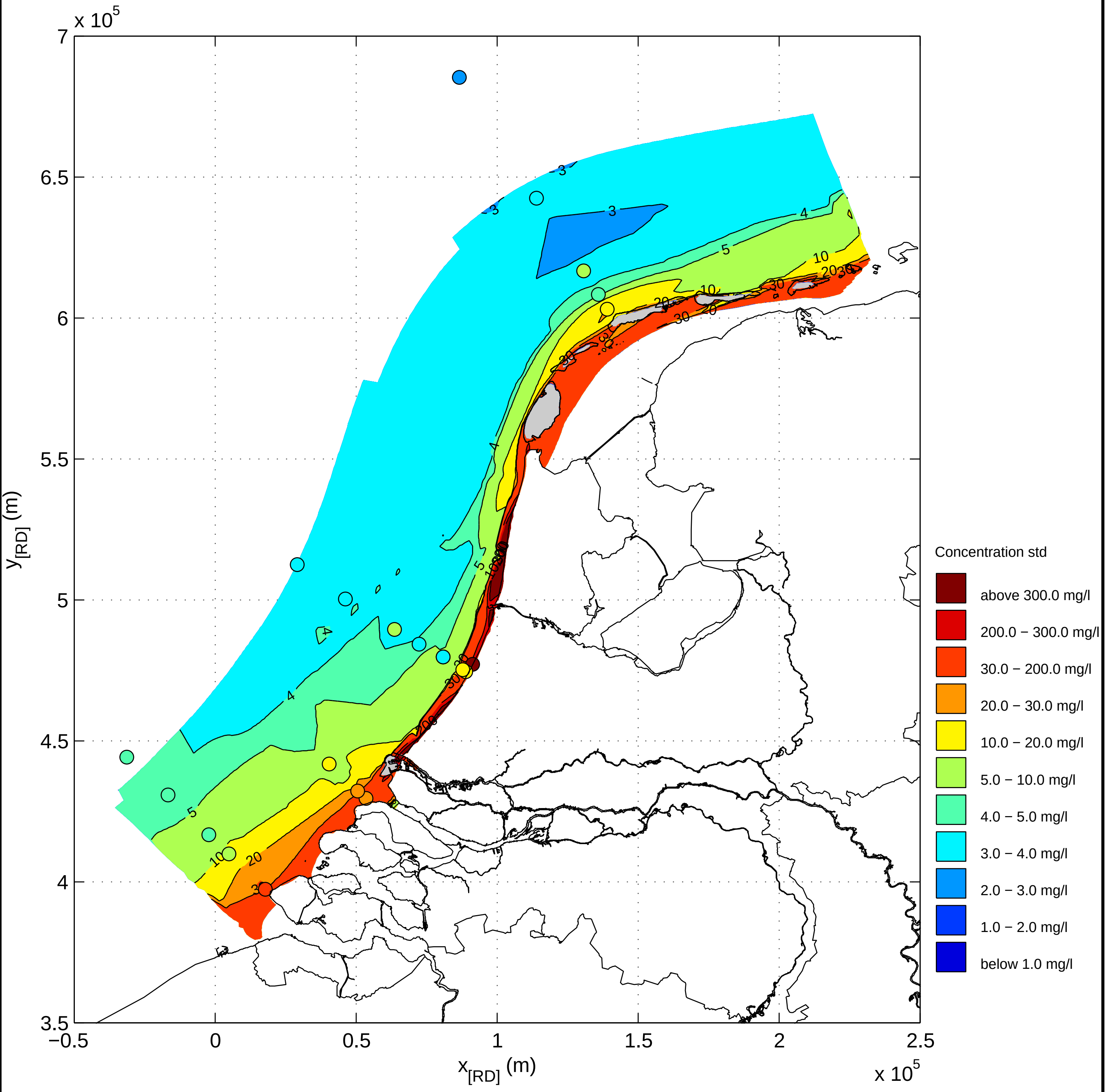

Standard deviation of total suspended solids concentration (mg/l) filled contours present the interpolated 1975−1983 waterbase data coloured symbols present the 1984−2008 waterbase data	1975−1983 and 1984−2008	
Alkyon Hydraulic Consultancy & Research	A2273	Fig.2.8

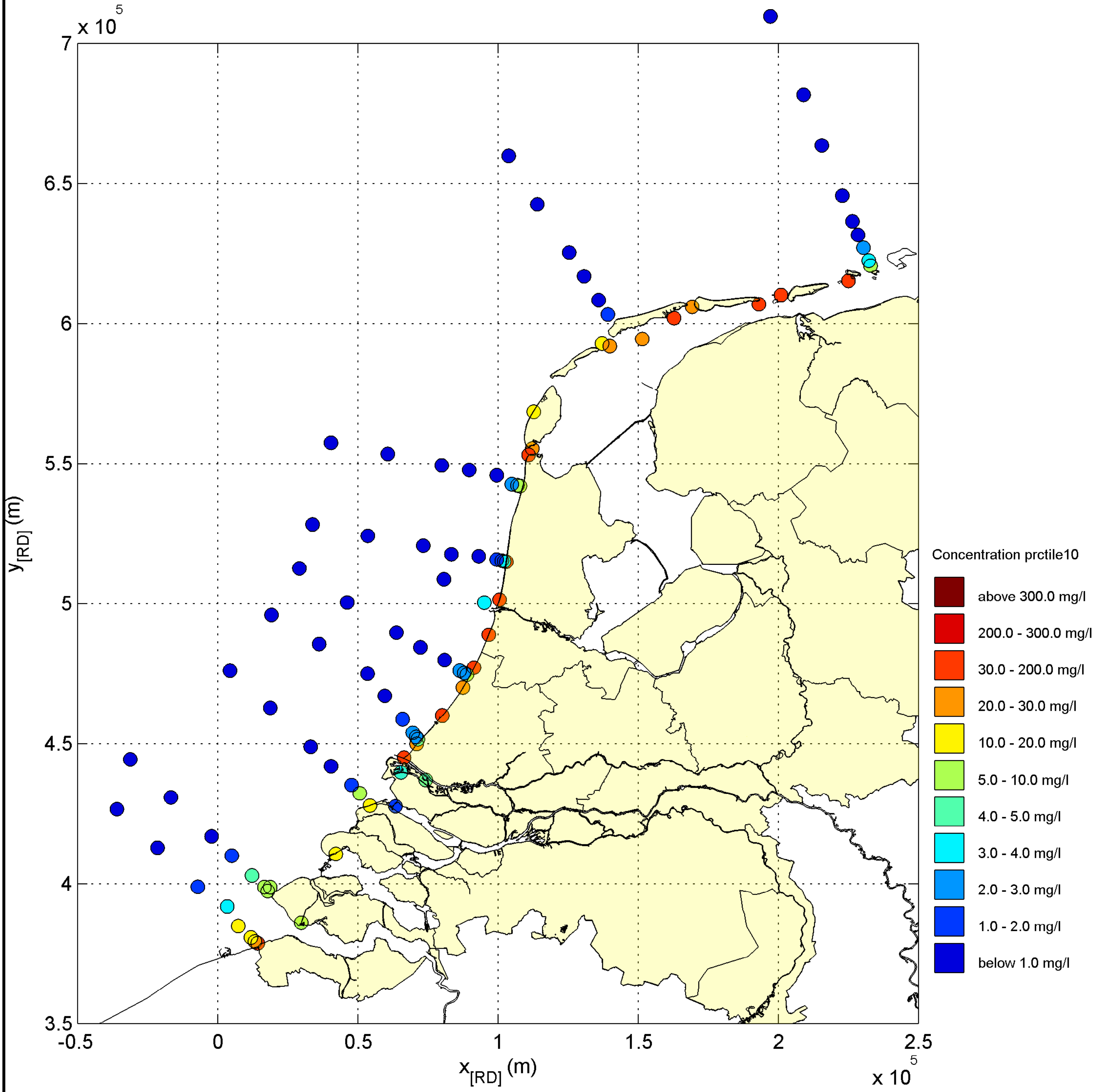

10th percentile of total suspended solids concentration (mg/l) for 96 stations along the Dutch coast based on waterbase data between 1975 and 1983	Waterbase 1975-1983	
Alkyon Hydraulic Consultancy & Research	A2273	Fig.2.9

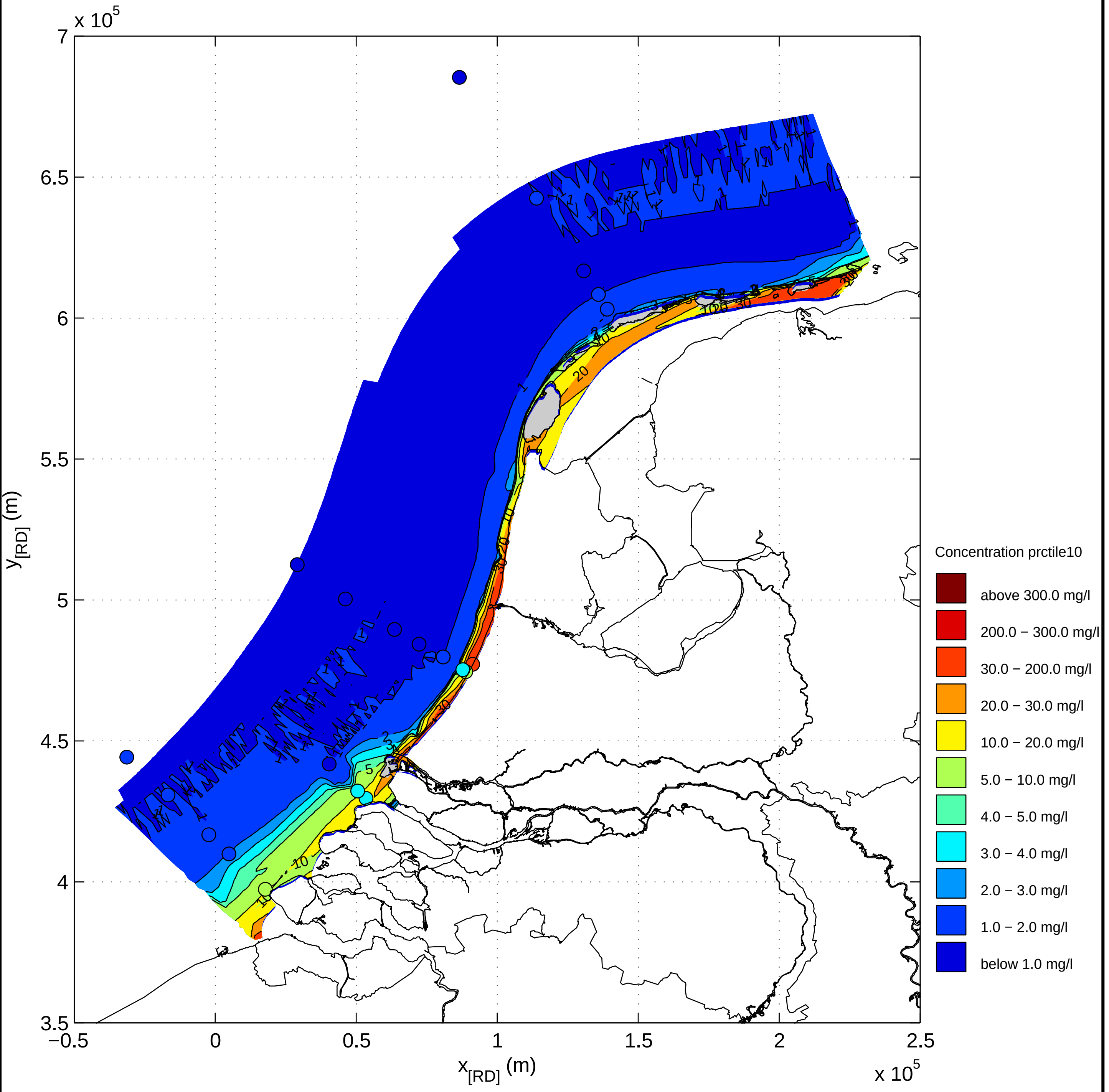

10th percentile of total suspended solids concentration (mg/l) filled contours present the interpolated 1975−1983 waterbase data coloured symbols present the 1984−2008 waterbase data	1975−1983 and 1984−2008	
Alkyon Hydraulic Consultancy & Research	A2273	Fig.2.10

A2273_MWTL_1975_1983_median

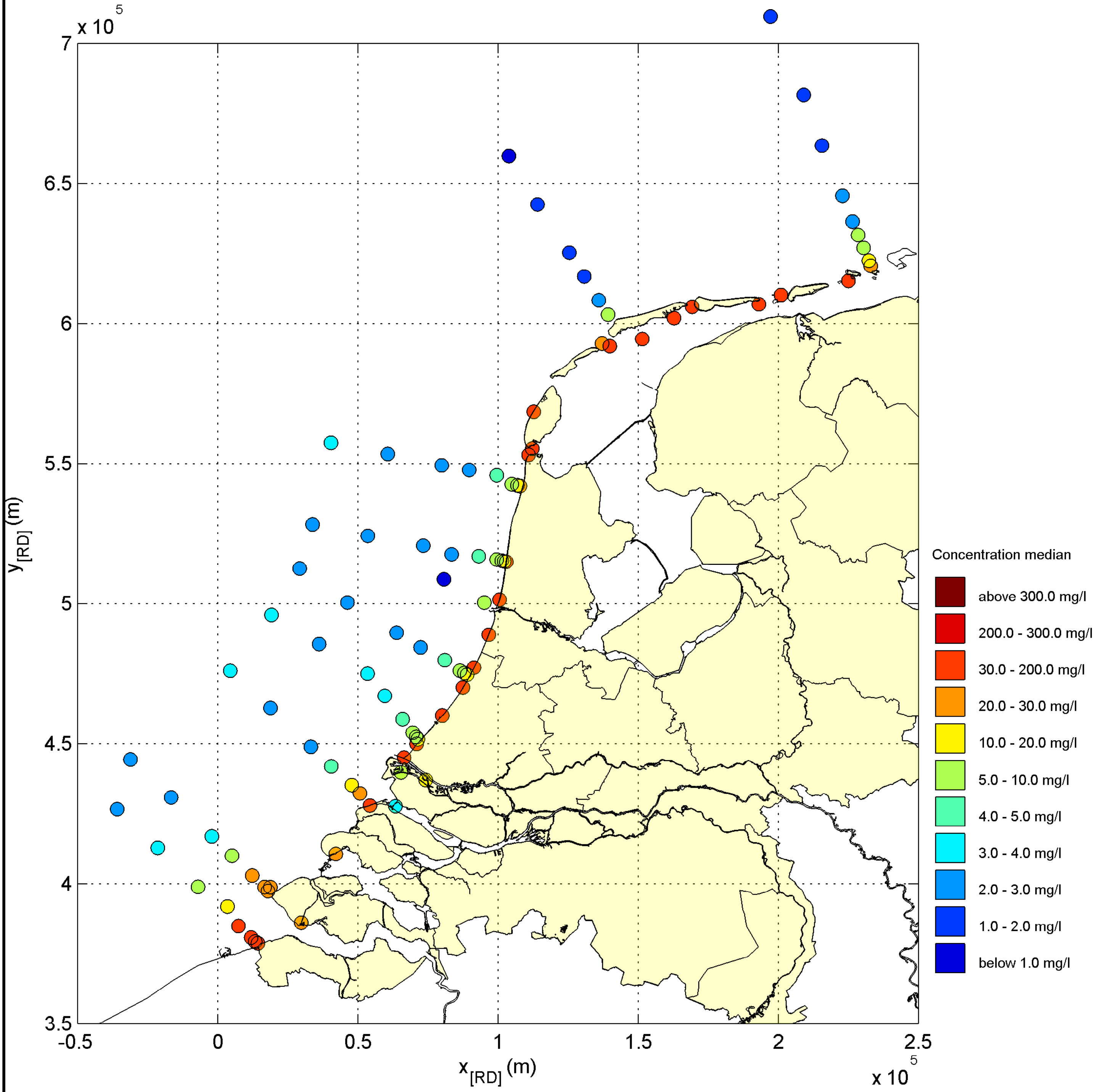

50th percentile (median) of total suspended solids concentration (mg/l) for 96 stations along the Dutch coast based on waterbase data between 1975 and 1983	Waterbase 1975-1983	
Alkyon Hydraulic Consultancy & Research	A2273	Fig.2.10a

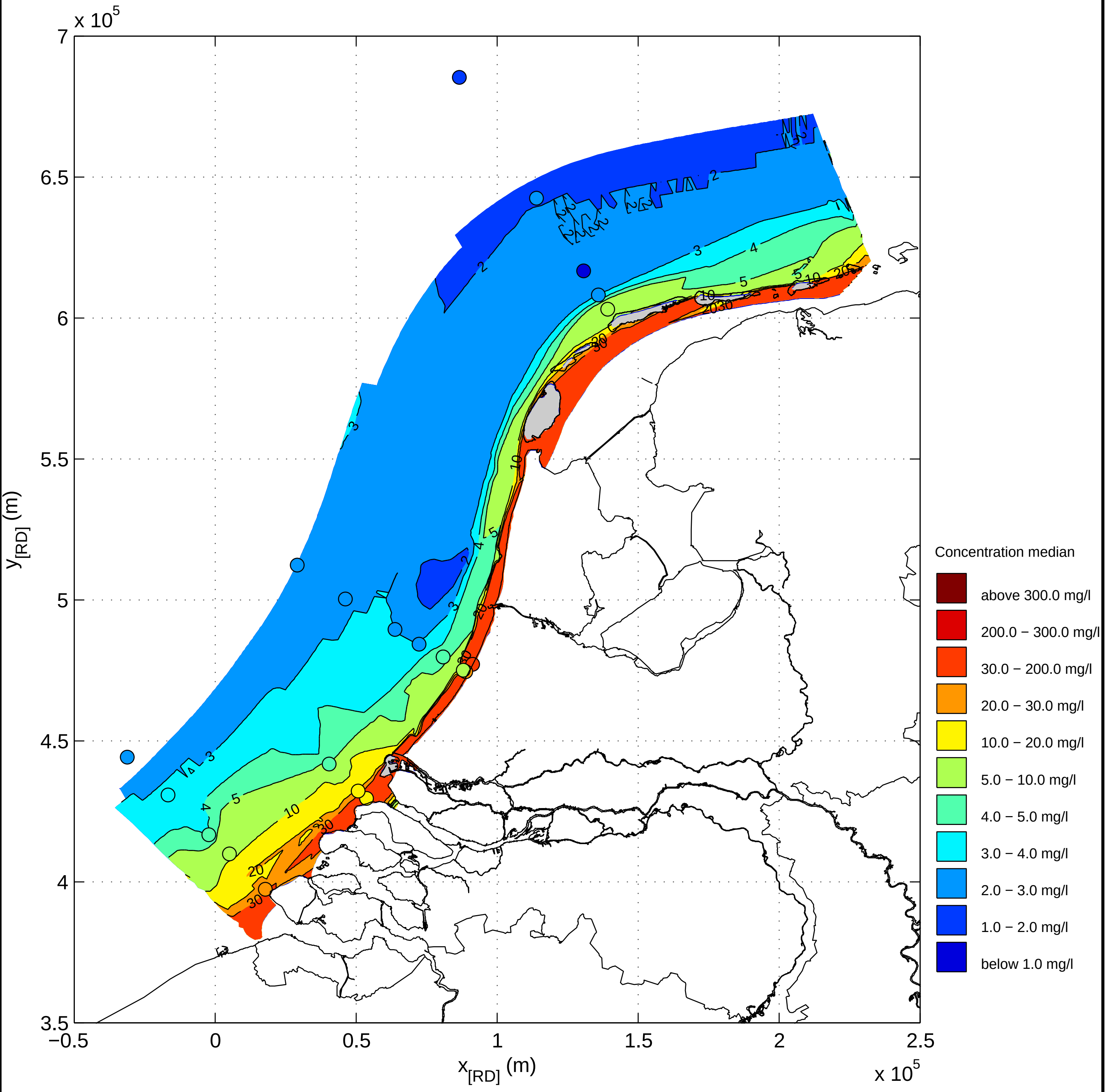

50th percentile (median) of total suspended solids concentration (mg/l) filled contours present the interpolated 1975−1983 waterbase data coloured symbols present the 1984−2008 waterbase data	1975−1983 and 1984−2008	
Alkyon Hydraulic Consultancy & Research	A2273	Fig.2.10b

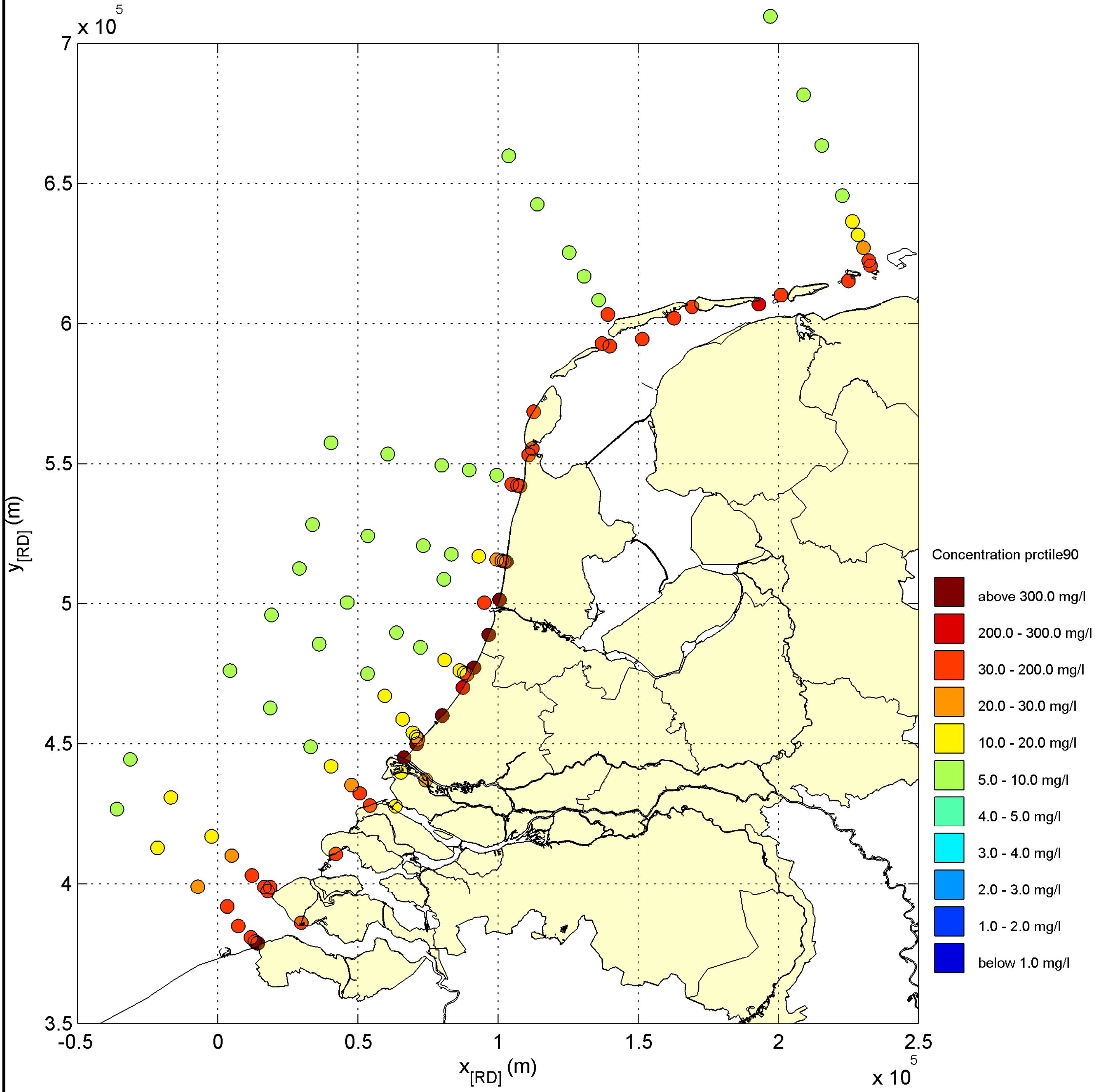

90th percentile of total suspended solids concentration (mg/l) for 96 stations along the Dutch coast based on waterbase data between 1975 and 1983	Waterbase 1975-1983	
Alkyon Hydraulic Consultancy & Research	A2273	Fig.2.11

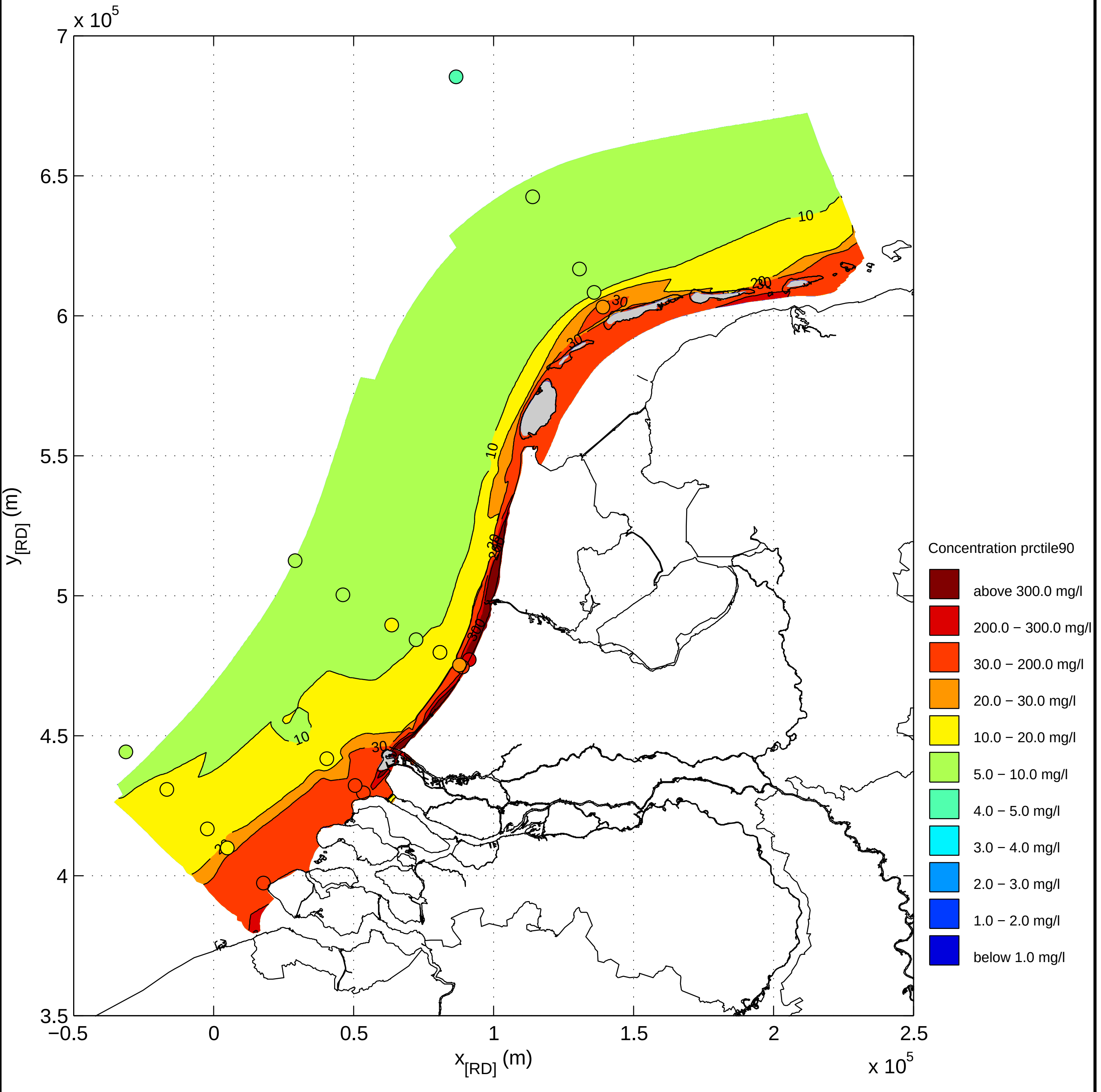

90th percentile of total suspended solids concentration (mg/l) filled contours present the interpolated 1975−1983 waterbase data coloured symbols present the 1984−2008 waterbase data	1975−1983 and 1984−2008	
Alkyon Hydraulic Consultancy & Research	A2273	Fig.2.12

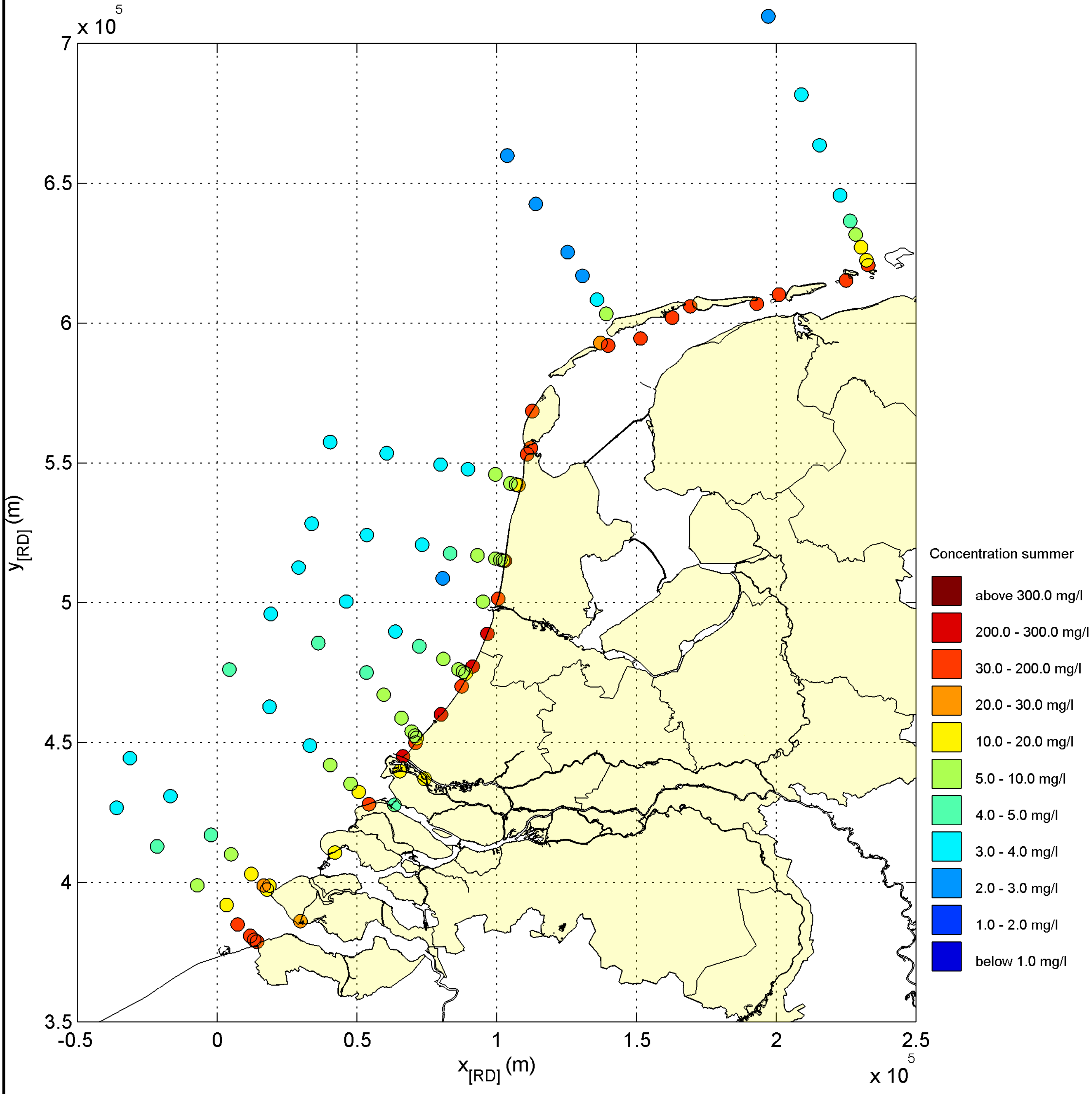

Summer mean of total suspended solids concentration (mg/l) for 96 stations along the Dutch coast based on waterbase data between 1975 and 1983	Waterbase 1975-1983	
Alkyon Hydraulic Consultancy & Research	A2273	Fig.2.13

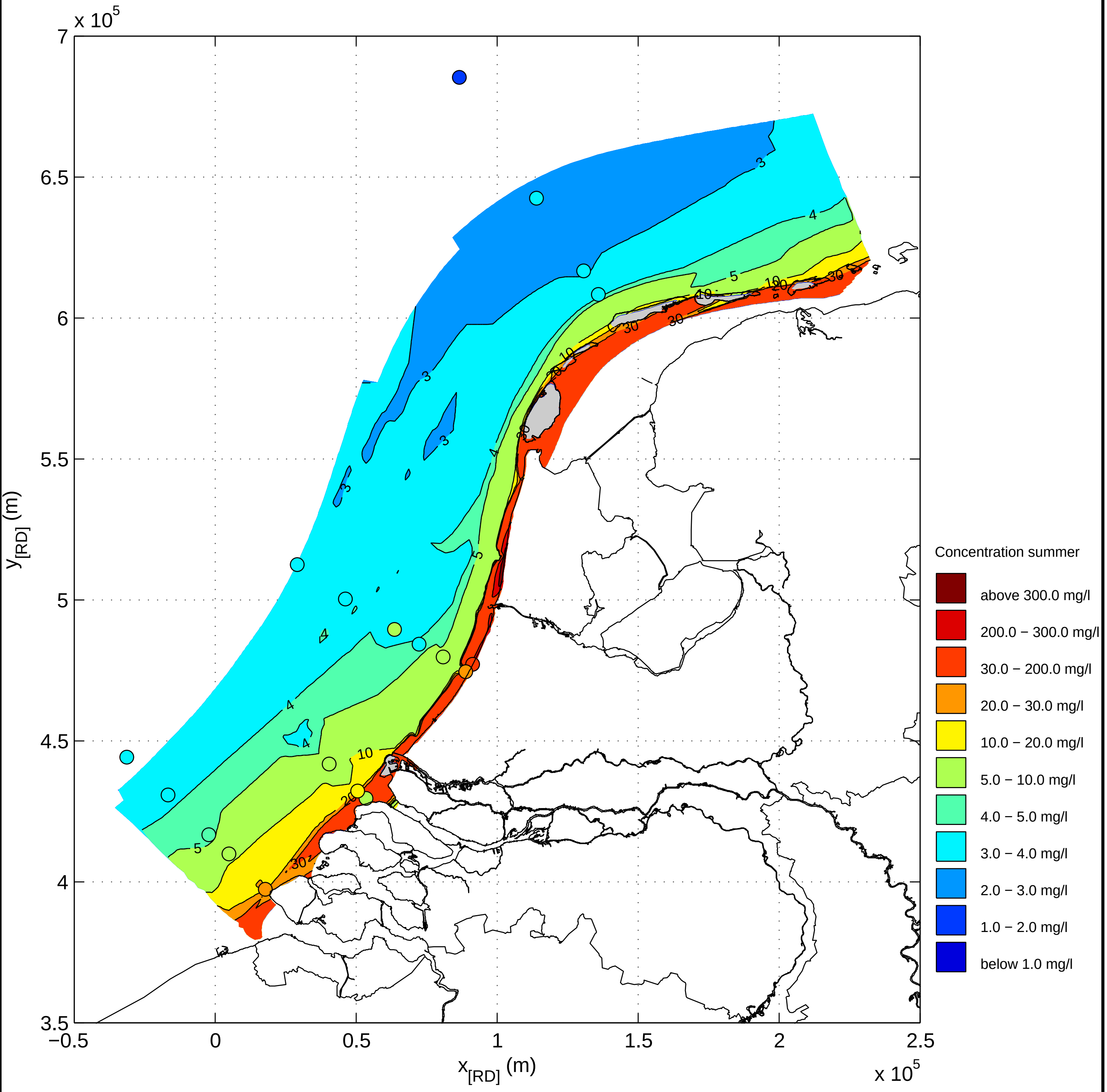

Summer mean of total suspended solids concentration (mg/l) filled contours present the interpolated 1975−1983 waterbase data coloured symbols present the 1984−2008 waterbase data	1975−1983 and 1984−2008	
Alkyon Hydraulic Consultancy & Research	A2273	Fig.2.14

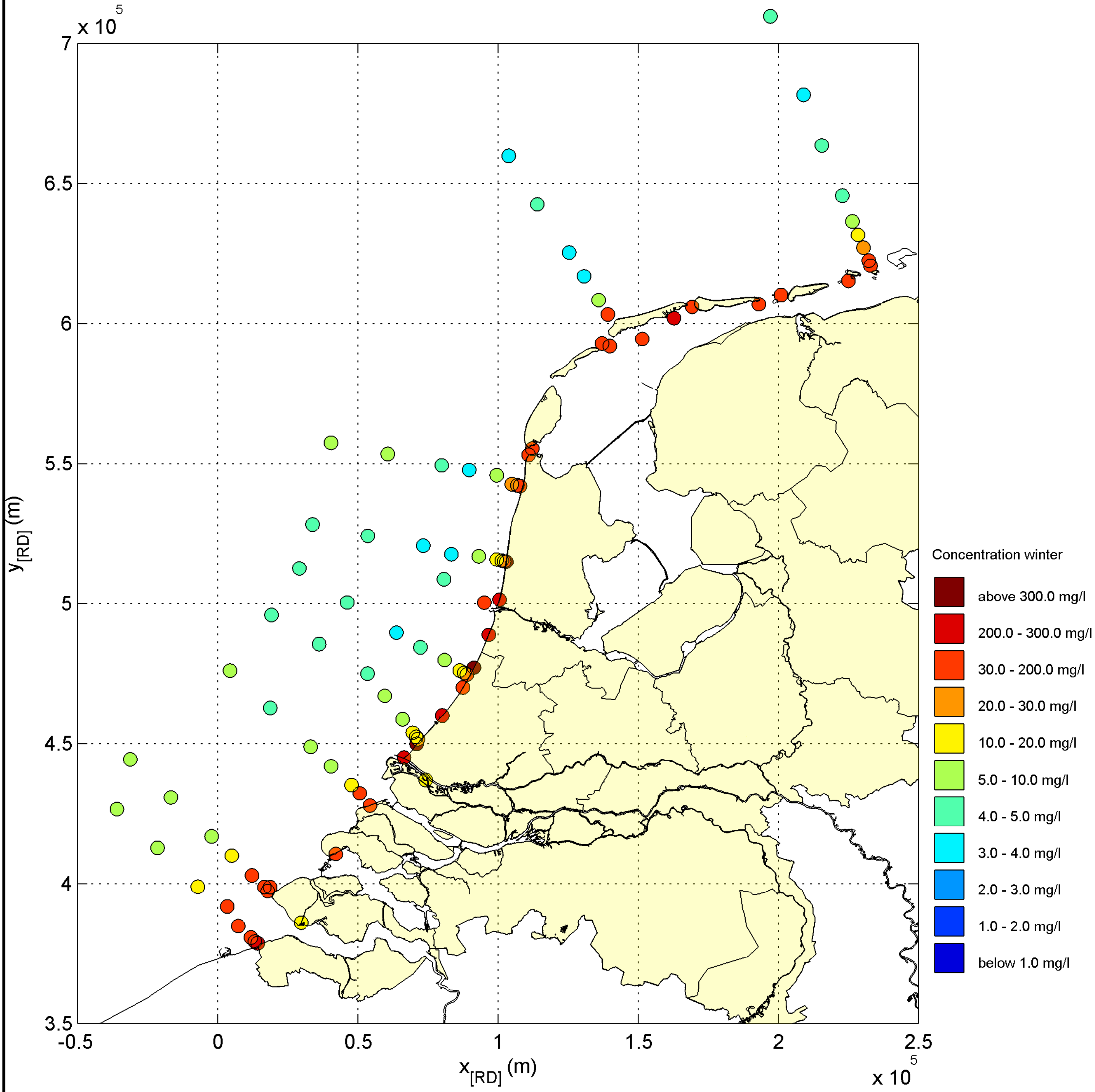

Winter mean of total suspended solids concentration (mg/l) for 96 stations along the Dutch coast based on waterbase data between 1975 and 1983	Waterbase 1975-1983	
Alkyon Hydraulic Consultancy & Research	A2273	Fig.2.15

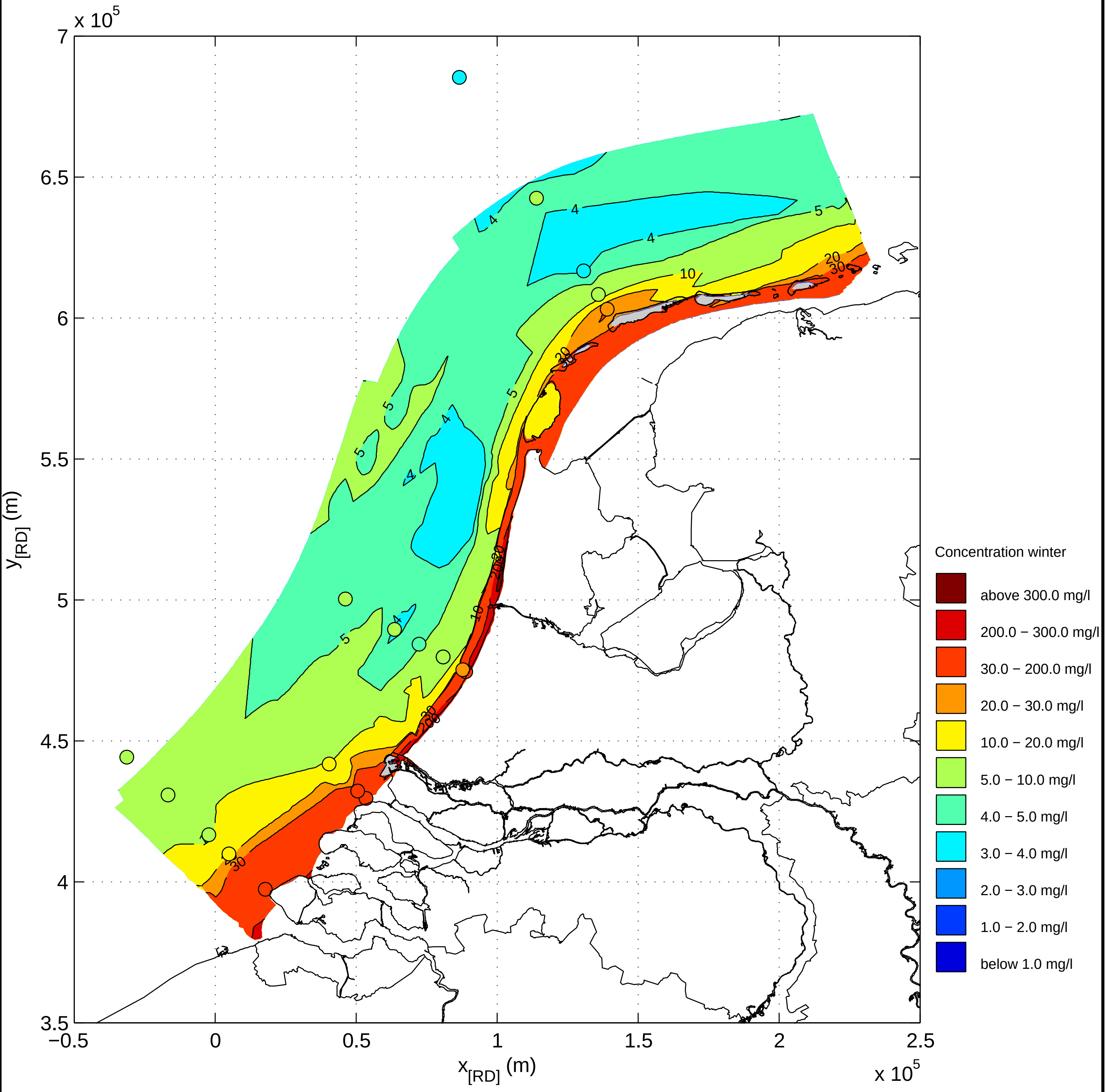

Winter mean of total suspended solids concentration (mg/l) filled contours present the interpolated 1975−1983 waterbase data coloured symbols present the 1984−2008 waterbase data	1975−1983 and 1984−2008
Alkyon Hydraulic Consultancy & Research	A2273 Fig.2.16

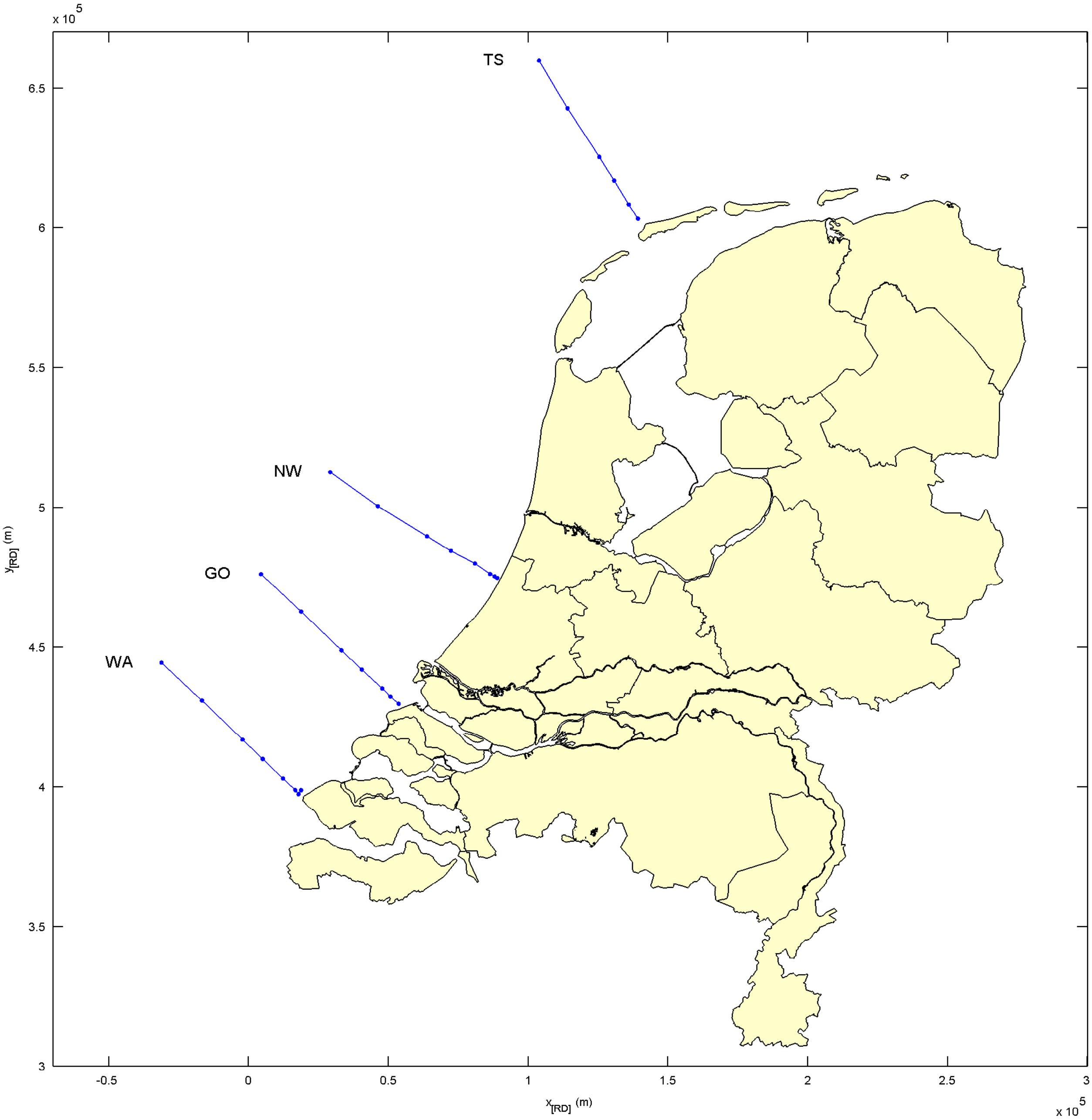

North Sea transects in which suspended matter concentration data is available from Waterbase for the period 1975-2008	Waterbase 1975-2008	
Alkyon Hydraulic Consultancy & Research	A2273	Fig.2.17

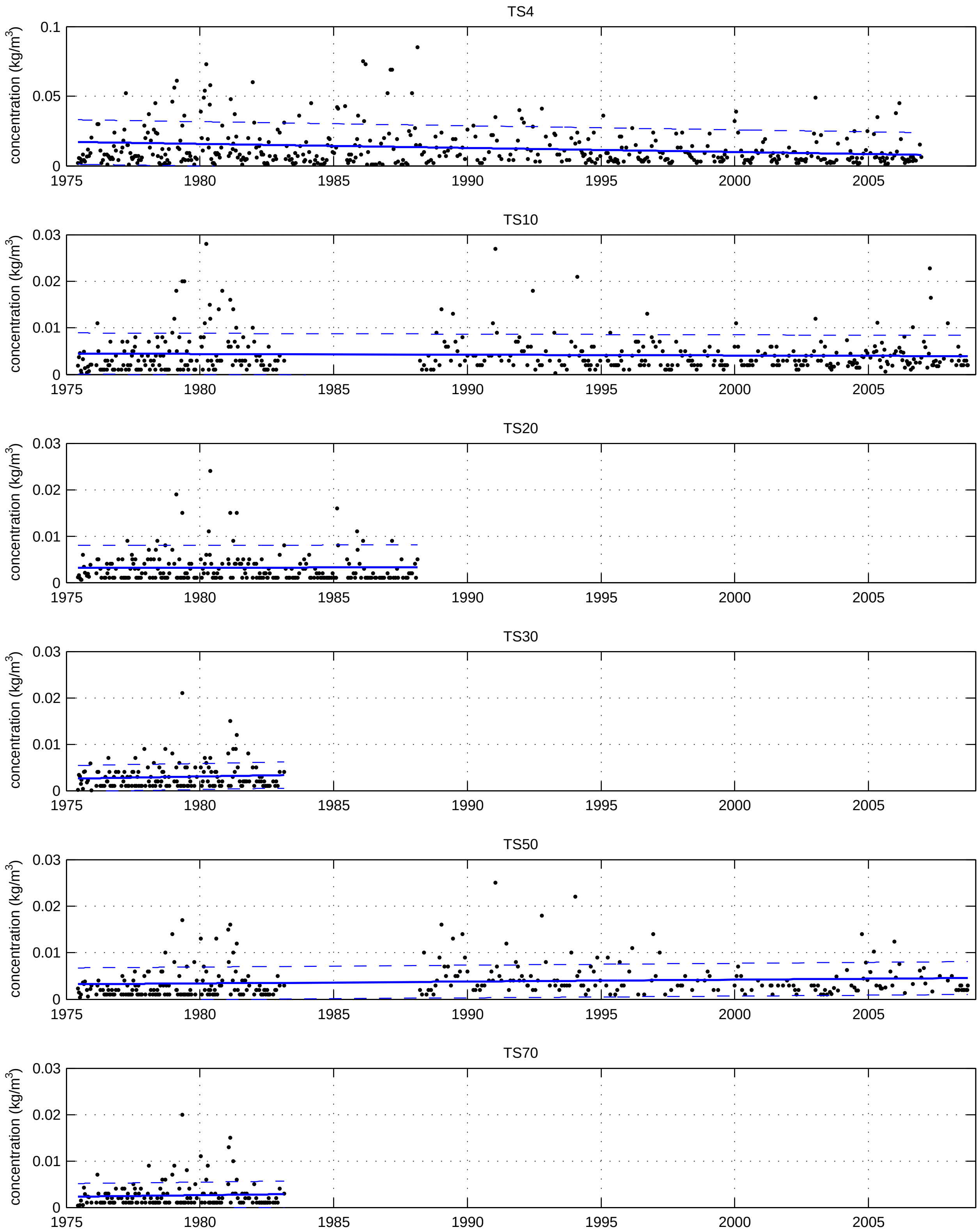

name	mean (x10^{-3} kg/m^3)	geomean (x10^{-3} kg/m^3)	trimmean (x10^{-3} kg/m^3)	std (x10^{-3} kg/m^3)	trend (x10^{-3} kg/m^3/year)	trend (95% low)	trend (95% up)
TS4	12.77	7.64	11.90	16.14	−0.29	−0.44	−0.15
TS10	4.19	3.05	3.96	4.42	−0.02	−0.05	0.02
TS20	3.19	2.09	2.89	4.81	0.01	−0.16	0.18
TS30	2.97	2.13	2.81	2.79	0.10	−0.11	0.30
TS50	3.77	2.74	3.64	3.52	0.04	0.00	0.08
TS70	2.57	1.83	2.40	2.79	0.07	−0.14	0.28

Time series of total suspended matter concentration (kg/m^3), linear trends and statistical parameters based on 1975−2008 Waterbase data
Terschelling transect

Alkyon Hydraulic Consultancy & Research | A2273 | Fig.2.18

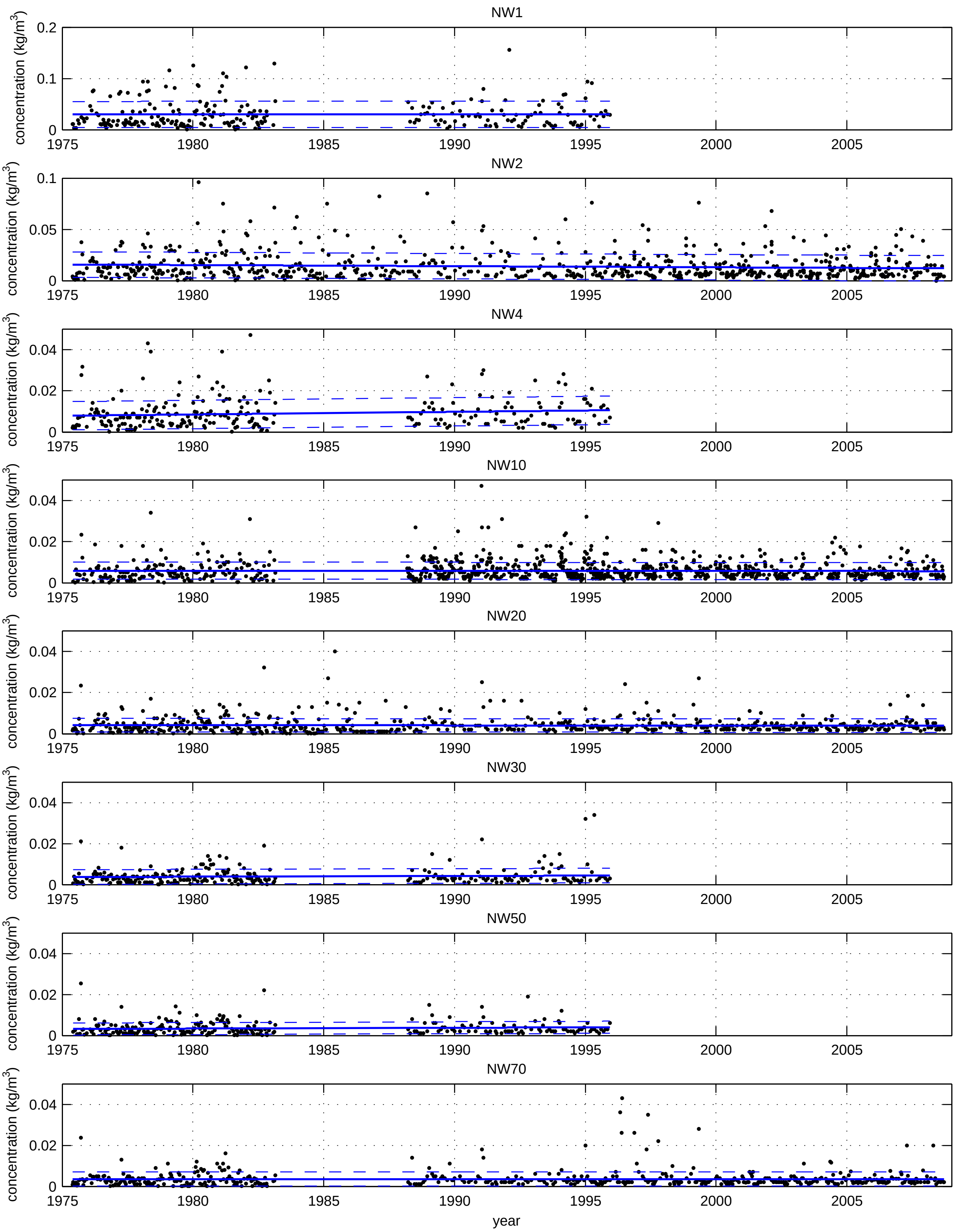

name	mean (x10^{-3} kg/m^3)	geomean (x10^{-3} kg/m^3)	trimmean (x10^{-3} kg/m^3)	std (x10^{-3} kg/m^3)	trend (x10^{-3} kg/m^3/year)	trend (95% low)	trend (95% up)
NW1	29.84	20.93	29.28	25.41	0.03	−0.46	0.51
NW2	13.69	9.53	13.23	12.44	−0.11	−0.20	−0.02
NW4	8.94	6.64	8.71	6.88	0.13	−0.00	0.26
NW10	5.78	4.58	5.65	4.14	−0.01	−0.04	0.02
NW20	4.01	2.91	3.91	3.26	−0.01	−0.03	0.02
NW30	3.96	2.77	3.80	3.56	0.03	−0.04	0.10
NW50	3.49	2.41	3.38	2.93	0.04	−0.02	0.10
NW70	3.53	2.52	3.35	3.46	−0.00	−0.03	0.03

Time series of total suspended matter concentration (kg/m^3), linear trends and statistical parameters based on 1975−2008 Waterbase data Noordwijk transect

Alkyon Hydraulic Consultancy & Research | A2273 | Fig.2.19

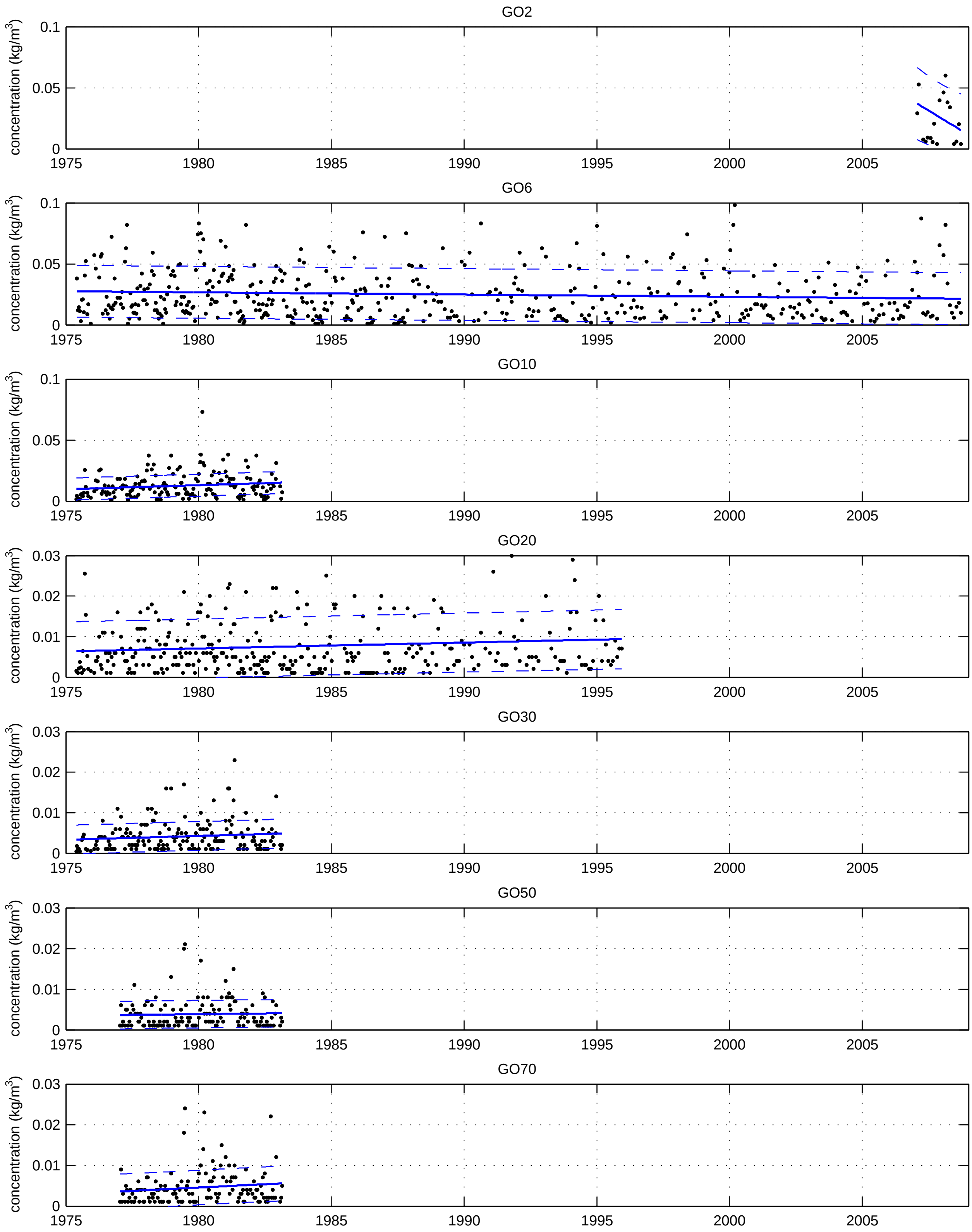

name	mean ($x10^{-3}$ kg/m^3)	geomean ($x10^{-3}$ kg/m^3)	trimmean ($x10^{-3}$ kg/m^3)	std ($x10^{-3}$ kg/m^3)	trend ($x10^{-3}$ kg/m^3/year)	trend (95% low)	trend (95% up)
GO2	26.57	15.93	26.57	27.38	−13.17	−38.82	12.48
GO6	24.92	16.79	24.28	21.27	−0.18	−0.37	0.01
GO10	12.44	9.00	12.28	9.07	0.67	0.07	1.28
GO20	7.64	4.98	7.43	7.30	0.15	0.01	0.28
GO30	4.12	2.91	4.02	3.54	0.19	−0.06	0.43
GO50	3.85	2.77	3.75	3.35	0.07	−0.25	0.39
GO70	4.53	3.17	4.41	4.26	0.33	−0.08	0.73

Time series of total suspended matter concentration (kg/m^3), linear trends and statistical parameters based on 1975−2008 Waterbase data Goeree transect

Alkyon Hydraulic Consultancy & Research | A2273 | Fig.2.20

waterbase_timeseries03

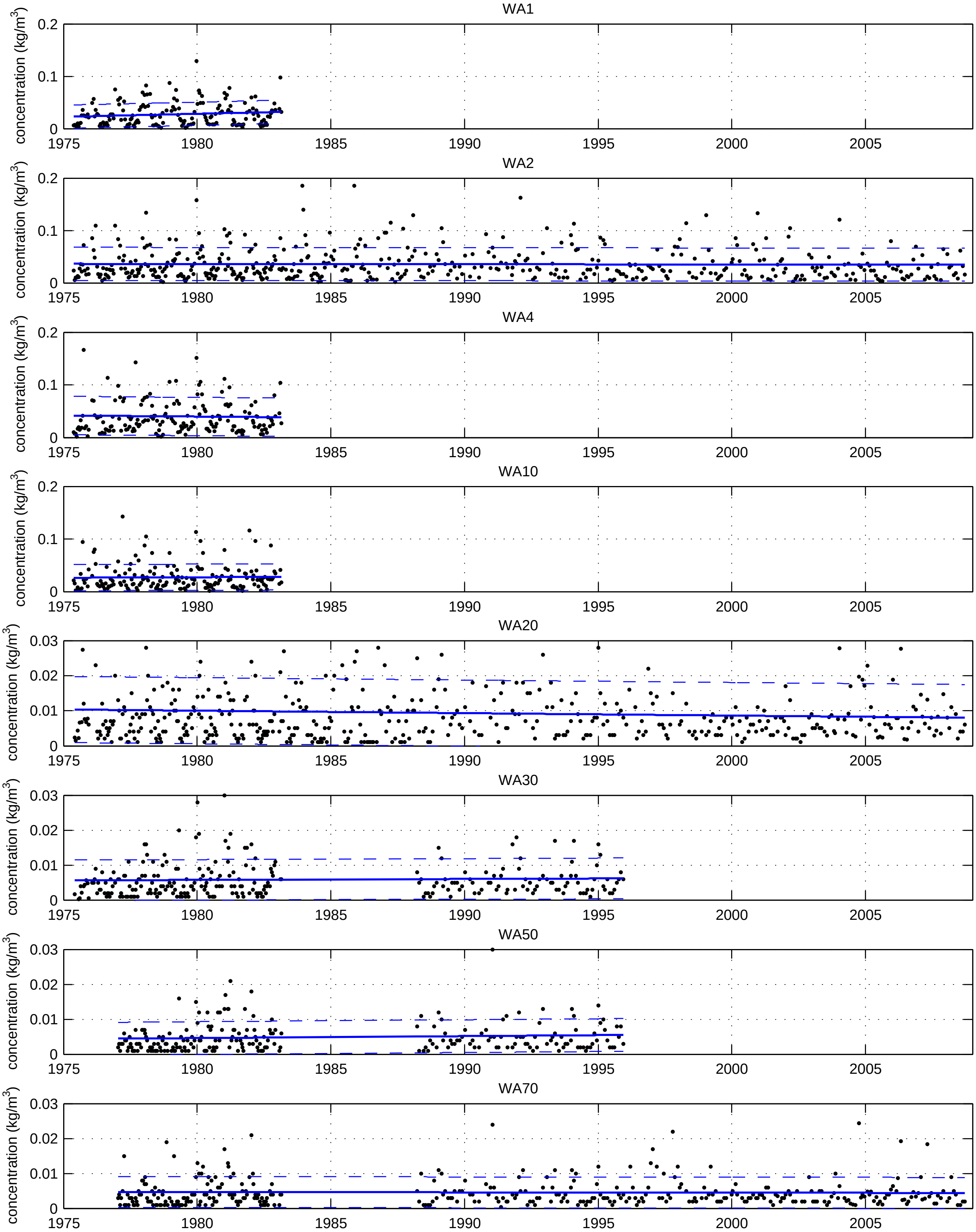

name	mean (x10^{-3} kg/m^3)	geomean (x10^{-3} kg/m^3)	trimmean (x10^{-3} kg/m^3)	std (x10^{-3} kg/m^3)	trend (x10^{-3} kg/m^3/year)	trend (95% low)	trend (95% up)
WA1	27.44	18.77	26.73	22.23	1.16	−0.32	2.64
WA2	35.50	24.88	34.27	31.46	−0.05	−0.33	0.23
WA4	40.05	28.22	38.36	36.18	−0.40	−2.78	1.98
WA10	27.21	18.52	26.33	24.78	0.21	−1.46	1.87
WA20	9.35	6.22	8.95	9.42	−0.07	−0.15	0.01
WA30	5.84	4.09	5.52	5.79	0.03	−0.08	0.14
WA50	4.86	3.47	4.63	4.67	0.06	−0.04	0.15

Time series of total suspended matter concentration (kg/m^3), linear trends and statistical parameters based on 1975−2008 Waterbase data Walcheren transect

Alkyon Hydraulic Consultancy & Research | A2273 | Fig.2.21

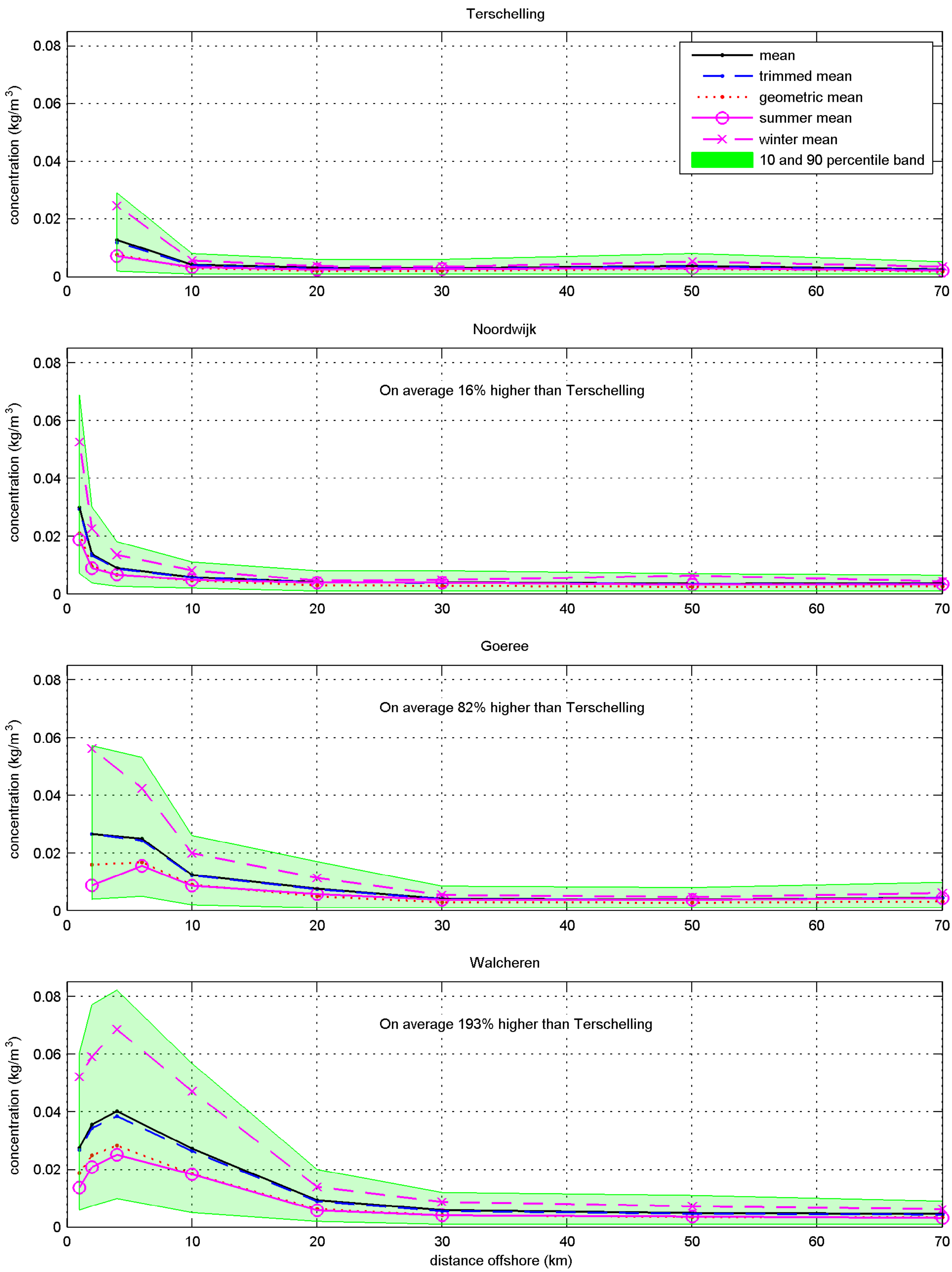

Cross-shore distribution of total suspended matter concentration (kg/m^3) Statistical parameters based on 1975-2008 Waterbase data Terschelling, Noordwijk, Goeree and Walcheren transects	Waterbase 1975-2008	
Alkyon Hydraulic Consultancy & Research	A2273	Fig.2.22

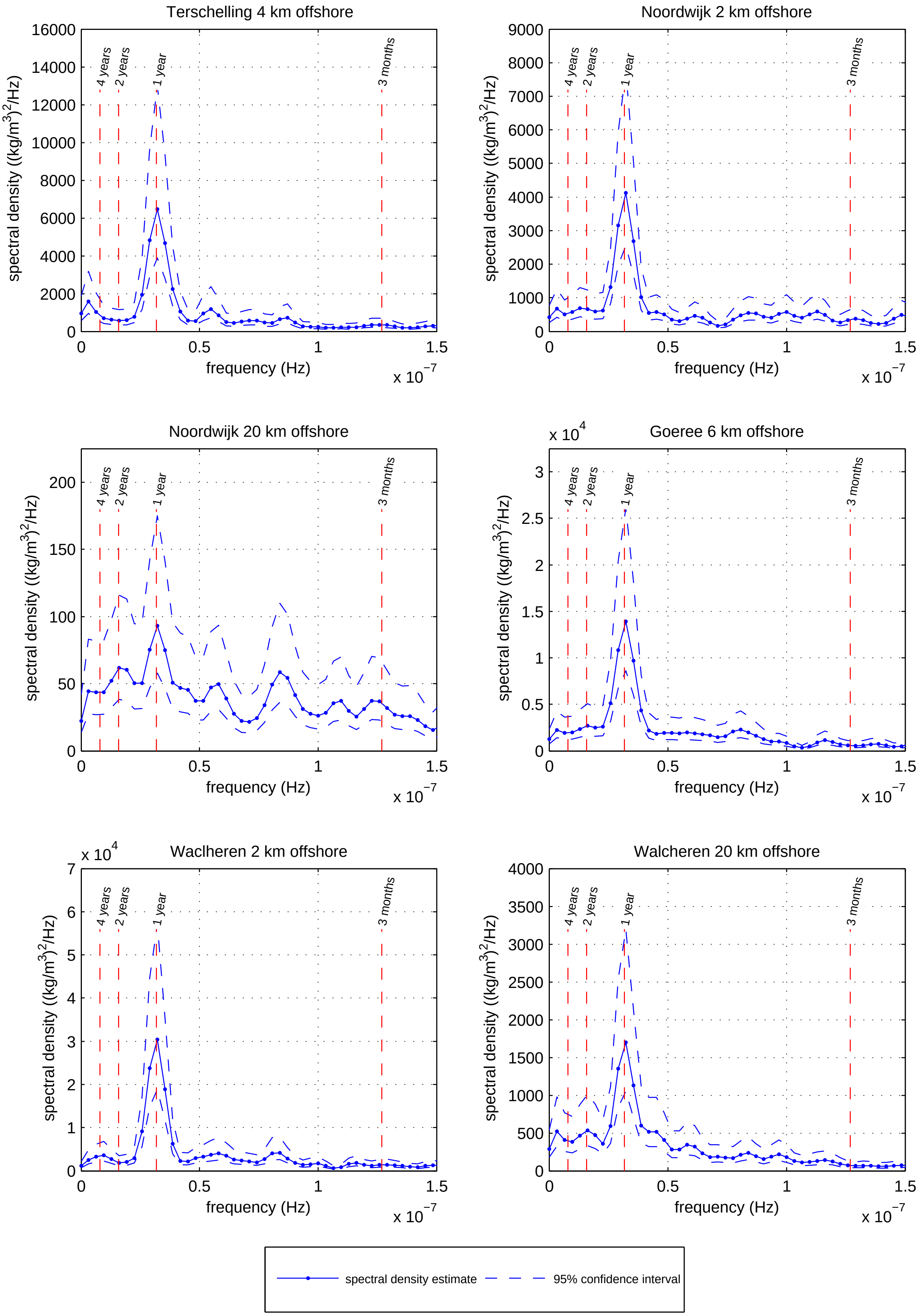

Power spectral density of suspended matter concentration for 6 different stations along the Dutch coast based on 1975−2008 Waterbase data	Waterbase 1975−2008	
Alkyon Hydraulic Consultancy & Research	A2273	Fig.2.23

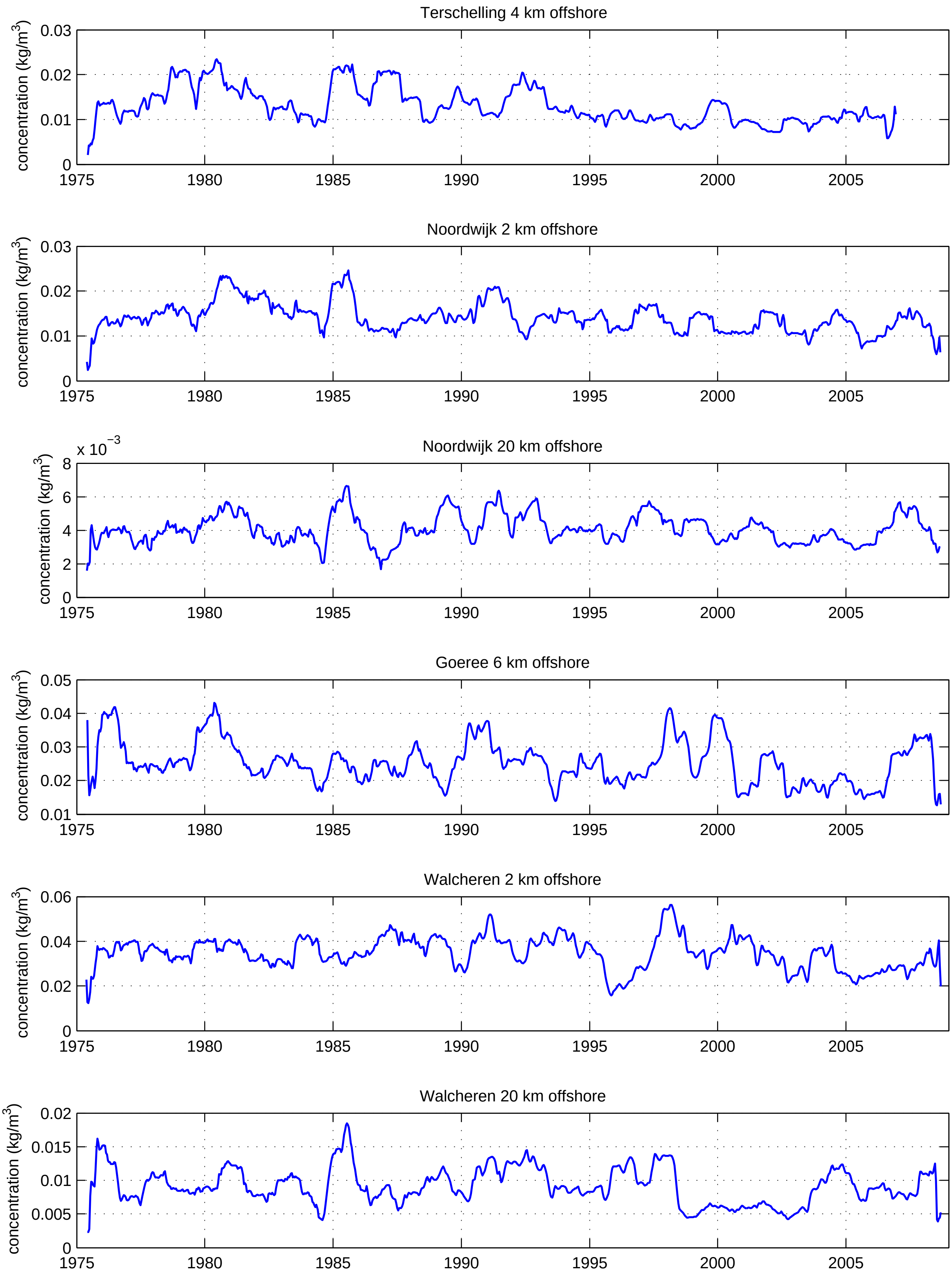

Moving averages (2 year window) of the suspended matter concentration for 6 different stations along the Dutch coast based on 1975−2008 Waterbase data	Waterbase 1975−2008	
Alkyon Hydraulic Consultancy & Research	A2273	Fig.2.24

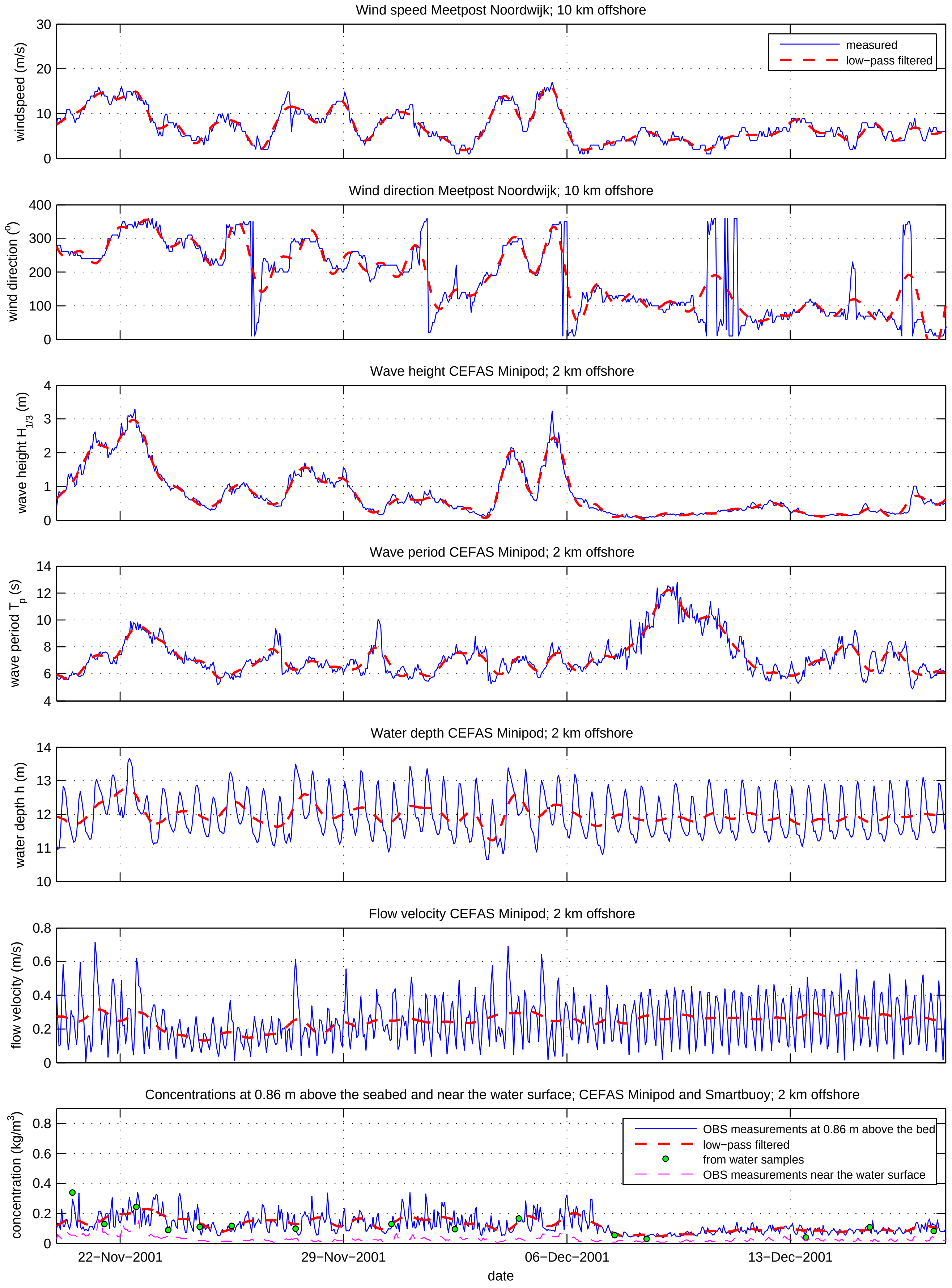

Conditions during the Noordwijk 2−1 measurements CEFAS Minipod and Smartbuoy deployment 180 The measurement period is 669 hours (nearly 28 days).	CEFAS Minipod and Smartbuoy	
Alkyon Hydraulic Consultancy & Research	A2273	Fig.2.25

CEFAS_plot_data02

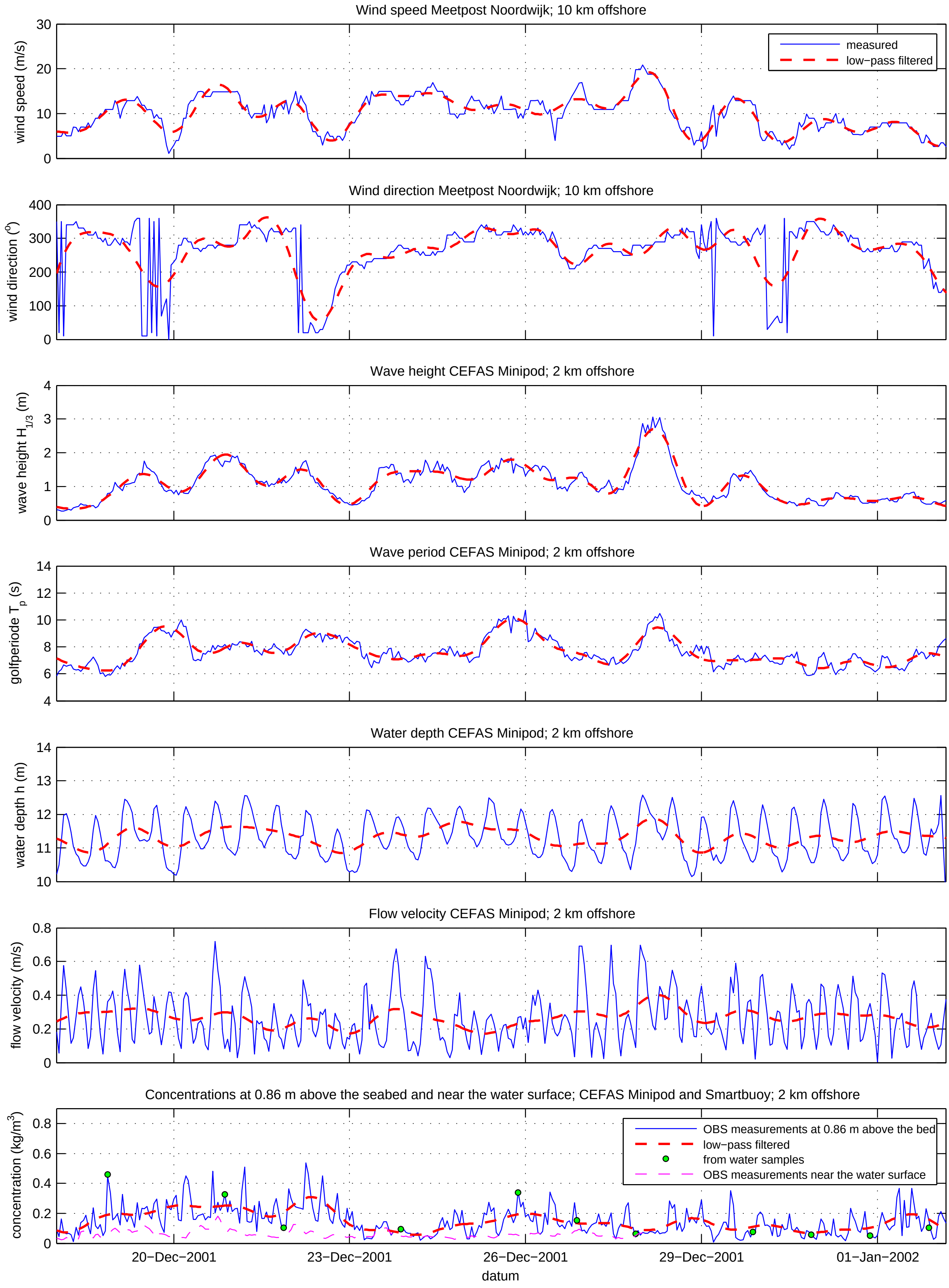

Conditions during the Noordwijk 2−2 measurements CEFAS Minipod and Smartbuoy deployment 181 The measurement period is 364 hours (just over 15 days).	CEFAS Minipod and Smartbuoy	
Alkyon Hydraulic Consultancy & Research	A2273	Fig.2.26

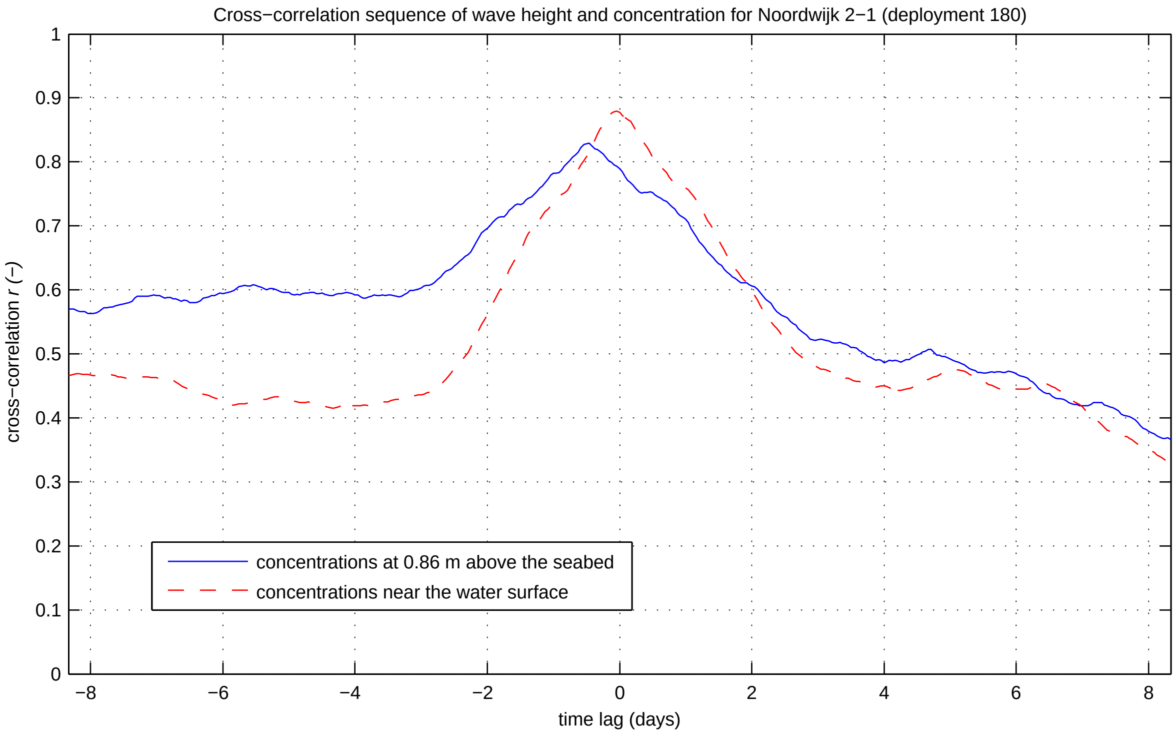

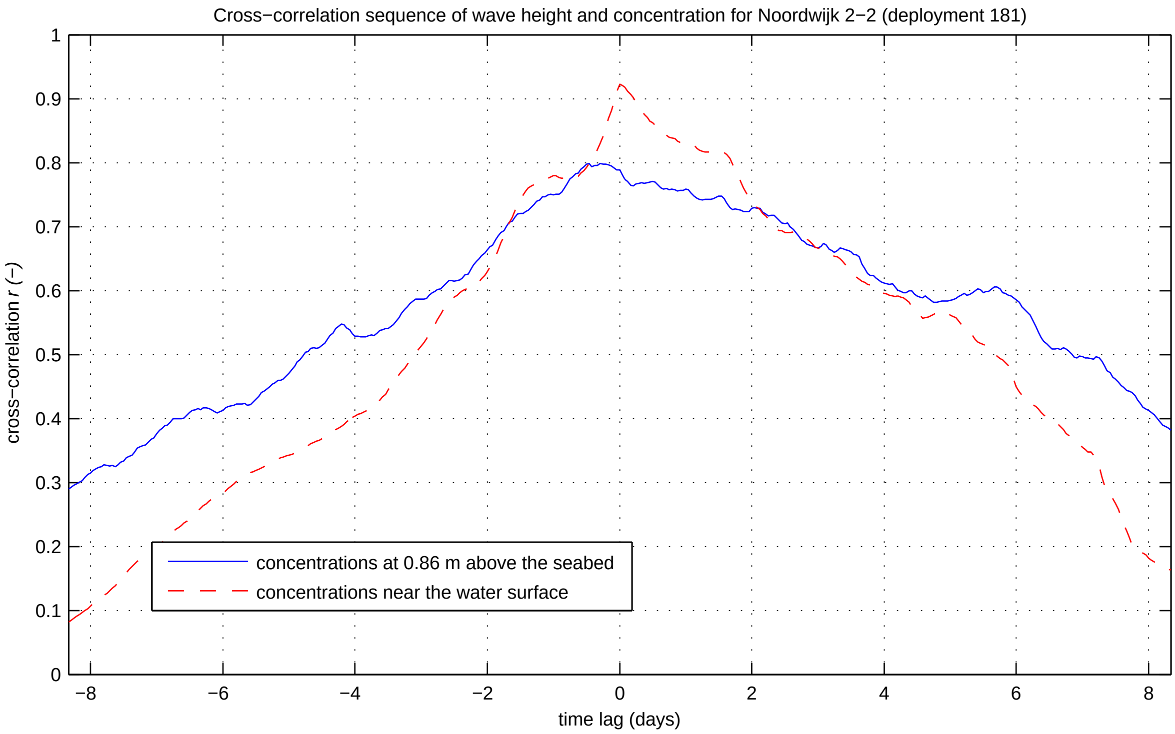

Cross−correlation sequence of wave height and concentration CEFAS Minipod and Smartbuoy deployment 180 and 181 Noordwijk 2 km offshore	CEFAS Minipod and Smartbuoy	
Alkyon Hydraulic Consultancy & Research	A2273	Fig.2.27

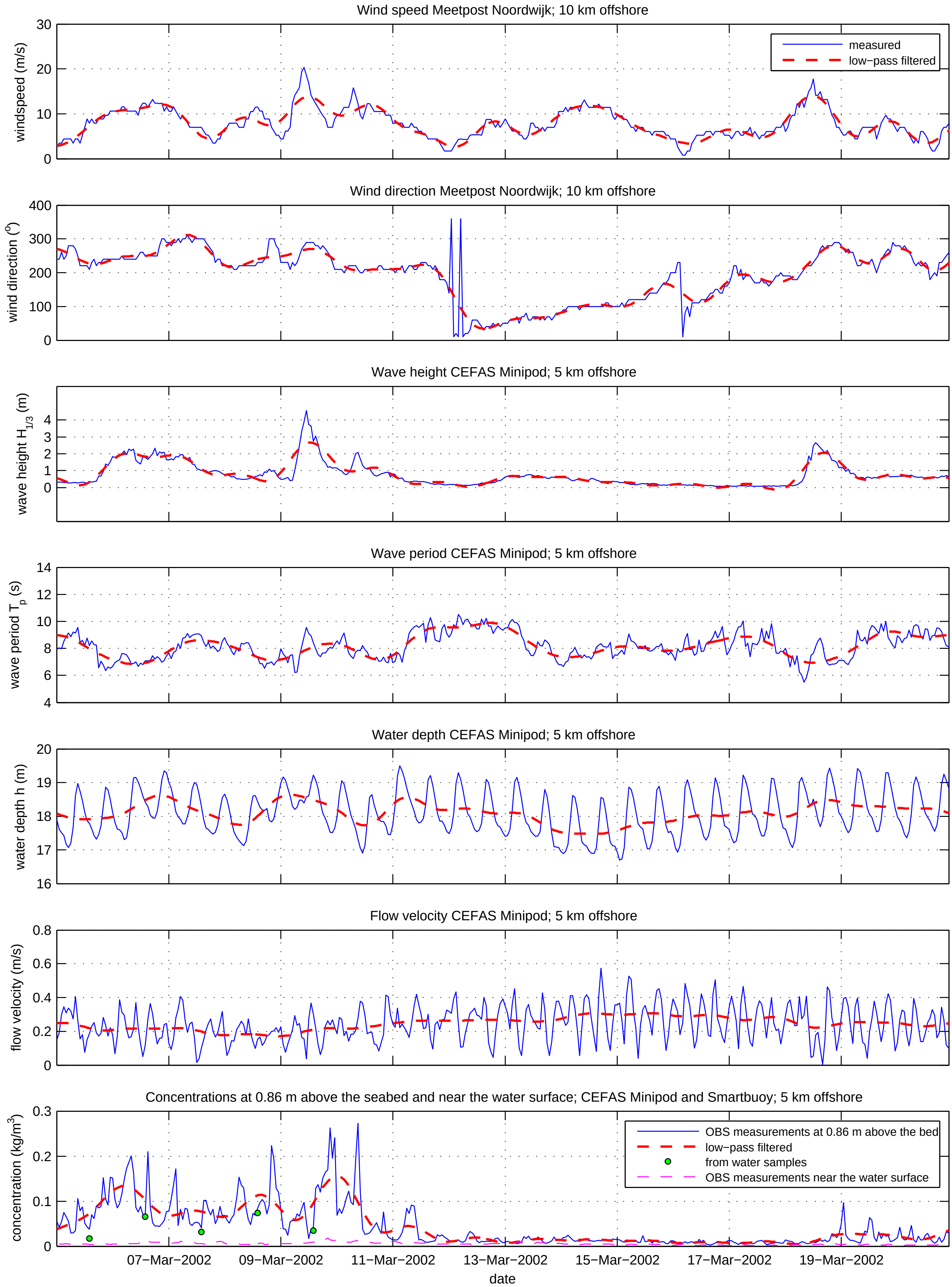

Conditions during the Noordwijk 5−1 measurements CEFAS Minipod and Smartbuoy deployment 182 The measurement period is 382 hours (nearly 16 days).	CEFAS Minipod and Smartbuoy	
Alkyon Hydraulic Consultancy & Research	A2273	Fig.2.28

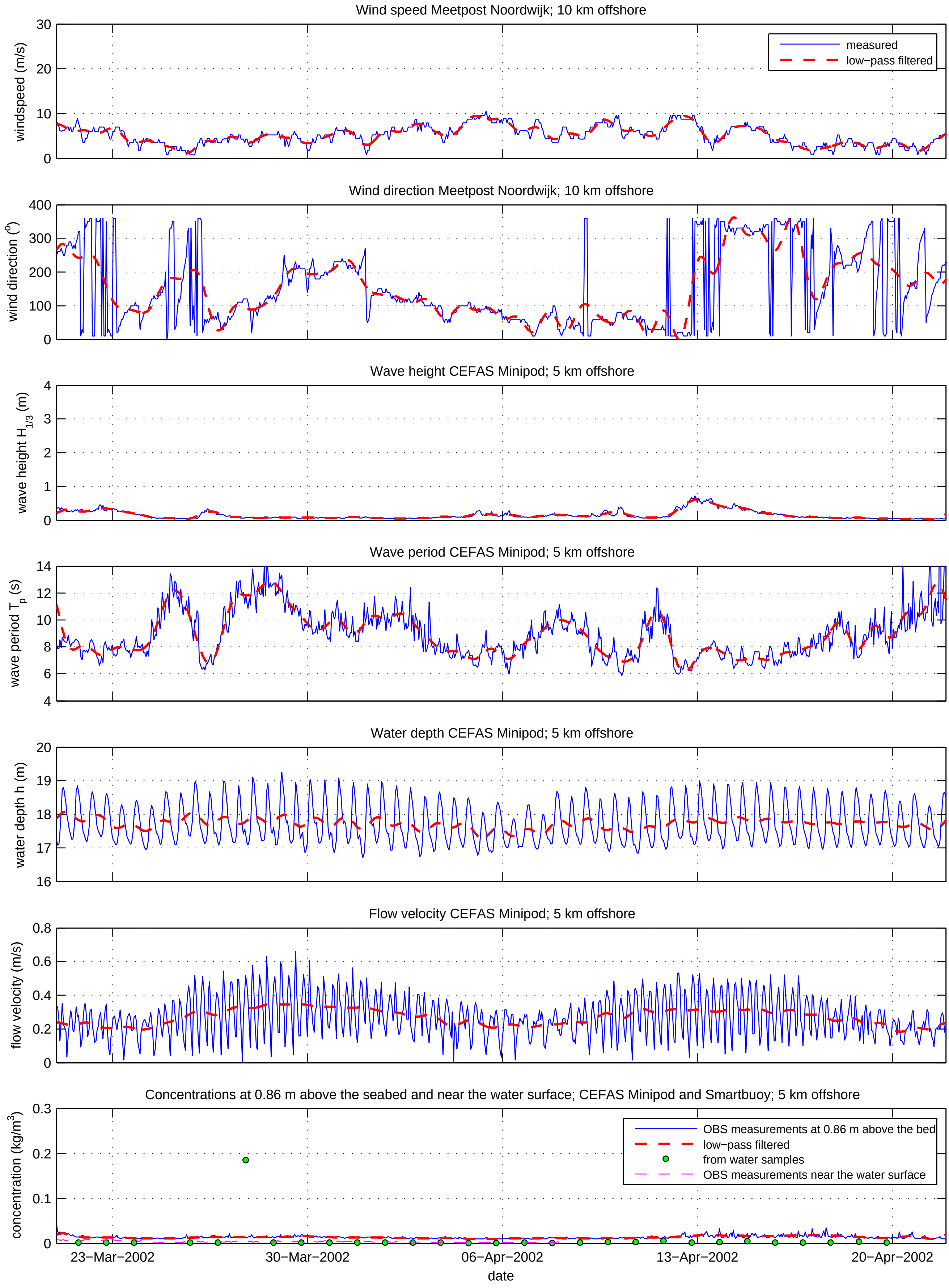

Conditions during the Noordwijk 5−2 measurements CEFAS Minipod and Smartbuoy deployment 183 The measurement period is 766 hours (nearly 32 days).	CEFAS Minipod and Smartbuoy	
Alkyon Hydraulic Consultancy & Research	A2273	Fig.2.29

Cross−correlation sequence of wave height and concentration for Noordwijk 5−1 (deployment 182)

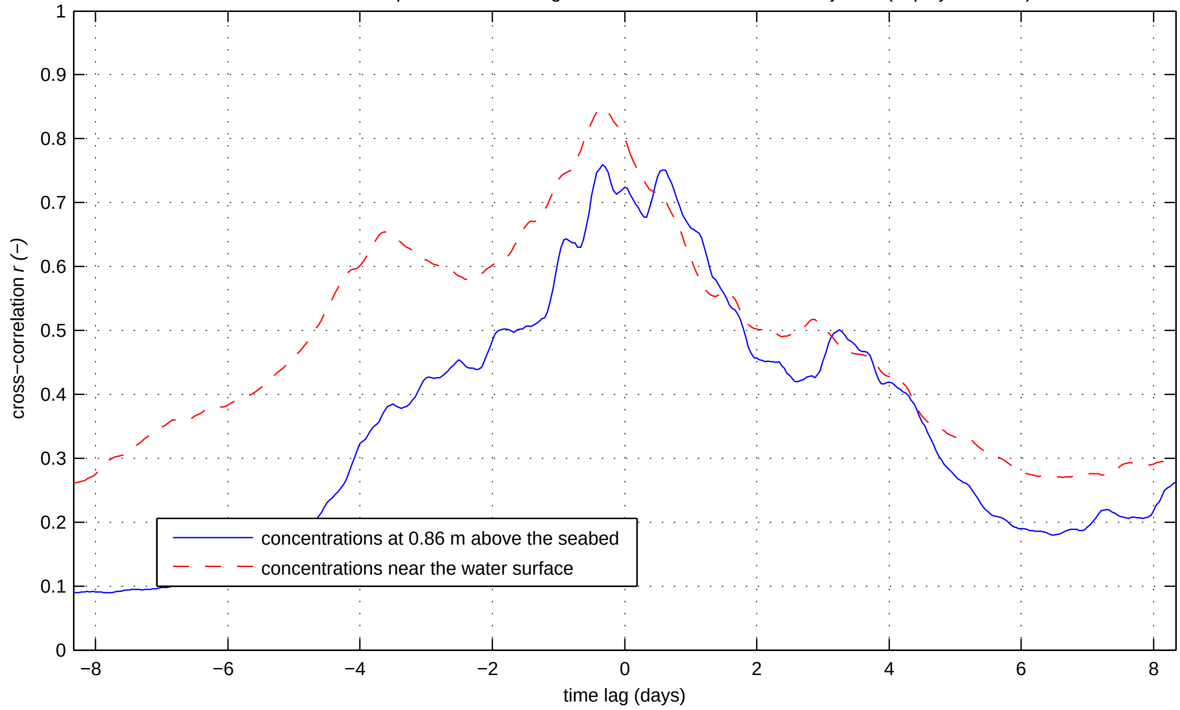

Cross−correlation sequence of wave height and concentration for Noordwijk 5−2 (deployment 183)

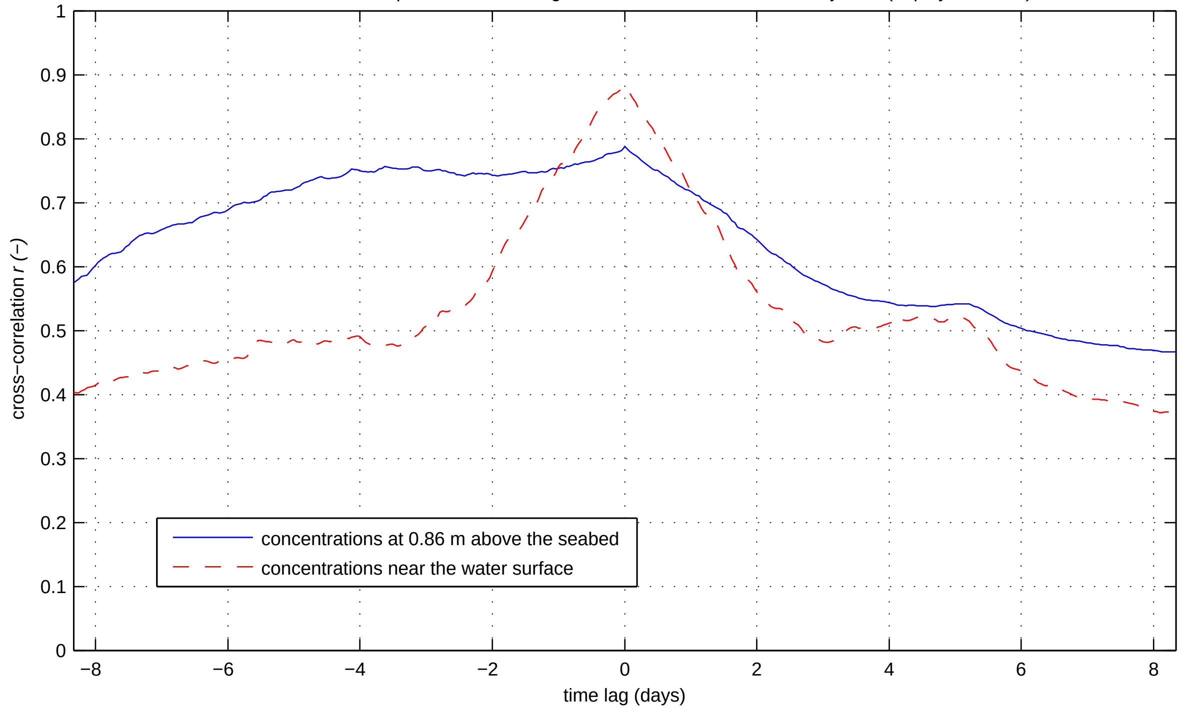

Cross−correlation sequence of wave height and concentration CEFAS Minipod and Smartbuoy deployment 182 and 183 Noordwijk 5 km offshore	CEFAS Minipod and Smartbuoy	
Alkyon Hydraulic Consultancy & Research	A2273	Fig.2.30

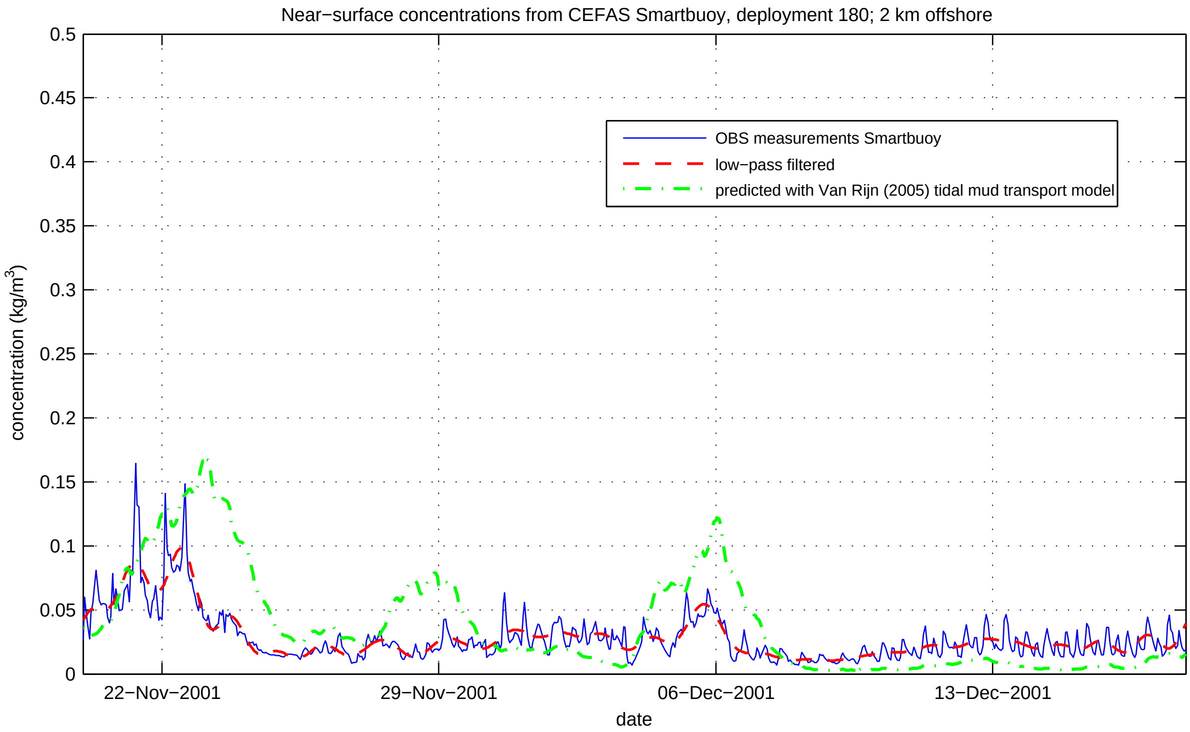

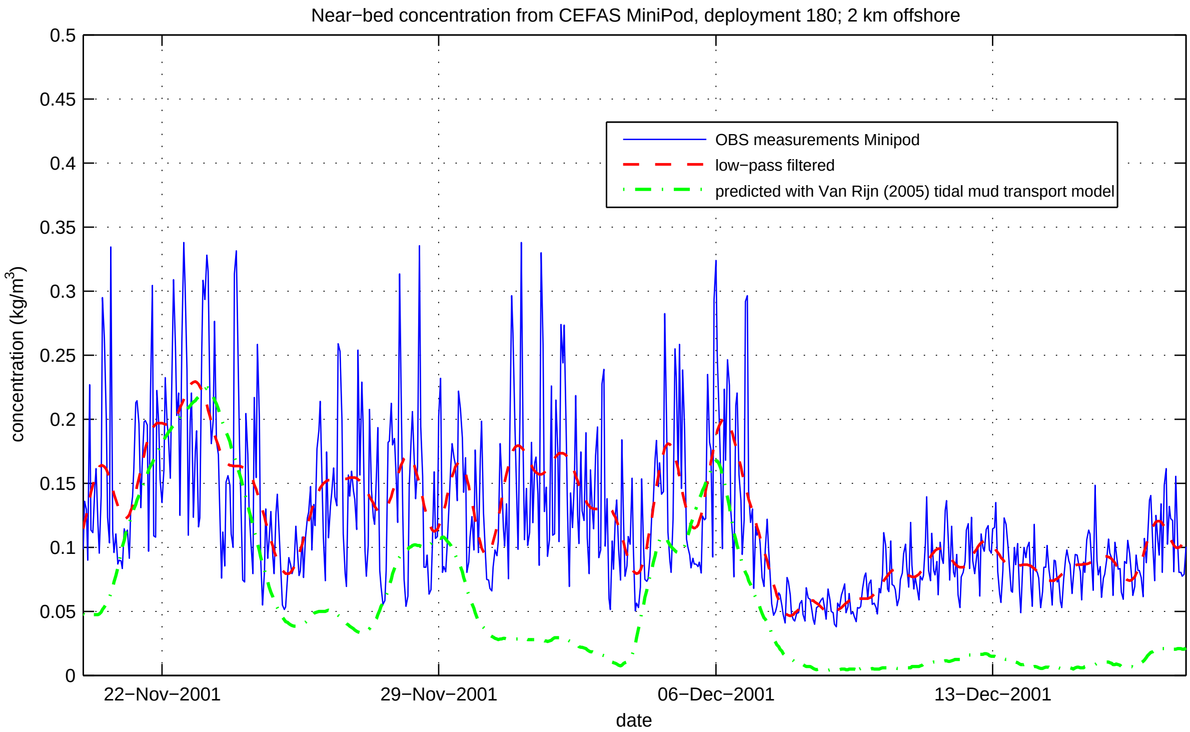

Comparison of measured and predicted concentrations CEFAS Minipod and Smartbuoy deployment 180 Predictions made with Van Rijn (2005) tidal mud transport model	CEFAS Minipod and Smartbuoy	
Alkyon Hydraulic Consultancy & Research	A2273	Fig.2.31

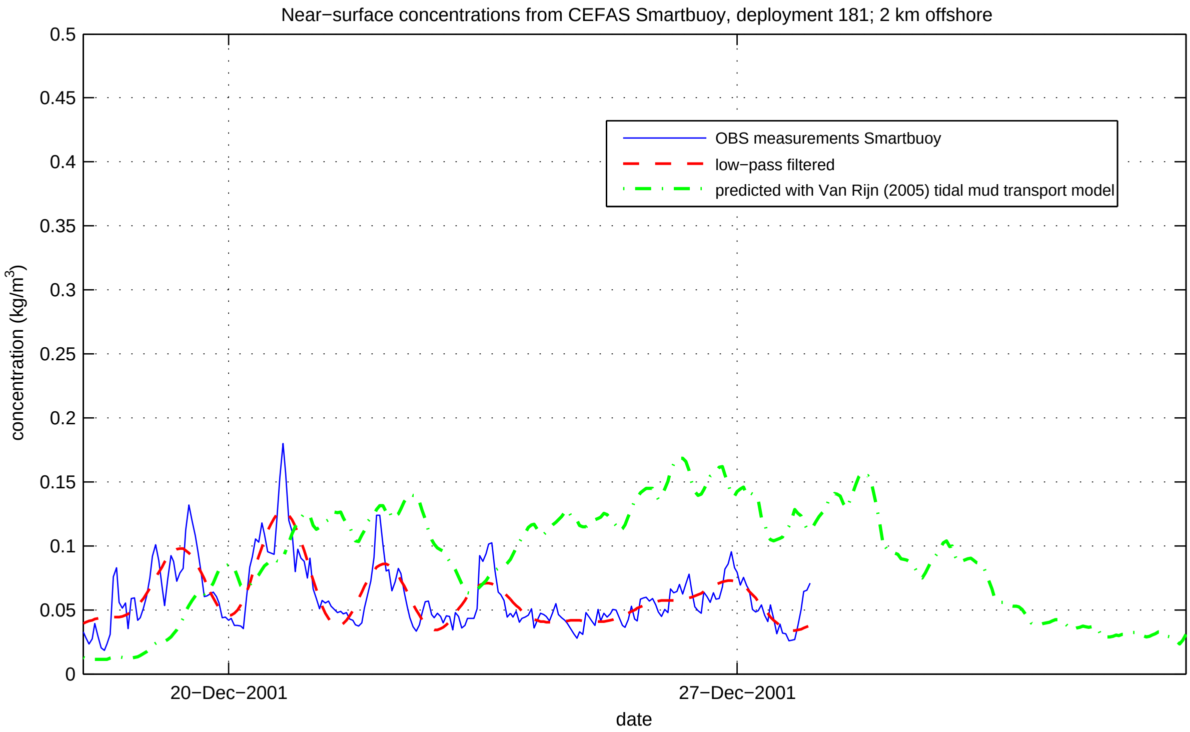

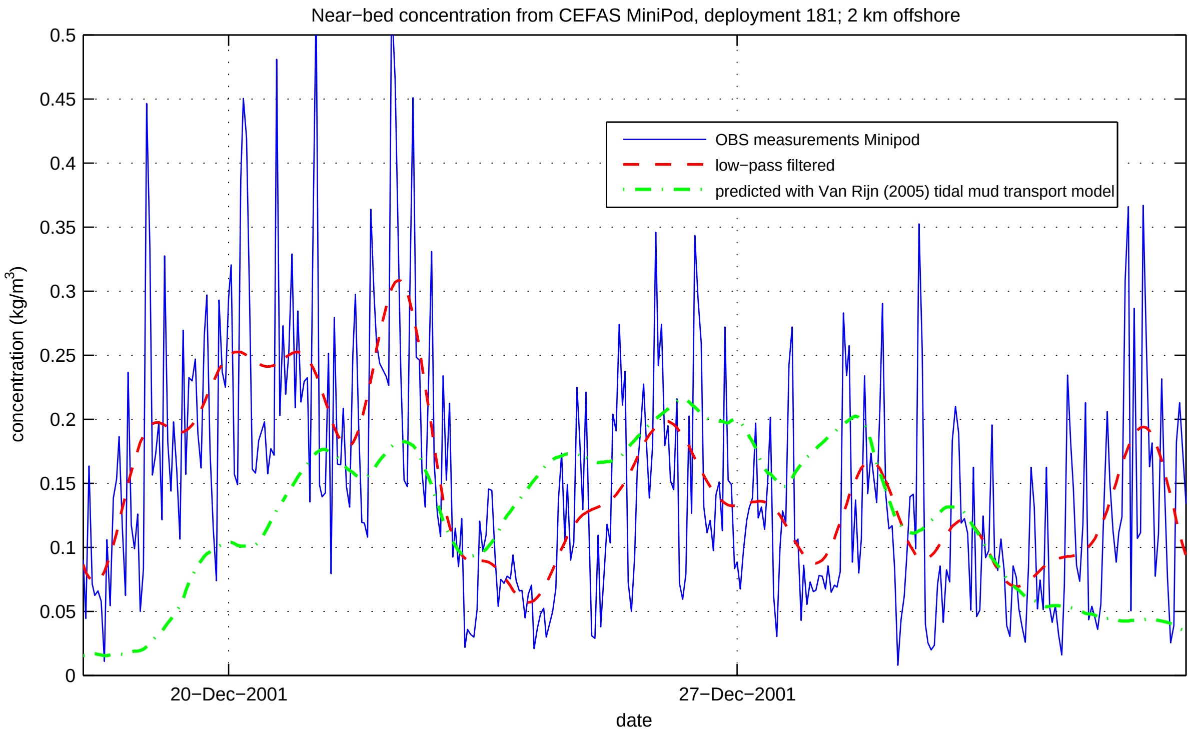

Comparison of measured and predicted concentrations CEFAS Minipod and Smartbuoy deployment 181 Predictions made with Van Rijn (2005) tidal mud transport model	CEFAS Minipod and Smartbuoy	
Alkyon Hydraulic Consultancy & Research	A2273	Fig.2.32

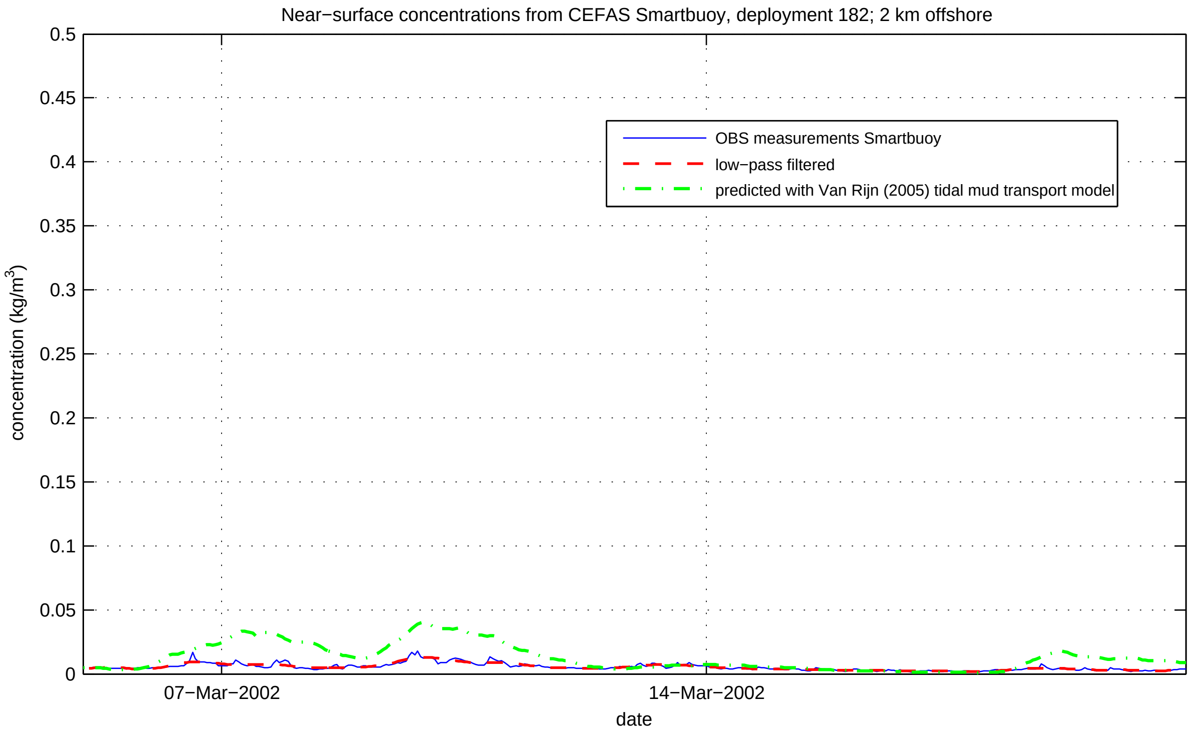

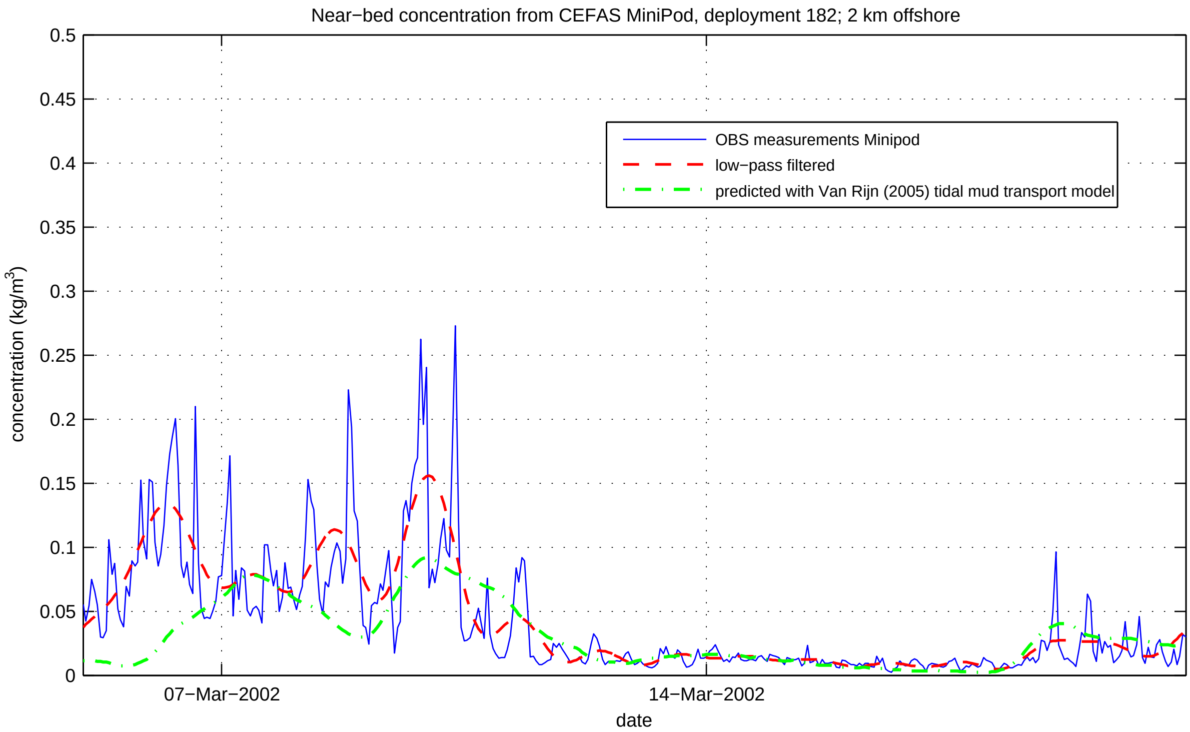

Comparison of measured and predicted concentrations CEFAS Minipod and Smartbuoy deployment 182 Predictions made with Van Rijn (2005) tidal mud transport model	CEFAS Minipod and Smartbuoy
Alkyon Hydraulic Consultancy & Research	A2273 / Fig.2.33

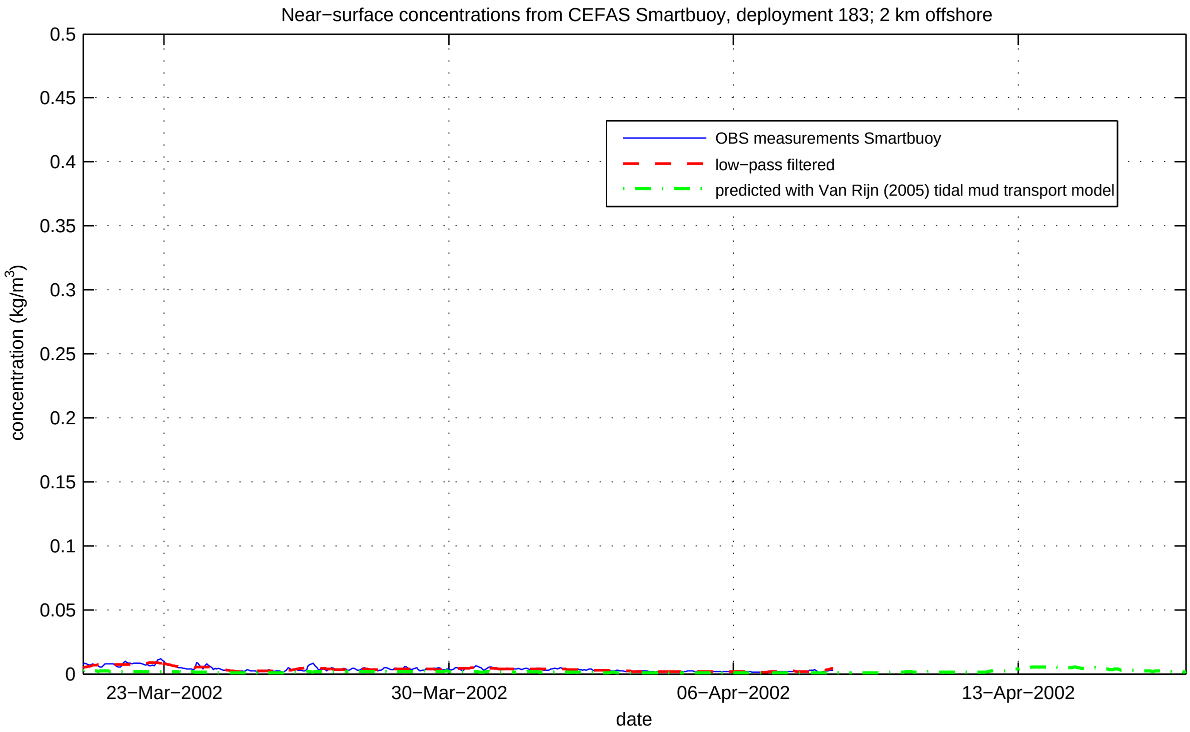

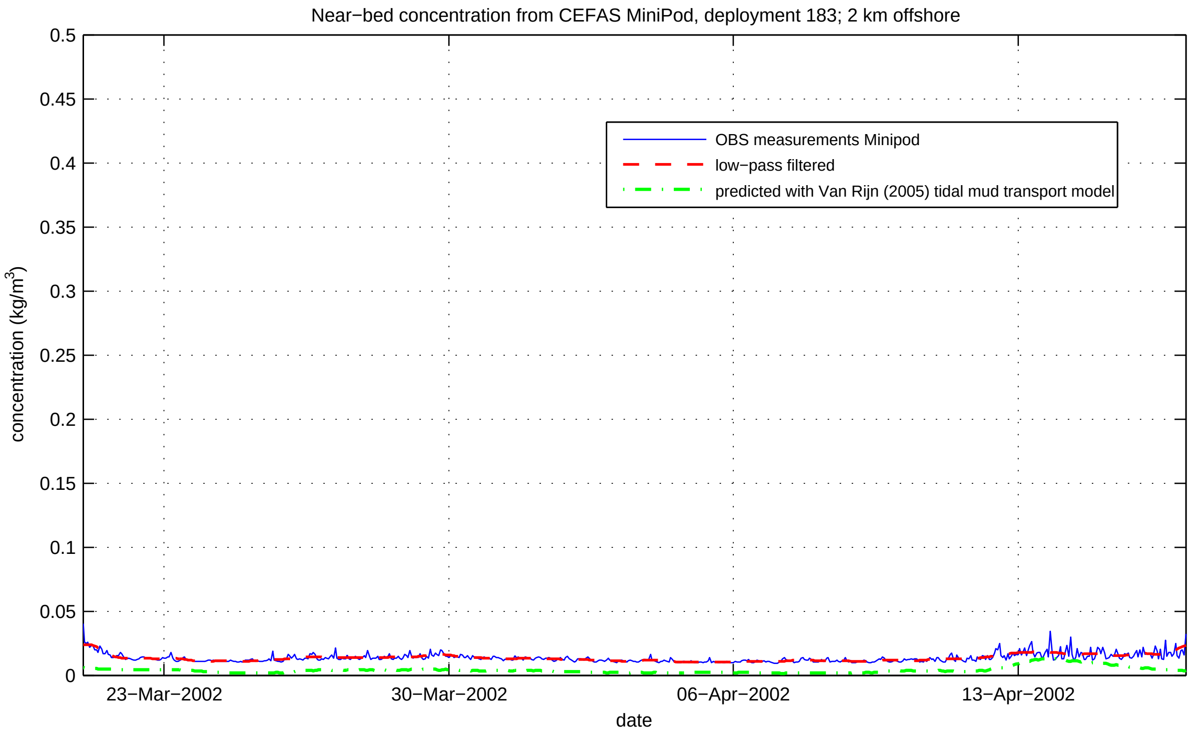

Comparison of measured and predicted concentrations
CEFAS Minipod and Smartbuoy deployment 183
Predictions made with Van Rijn (2005) tidal mud transport model

CEFAS Minipod and Smartbuoy

Alkyon Hydraulic Consultancy & Research

A2273

Fig.2.34

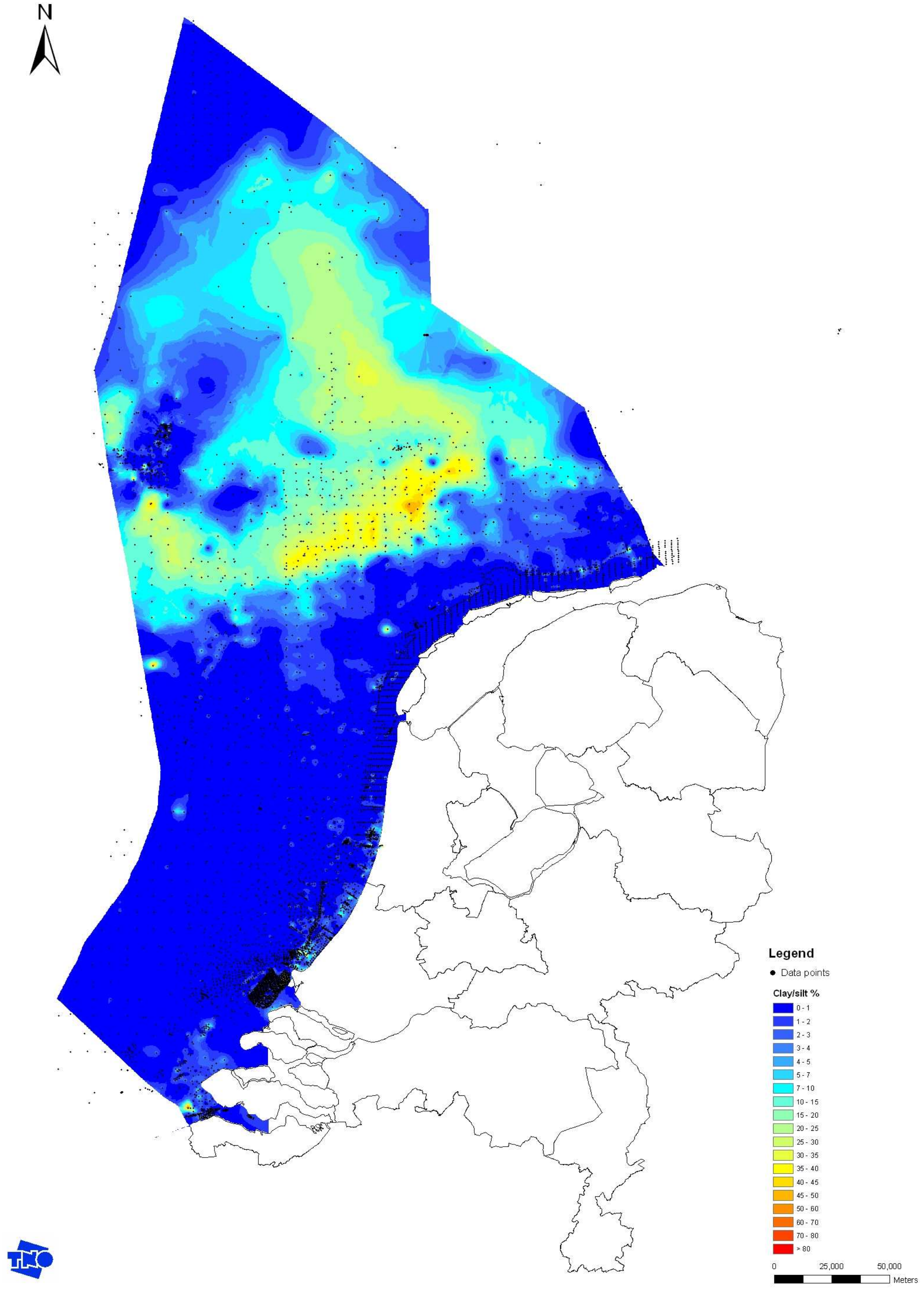

Percentage of clay/silt in the North Sea Map produced by Deltares / TNO Built Environment and Geosciences − Geological Survey of the Netherlands.	Deltares / TNO	
Alkyon Hydraulic Consultancy & Research	A2273	Fig.2.34b

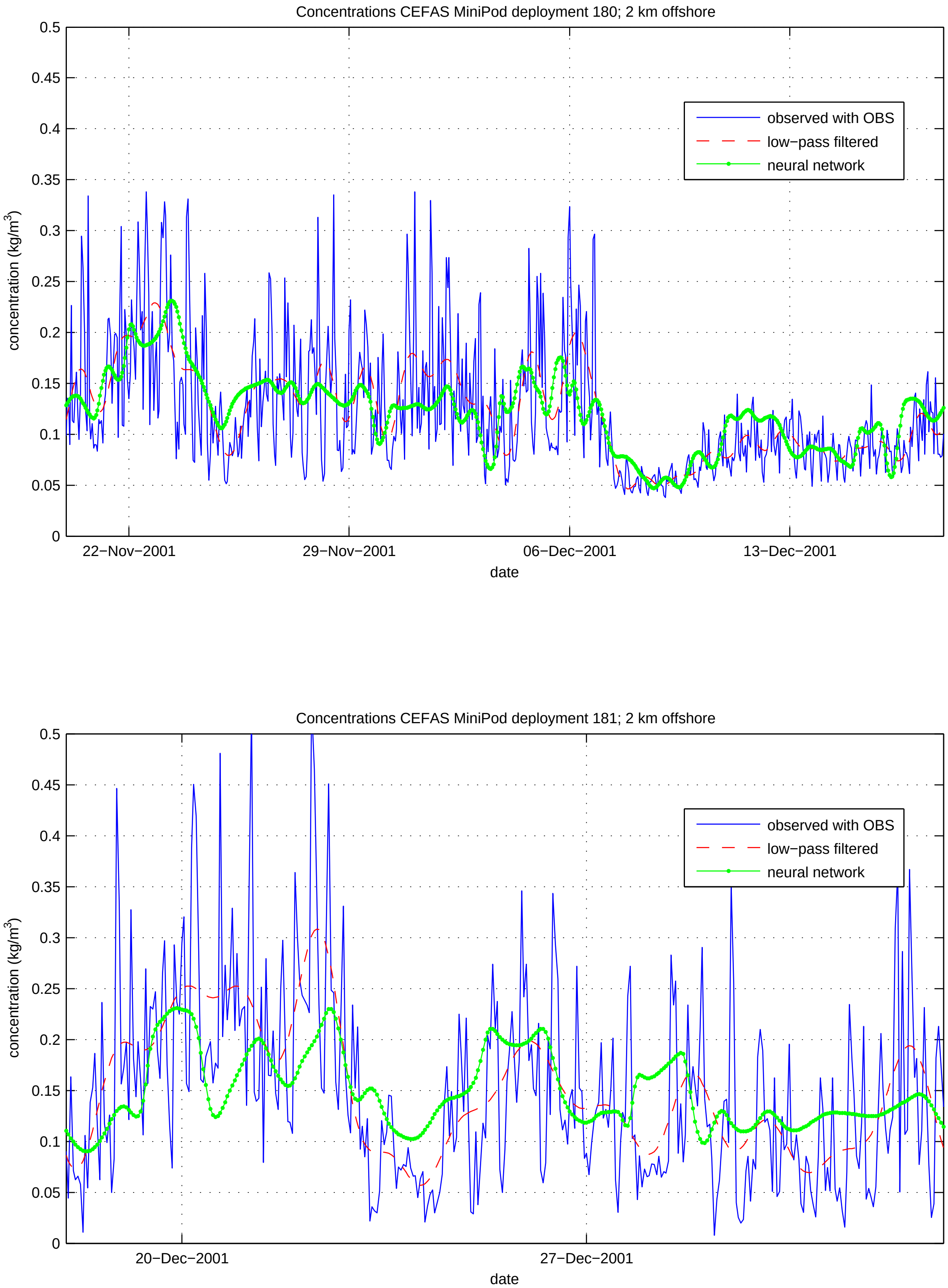

Measured, low−pass filtered and neural network predicted concentrations using wave height, wave period and water depth as input CEFAS Minipod deployment 180 and 181	CEFAS Minipod and Neural Network	
Alkyon Hydraulic Consultancy & Research	A2273	Fig.2.35

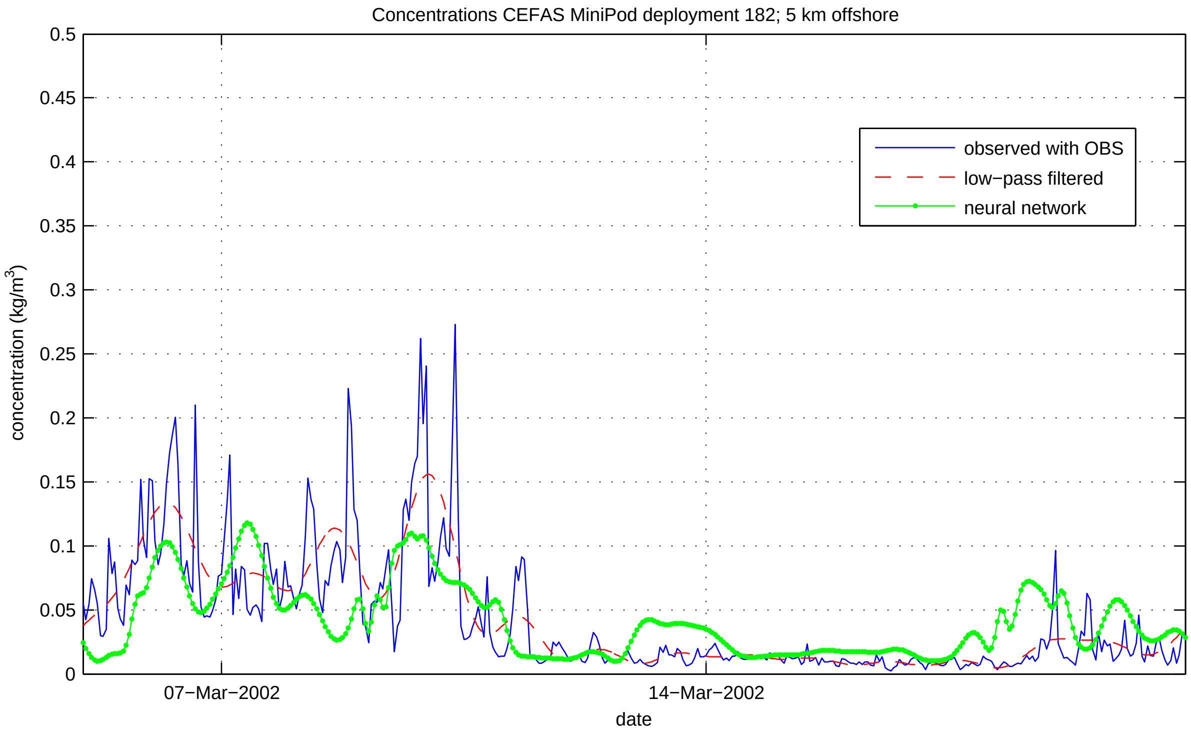

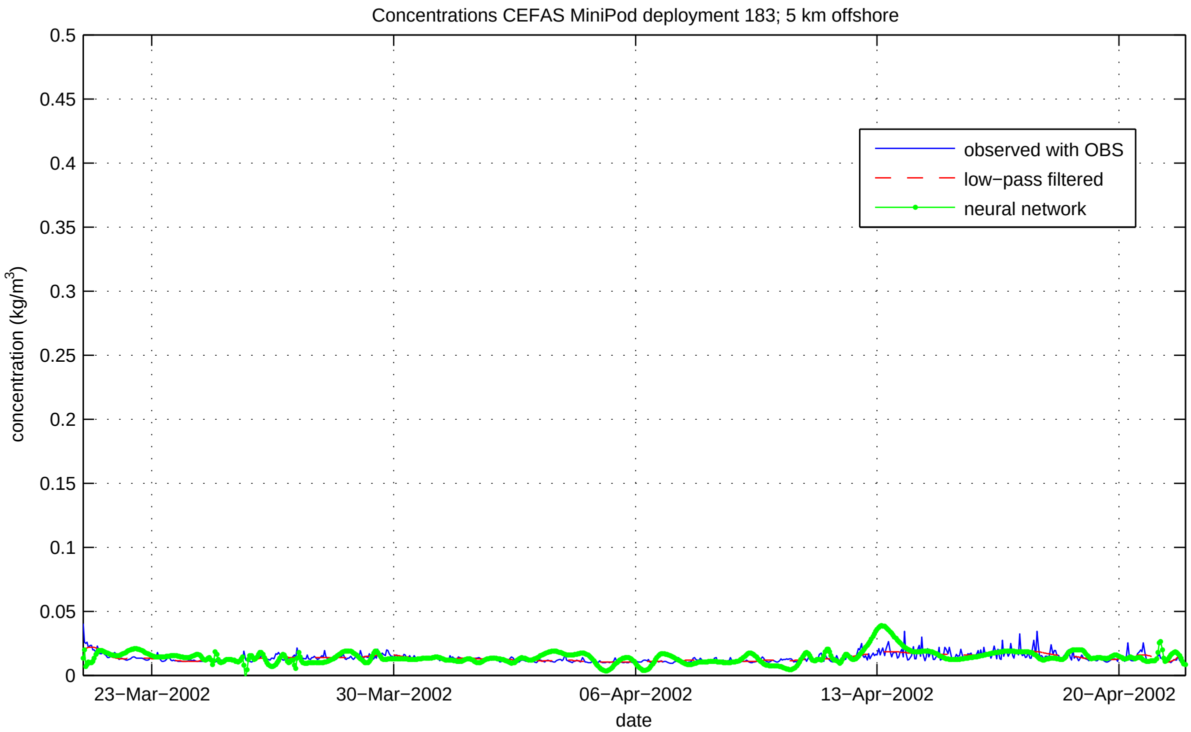

Measured, low−pass filtered and neural network predicted concentrations
using wave height, wave period and water depth as input
CEFAS Minipod deployment 182 and 183

CEFAS Minipod and Neural Network

Alkyon Hydraulic Consultancy & Research

A2273

Fig.2.36

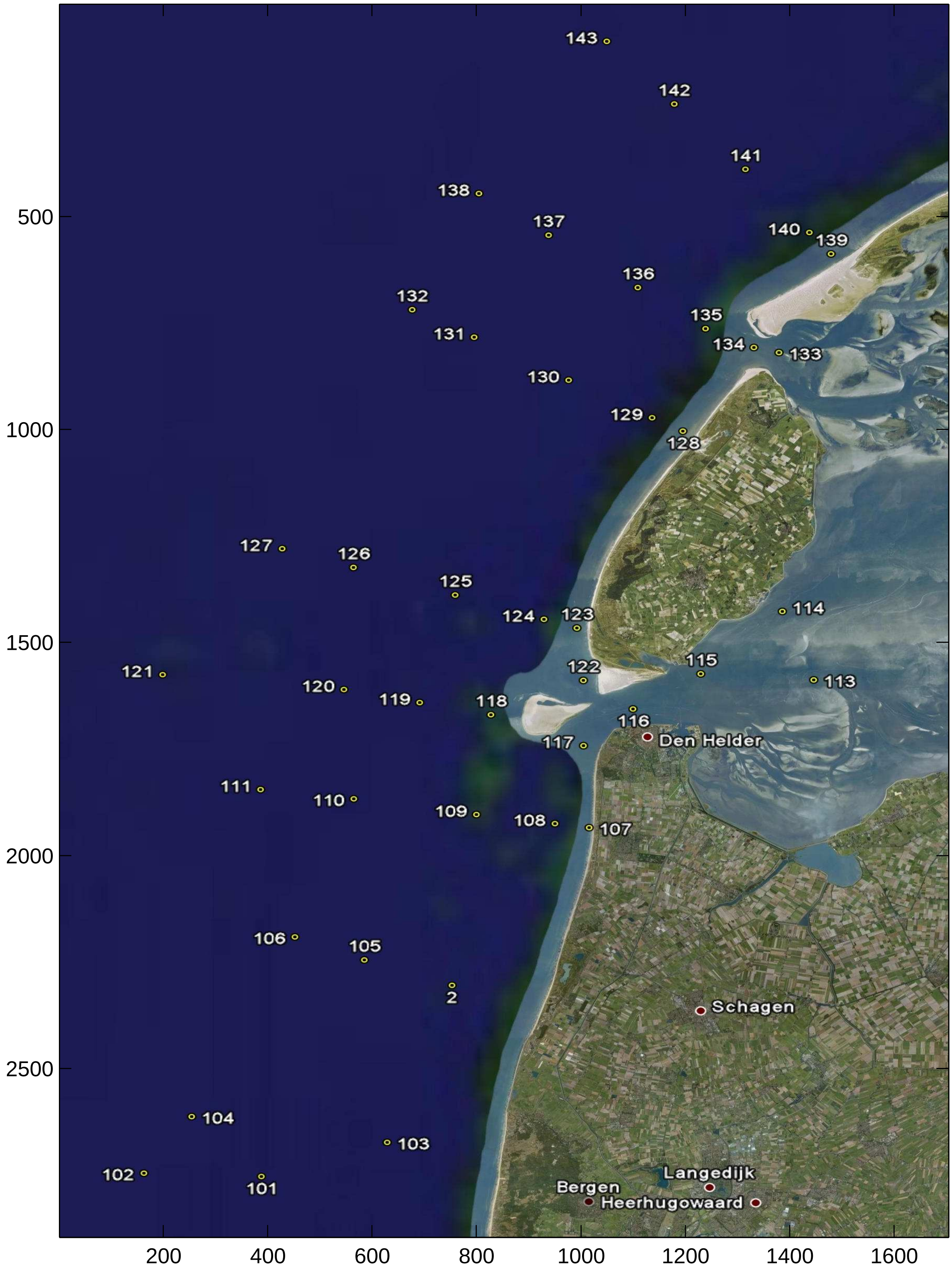

Locations T0 measurement campaign silt profiler observations 22−24 May 2007	Silt Profiler	
Alkyon Hydraulic Consultancy & Research	A2273	Fig.2.37

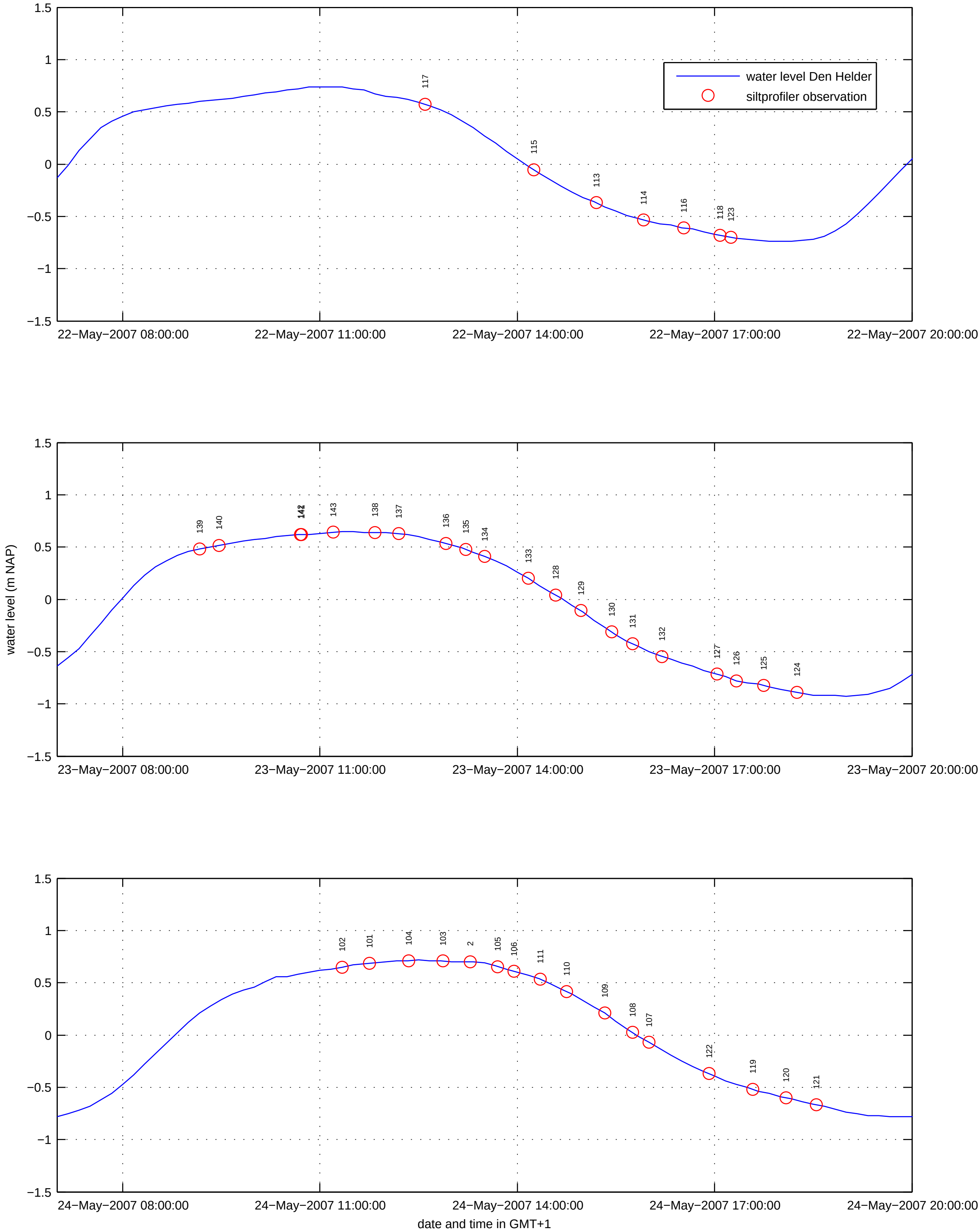

Date and time of T0 silt profiler measurements
using water level at Den Helder as reference
22−24 May 2007

Silt Profiler		
Alkyon Hydraulic Consultancy & Research	A2273	Fig.2.38

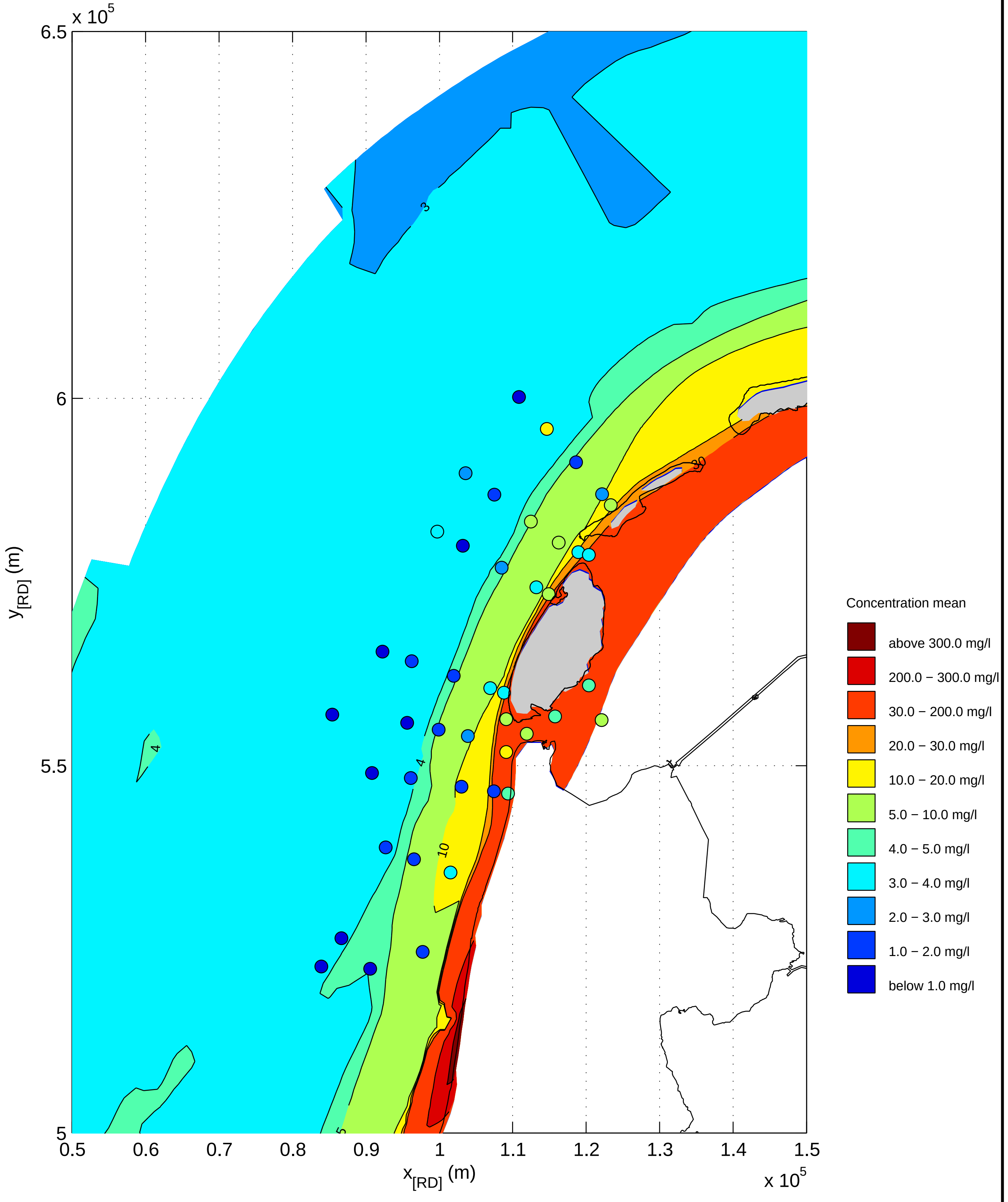

Mean of total suspended solids concentration (mg/l) filled contours present the interpolated 1975−1983 waterbase data coloured symbols present the T0 silt profiler data	1975−1983 and T0 2007	
Alkyon Hydraulic Consultancy & Research	A2273	Fig.2.39

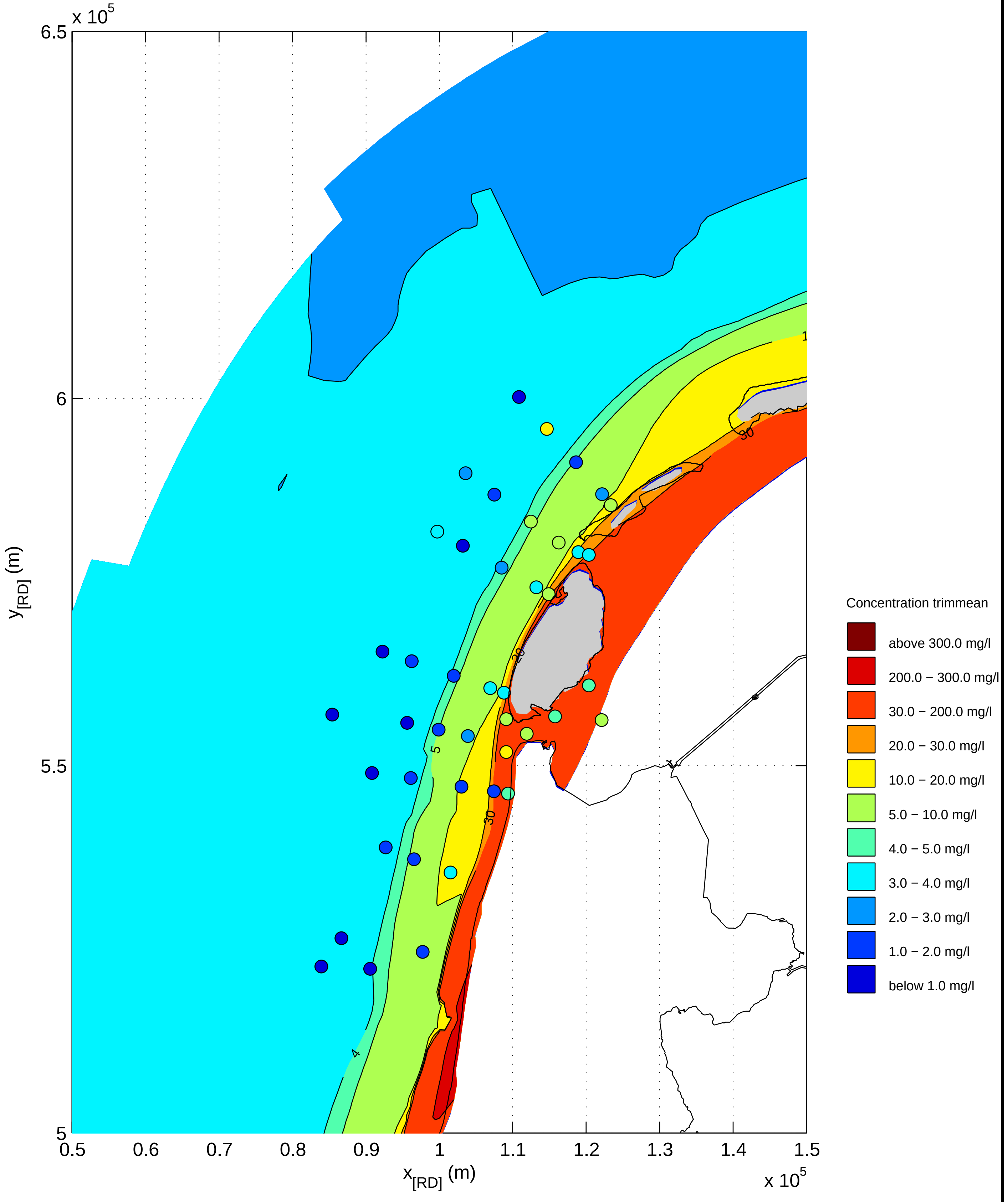

Trimmed mean of total suspended solids concentration (mg/l) filled contours present the interpolated 1975−1983 waterbase data coloured symbols present the T0 silt profiler data	1975−1983 and T0 2007	
Alkyon Hydraulic Consultancy & Research	A2273	Fig.2.40

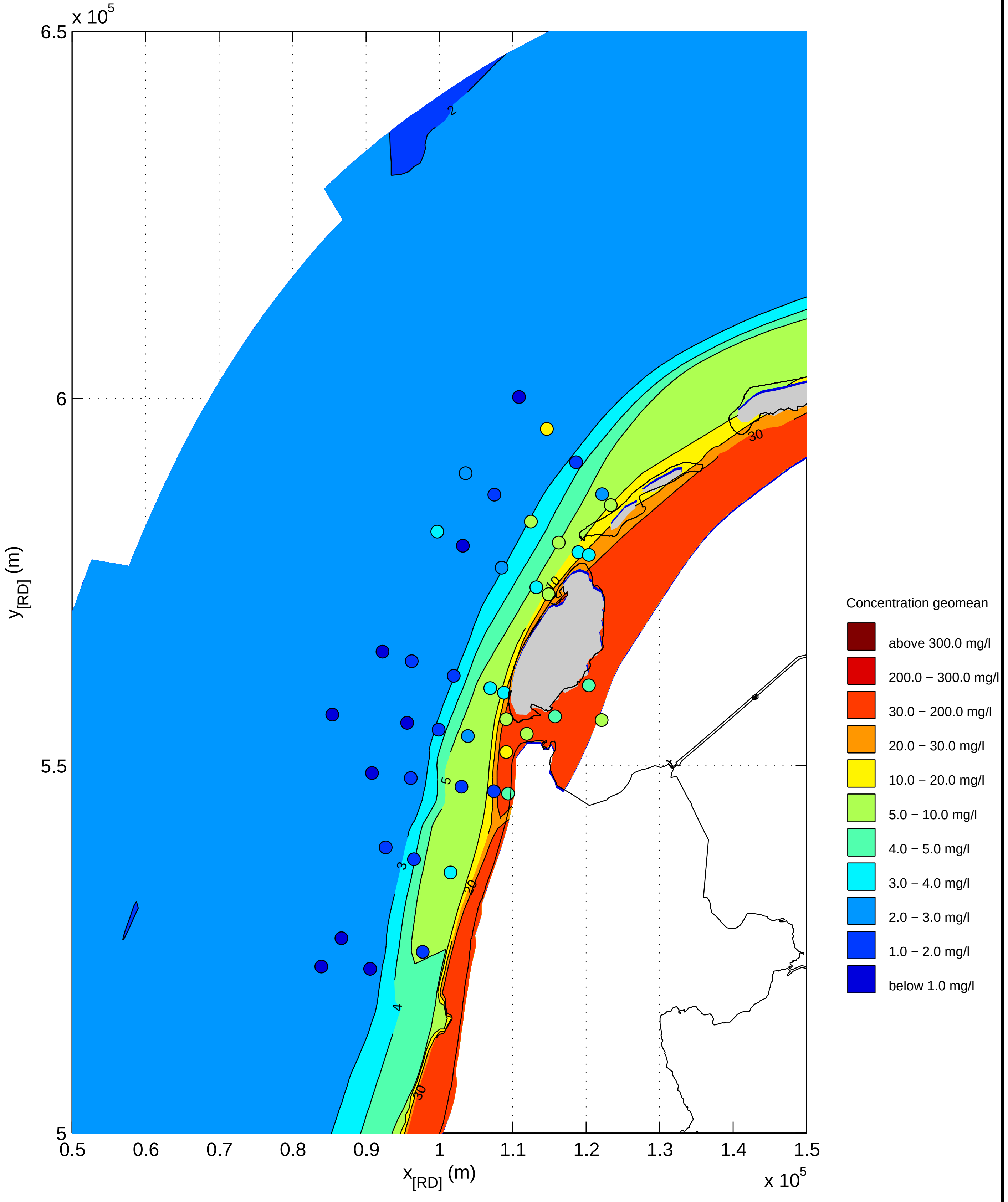

Geometric mean of total suspended solids concentration (mg/l) filled contours present the interpolated 1975−1983 waterbase data coloured symbols present the T0 silt profiler data	1975−1983 and T0 2007	
Alkyon Hydraulic Consultancy & Research	A2273	Fig.2.41

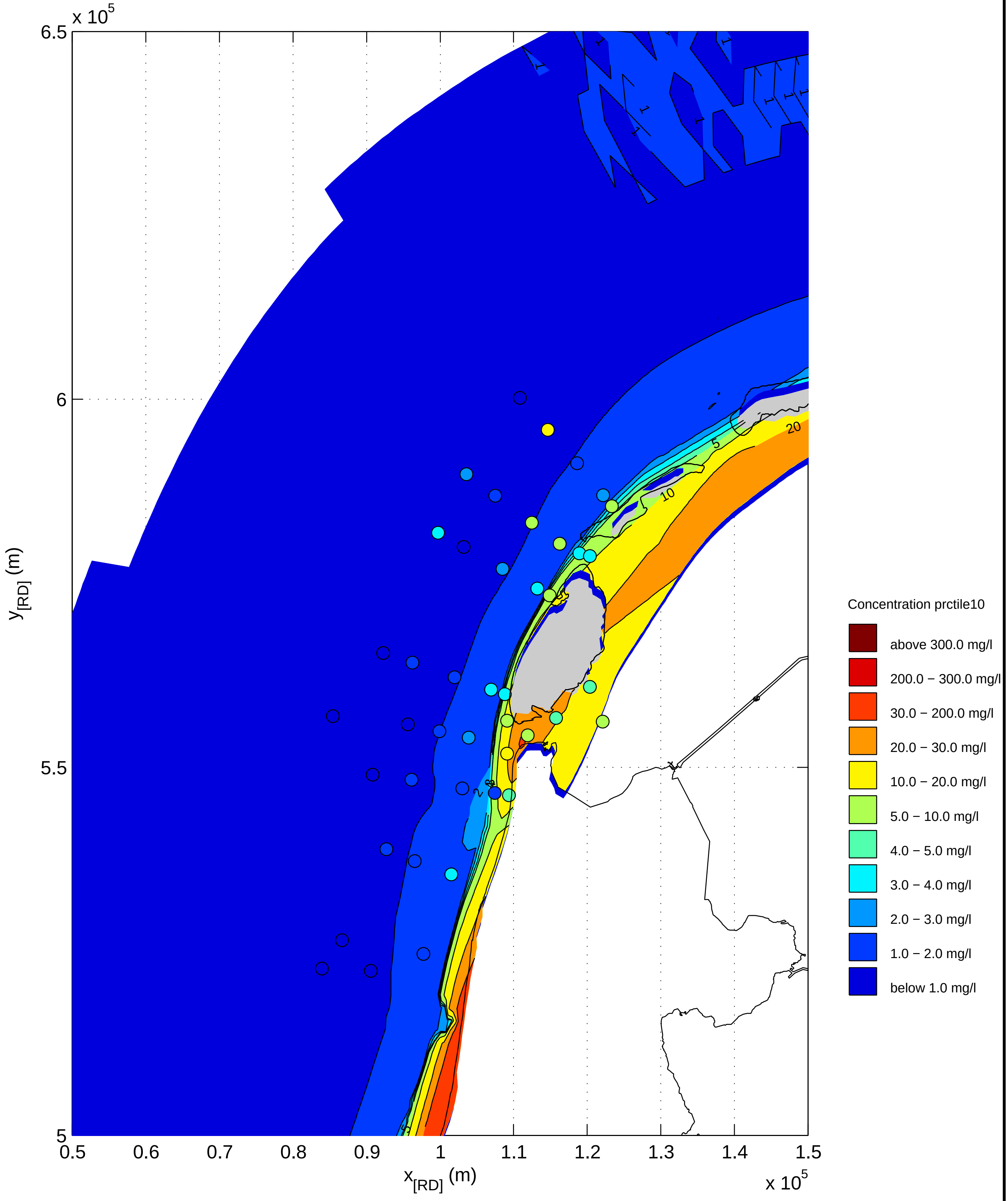

10^{th} percentile of total suspended solids concentration (mg/l) filled contours present the interpolated 1975−1983 waterbase data coloured symbols present the T0 silt profiler data	1975−1983 and T0 2007	
Alkyon Hydraulic Consultancy & Research	A2273	Fig.2.42

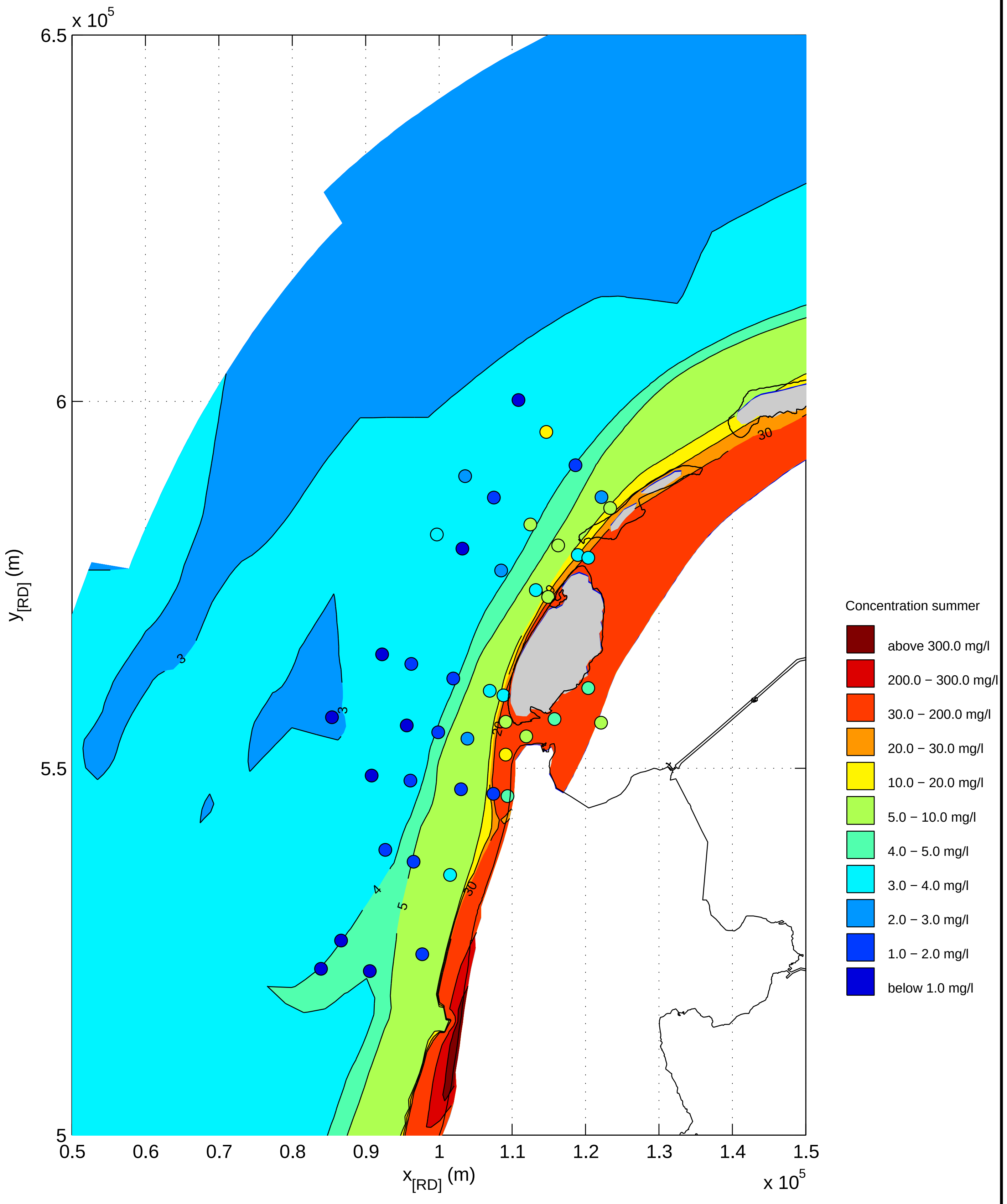

Summer mean of total suspended solids concentration (mg/l) filled contours present the interpolated 1975−1983 waterbase data coloured symbols present the T0 silt profiler data	1975−1983 and T0 2007	
Alkyon Hydraulic Consultancy & Research	A2273	Fig.2.43

Locations T1 measurement campaign silt profiler observations 17 September and 1 and 2 October 2007		
	Silt Profiler	
Alkyon Hydraulic Consultancy & Research	A2273	Fig. 2.44

plot_waterlevels_sepoct2007

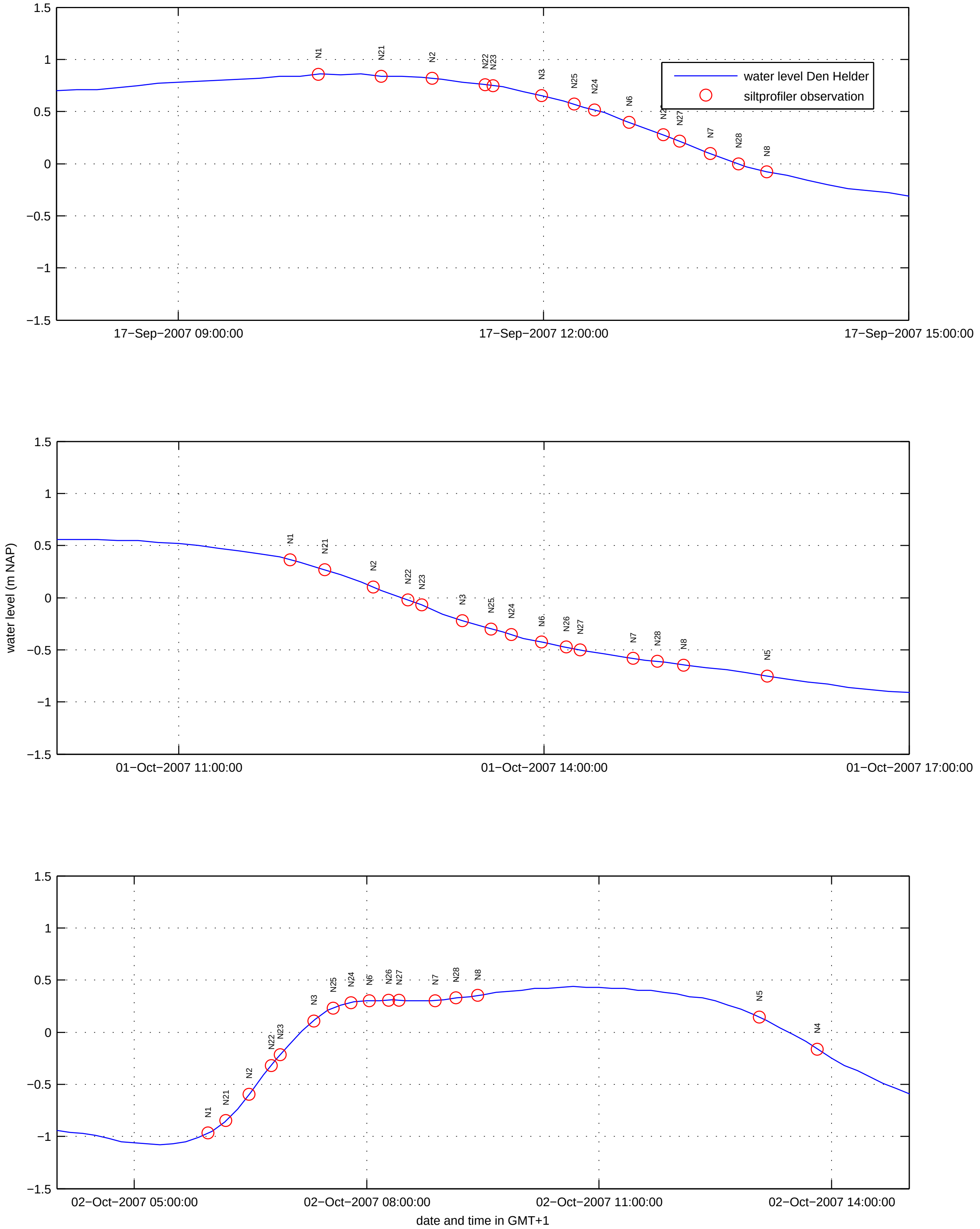

Date and time of T0 silt profiler measurements
using water level at Den Helder as reference
17 September and 1 and 2 October 2007

Silt Profiler

Alkyon Hydraulic Consultancy & Research

A2273

Fig. 2.45

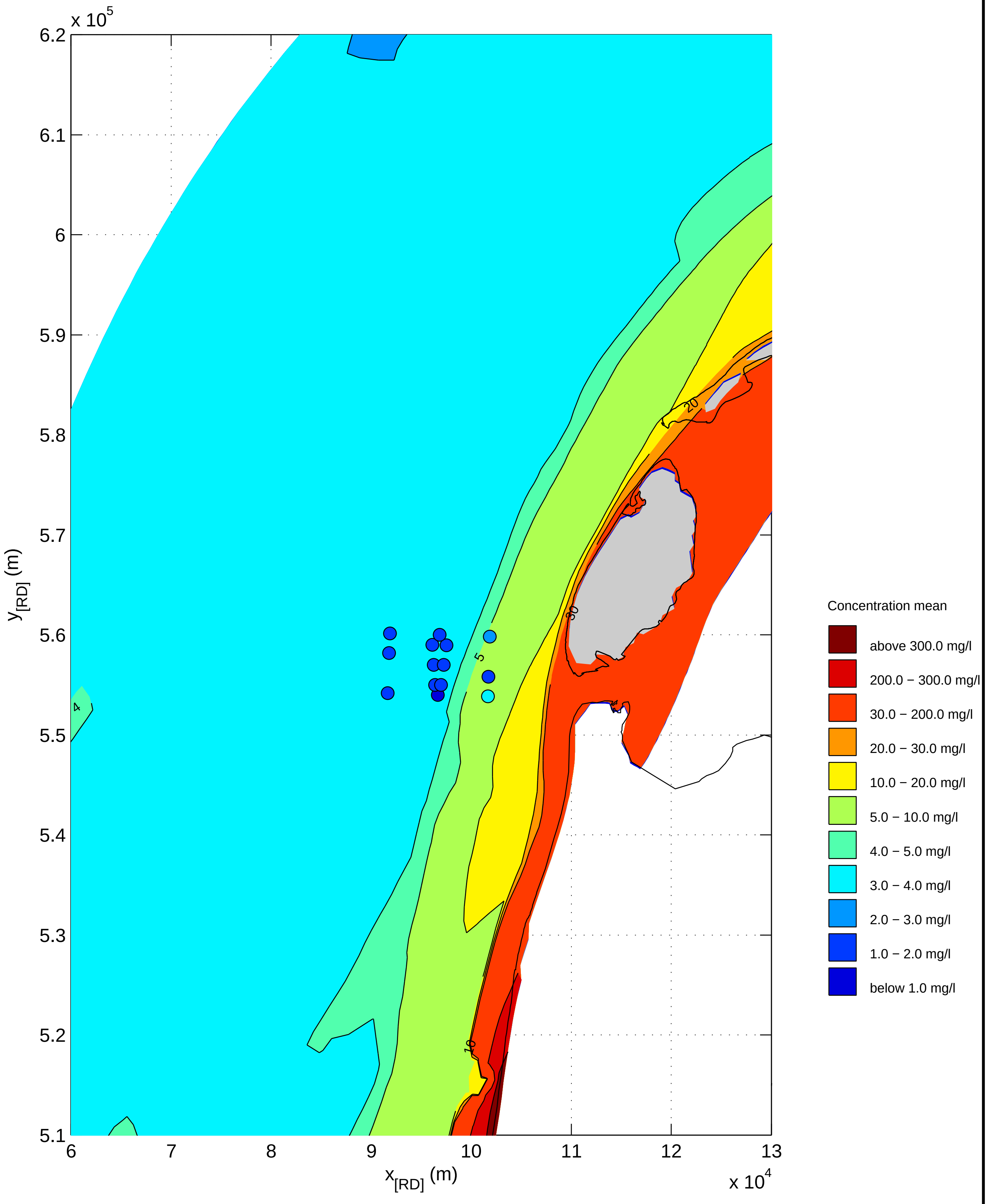

Mean of total suspended solids concentration (mg/l) filled contours present the interpolated 1975−1983 waterbase data coloured symbols present the T1 silt profiler data on 17 September 2007	1975−1983 and T1 2007	
Alkyon Hydraulic Consultancy & Research	A2273	Fig. 2.46

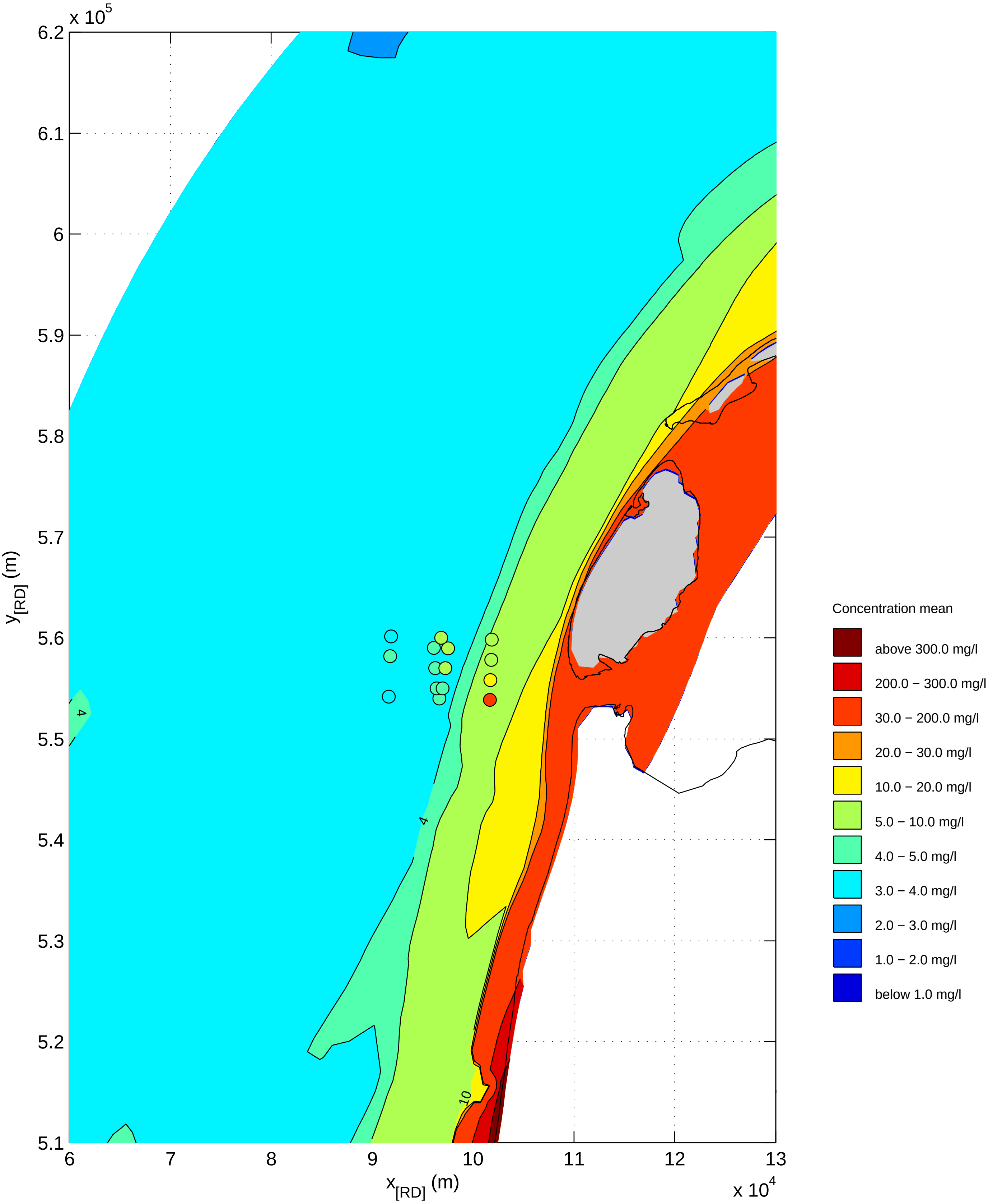

Mean of total suspended solids concentration (mg/l) filled contours present the interpolated 1975−1983 waterbase data coloured symbols present the T1 silt profiler data on 1 October 2007	1975−1983 and T1 2007	
Alkyon Hydraulic Consultancy & Research	A2273	Fig. 2.47

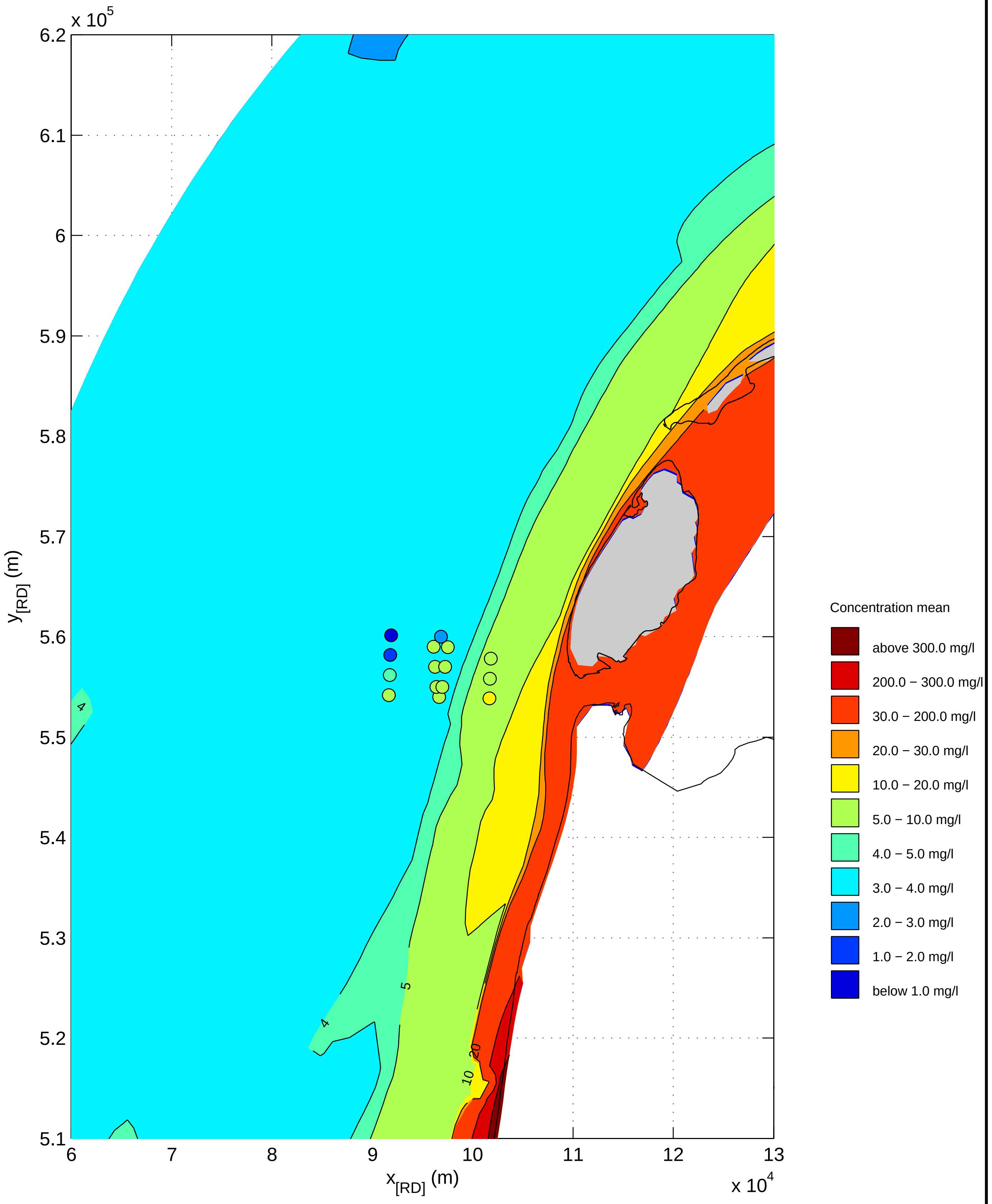

Mean of total suspended solids concentration (mg/l) filled contours present the interpolated 1975−1983 waterbase data coloured symbols present the T1 silt profiler data on 2 October 2007	1975−1983 and T1 2007	
Alkyon Hydraulic Consultancy & Research	A2273	Fig. 2.48

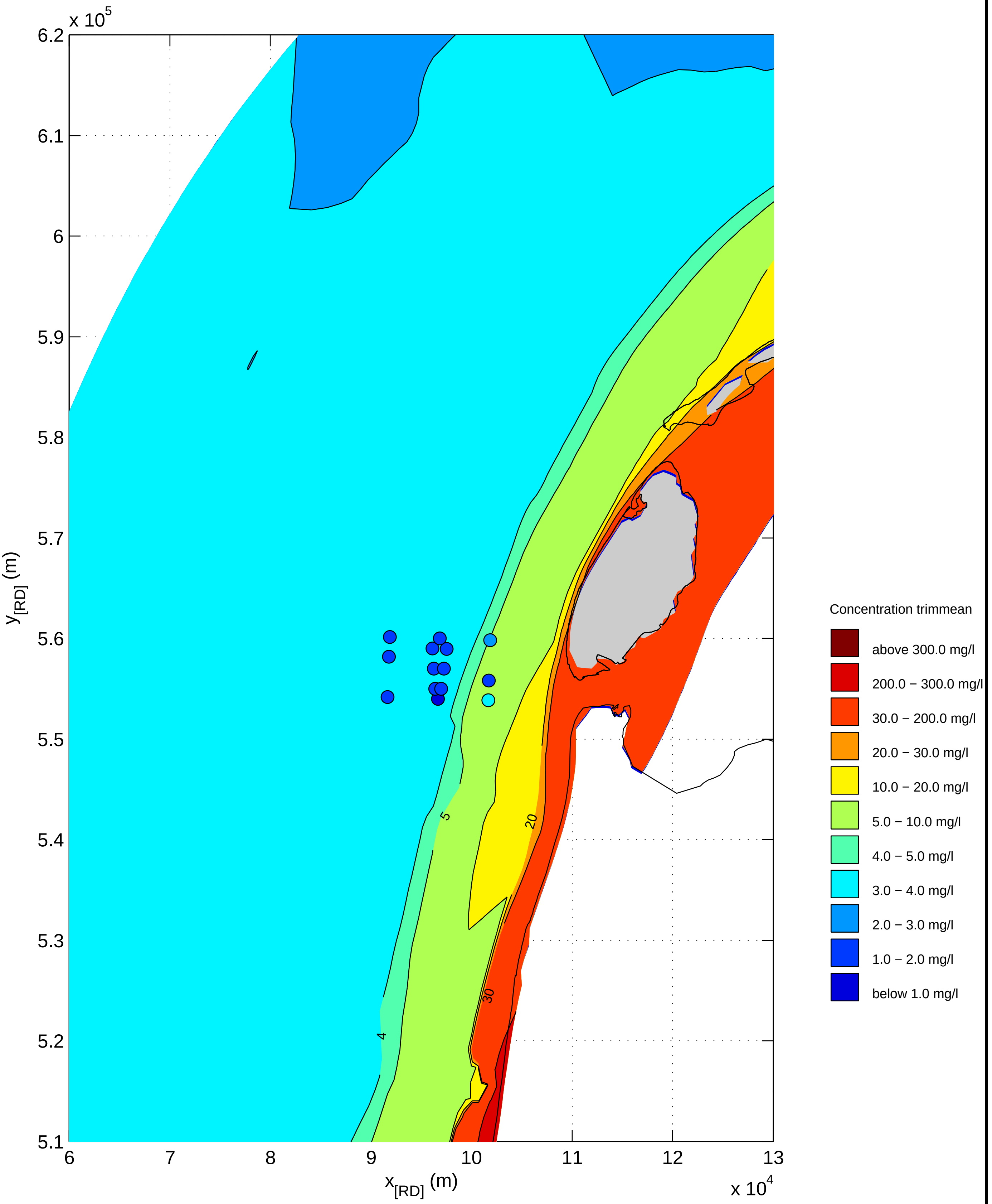

Trimmed mean of total suspended solids concentration (mg/l) filled contours present the interpolated 1975−1983 waterbase data coloured symbols present the T1 silt profiler data on 17 September 2007	1975−1983 and T1 2007	
Alkyon Hydraulic Consultancy & Research	A2273	Fig. 2.49

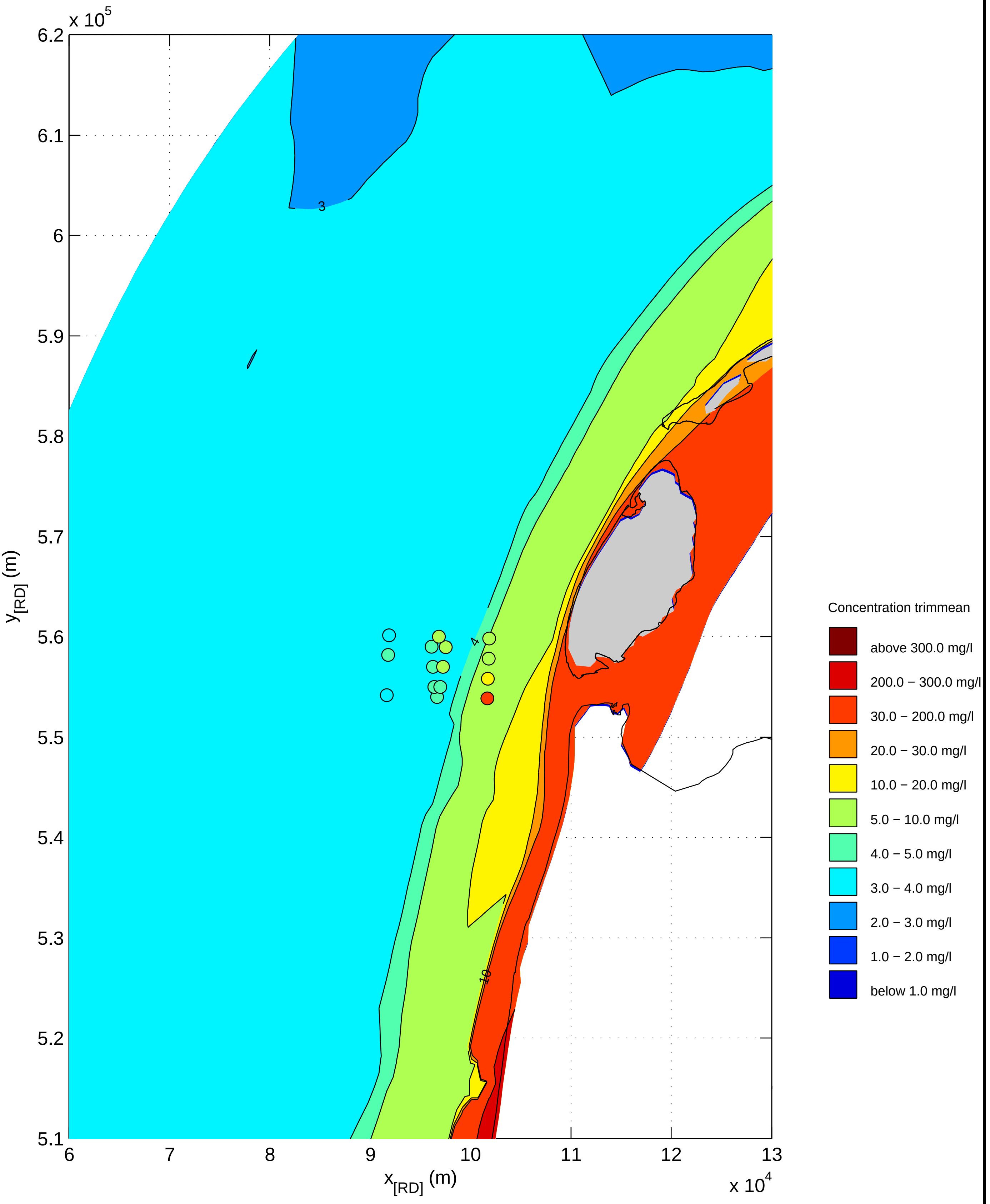

Trimmed mean of total suspended solids concentration (mg/l) filled contours present the interpolated 1975−1983 waterbase data coloured symbols present the T1 silt profiler data on 1 October 2007	1975−1983 and T1 2007	
Alkyon Hydraulic Consultancy & Research	A2273	Fig. 2.50

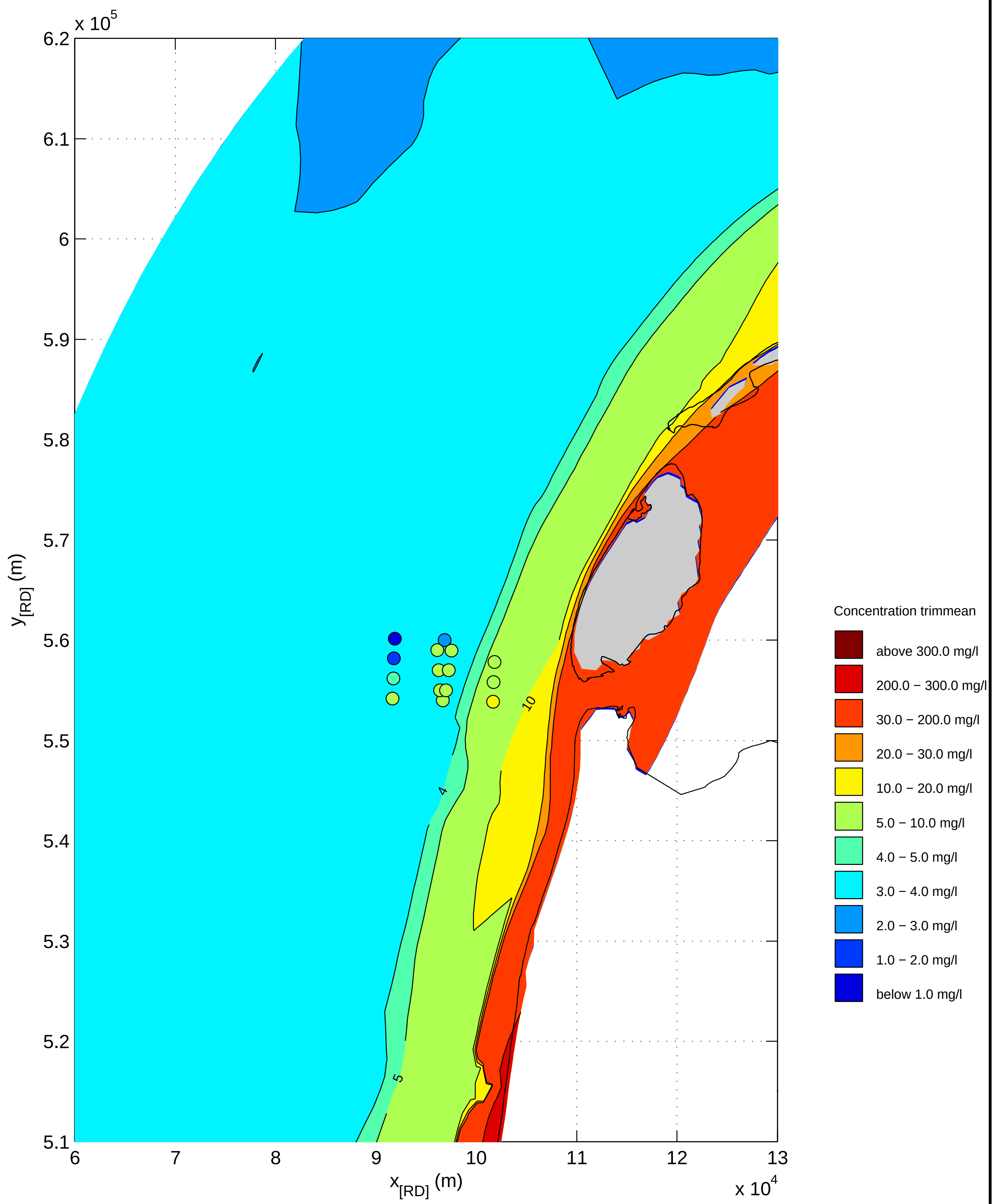

Trimmed mean of total suspended solids concentration (mg/l) filled contours present the interpolated 1975−1983 waterbase data coloured symbols present the T1 silt profiler data on 2 October 2007	1975−1983 and T1 2007	
Alkyon Hydraulic Consultancy & Research	A2273	Fig. 2.51

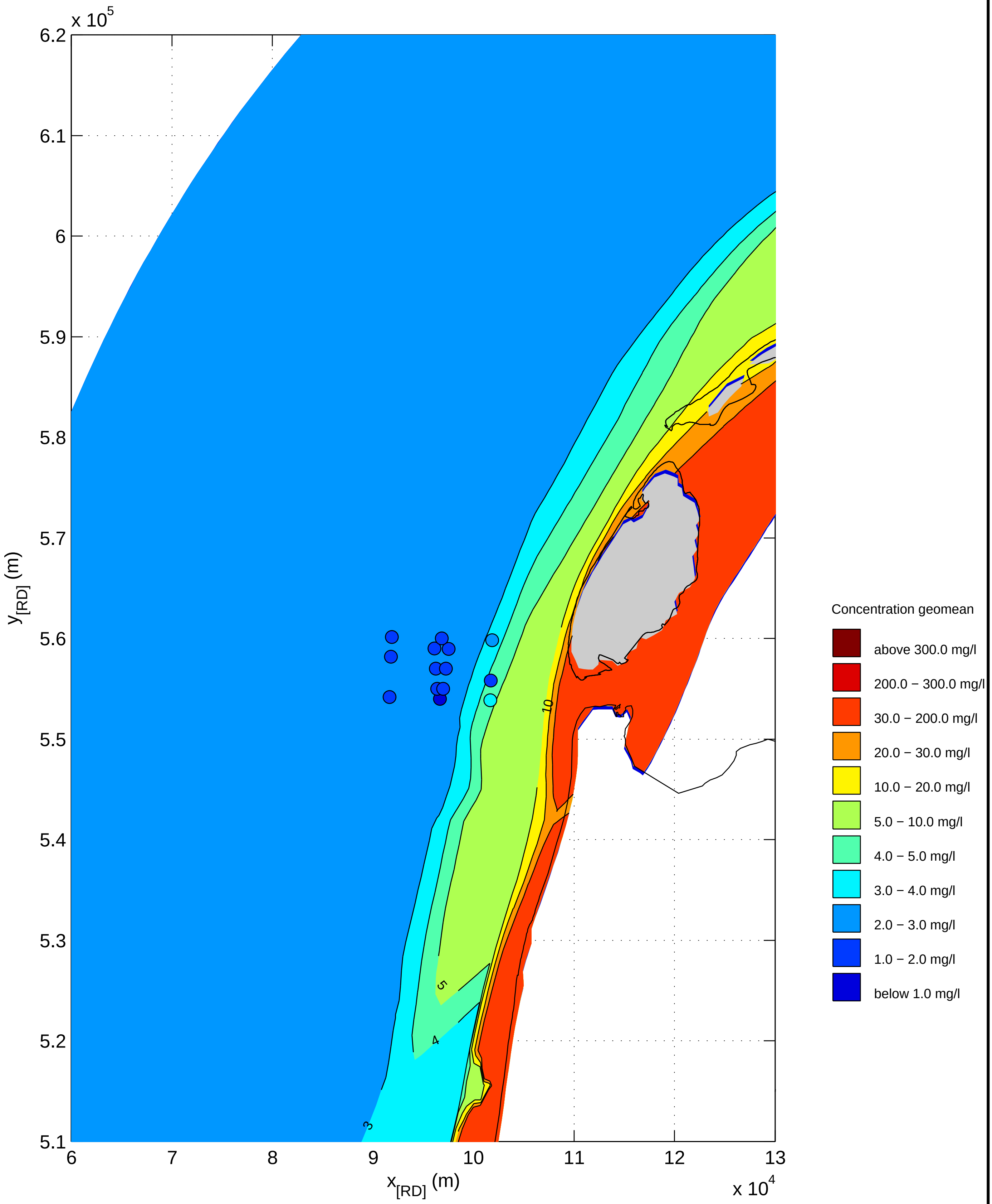

Geometric mean of total suspended solids concentration (mg/l) filled contours present the interpolated 1975−1983 waterbase data coloured symbols present the T1 silt profiler data on 17 September 2007	1975−1983 and T1 2007	
Alkyon Hydraulic Consultancy & Research	A2273	Fig. 2.52

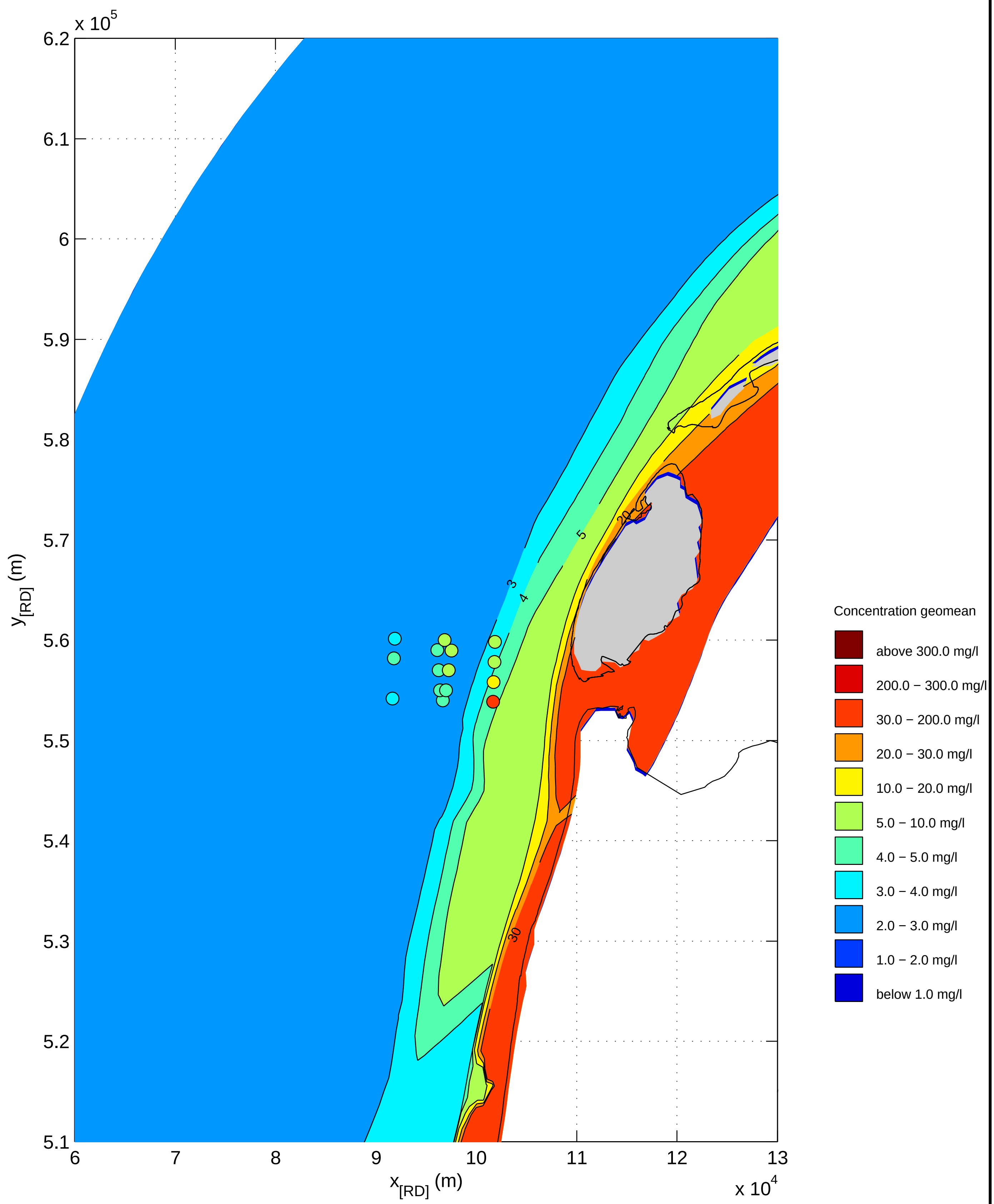

Geometric mean of total suspended solids concentration (mg/l) filled contours present the interpolated 1975−1983 waterbase data coloured symbols present the T1 silt profiler data on 1 October 2007	1975−1983 and T1 2007	
Alkyon Hydraulic Consultancy & Research	A2273	Fig. 2.53

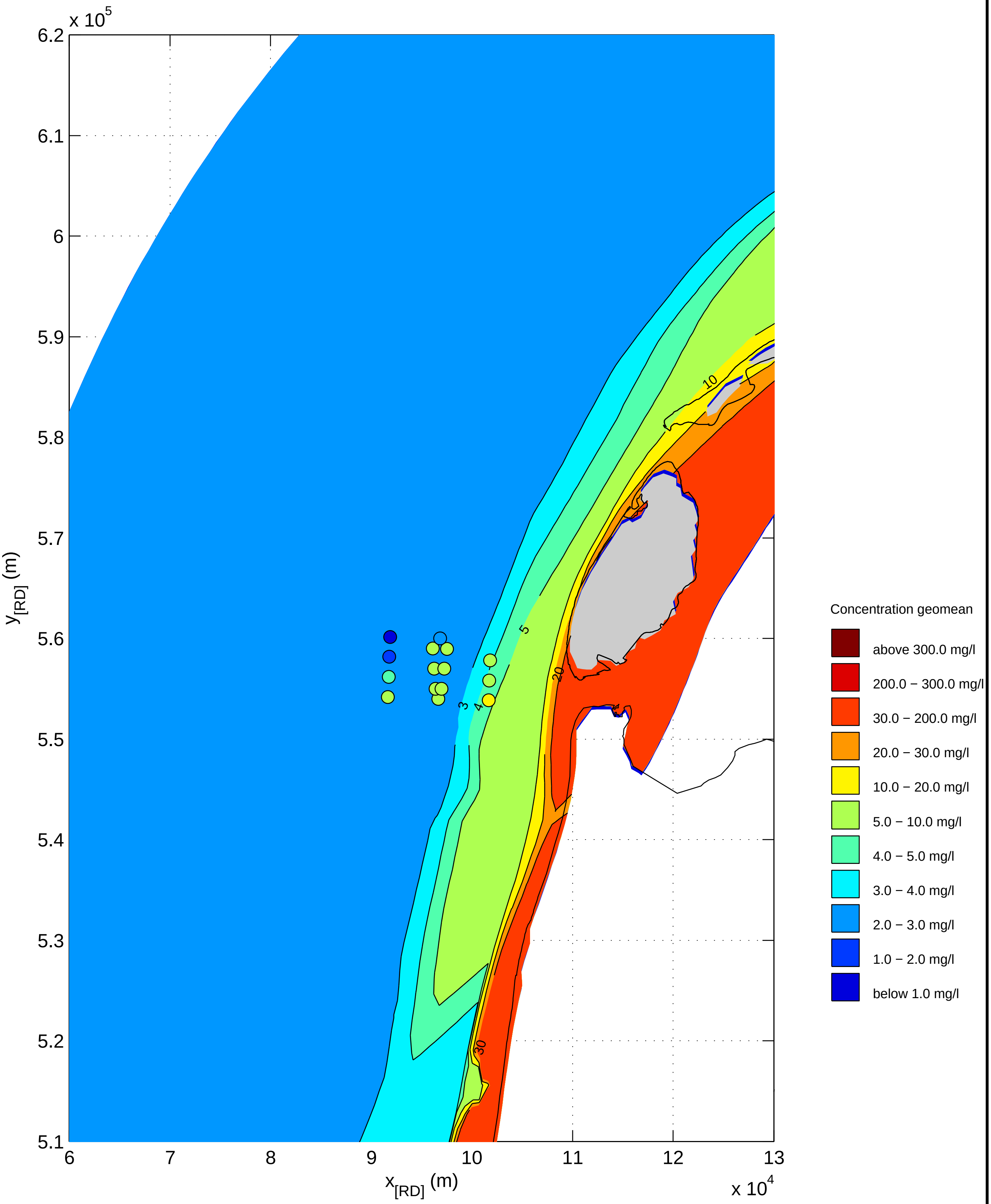

Geometric mean of total suspended solids concentration (mg/l) filled contours present the interpolated 1975−1983 waterbase data coloured symbols present the T1 silt profiler data on 2 October 2007	1975−1983 and T1 2007	
Alkyon Hydraulic Consultancy & Research	A2273	Fig. 2.54

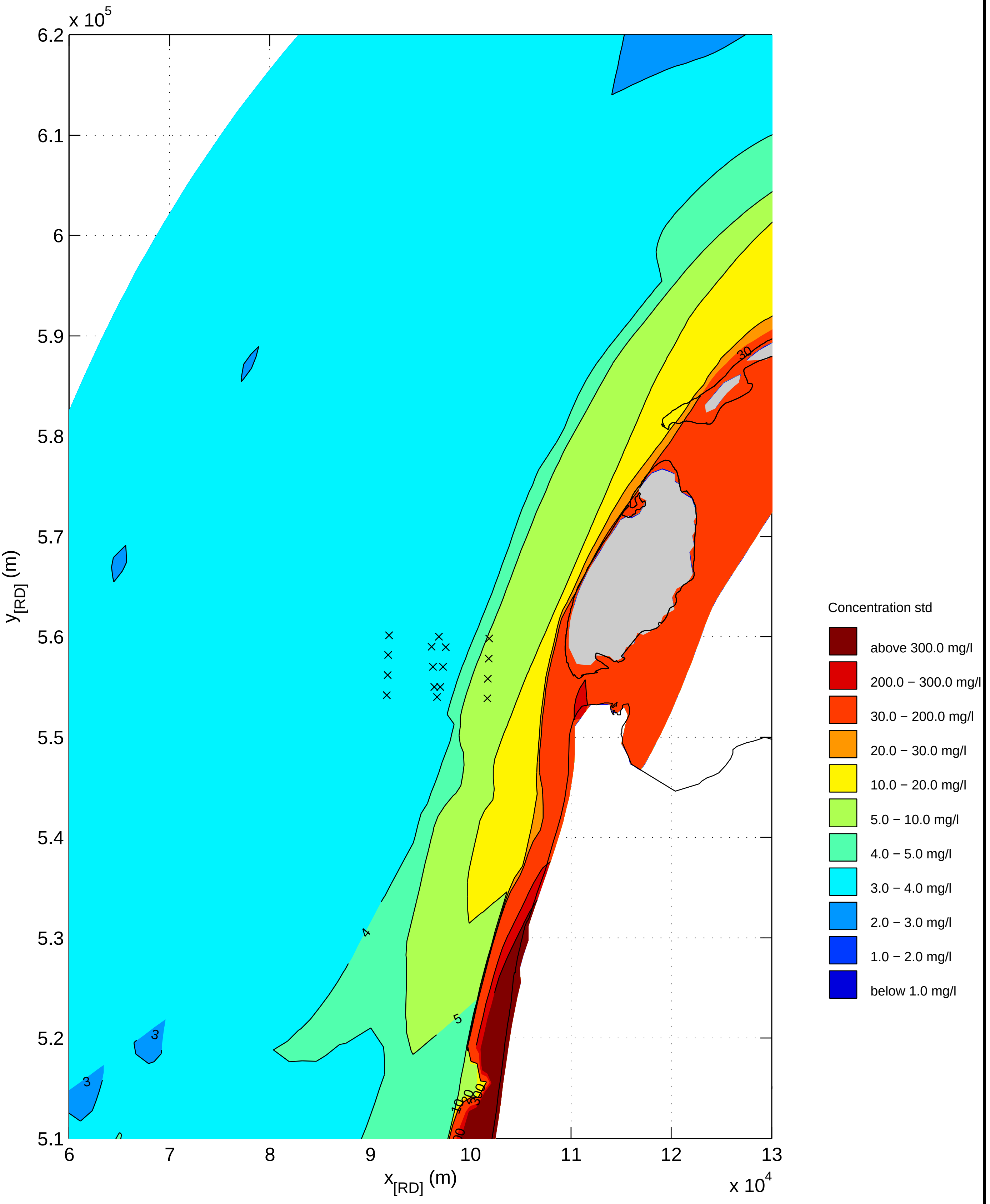

Standard deviation of total suspended solids concentration (mg/l)
filled contours present the interpolated 1975−1983 waterbase data
x−marks denote locations of T1 observations on 17 Sep, 1 Oct and 2 Oct 2007

Standard deviation of total suspended solids concentration (mg/l) filled contours present the interpolated 1975−1983 waterbase data x−marks denote locations of T1 observations on 17 Sep, 1 Oct and 2 Oct 2007	1975−1983 and T1 2007	
Alkyon Hydraulic Consultancy & Research	A2273	Fig. 2.55

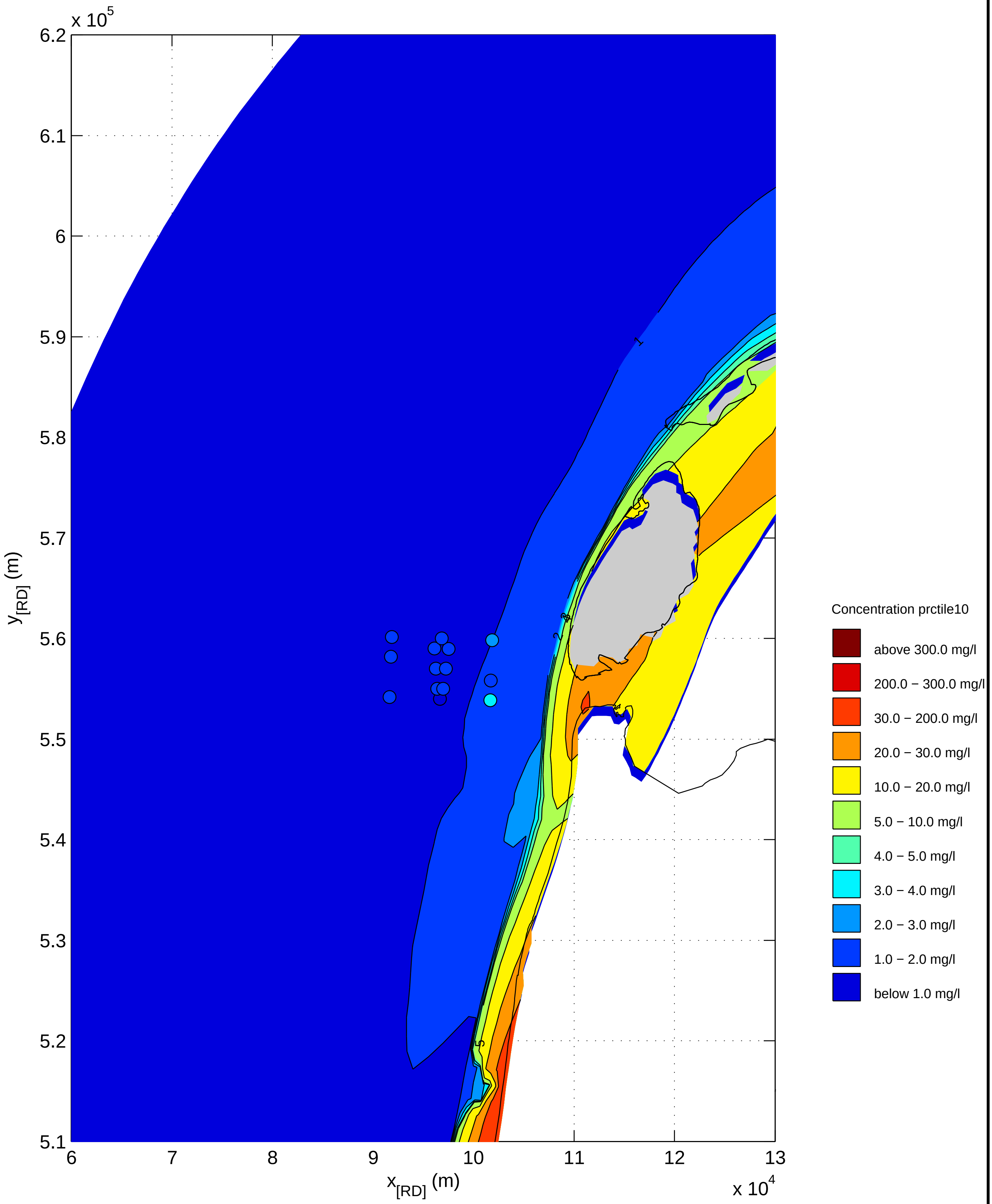

10th percentile of total suspended solids concentration (mg/l) filled contours present the interpolated 1975−1983 waterbase data coloured symbols present the T1 silt profiler data on 17 September 2007	1975−1983 and T1 2007	
Alkyon Hydraulic Consultancy & Research	A2273	Fig. 2.56

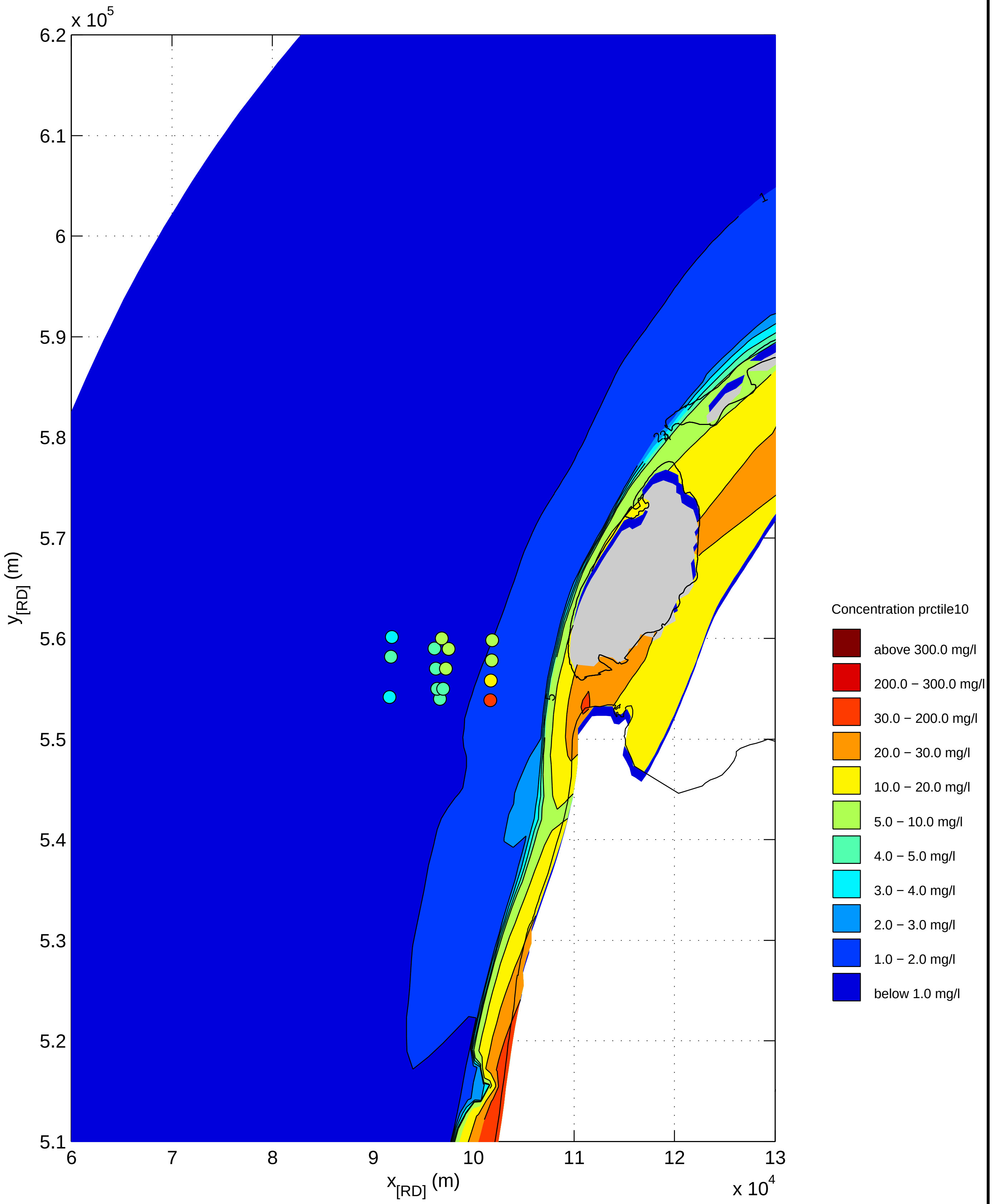

10th percentile of total suspended solids concentration (mg/l) filled contours present the interpolated 1975−1983 waterbase data coloured symbols present the T1 silt profiler data on 1 October 2007	1975−1983 and T1 2007	
Alkyon Hydraulic Consultancy & Research	A2273	Fig. 2.57

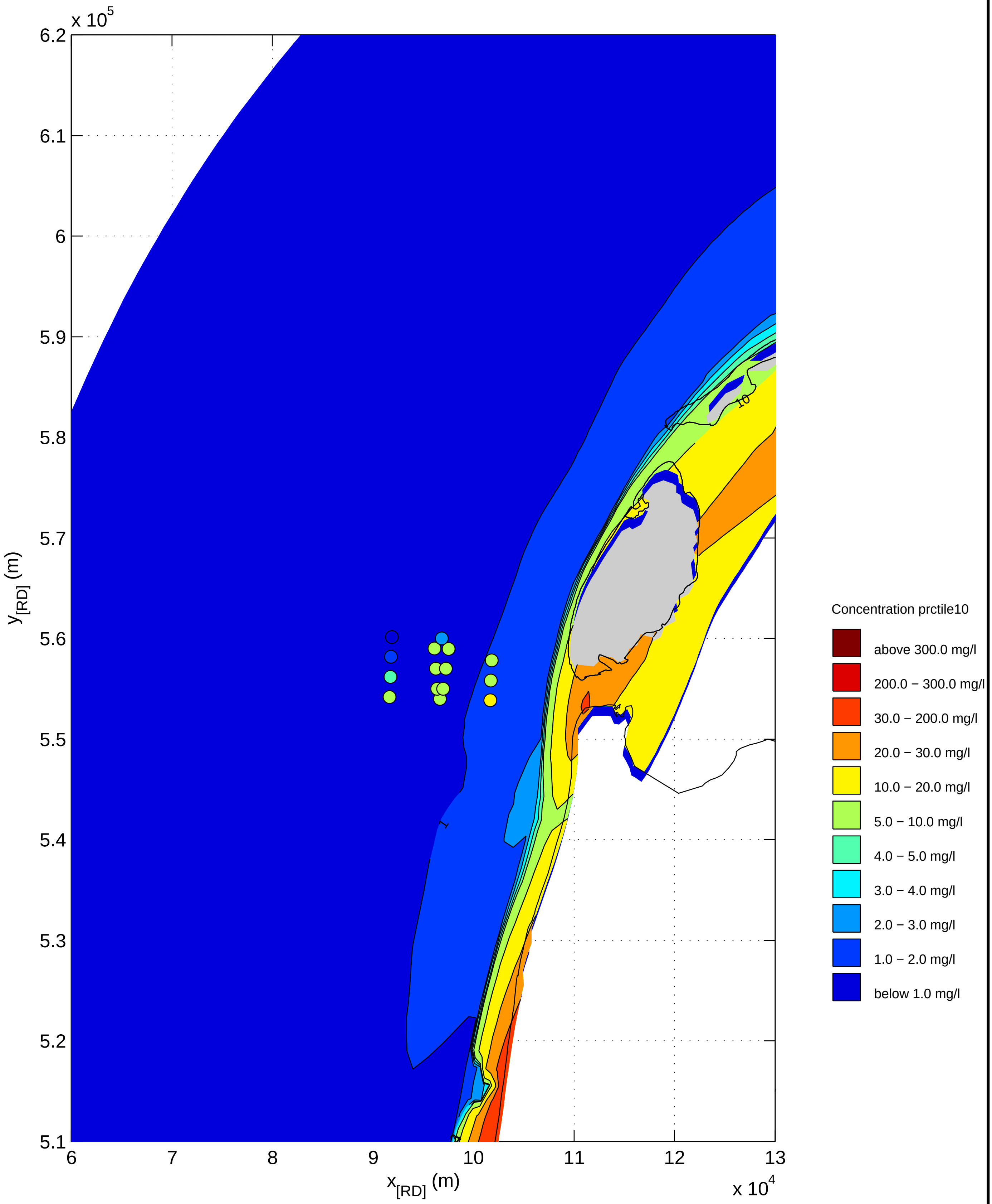

10^{th} percentile of total suspended solids concentration (mg/l) filled contours present the interpolated 1975−1983 waterbase data coloured symbols present the T1 silt profiler data on 2 October 2007	1975−1983 and T1 2007	
Alkyon Hydraulic Consultancy & Research	A2273	Fig. 2.58

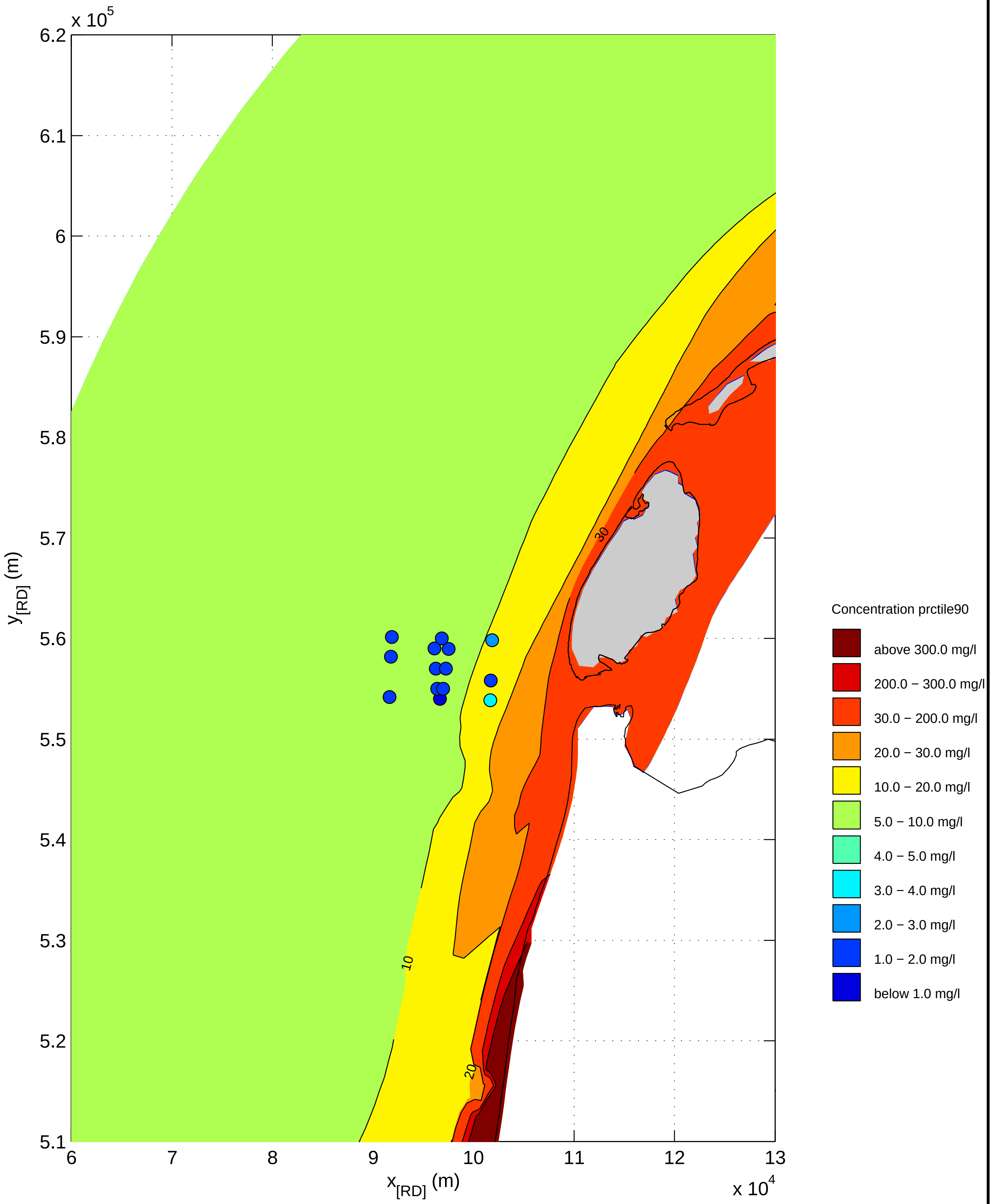

50th percentile (median) of total suspended solids concentration (mg/l) filled contours present the interpolated 1975−1983 waterbase data coloured symbols present the T1 silt profiler data on 17 September 2007	1975−1983 and T1 2007	
Alkyon Hydraulic Consultancy & Research	A2273	Fig. 2.59

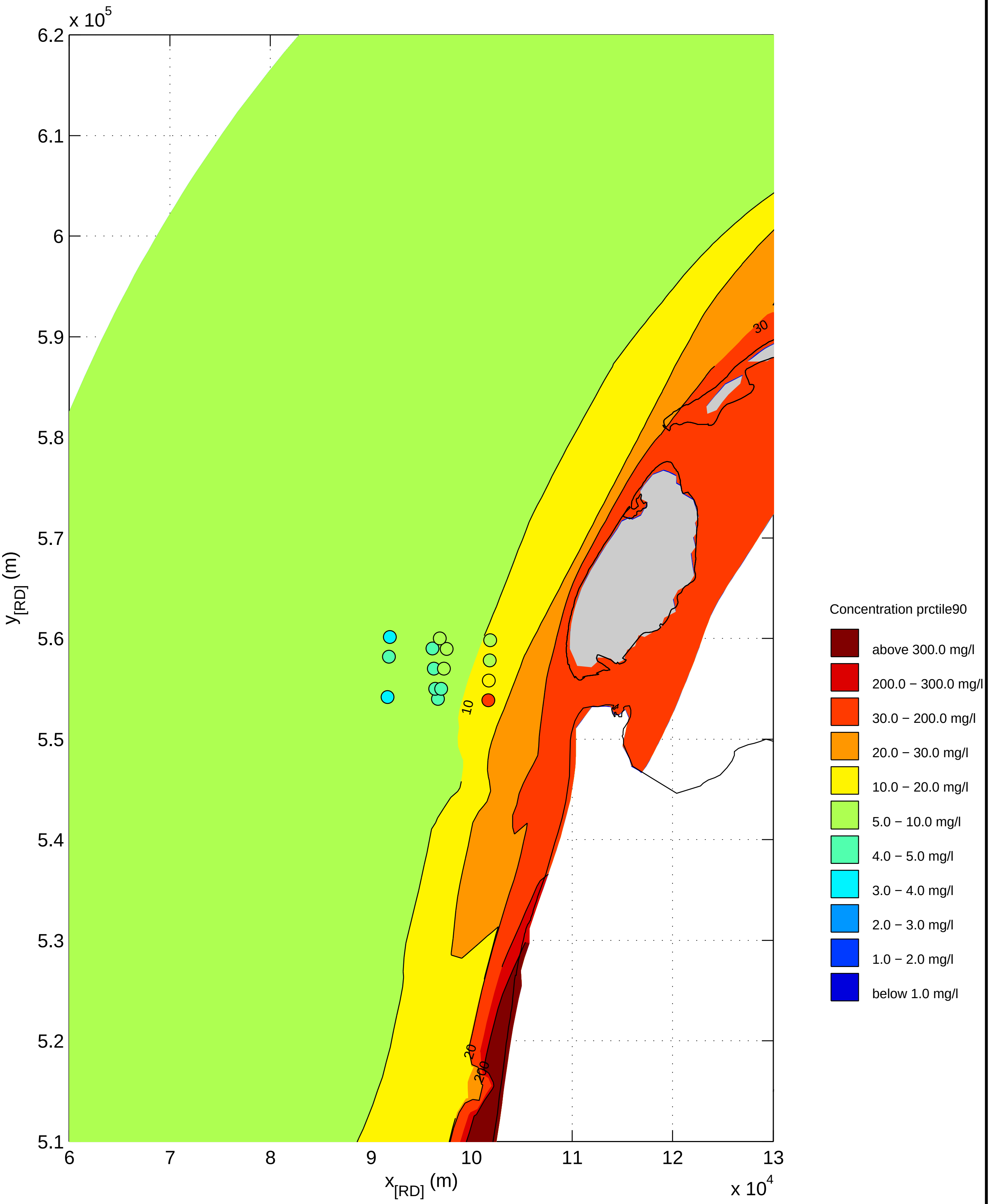

50th percentile (median) of total suspended solids concentration (mg/l) filled contours present the interpolated 1975−1983 waterbase data coloured symbols present the T1 silt profiler data on 1 October 2007	1975−1983 and T1 2007	
Alkyon Hydraulic Consultancy & Research	A2273	Fig. 2.60

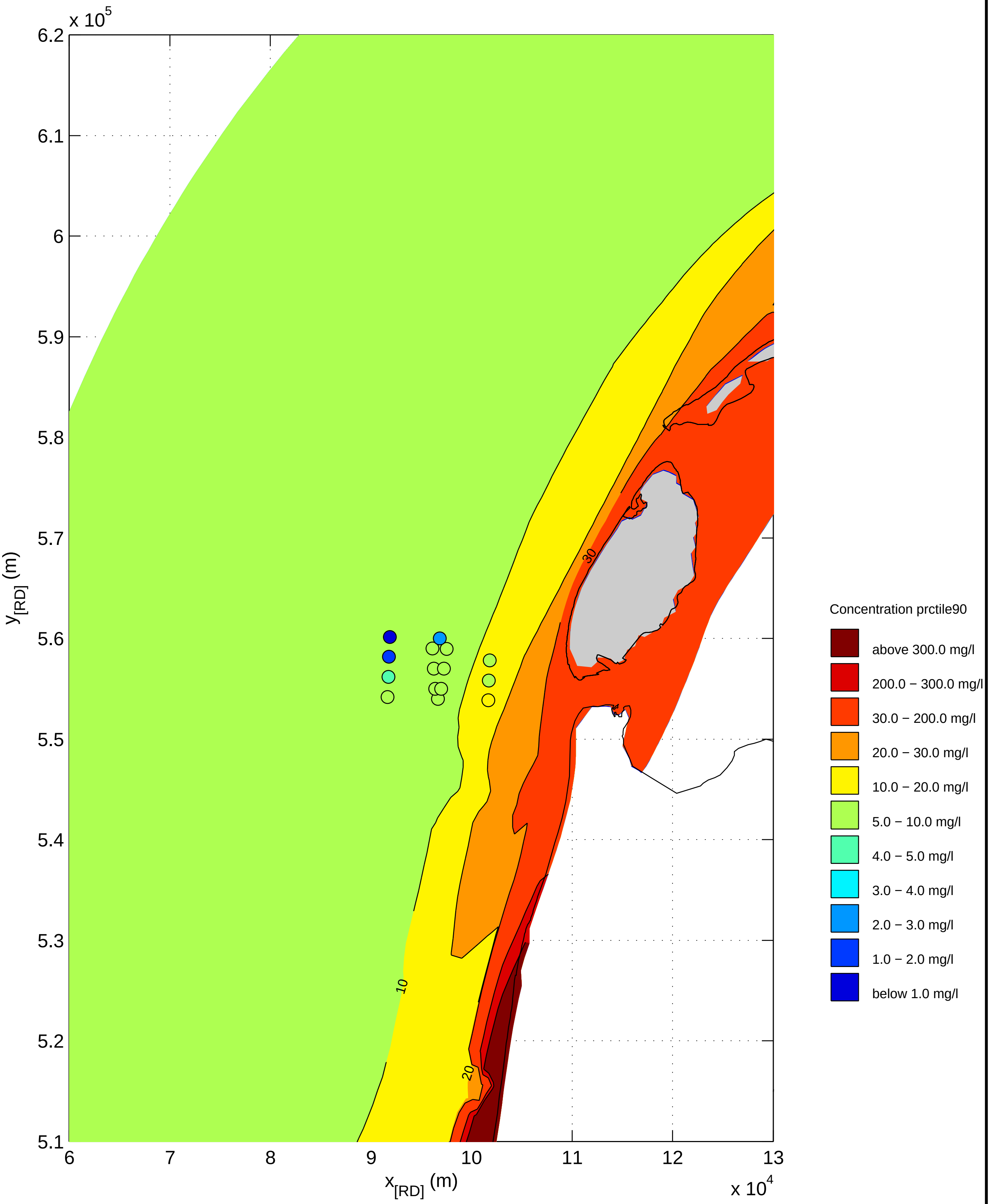

50th percentile (median) of total suspended solids concentration (mg/l) filled contours present the interpolated 1975−1983 waterbase data coloured symbols present the T1 silt profiler data on 2 October 2007	1975−1983 and T1 2007	
Alkyon Hydraulic Consultancy & Research	A2273	Fig. 2.61

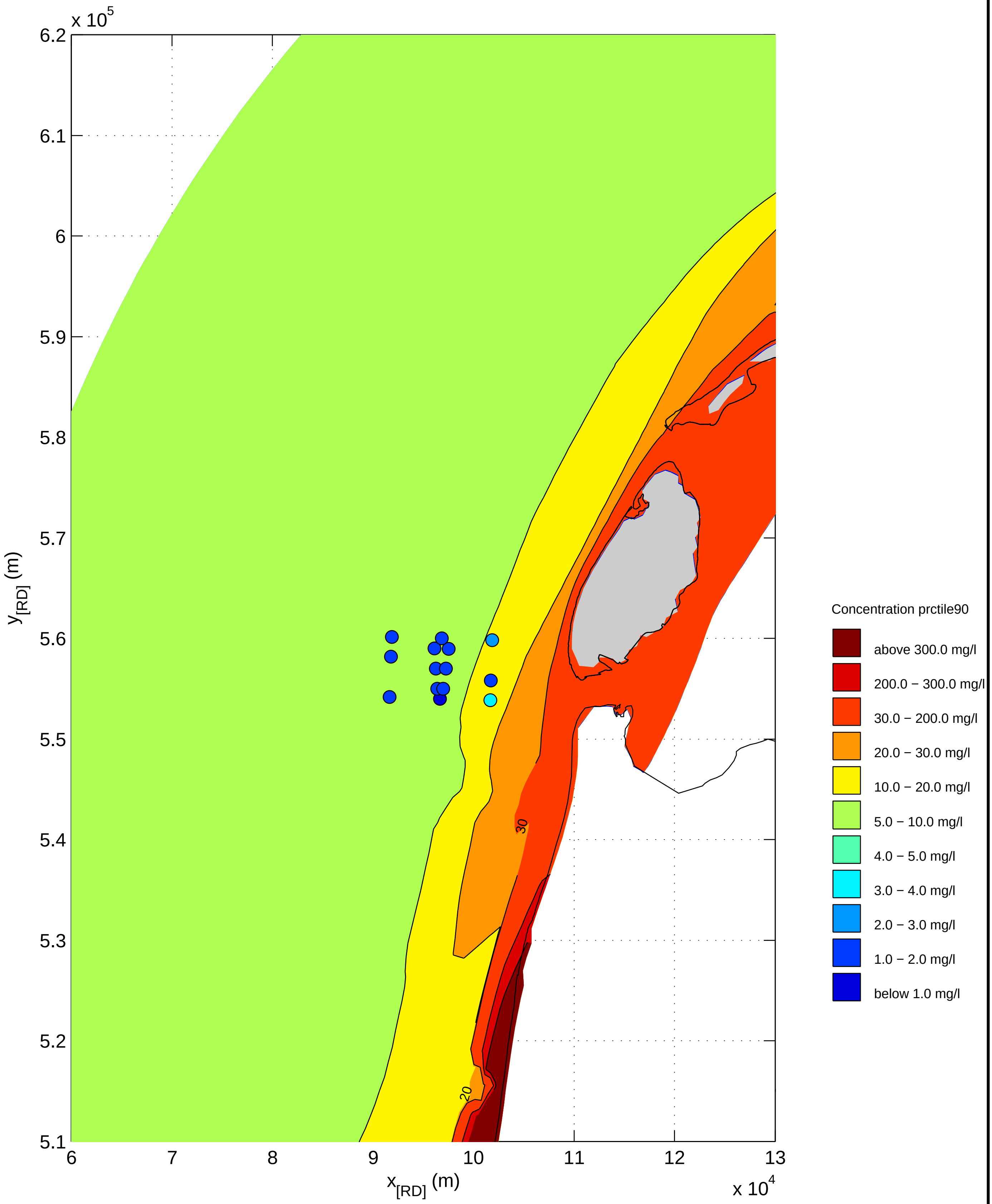

90th percentile of total suspended solids concentration (mg/l) filled contours present the interpolated 1975−1983 waterbase data coloured symbols present the T1 silt profiler data on 17 September 2007	1975−1983 and T1 2007	
Alkyon Hydraulic Consultancy & Research	A2273	Fig. 2.62

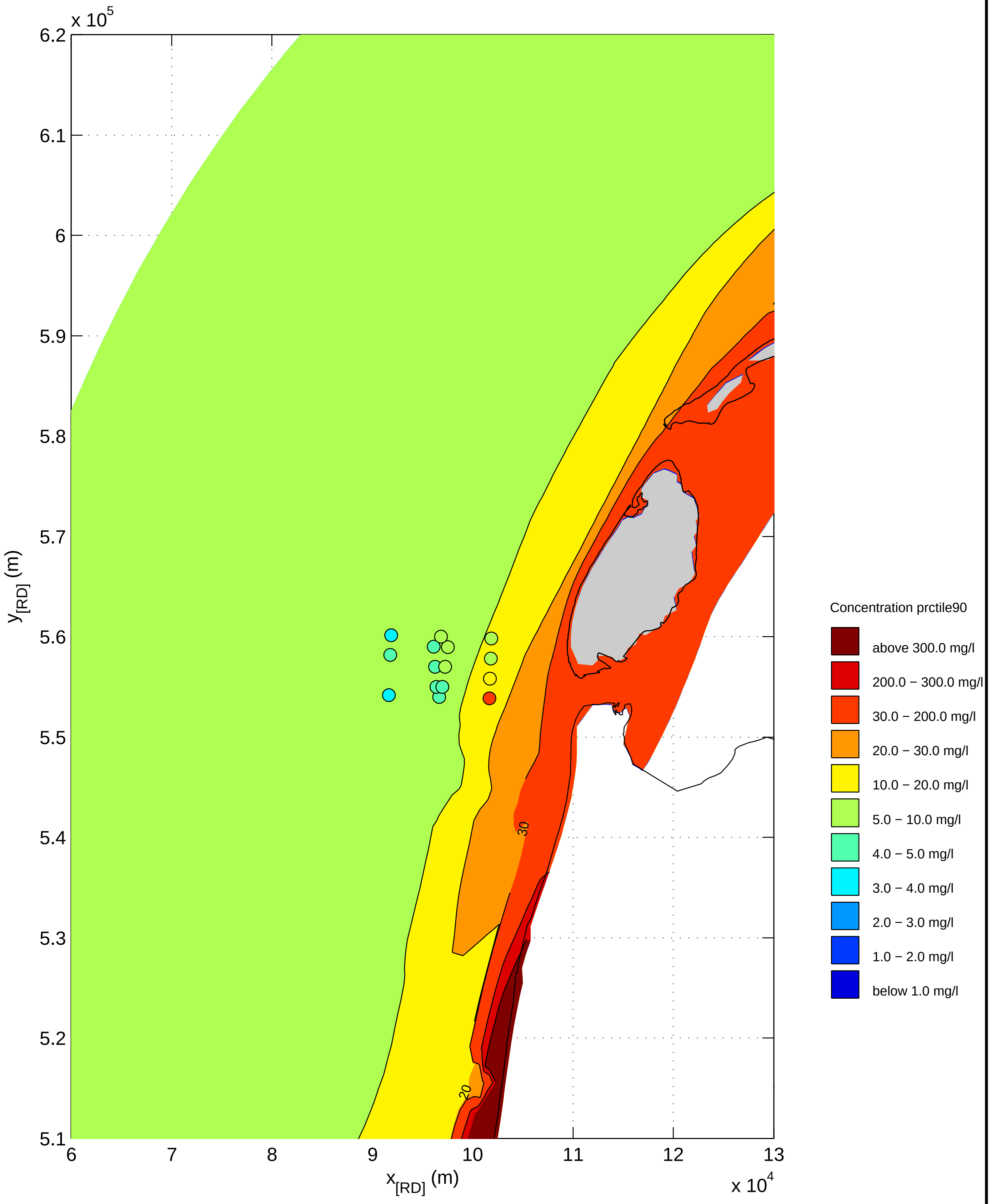

90^{th} percentile of total suspended solids concentration (mg/l) filled contours present the interpolated 1975−1983 waterbase data coloured symbols present the T1 silt profiler data on 1 October 2007	1975−1983 and T1 2007	
Alkyon Hydraulic Consultancy & Research	A2273	Fig. 2.63

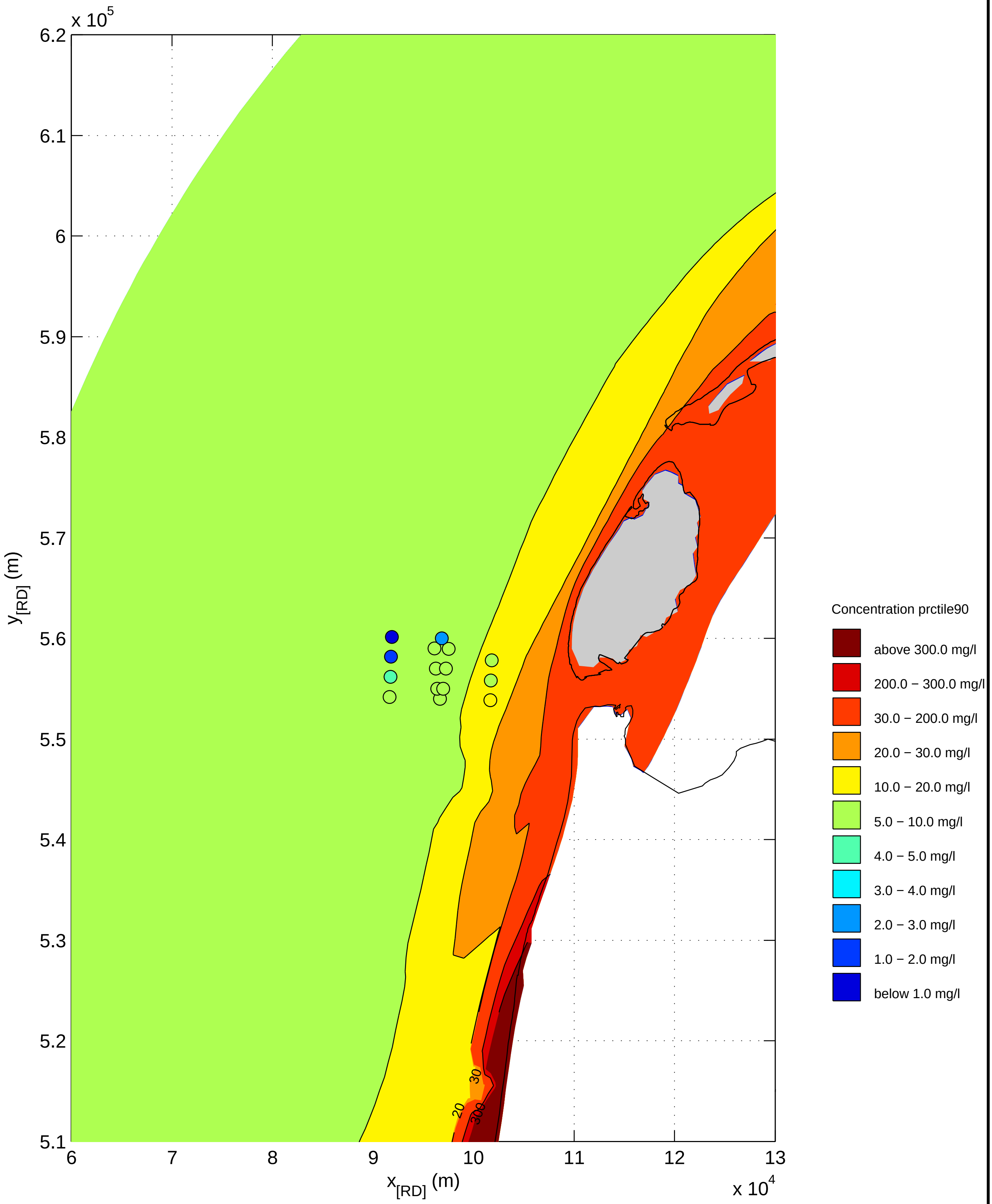

90th percentile of total suspended solids concentration (mg/l) filled contours present the interpolated 1975−1983 waterbase data coloured symbols present the T1 silt profiler data on 2 October 2007	1975−1983 and T1 2007	
Alkyon Hydraulic Consultancy & Research	A2273	Fig. 2.64

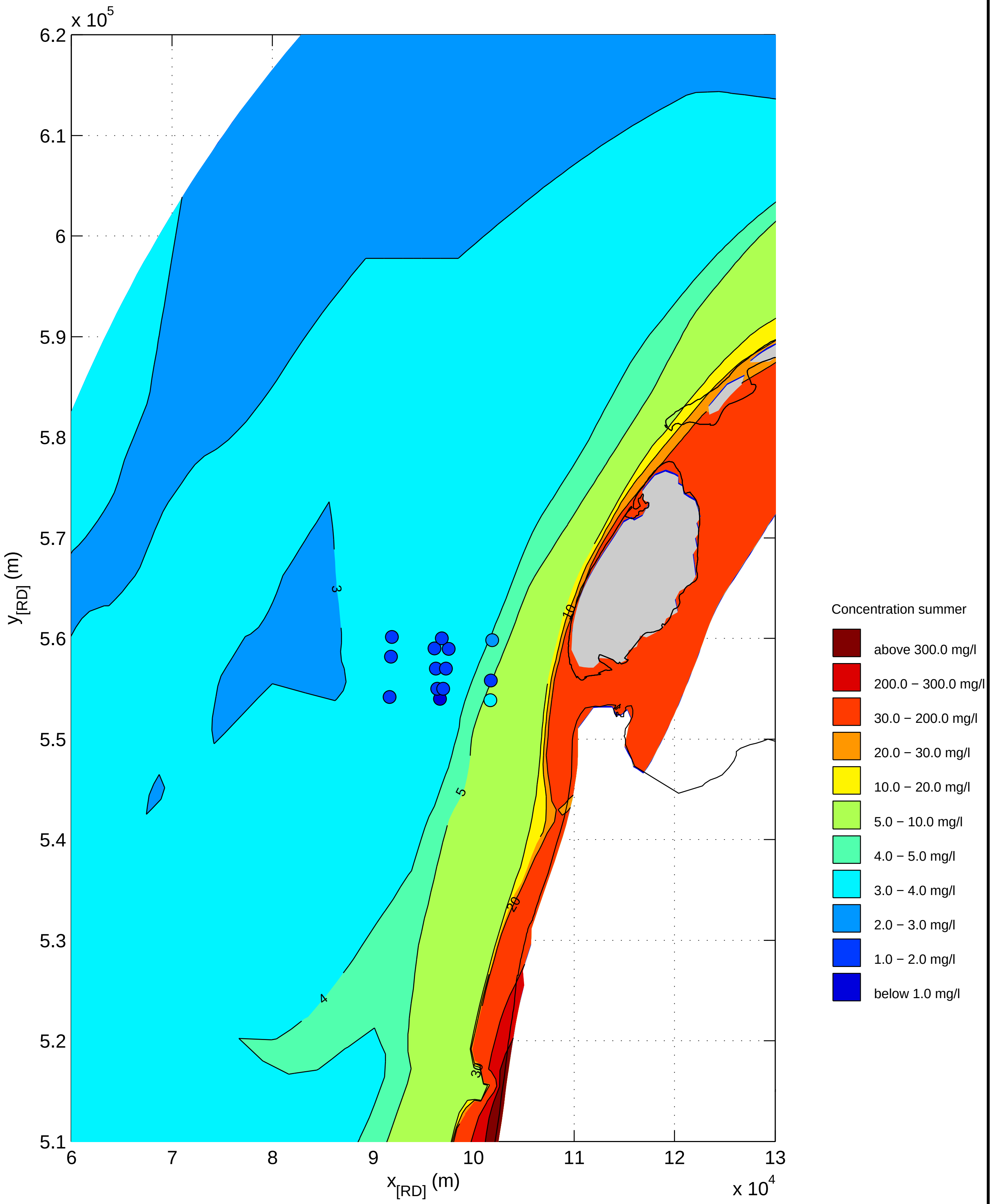

Summer mean of total suspended solids concentration (mg/l) filled contours present the interpolated 1975−1983 waterbase data coloured symbols present the T1 silt profiler data on 17 September 2007	1975−1983 and T1 2007	
Alkyon Hydraulic Consultancy & Research	A2273	Fig. 2.65

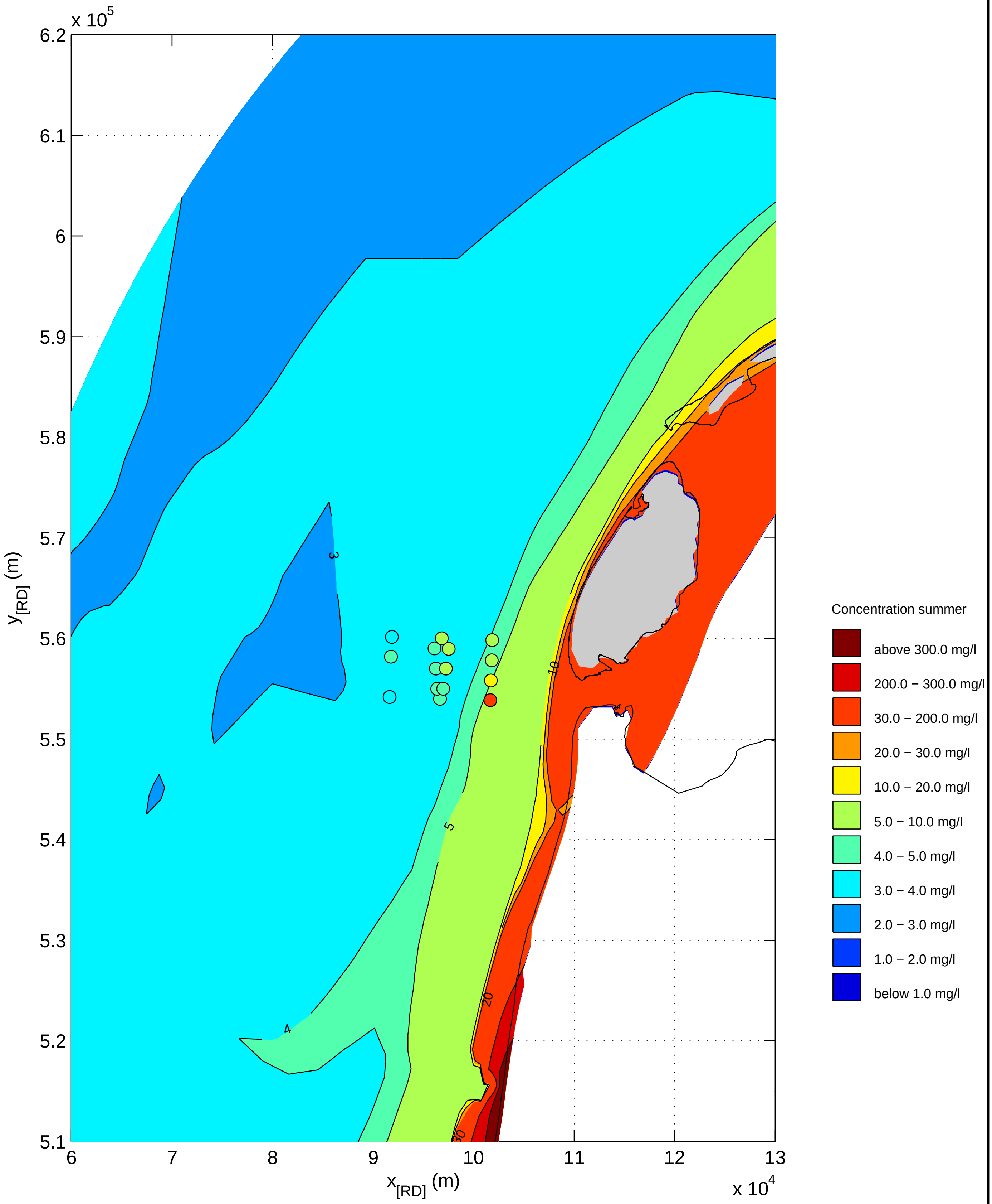

Summer mean of total suspended solids concentration (mg/l) filled contours present the interpolated 1975−1983 waterbase data coloured symbols present the T1 silt profiler data on 1 October 2007	1975−1983 and T1 2007	
Alkyon Hydraulic Consultancy & Research	A2273	Fig. 2.66

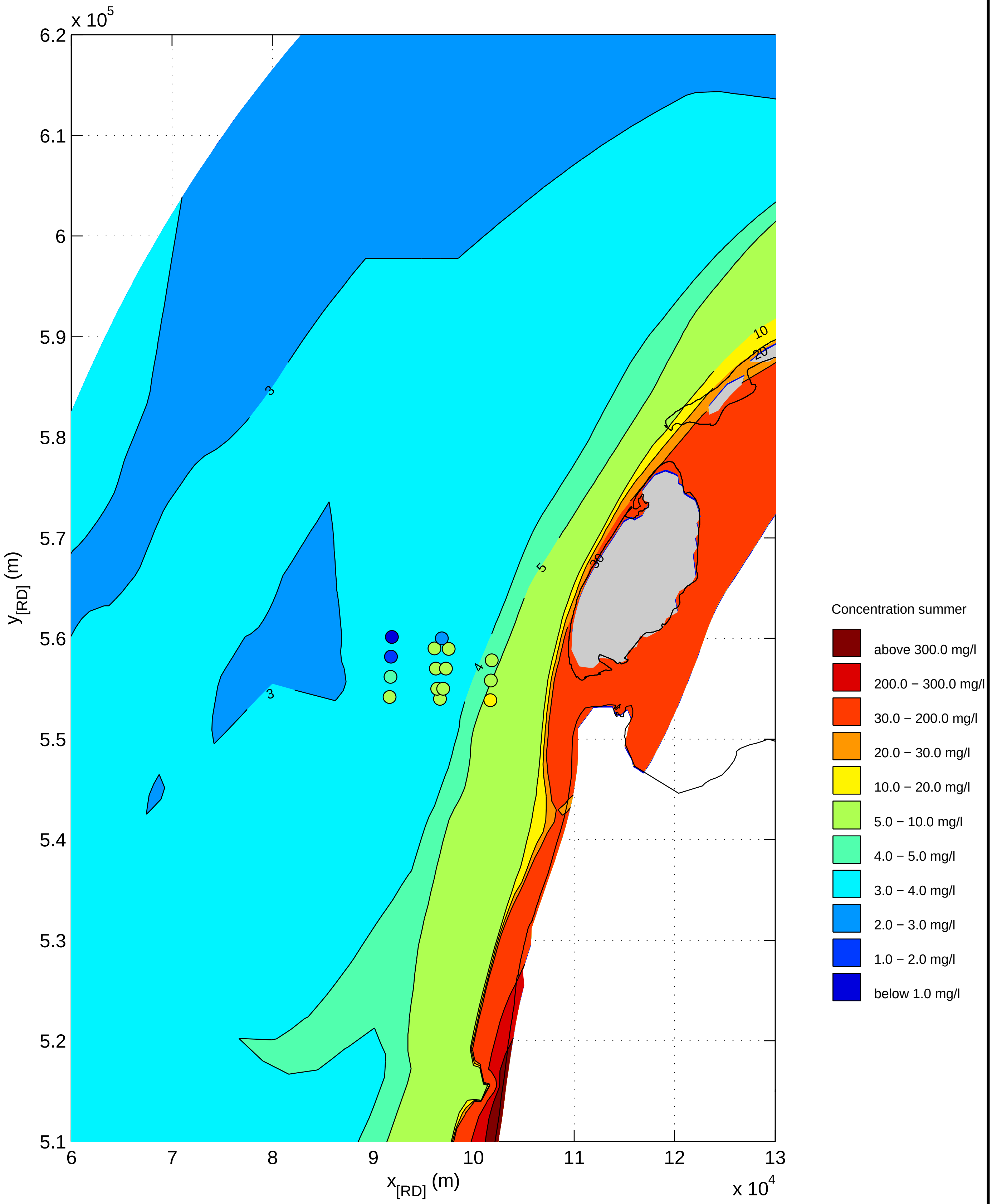

Summer mean of total suspended solids concentration (mg/l) filled contours present the interpolated 1975−1983 waterbase data coloured symbols present the T1 silt profiler data on 2 October 2007	1975−1983 and T1 2007	
Alkyon Hydraulic Consultancy & Research	A2273	Fig. 2.67

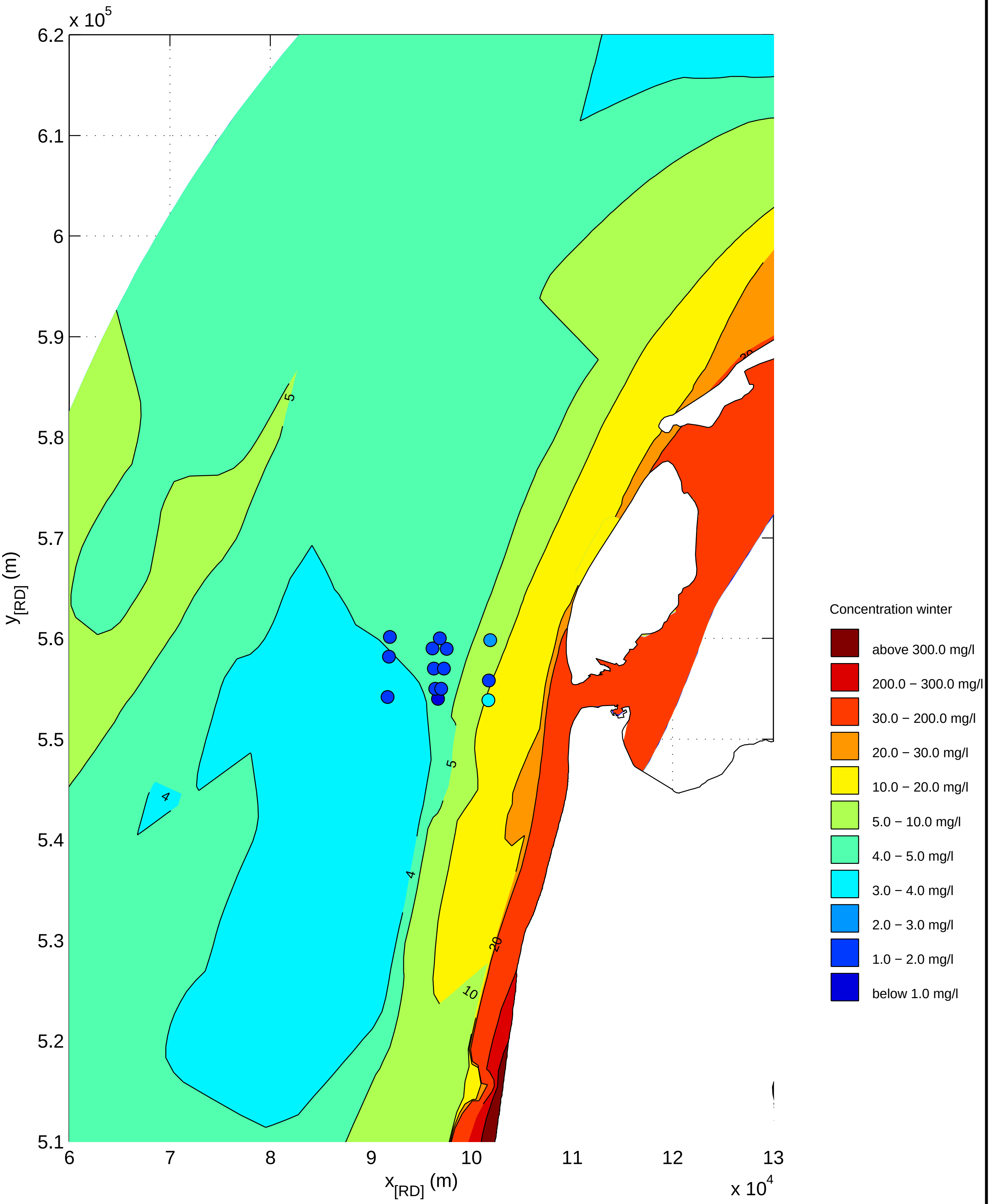

Winter mean of total suspended solids concentration (mg/l) filled contours present the interpolated 1975−1983 waterbase data coloured symbols present the T1 silt profiler data on 17 September 2007	1975−1983 and T1 2007	
Alkyon Hydraulic Consultancy & Research	A2273	Fig. 2.68

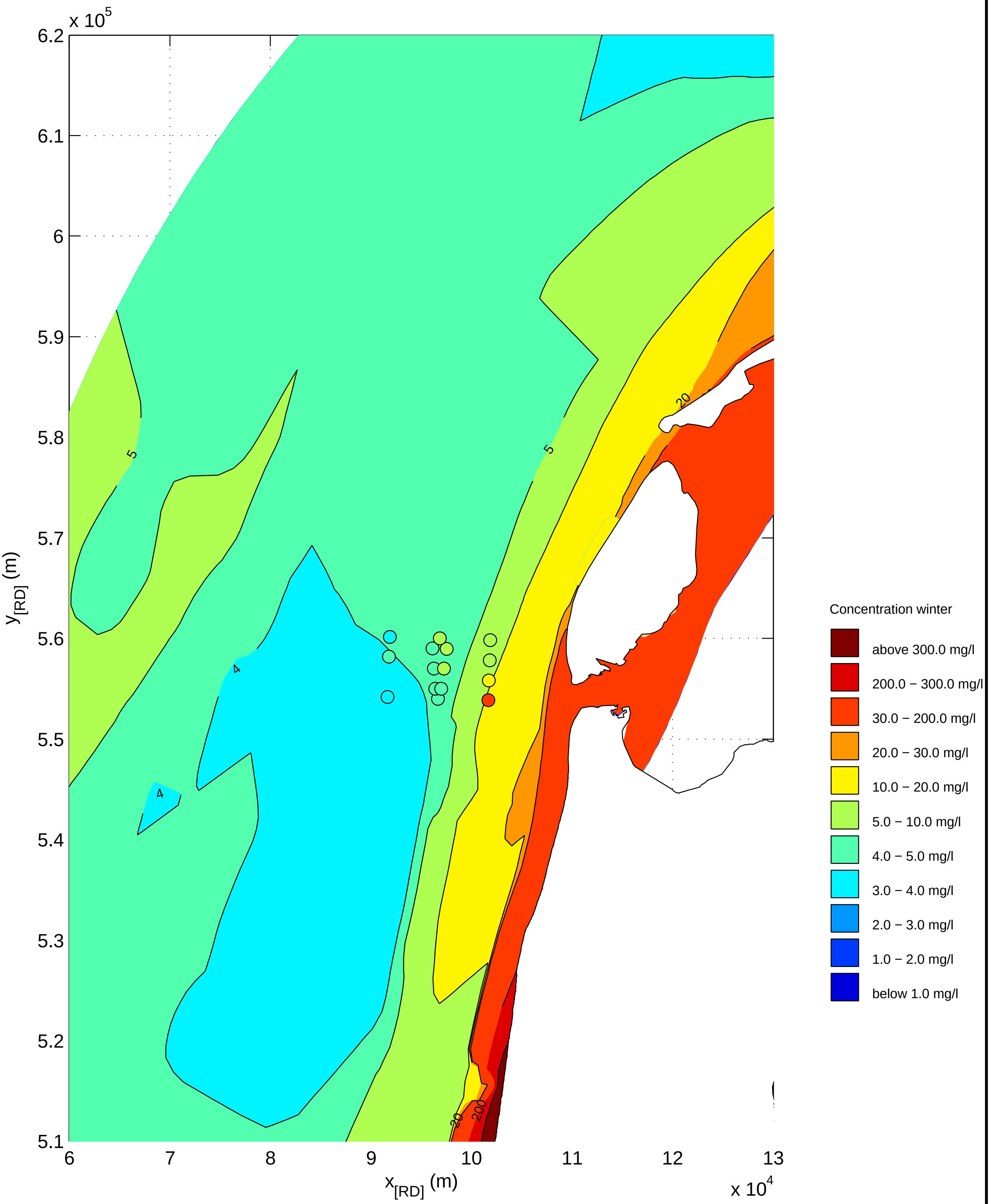

Winter mean of total suspended solids concentration (mg/l) filled contours present the interpolated 1975−1983 waterbase data coloured symbols present the T1 silt profiler data on 1 October 2007	1975−1983 and T1 2007	
Alkyon Hydraulic Consultancy & Research	A2273	Fig. 2.69

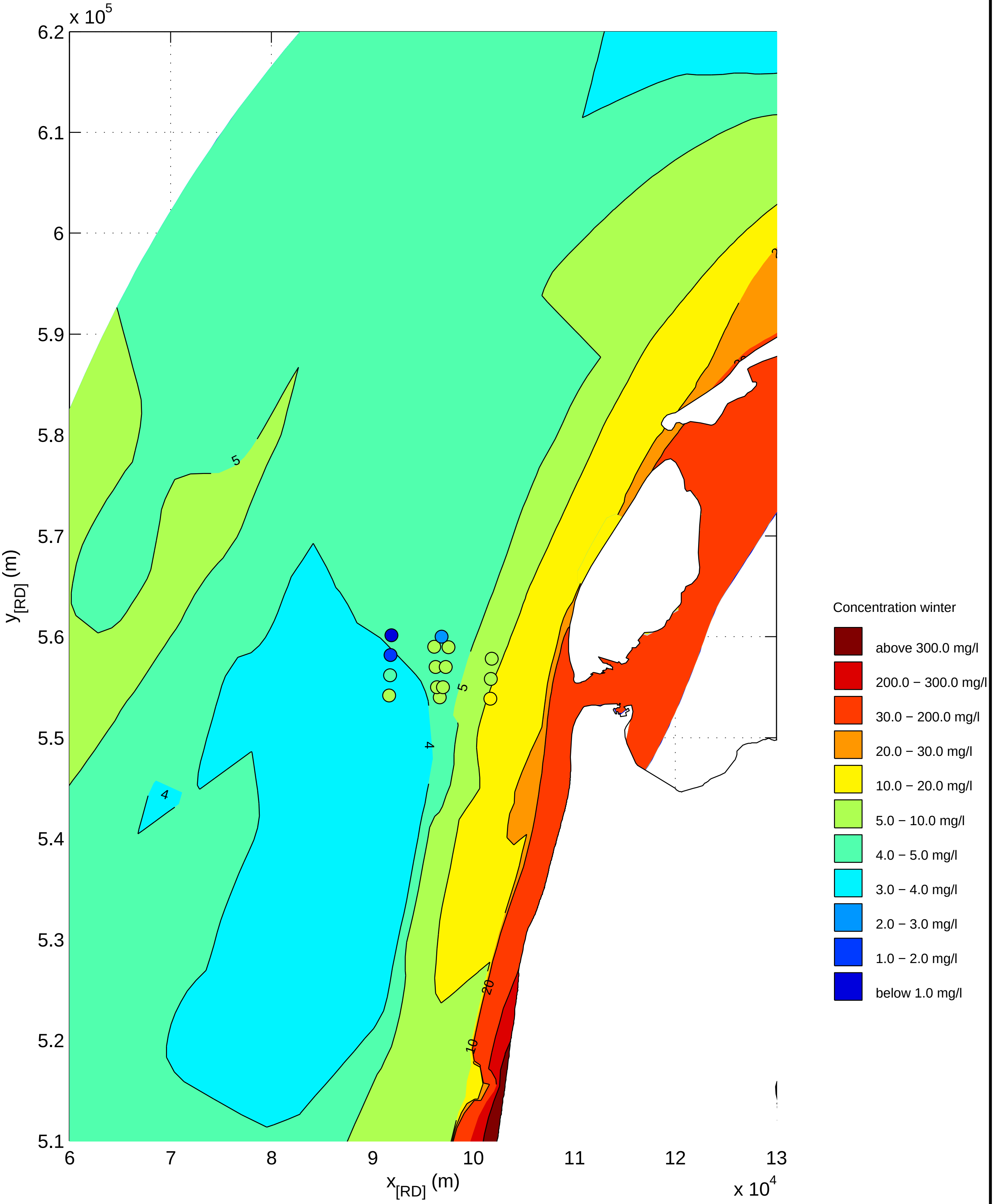

Winter mean of total suspended solids concentration (mg/l) filled contours present the interpolated 1975−1983 waterbase data coloured symbols present the T1 silt profiler data on 2 October 2007	1975−1983 and T1 2007	
Alkyon Hydraulic Consultancy & Research	A2273	Fig. 2.70

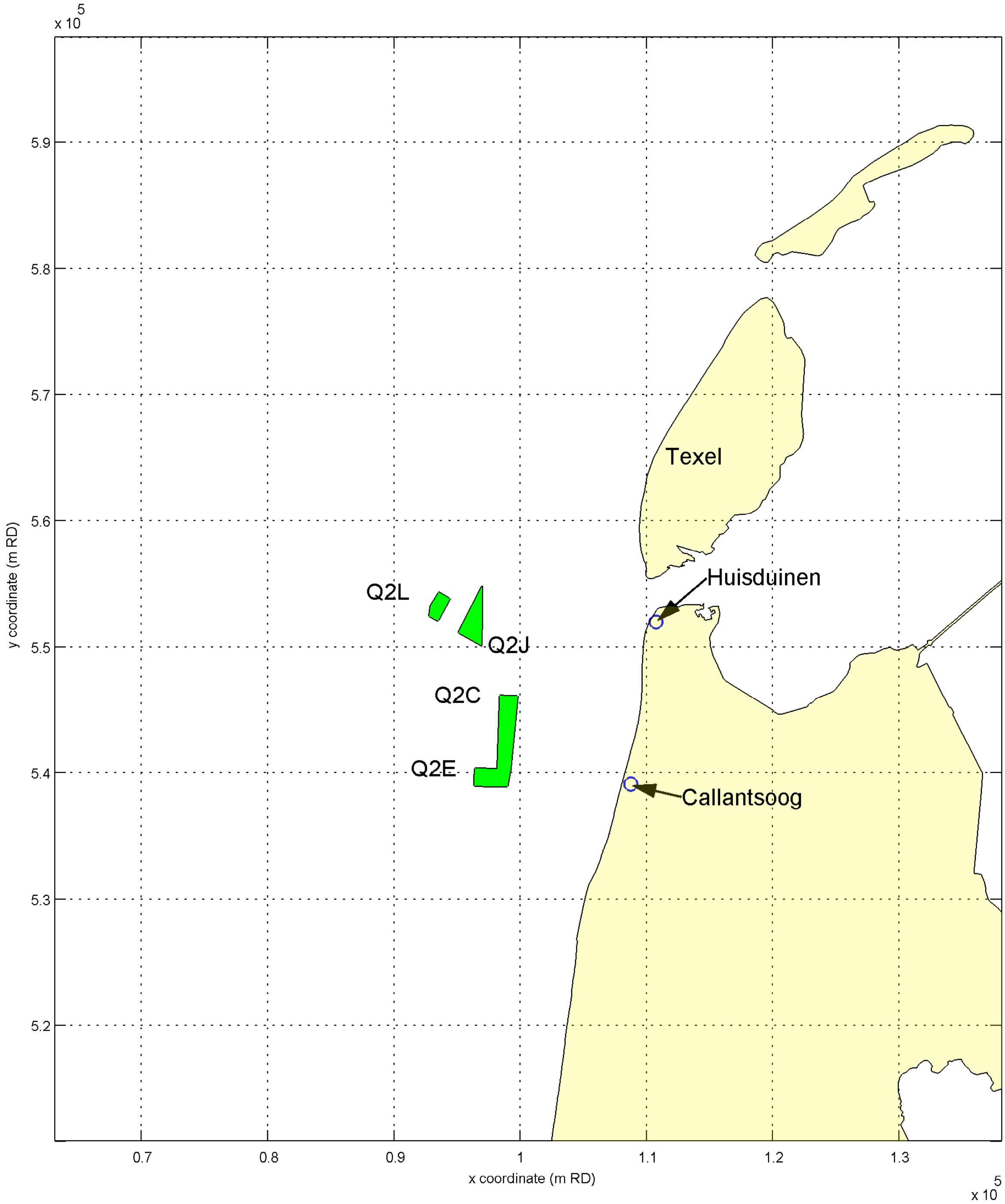

Sand extraction locations offshore Huisduinen (Q2L and Q2J) and Callantsoog (Q2C and Q2E)	Noordzee	
Alkyon Hydraulic Consultancy & Research	A2273	Fig. 3.1

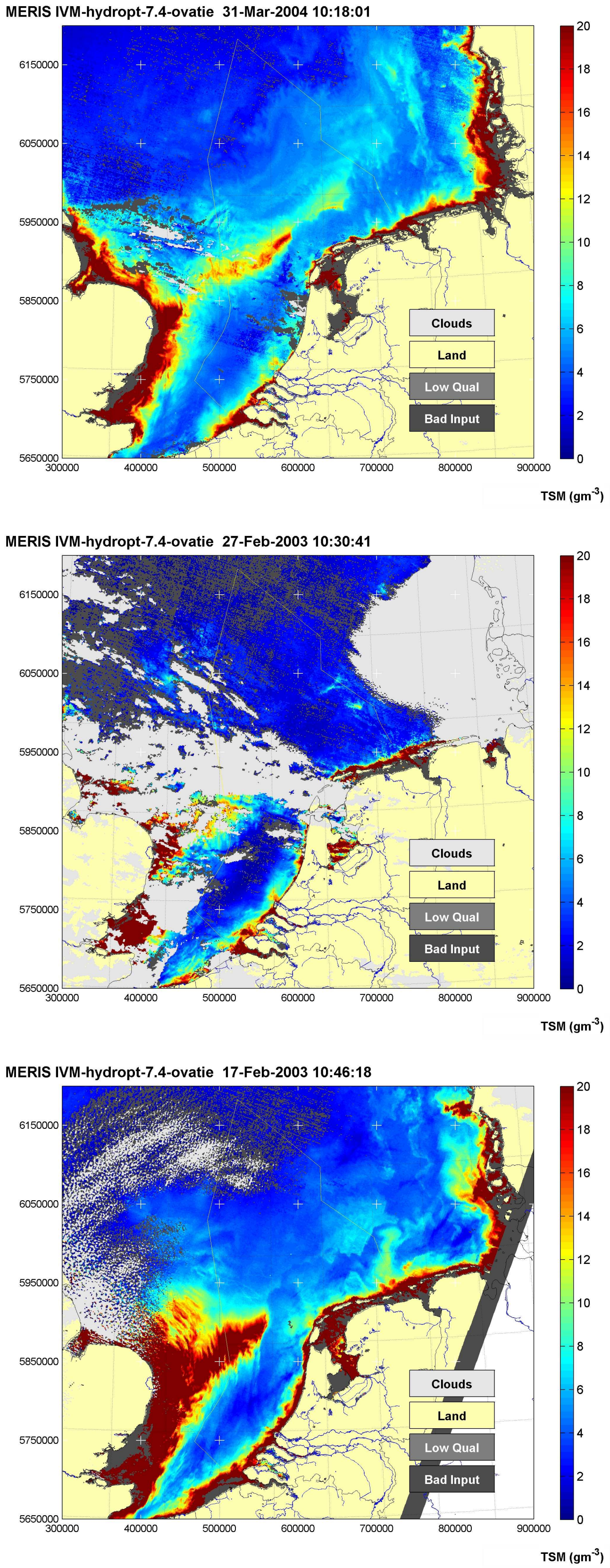

Surface SPM concentrations during different conditions
Bulges along Dutch coast may result from
(a) high discharge (b) tide (c) dredge spoil

IVM

Alkyon Hydraulic Consultancy & Research | A2273 | Fig.3.2

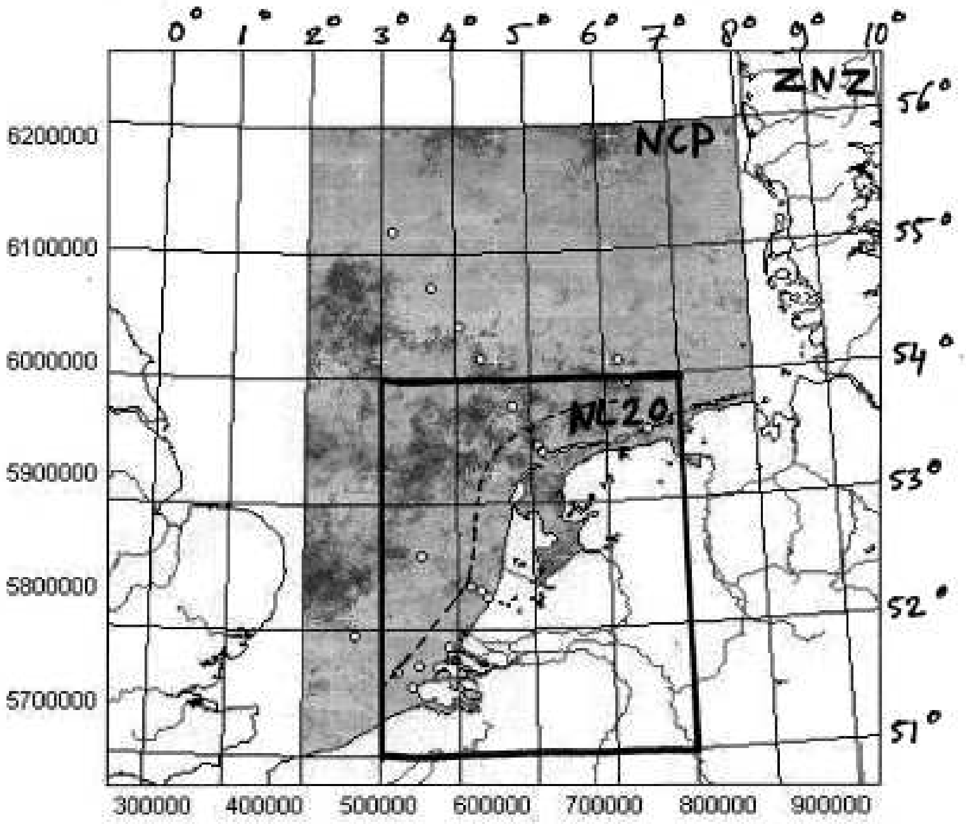

Study area remote sensing data		
	IVM	
Alkyon Hydraulic Consultancy & Research	A2273	Fig.3.3

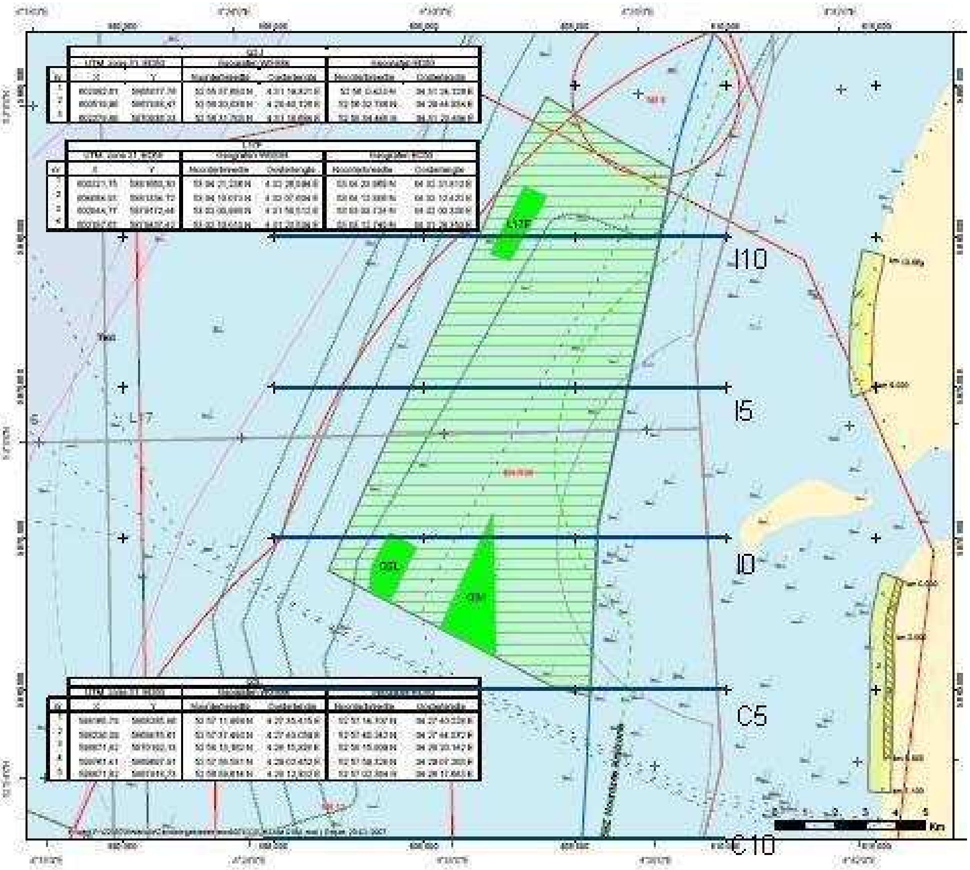

Five cross−shore transects from X is 595.000 to 610.000 m
The central transect (I0) goes through both Q2J and Q2L at Y 5.870.000
The others are located 5 and 10 km to the north and to the south

IVM

Alkyon Hydraulic Consultancy & Research

A2273

Fig.3.4

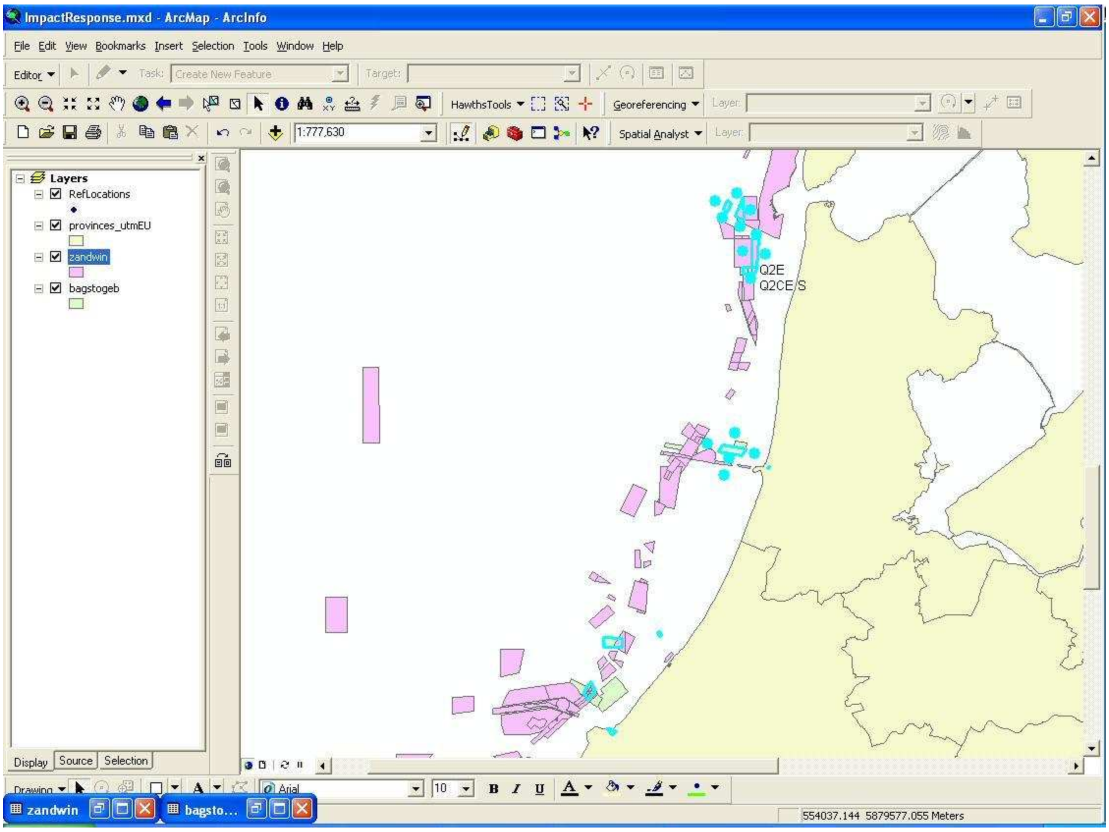

Studied sand extraction locations and dredge disposal sites.
Values were extracted at the centres and digitized points

IVM	
A2273	Fig.3.5

Alkyon Hydraulic Consultancy & Research

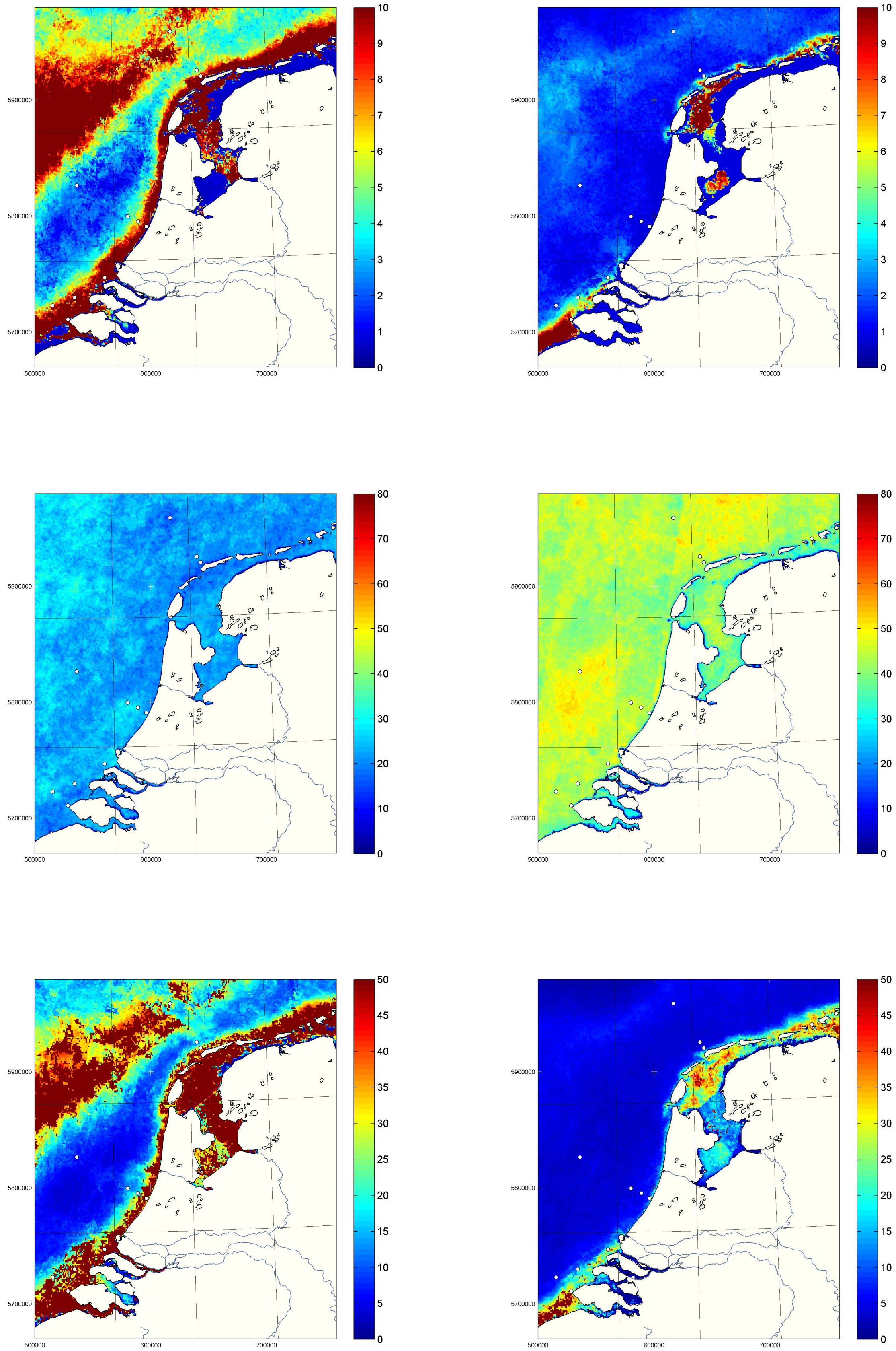

Examples of cell−based probability distributions of SPM concentrations (top) median, (centre) number of observations and (bottom) 95 percentile for two contrasting months, (left) February and (right) July

	IVM	
Alkyon Hydraulic Consultancy & Research	A2273	Fig.3.6

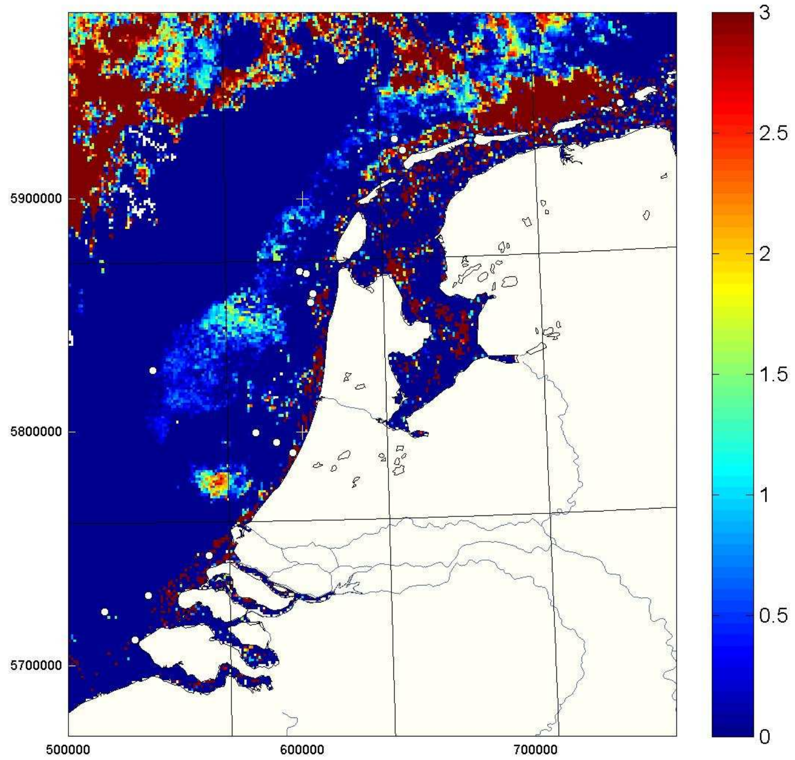

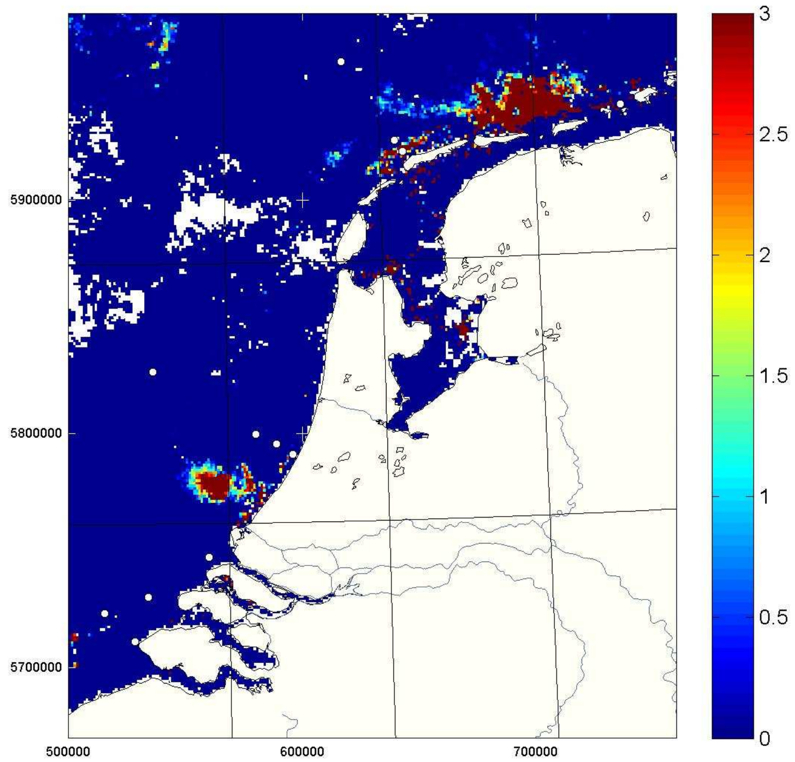

Outliers: top panel shows the composite April 2003 anomaly
with high values near Q2C and Q2E and Loswal Noordwest.
The bottom panel shows the individual map of 7 April 2003 causing the outlier

	IVM	
Alkyon Hydraulic Consultancy & Research	A2273	Fig.3.7

MERIS IVM-hydropt-7.4-ovatie 07-Apr-2003 09:59:55

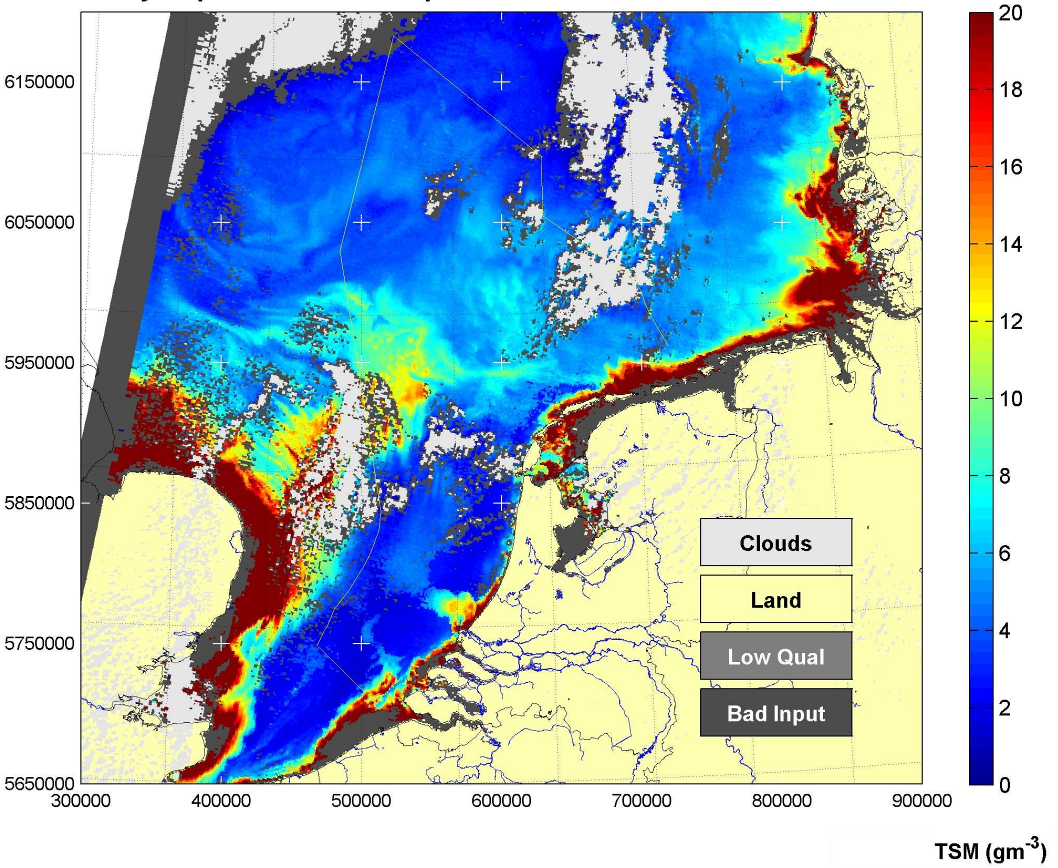

SPM quicklook with quality flags, confirming that the signal near Loswal Noordwest occurs in the water and not in the atmosphere.	IVM	
Alkyon Hydraulic Consultancy & Research	A2273	Fig.3.8

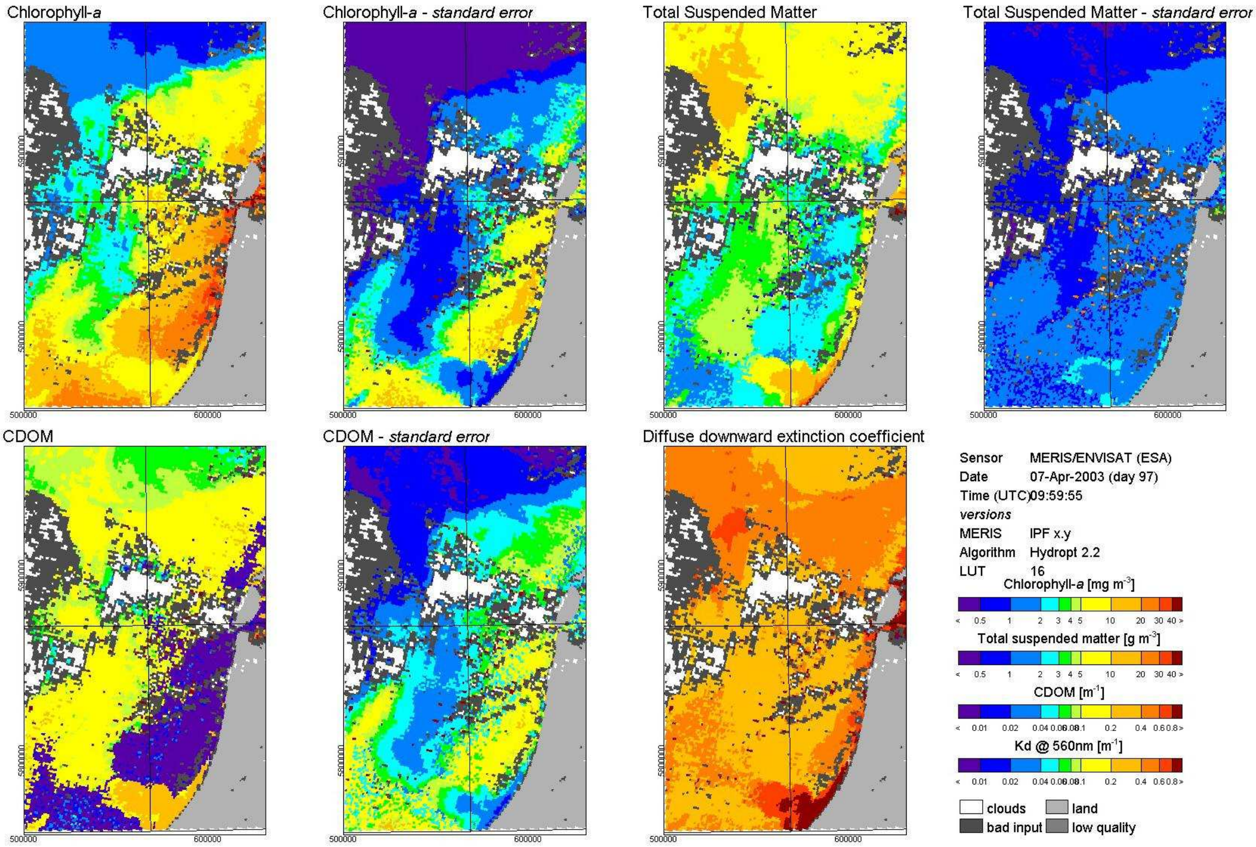

All optical water quality parameters and their estimated retrieval error products, confirms that the signal is truly caused by SPM (note the small error), and not caused by a scattering algal bloom.

IVM

Alkyon Hydraulic Consultancy & Research

A2273

Fig.3.9

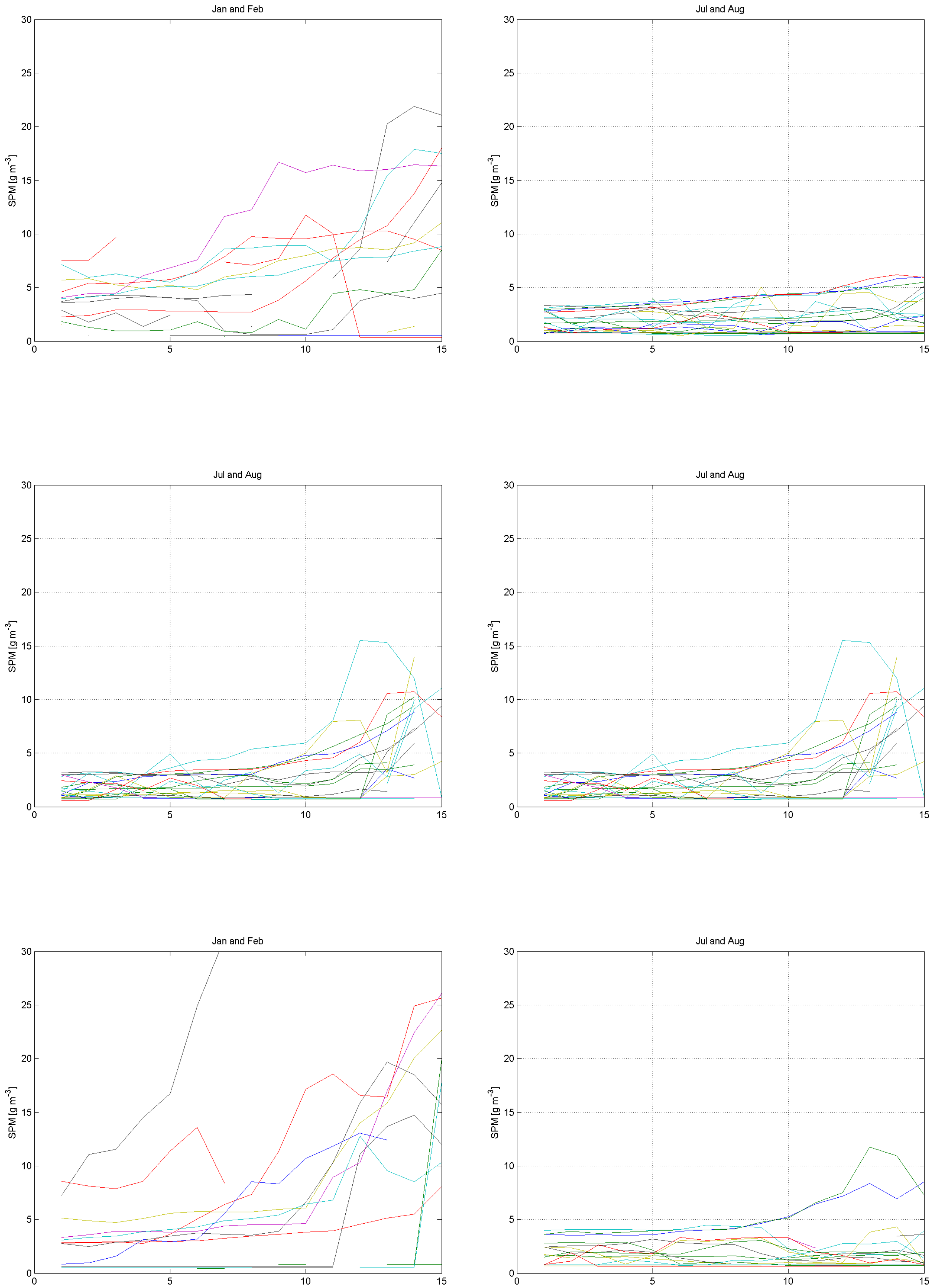

Examples of extracted SPM values along transects (top) I10 (centre) I0, (bottom) C10 confirming the large autonomous (T0) spatial and seasonal variation in the cross−shore gradient of SPM concentrations.

	IVM	
Alkyon Hydraulic Consultancy & Research	A2273	Fig.3.10

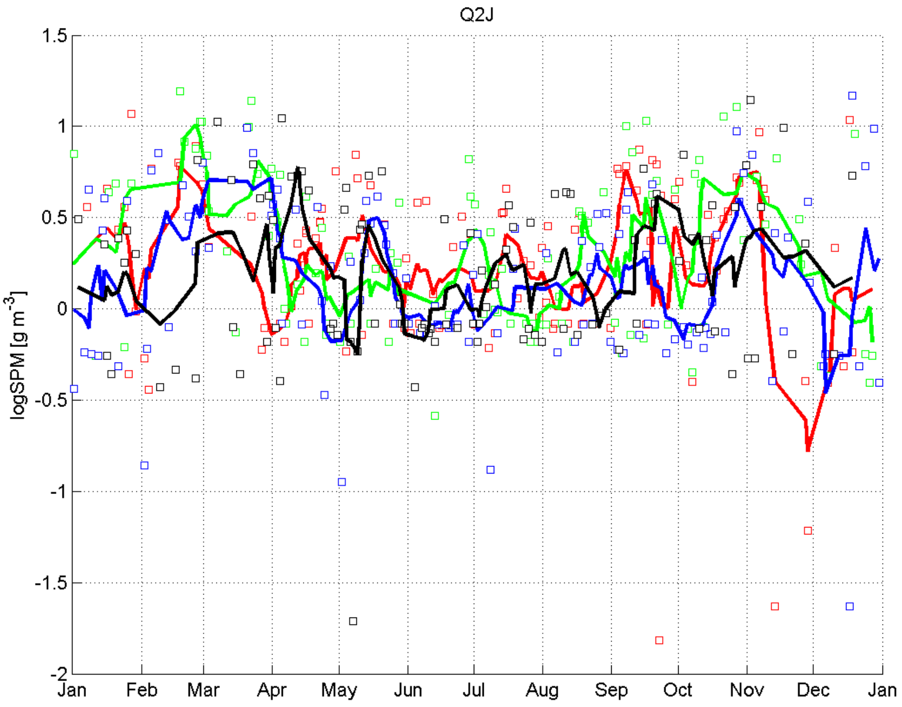

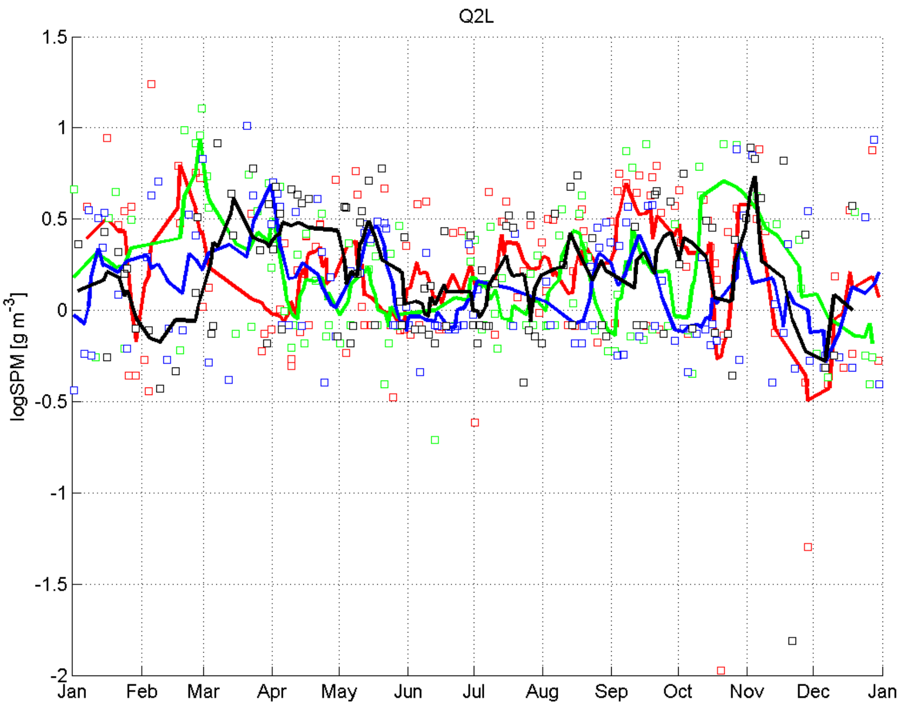

T0 time series (red = 2003, green =2004, blue = 2005, black = 2006) at the centre points of Q2J and Q2L. The (span) moving averages illustrate seasonality and inter−annual variation.	IVM	
Alkyon Hydraulic Consultancy & Research	A2273	Fig.3.11

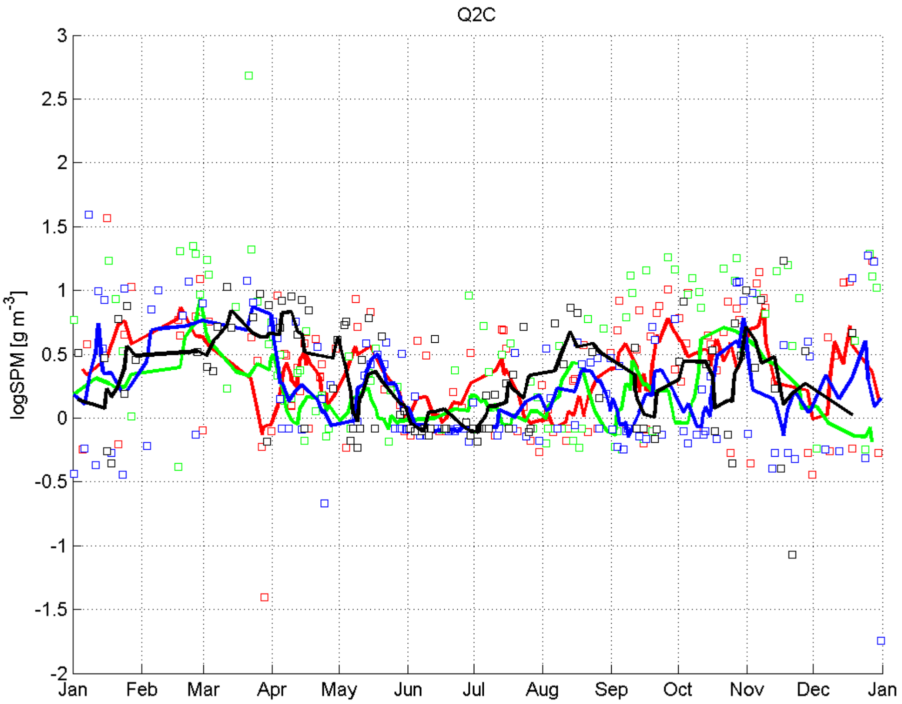

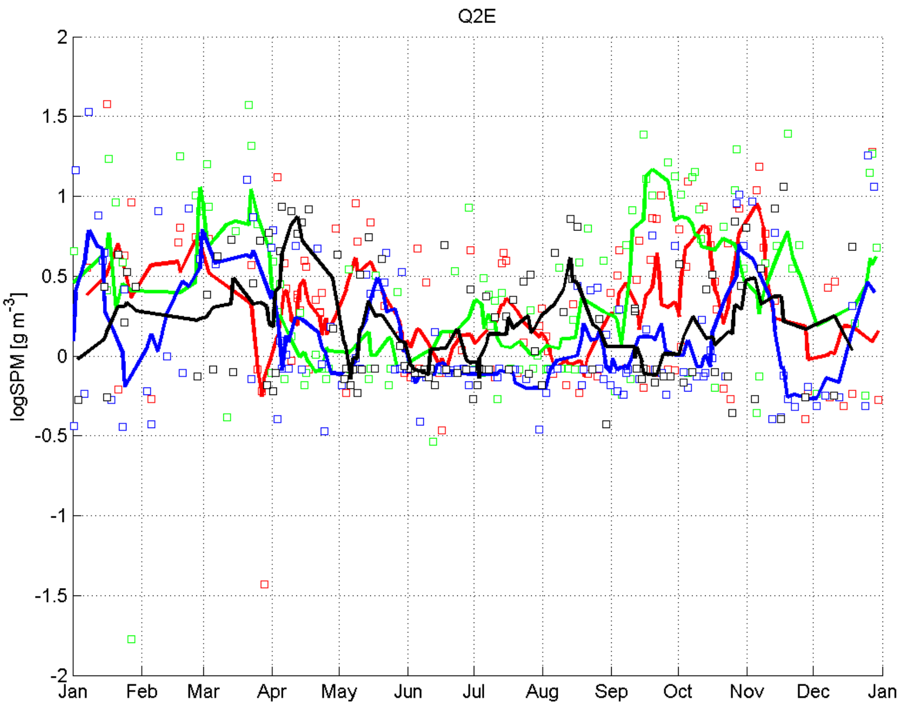

T0 time series (red = 2003, green =2004, blue = 2005, black = 2006)
at the centre points of Q2C and Q2E.
The (span) moving averages illustrate seasonality and inter−annual variation.

	IVM	
Alkyon Hydraulic Consultancy & Research	A2273	Fig.3.12

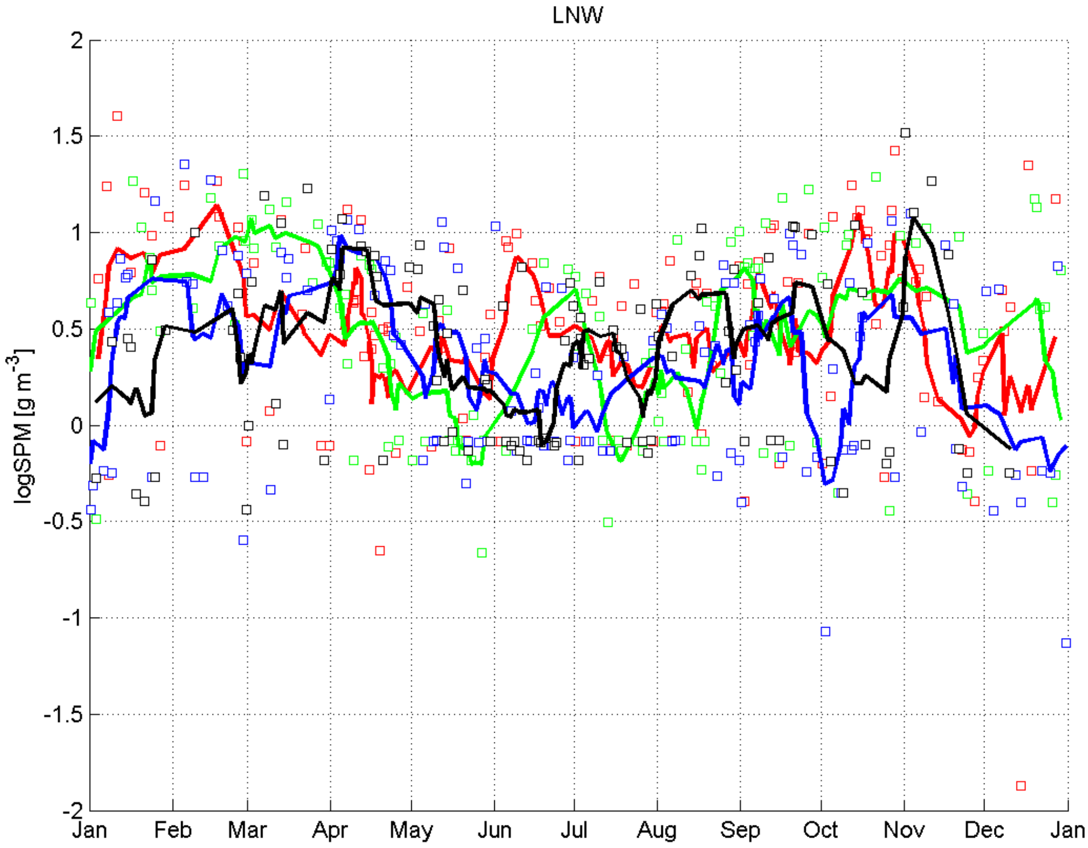

T0 time series (red = 2003, green =2004, blue = 2005, black = 2006) at the centre points of Loswal Noord. The (span) moving averages illustrate seasonality and inter−annual variation.	IVM	
Alkyon Hydraulic Consultancy & Research	A2273	Fig.3.13

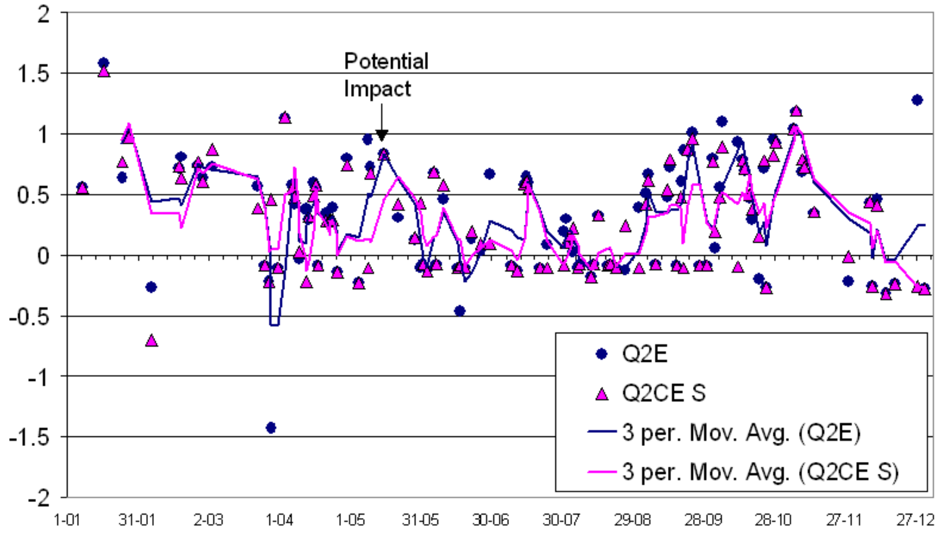

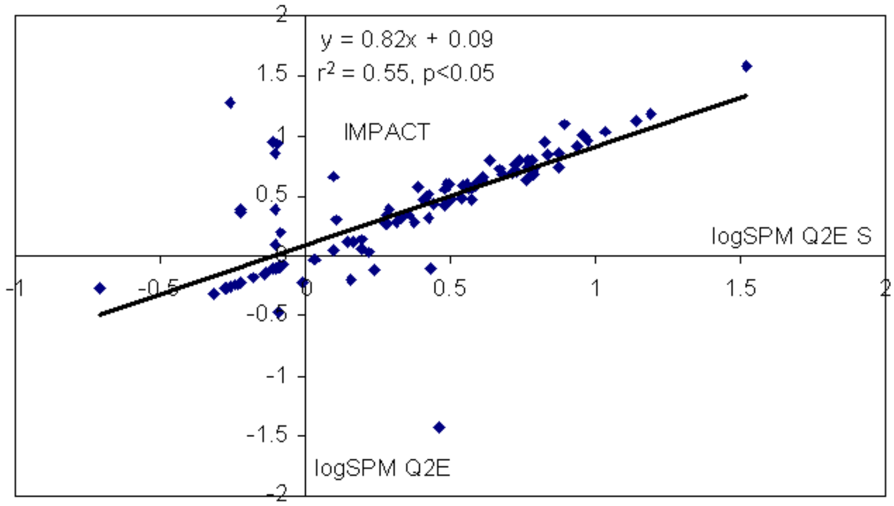

End of May impact site Q2E shows higher values than control site Q2CE S just to the south of Q2E. (see Fig 3.5 for sampling design.) Lower panel shows the correlation between Q2E and Q2CE S.

IVM

mean 2003−2006

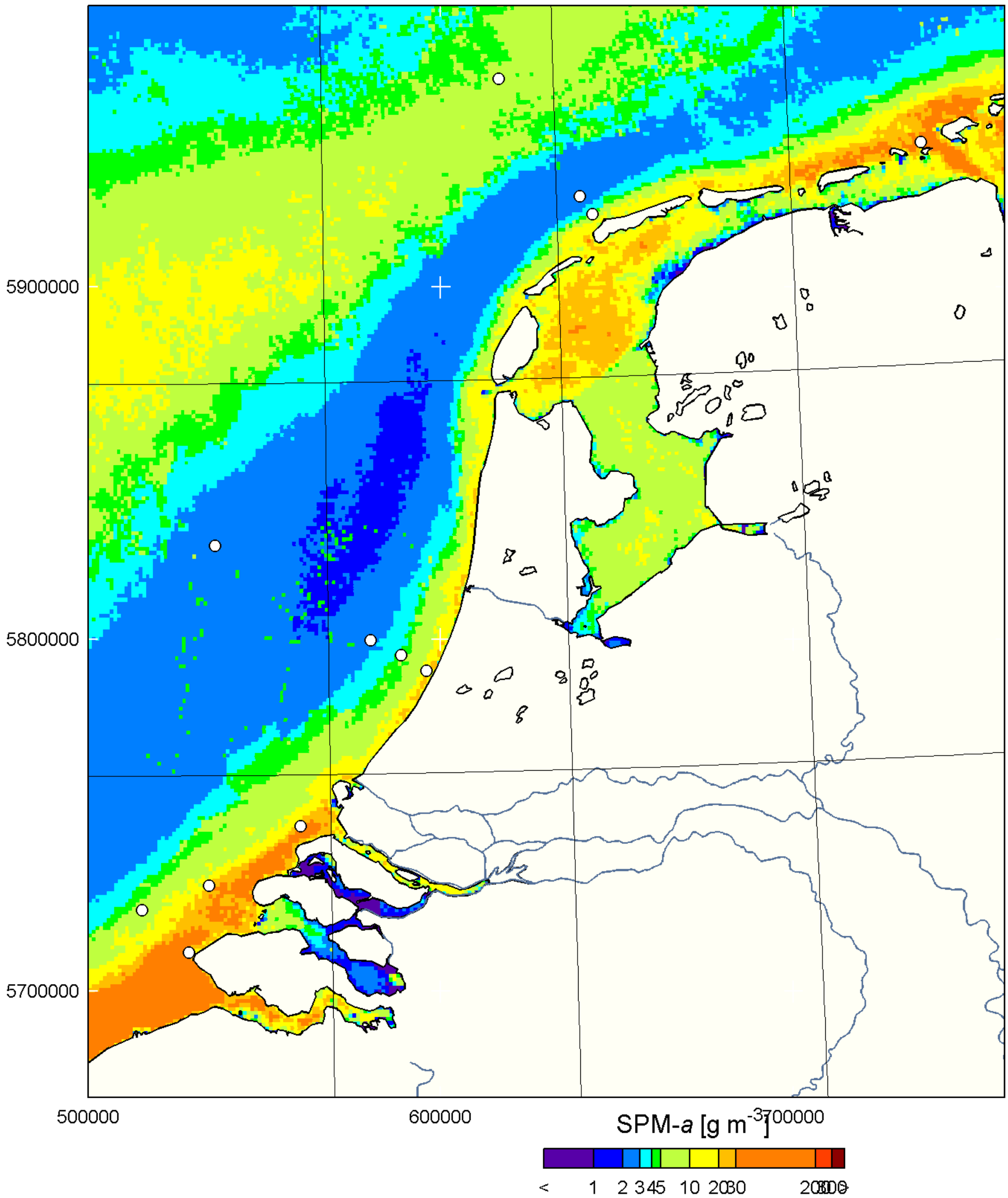

Mean values of SPM for 2003−2006 derived from
HYDROPT MERIS obervations

IVM

Alkyon Hydraulic Consultancy & Research

A2273

Fig.3.15

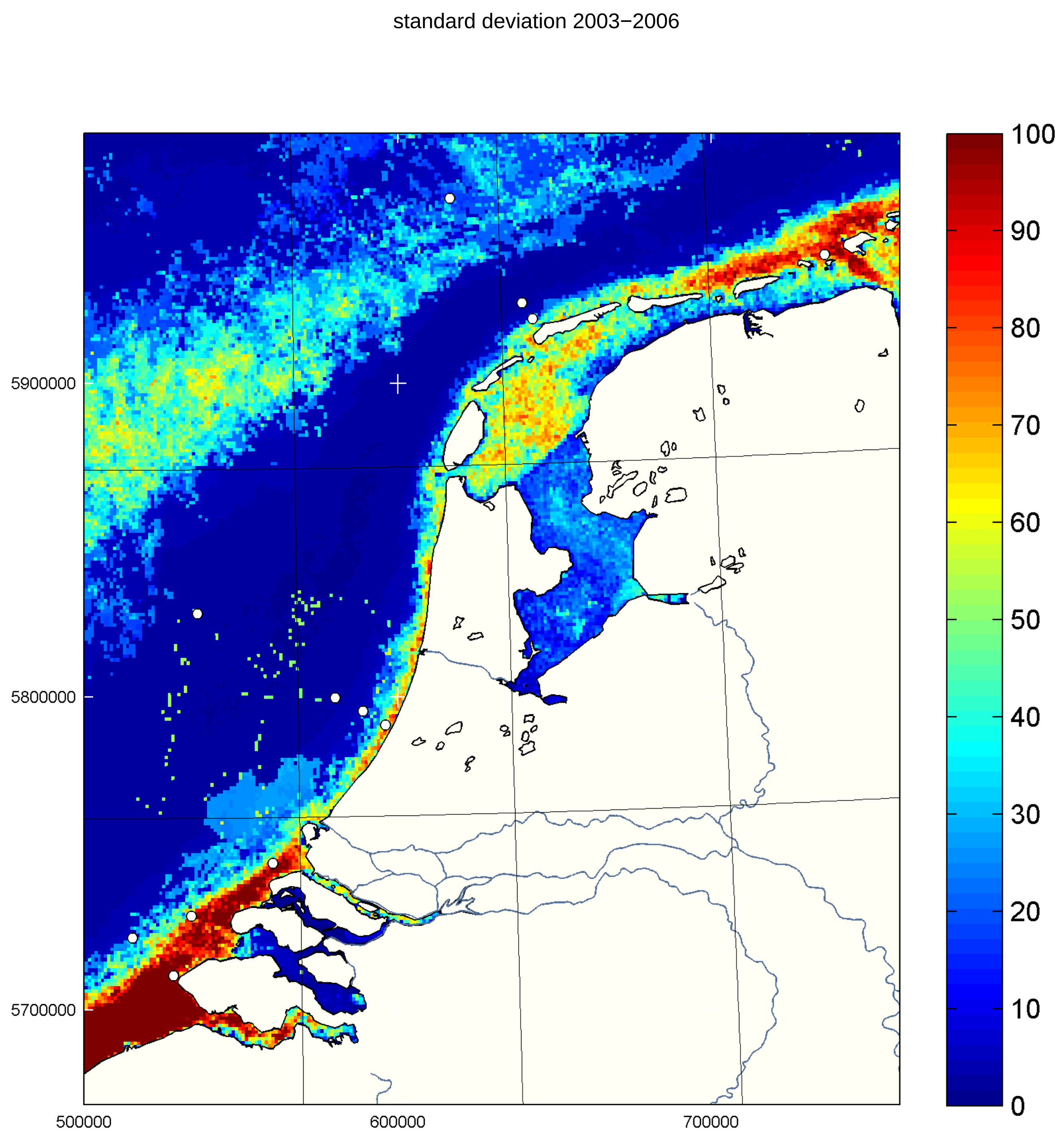

Standard deviation of SPM for 2003−2006 derived from HYDROPT MERIS obervations

	IVM	
Alkyon Hydraulic Consultancy & Research	A2273	Fig.3.16

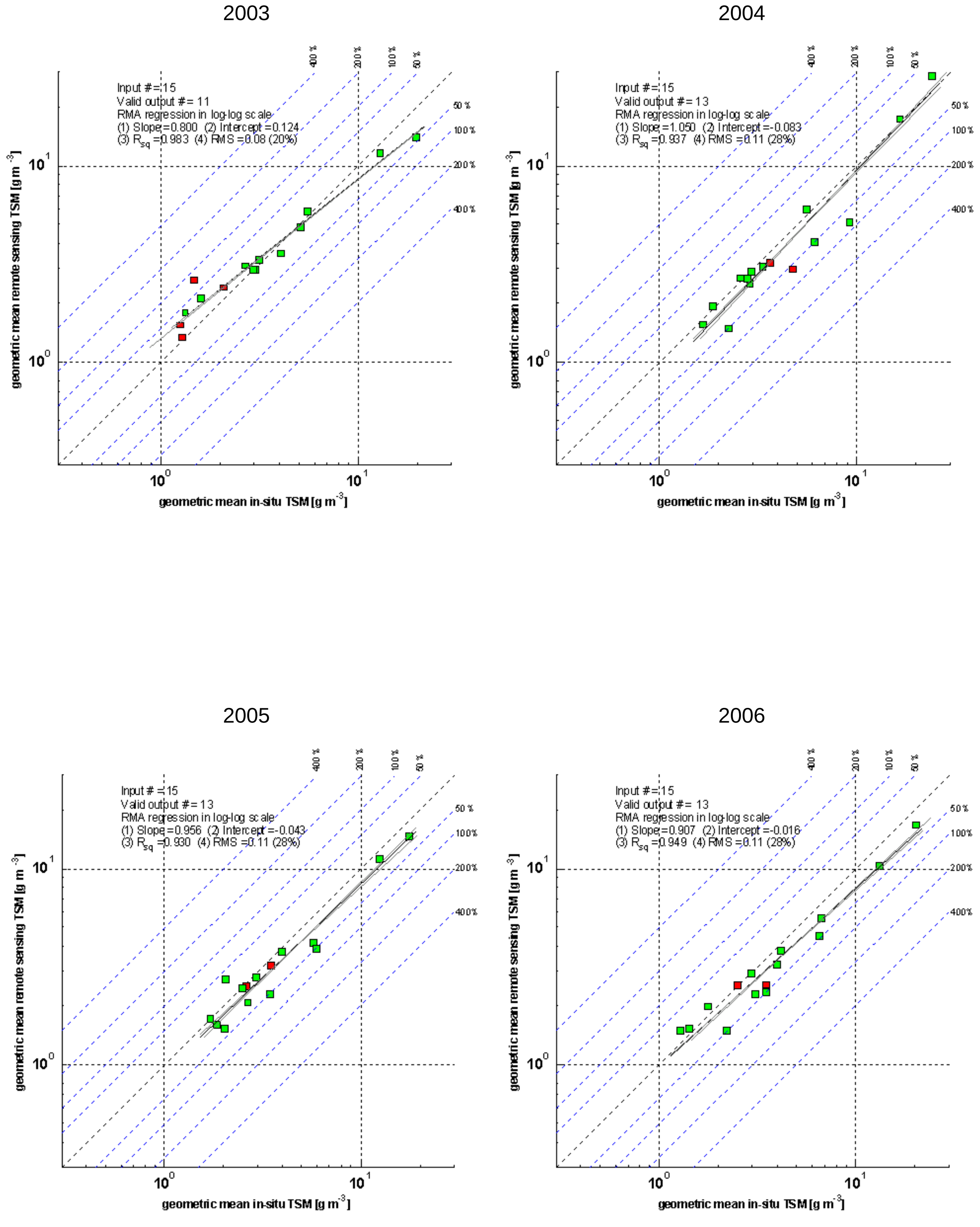

Comparison of annual geometric mean values of SPM as observed in−situ on MWTL monitoring stations with values derived from HYDROPT MERIS observations at MWTL locations (Peters et al., in prep.)		
	IVM	
Alkyon Hydraulic Consultancy & Research	A2273	Fig.3.17

Apr−2007

MERIS IVM-hydropt-7.4-ovatie 28-Apr-2007 10:26:37

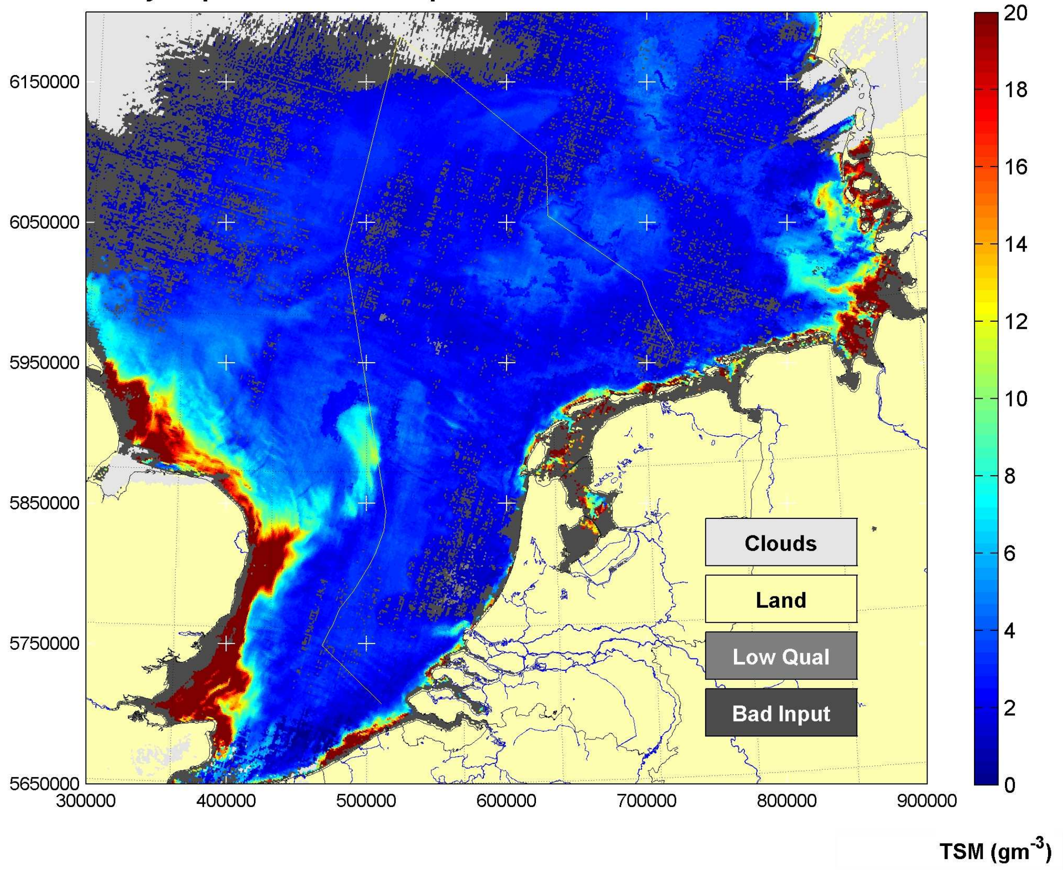

SPM quicklook with quality flags for conditions without sand mining 28−Apr−2007		
	IVM	
Alkyon Hydraulic Consultancy & Research	A2273	Fig. 3.18

May−2007

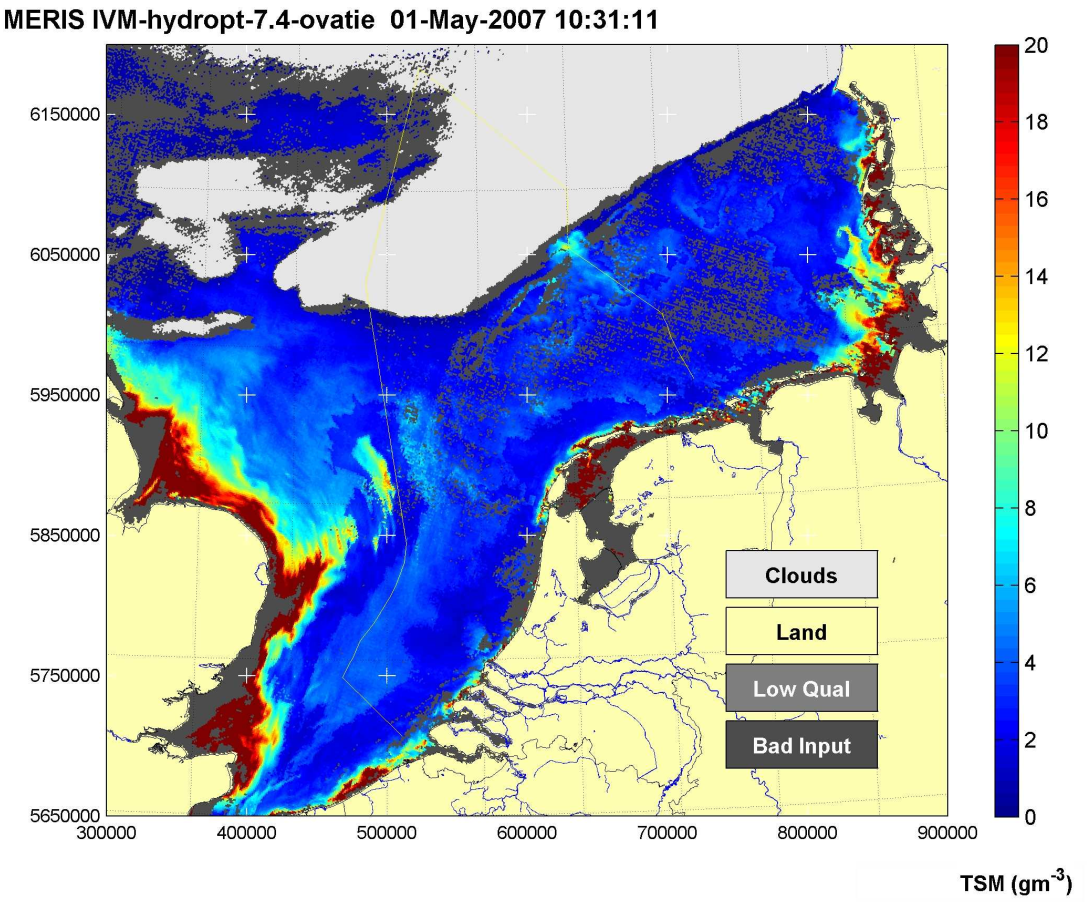

SPM quicklook with quality flags for conditions without sand mining 01−May−2007		
	IVM	
Alkyon Hydraulic Consultancy & Research	A2273	Fig. 3.19

May−2007

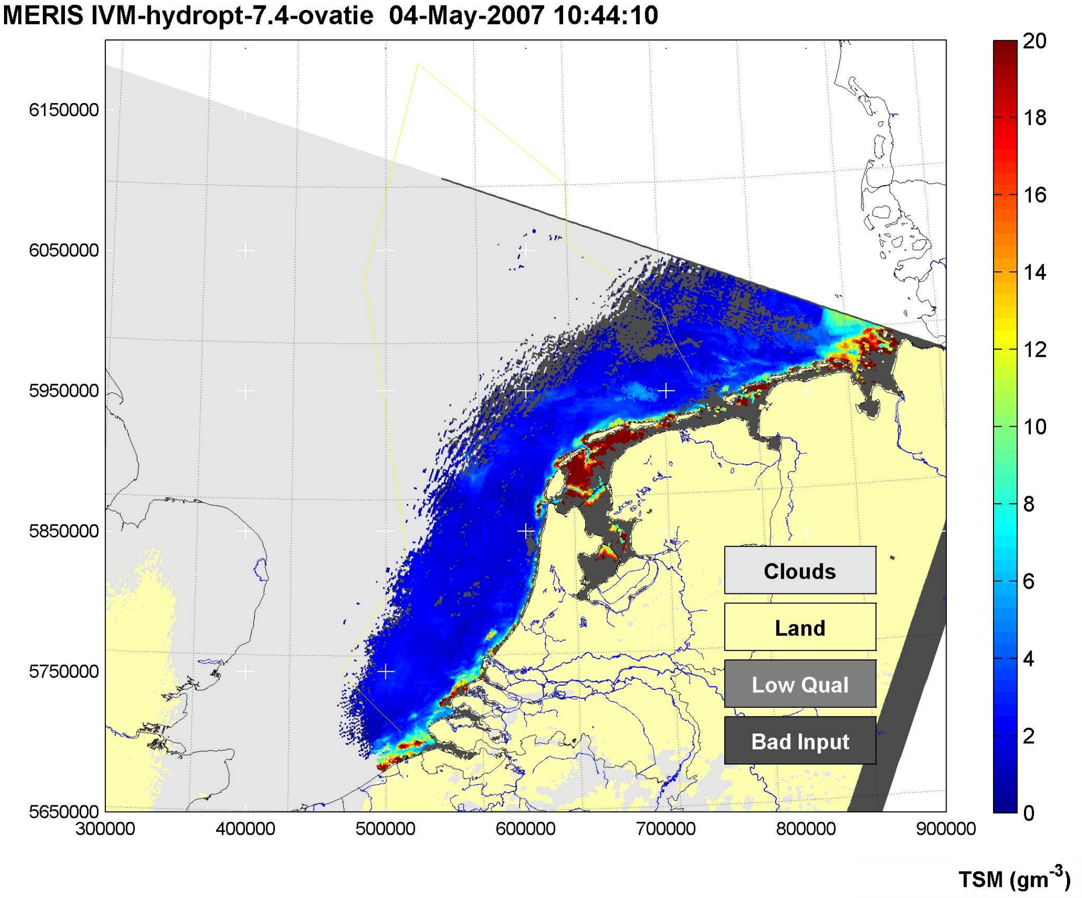

SPM quicklook with quality flags for conditions without sand mining 04−May−2007		
	IVM	
Alkyon Hydraulic Consultancy & Research	A2273	Fig. 3.20

May−2007

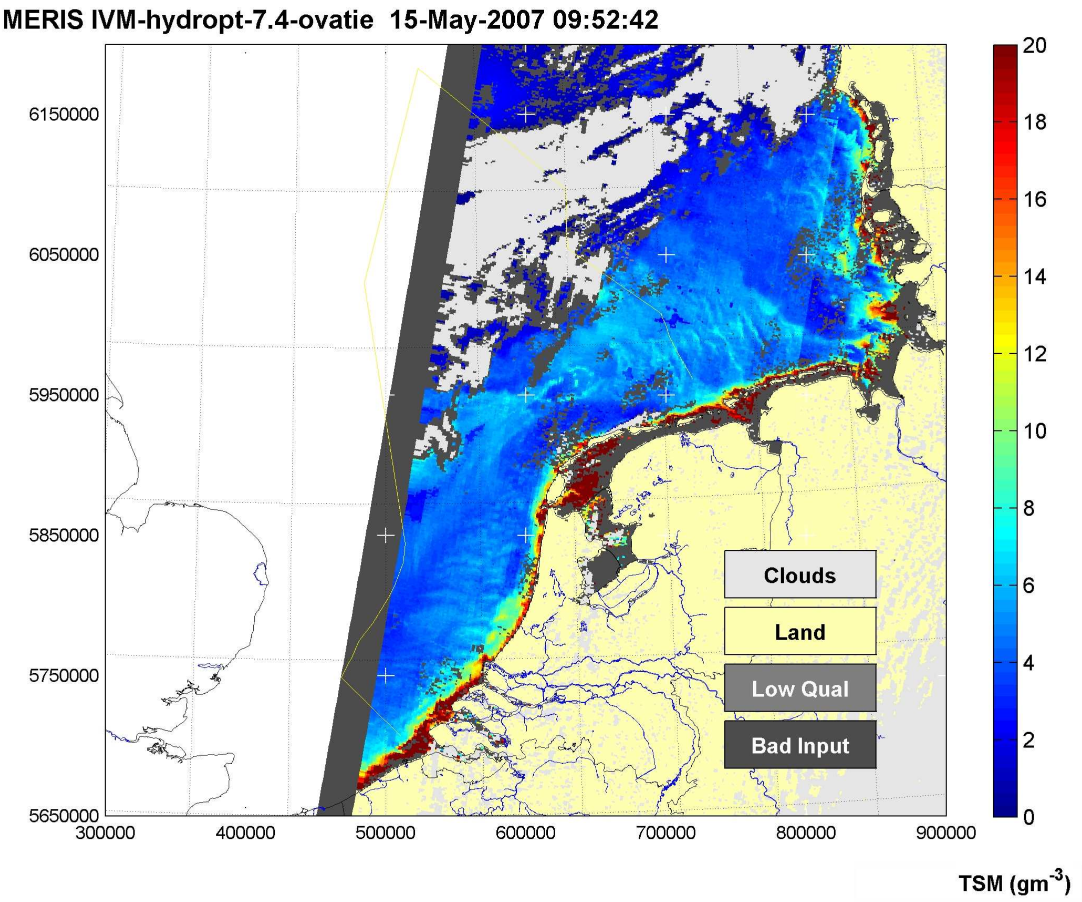

SPM quicklook with quality flags for conditions without sand mining 15−May−2007		
	IVM	
Alkyon Hydraulic Consultancy & Research	A2273	Fig. 3.21

May−2007

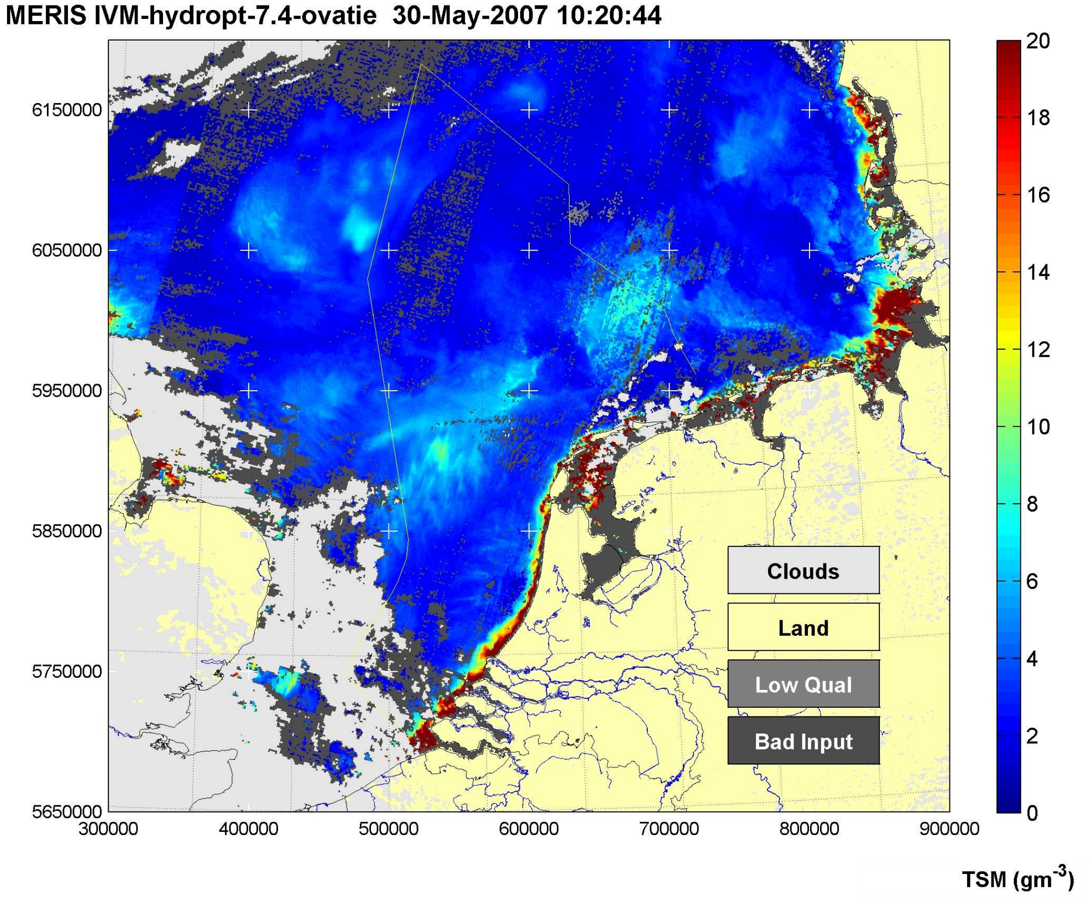

SPM quicklook with quality flags for conditions without sand mining 30−May−2007		
	IVM	
Alkyon Hydraulic Consultancy & Research	A2273	Fig. 3.22

Aug−2007

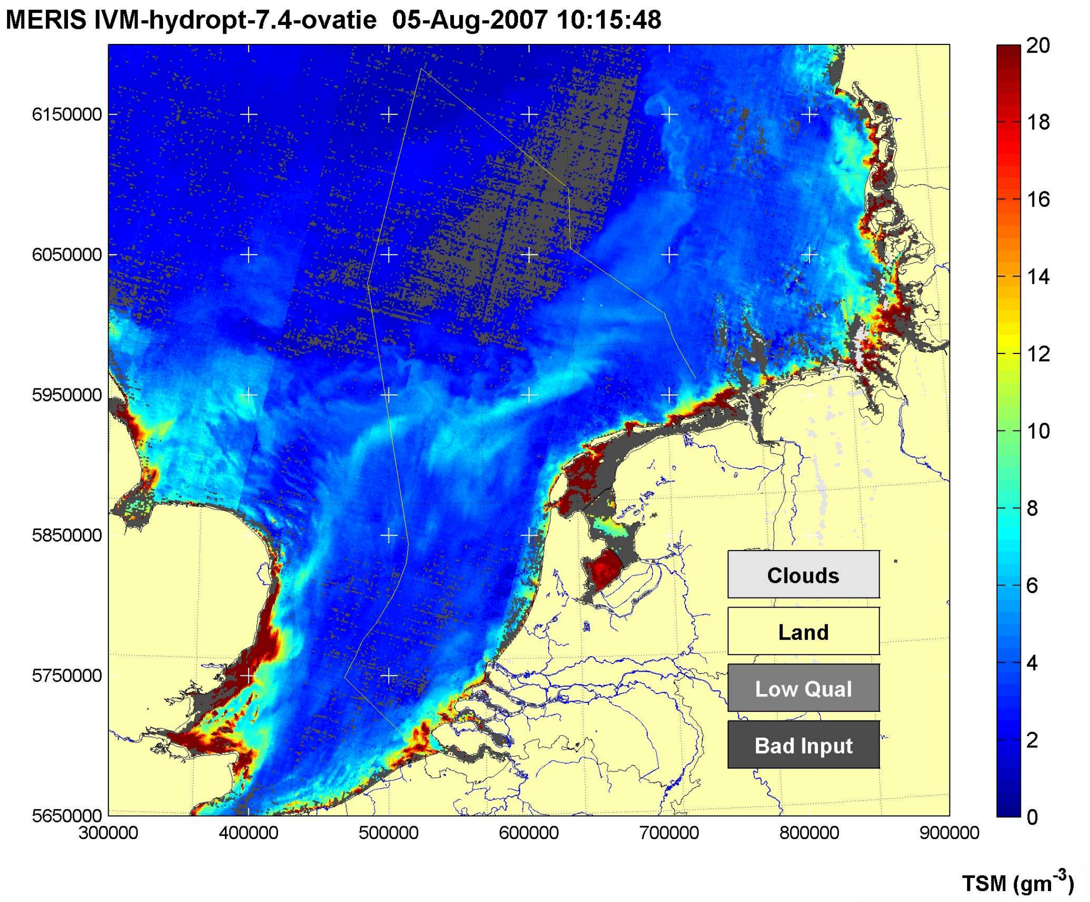

SPM quicklook with quality flags for conditions with sand mining 05−Aug−2007		
	IVM	
Alkyon Hydraulic Consultancy & Research	A2273	Fig. 3.23

Aug−2007

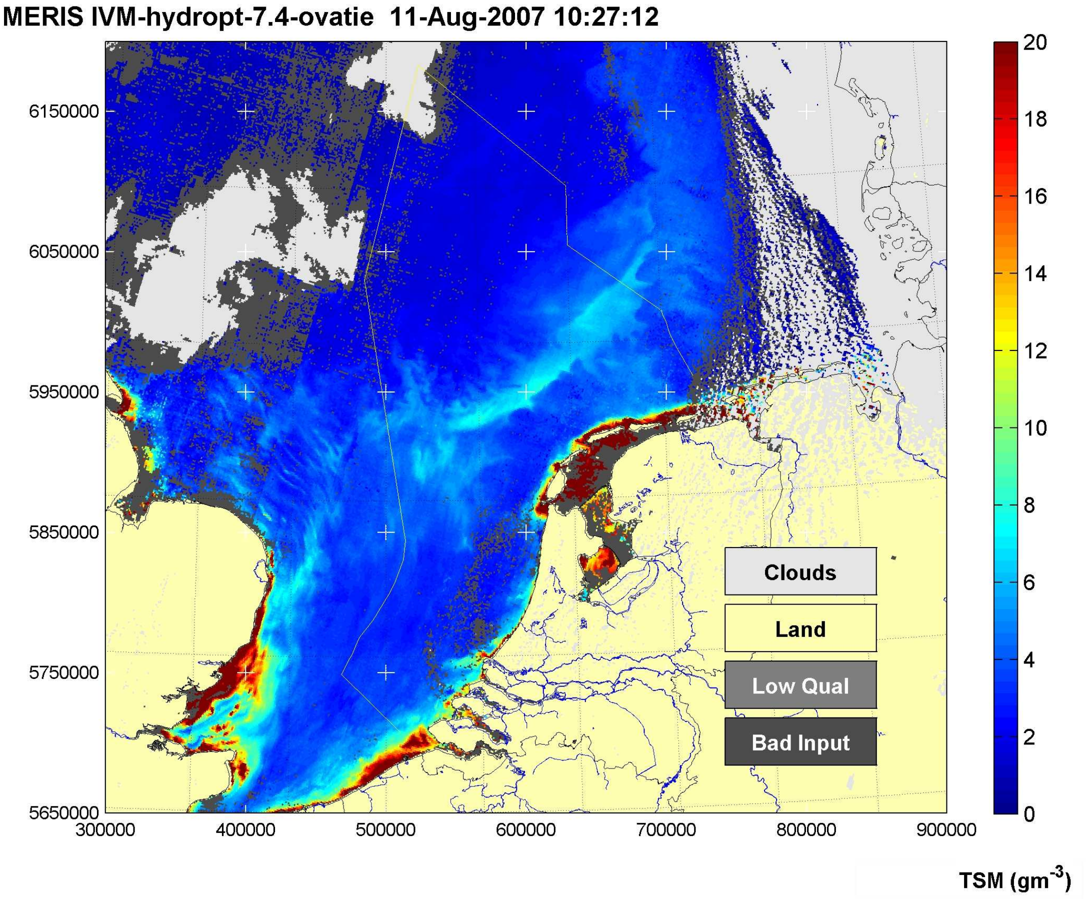

SPM quicklook with quality flags for conditions with sand mining 11−Aug−2007		
	IVM	
Alkyon Hydraulic Consultancy & Research	A2273	Fig. 3.24

Aug−2007

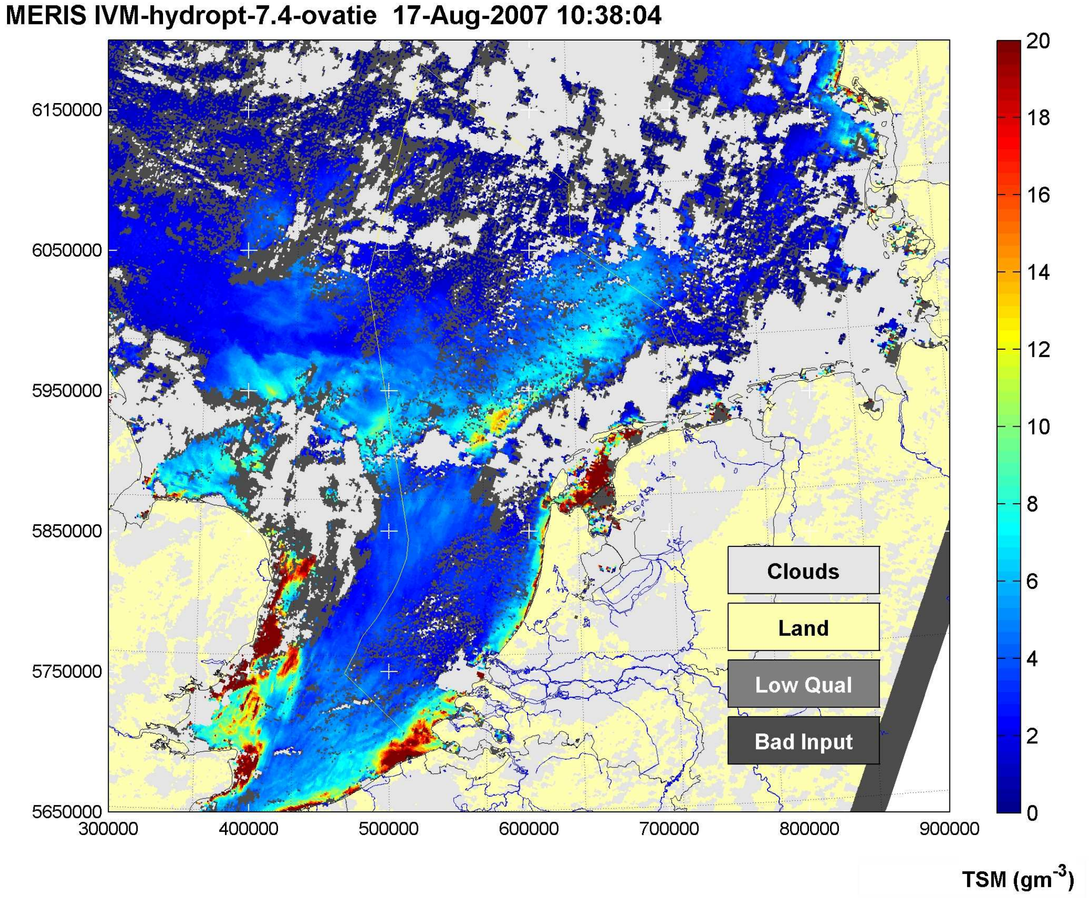

SPM quicklook with quality flags for conditions with sand mining 17−Aug−2007		
	IVM	
Alkyon Hydraulic Consultancy & Research	A2273	Fig. 3.25

Aug−2007

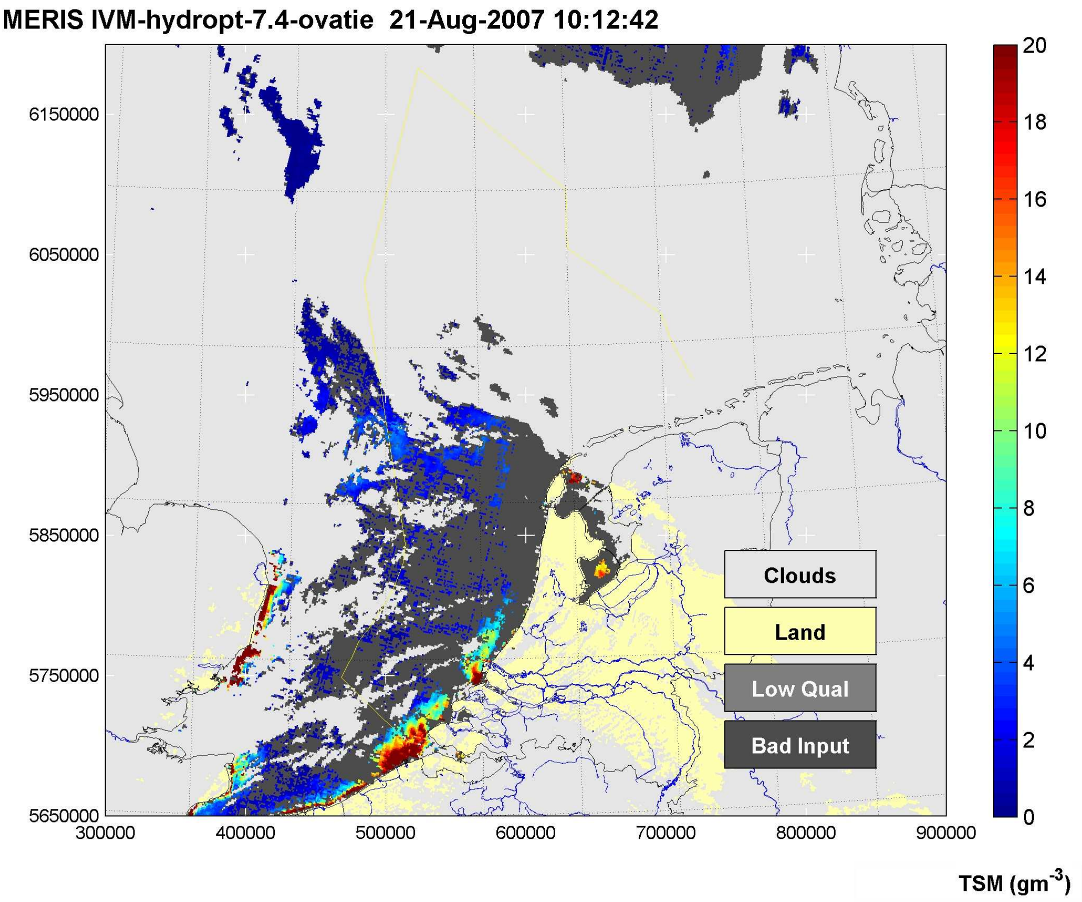

SPM quicklook with quality flags for conditions with sand mining 21−Aug−2007		
	IVM	
Alkyon Hydraulic Consultancy & Research	A2273	Fig. 3.26

Aug−2007

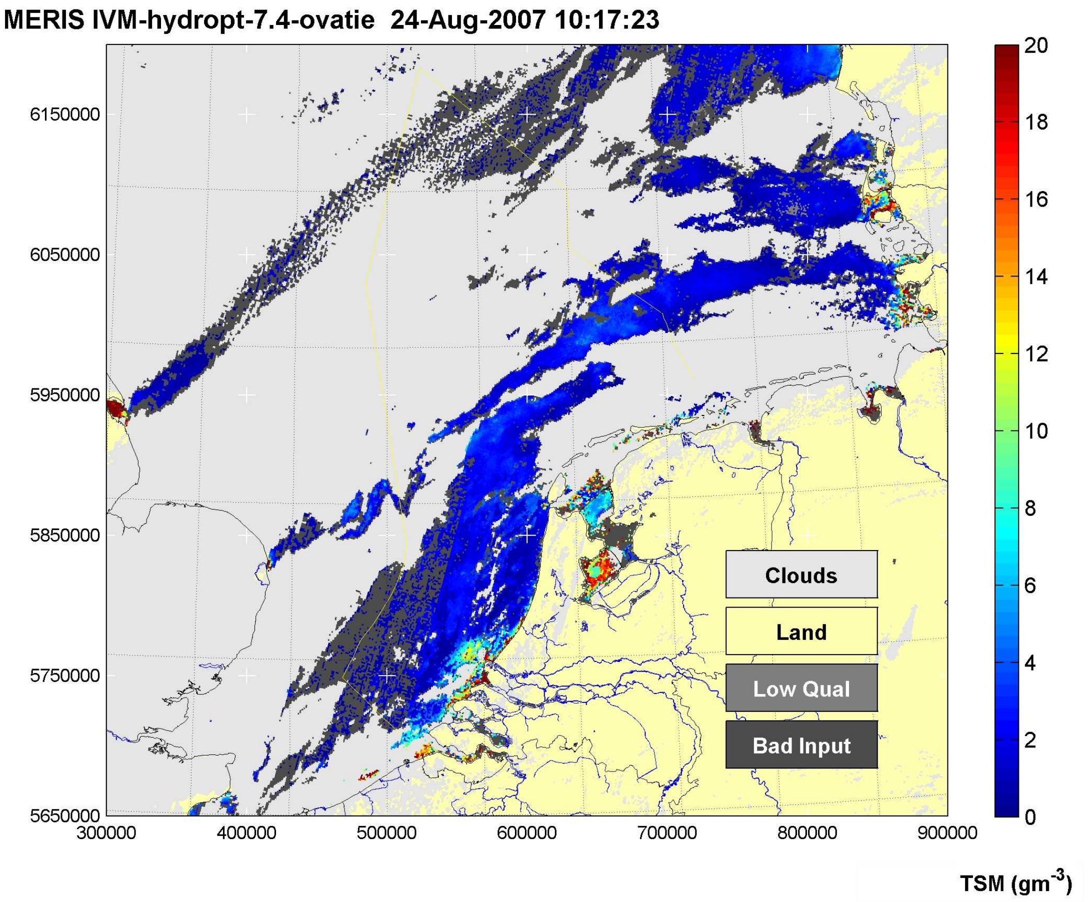

SPM quicklook with quality flags
for conditions with sand mining
24−Aug−2007

IVM

Alkyon Hydraulic Consultancy & Research | A2273 | Fig. 3.27

Sep−2007

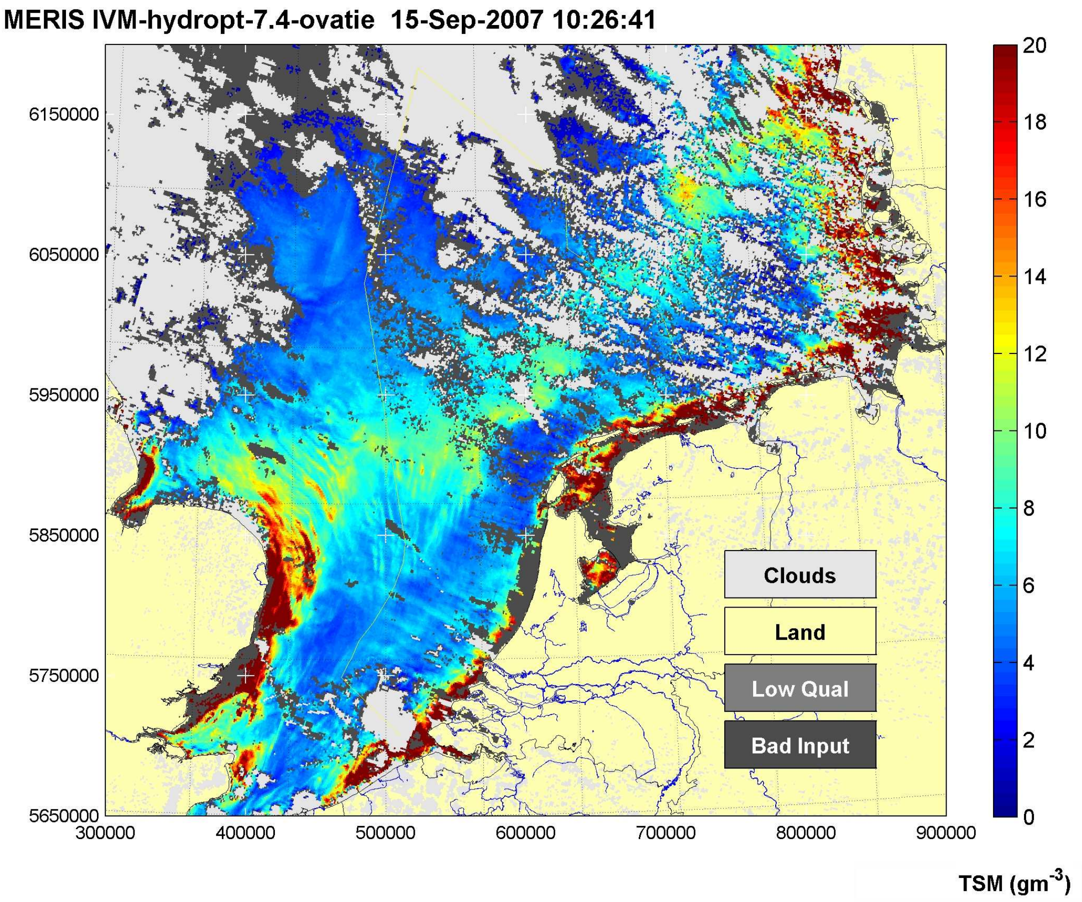

SPM quicklook with quality flags
for conditions with sand mining
15−Sep−2007

SPM quicklook with quality flags for conditions with sand mining 15−Sep−2007	IVM	
Alkyon Hydraulic Consultancy & Research	A2273	Fig. 3.28

Sep−2007

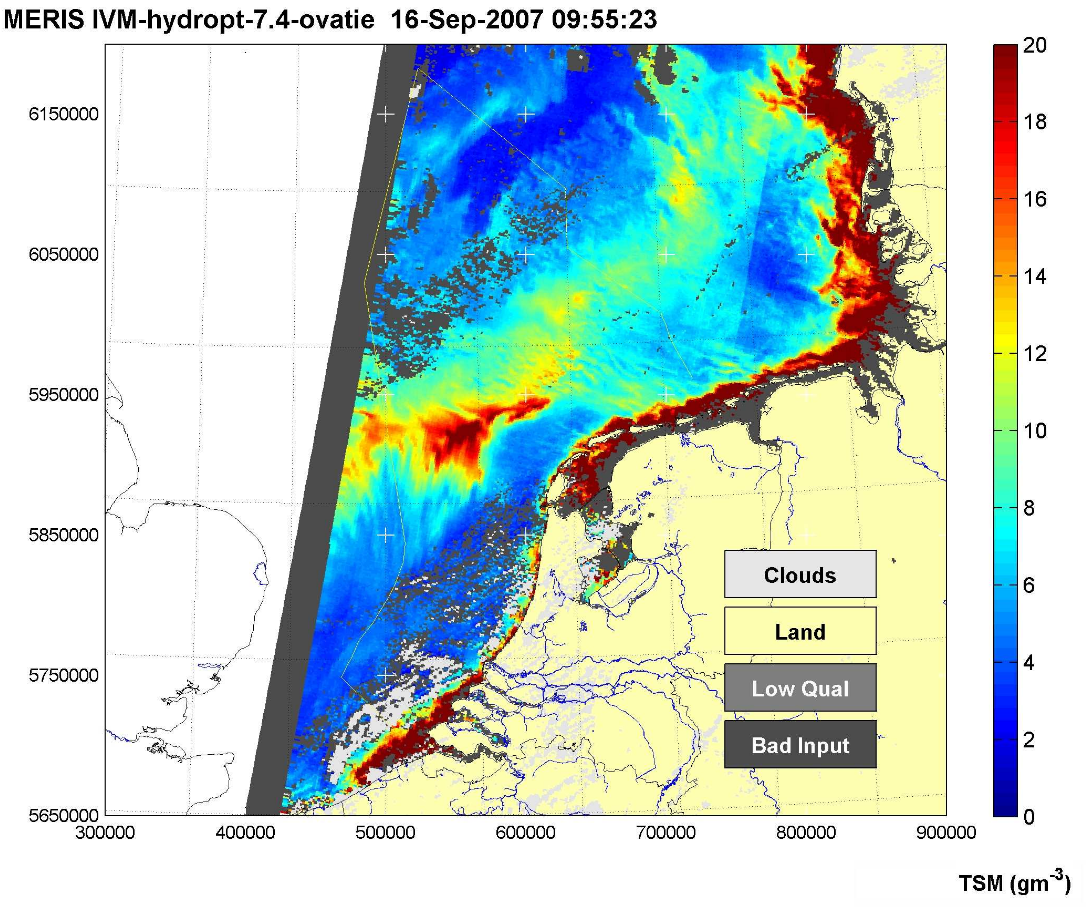

SPM quicklook with quality flags for conditions with sand mining 16−Sep−2007		
	IVM	
Alkyon Hydraulic Consultancy & Research	A2273	Fig. 3.29

Oct−2007

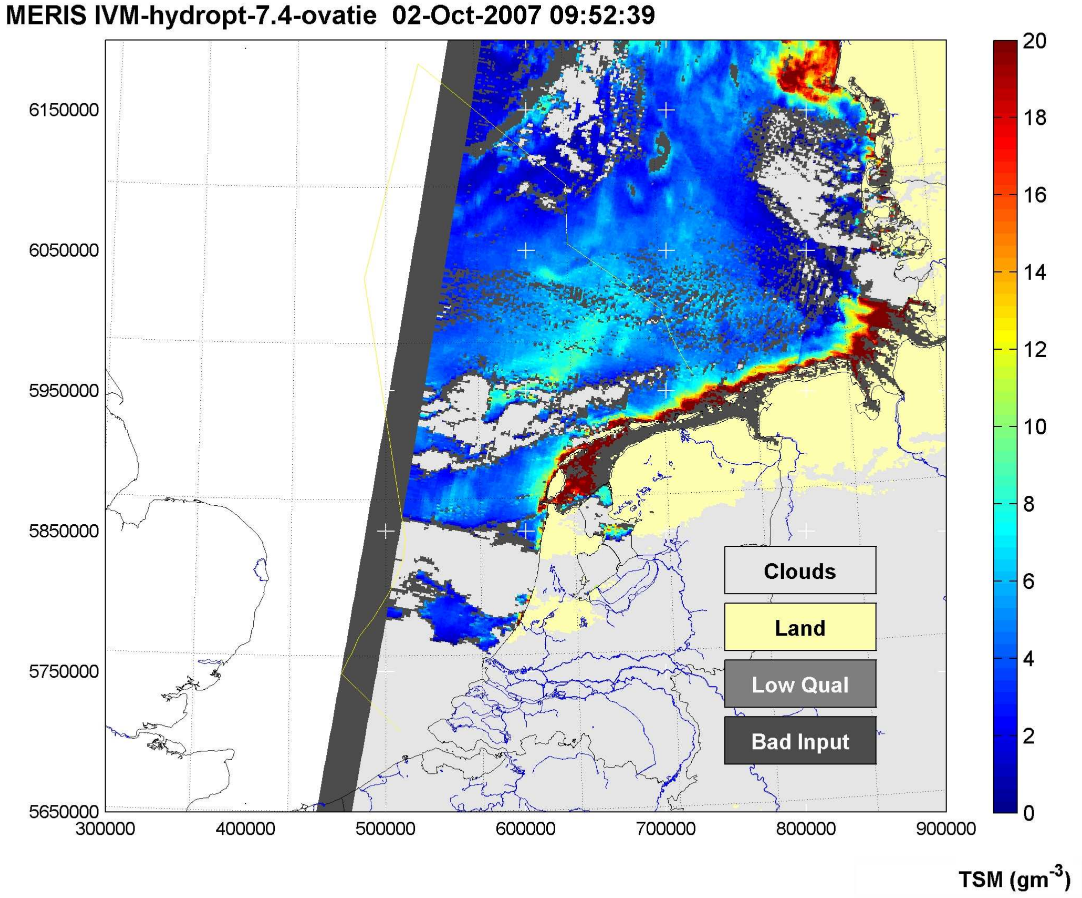

SPM quicklook with quality flags for conditions with sand mining 02−Oct−2007		
	IVM	
Alkyon Hydraulic Consultancy & Research	A2273	Fig. 3.30

Oct−2007

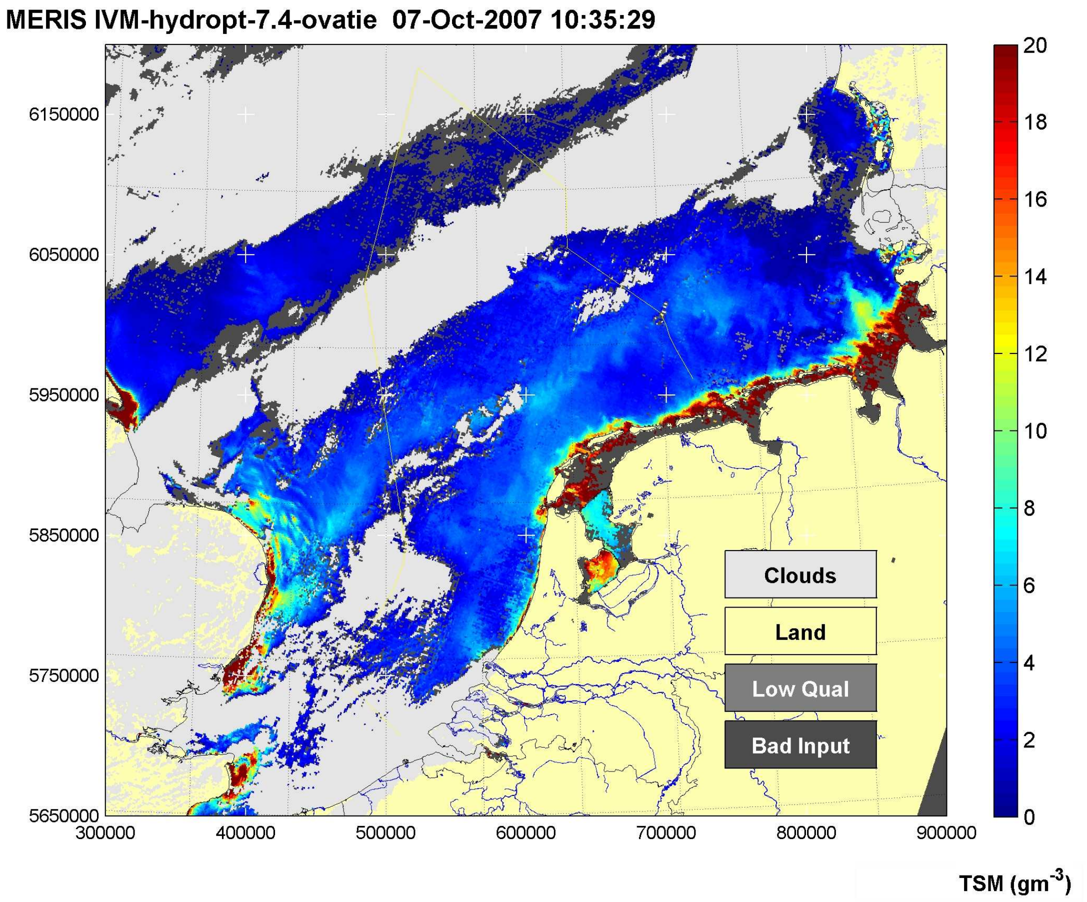

SPM quicklook with quality flags for conditions with sand mining 07−Oct−2007		
	IVM	
Alkyon Hydraulic Consultancy & Research	A2273	Fig. 3.31

Oct−2007

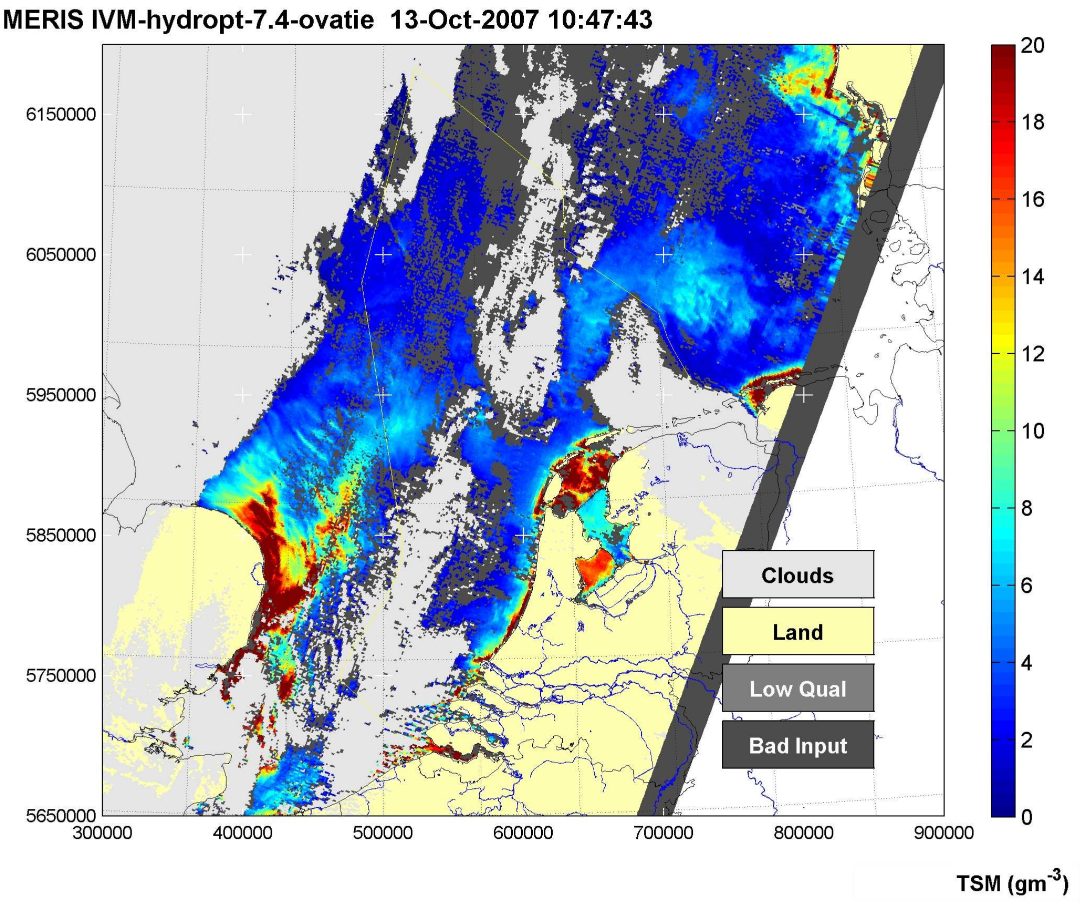

SPM quicklook with quality flags for conditions with sand mining 13−Oct−2007	IVM	
Alkyon Hydraulic Consultancy & Research	A2273	Fig. 3.32

Oct−2007

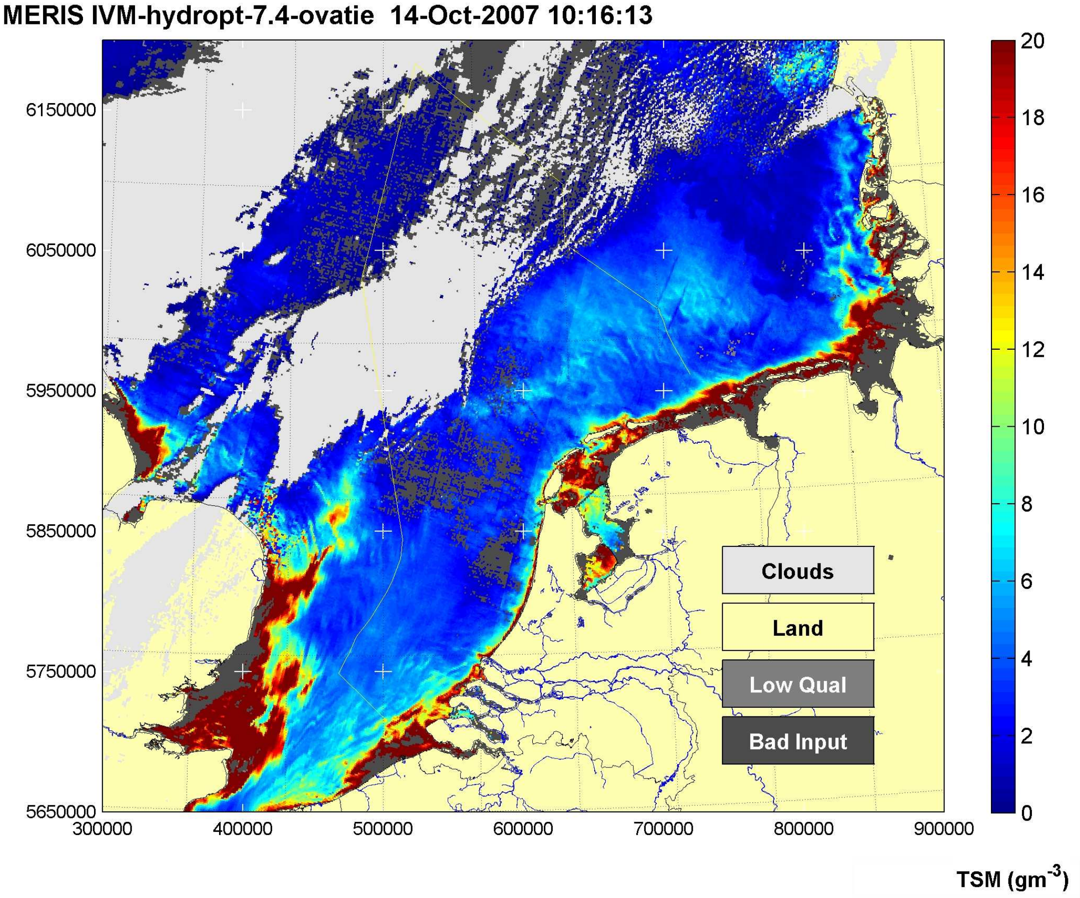

SPM quicklook with quality flags for conditions with sand mining 14−Oct−2007		
	IVM	
Alkyon Hydraulic Consultancy & Research	A2273	Fig. 3.33

Oct−2007

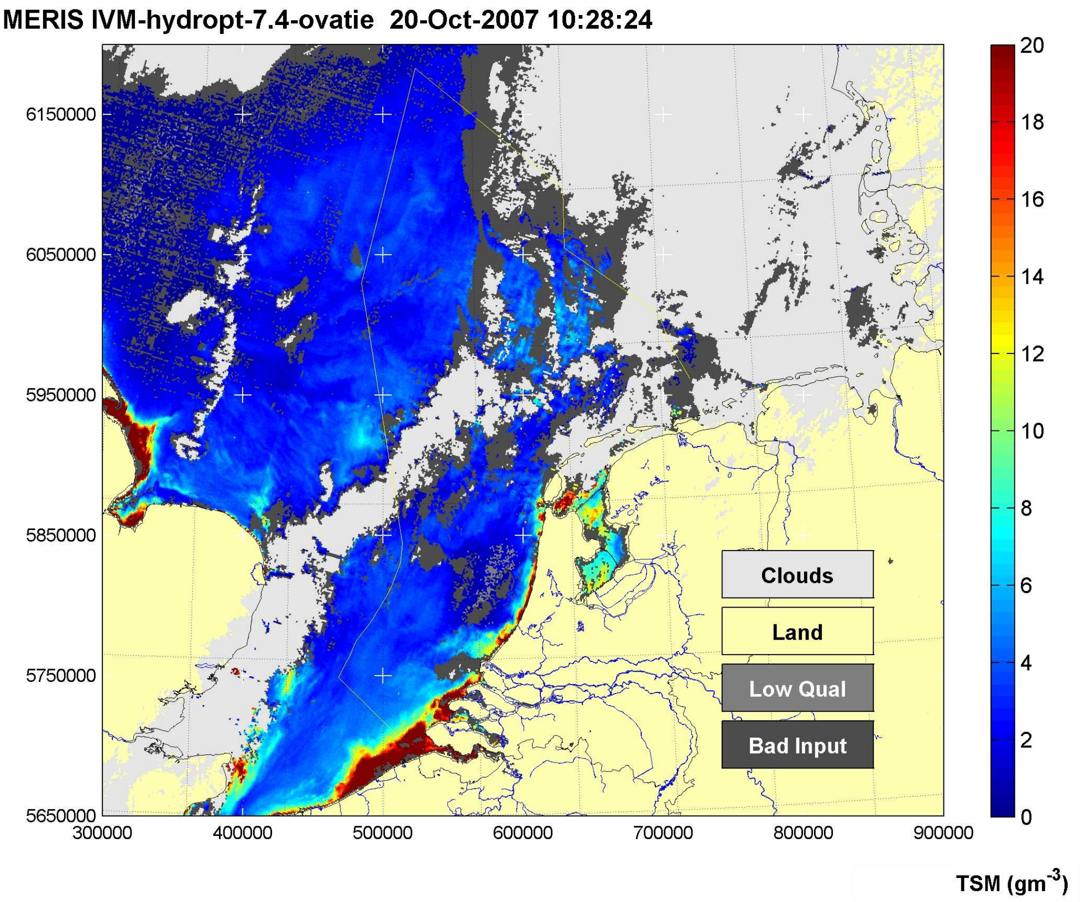

SPM quicklook with quality flags for conditions with sand mining 20−Oct−2007		
	IVM	
Alkyon Hydraulic Consultancy & Research	A2273	Fig. 3.34

Oct−2007

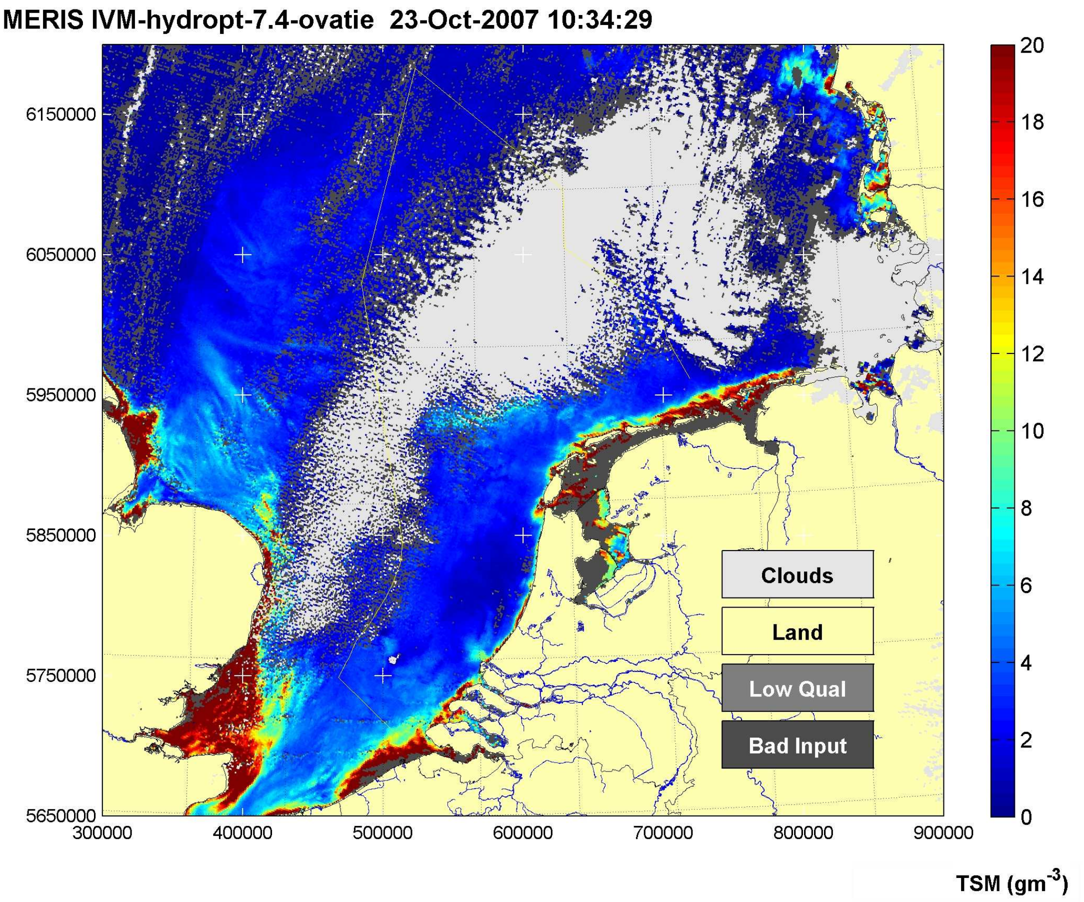

SPM quicklook with quality flags for conditions with sand mining 23−Oct−2007	IVM	
Alkyon Hydraulic Consultancy & Research	A2273	Fig. 3.35

Nov−2007

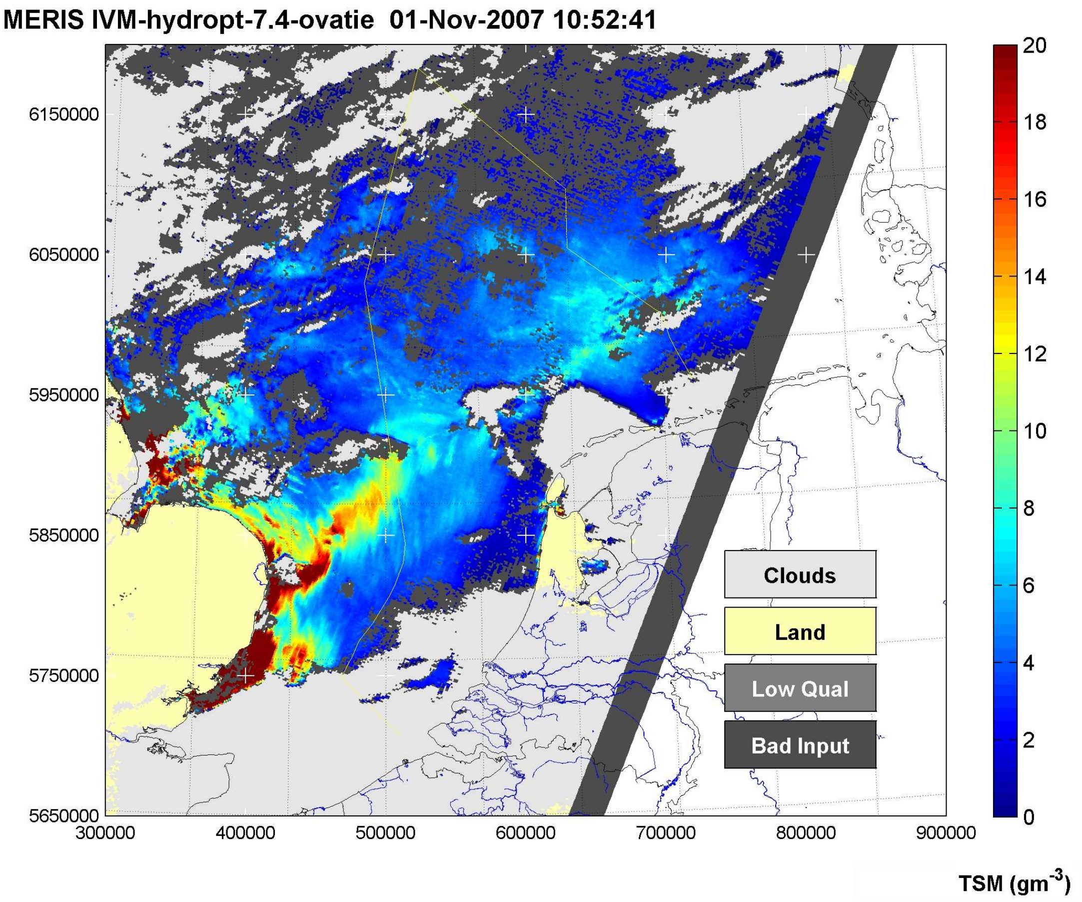

SPM quicklook with quality flags for conditions with sand mining 01−Nov−2007	IVM	
Alkyon Hydraulic Consultancy & Research	A2273	Fig. 3.36

Nov−2007

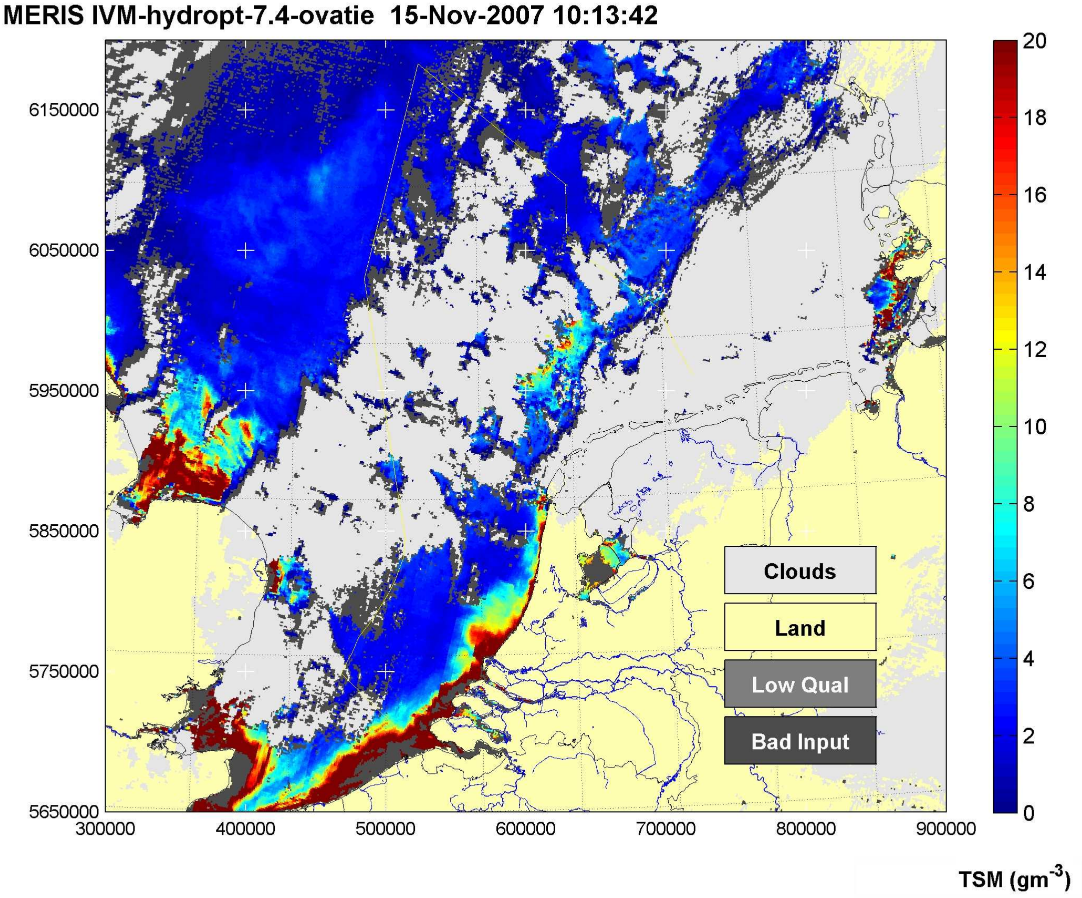

SPM quicklook with quality flags for conditions with sand mining 15−Nov−2007		
	IVM	
Alkyon Hydraulic Consultancy & Research	A2273	Fig. 3.37

Nov−2007

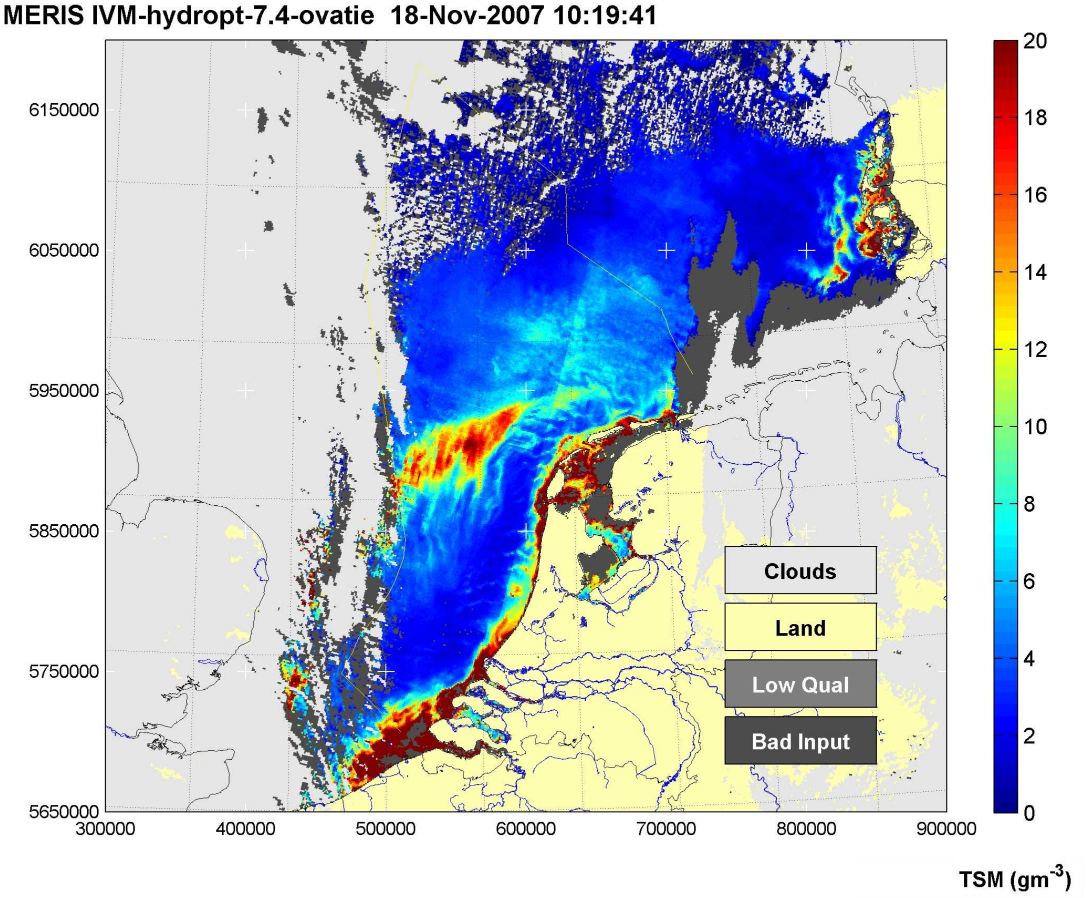

SPM quicklook with quality flags
for conditions with sand mining
18−Nov−2007

	IVM	
Alkyon Hydraulic Consultancy & Research	A2273	Fig. 3.38

Dec−2007

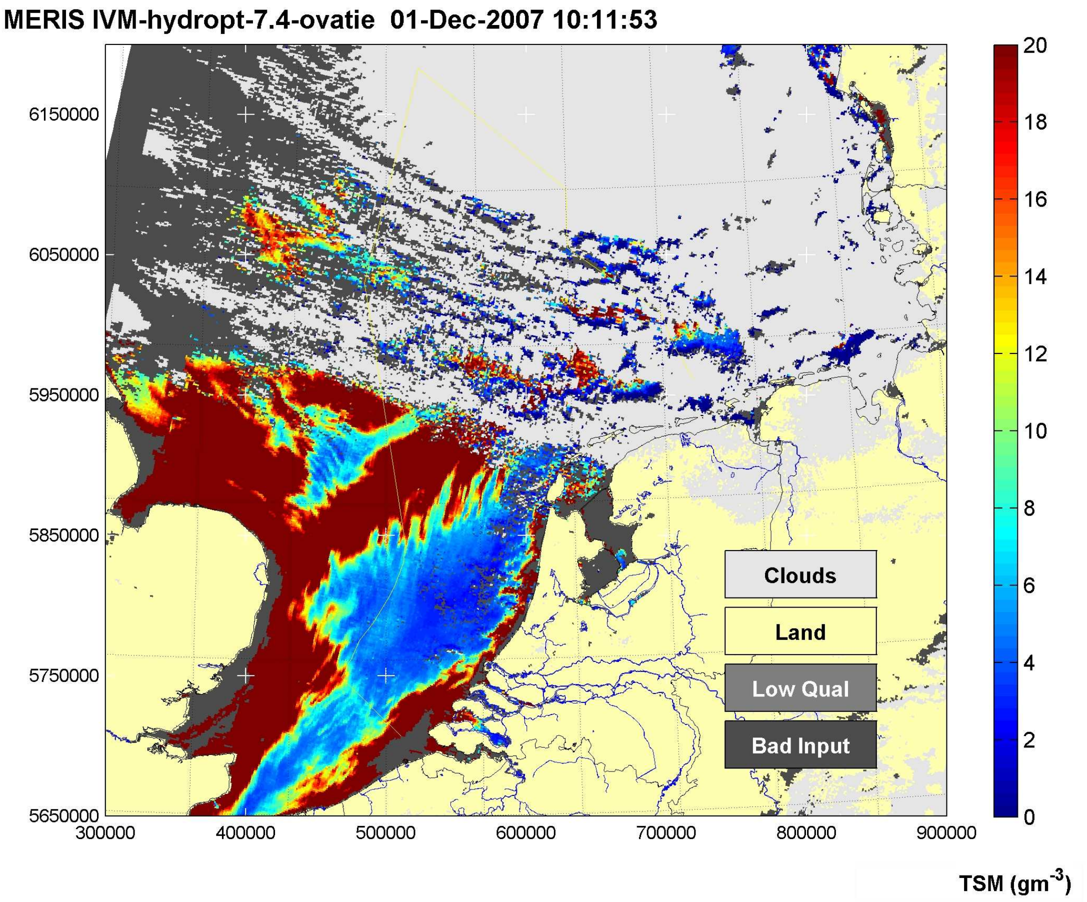

SPM quicklook with quality flags for conditions with sand mining 01−Dec−2007		
	IVM	
Alkyon Hydraulic Consultancy & Research	A2273	Fig. 3.39

Dec−2007

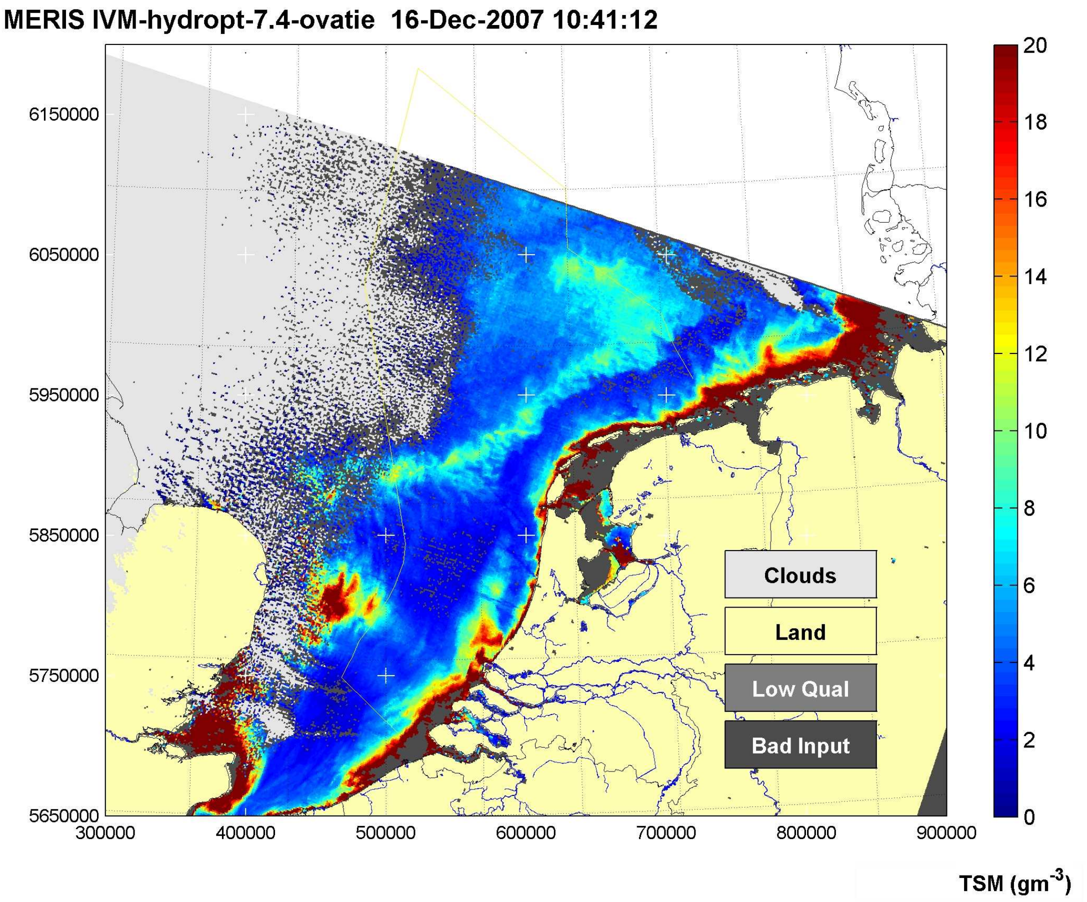

SPM quicklook with quality flags for conditions with sand mining 16−Dec−2007	IVM	
Alkyon Hydraulic Consultancy & Research	A2273	Fig. 3.40

Dec−2007

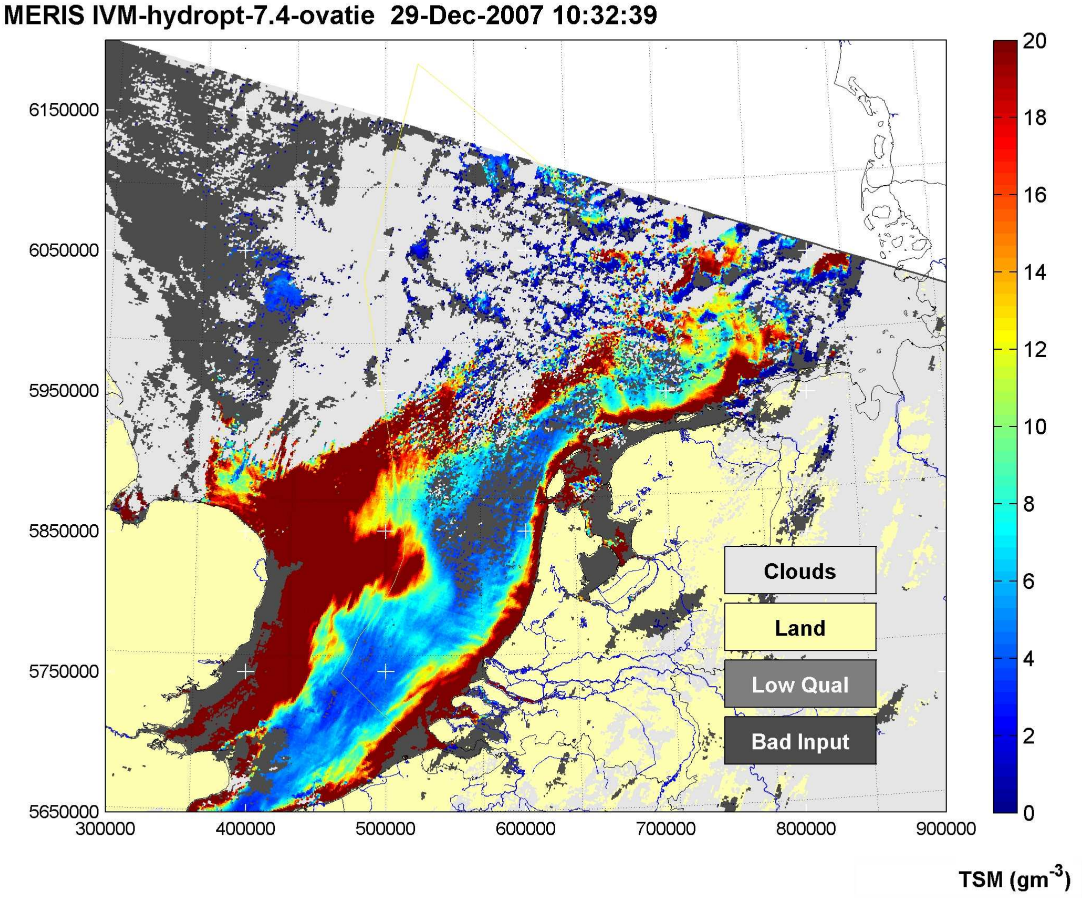

SPM quicklook with quality flags for conditions with sand mining 29−Dec−2007	IVM	
Alkyon Hydraulic Consultancy & Research	A2273	Fig. 3.41

05−Aug−2007

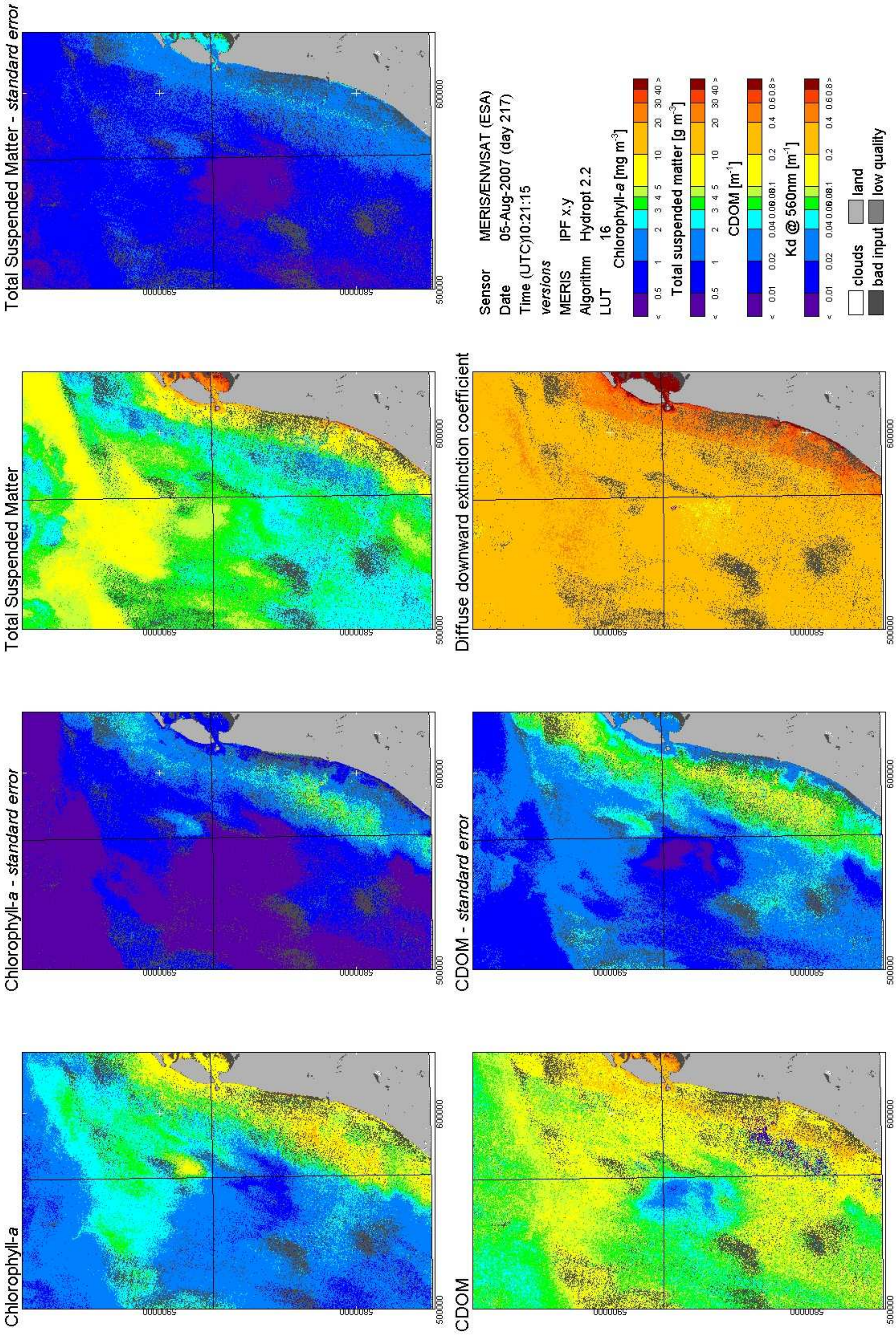

L2 data were browsed for higher reflectances near the mining locations and processed with optimised Ovatie SIOPs and L2 flag settings, ignoring PCD 1 13; 05−Aug−2007

IVM

Alkyon Hydraulic Consultancy & Research | A2273 | Fig. 3.42

07−Oct−2007

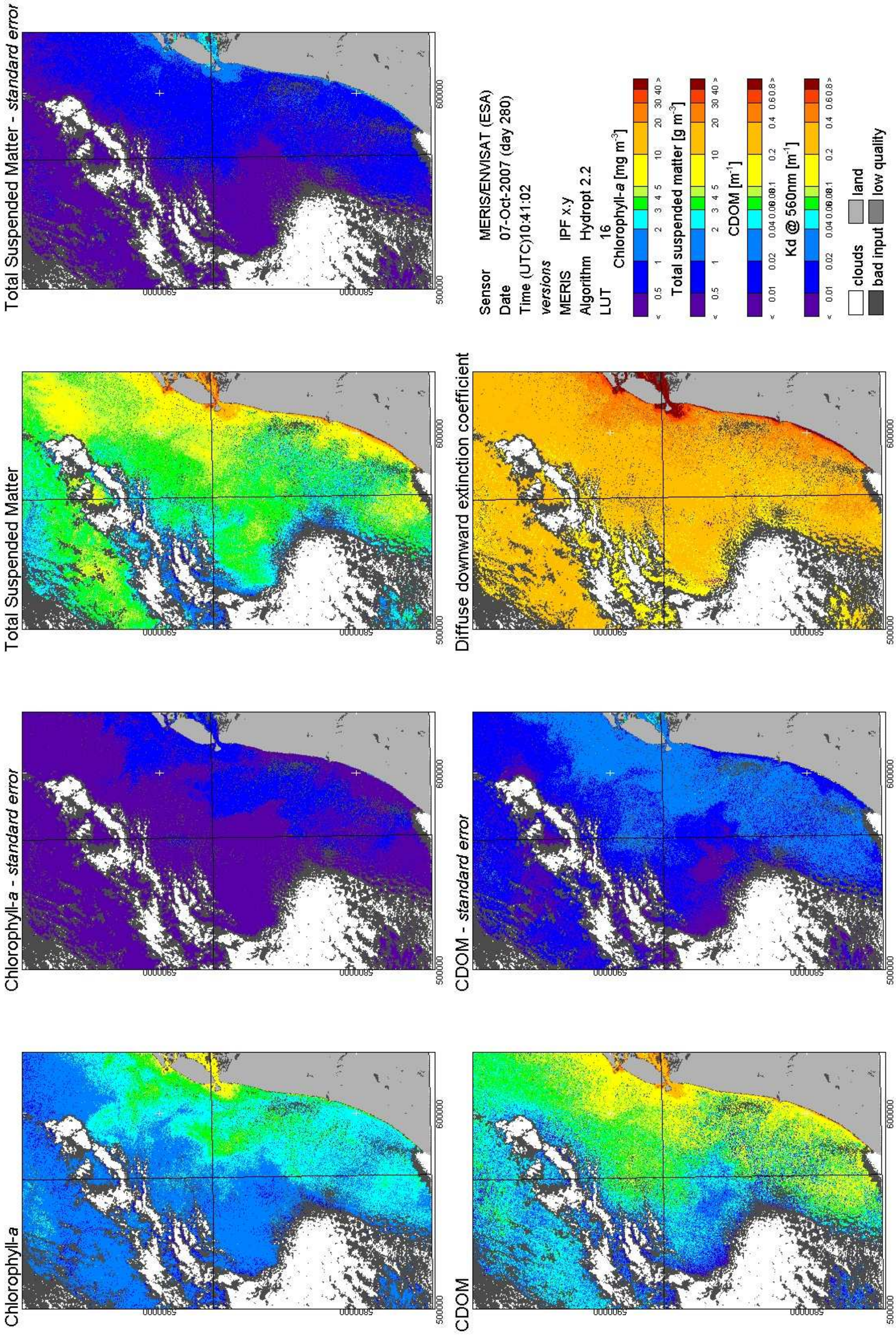

L2 data were browsed for higher reflectances near the mining locations and processed with optimised Ovatie SIOPs and L2 flag settings, ignoring PCD 1 13; 07−Oct−2007

	IVM	
Alkyon Hydraulic Consultancy & Research	A2273	Fig. 3.43

20−Oct−2007

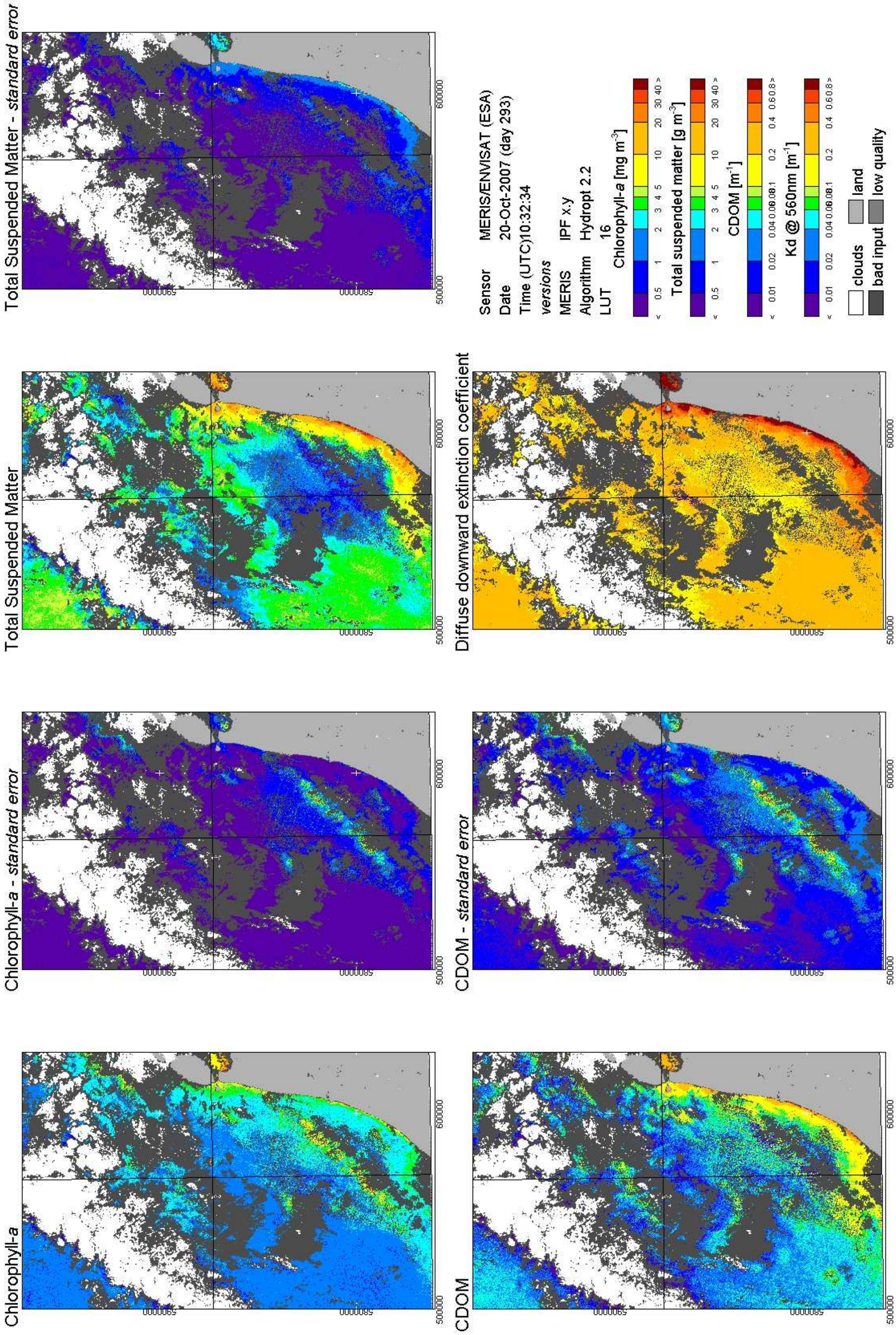

L2 data were browsed for higher reflectances near the mining locations and processed with optimised Ovatie SIOPs and L2 flag settings, ignoring PCD 1 13; 20−Oct−2007

	IVM	
Alkyon Hydraulic Consultancy & Research	A2273	Fig. 3.44

23−Oct−2007

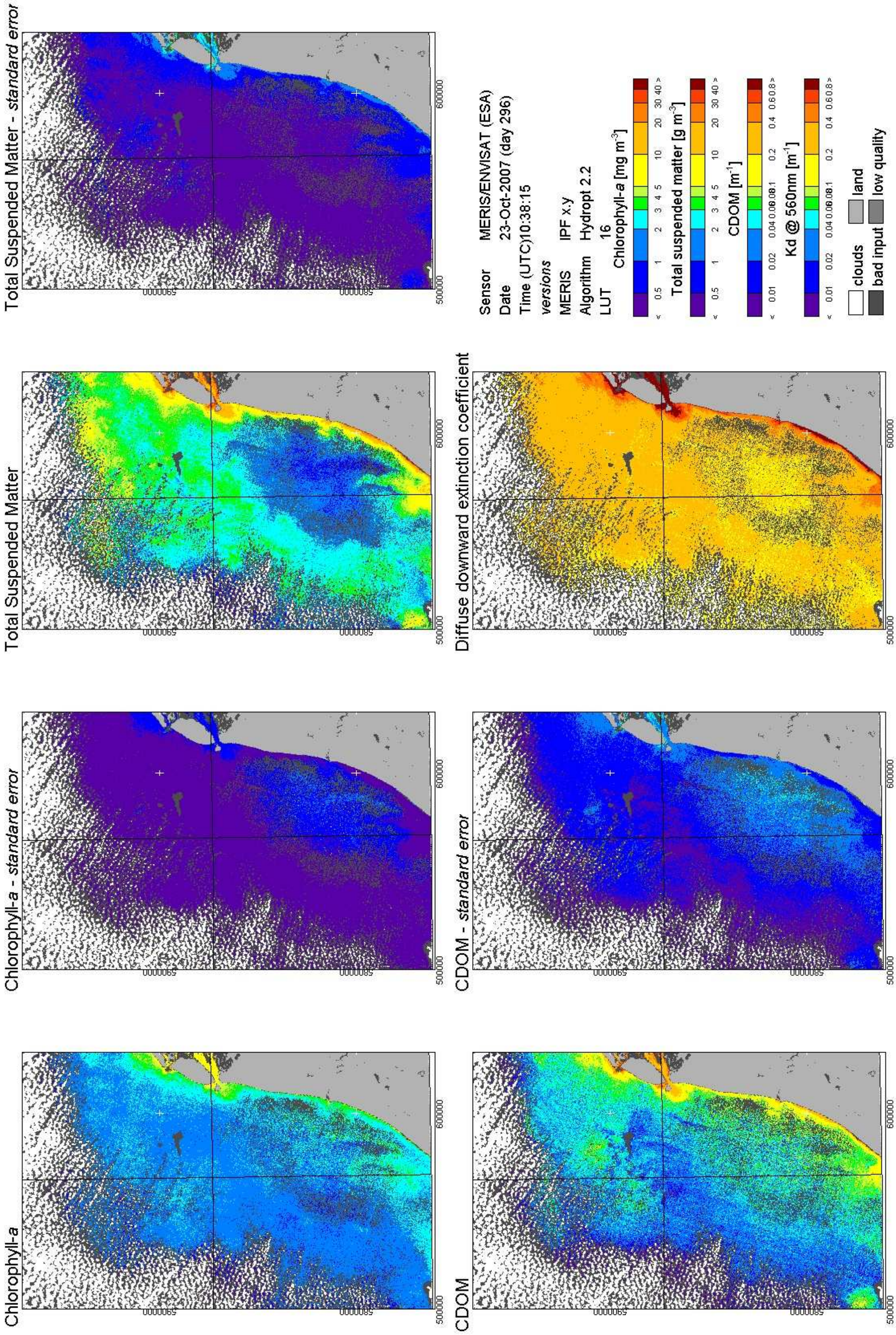

L2 data were browsed for higher reflectances near the mining locations
and processed with optimised Ovatie SIOPs and L2 flag settings,
ignoring PCD 1 13; 23−Oct−2007

	IVM	
Alkyon Hydraulic Consultancy & Research	A2273	Fig. 3.45

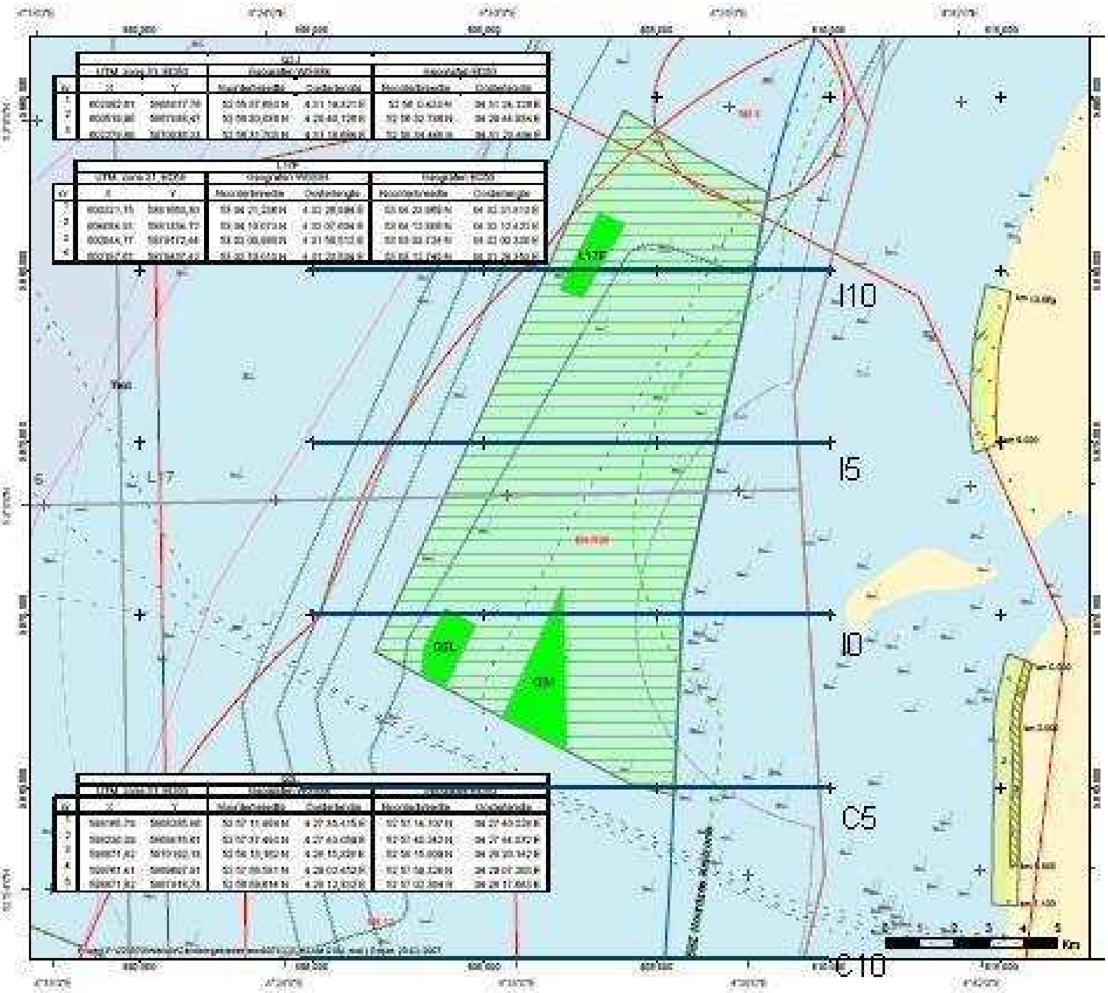

Five 15 km long cross−shore transects from X is 595.000 to 610.000 m.
The central transect (I0) goes through Q2J and Q2L at Y 5.870.000.
I5 and I10 are 5 and 10 km to the north; C5 and C10 are 5 and 10 km to the south

Alkyon Hydraulic Consultancy & Research	A2273	Fig. 3.46

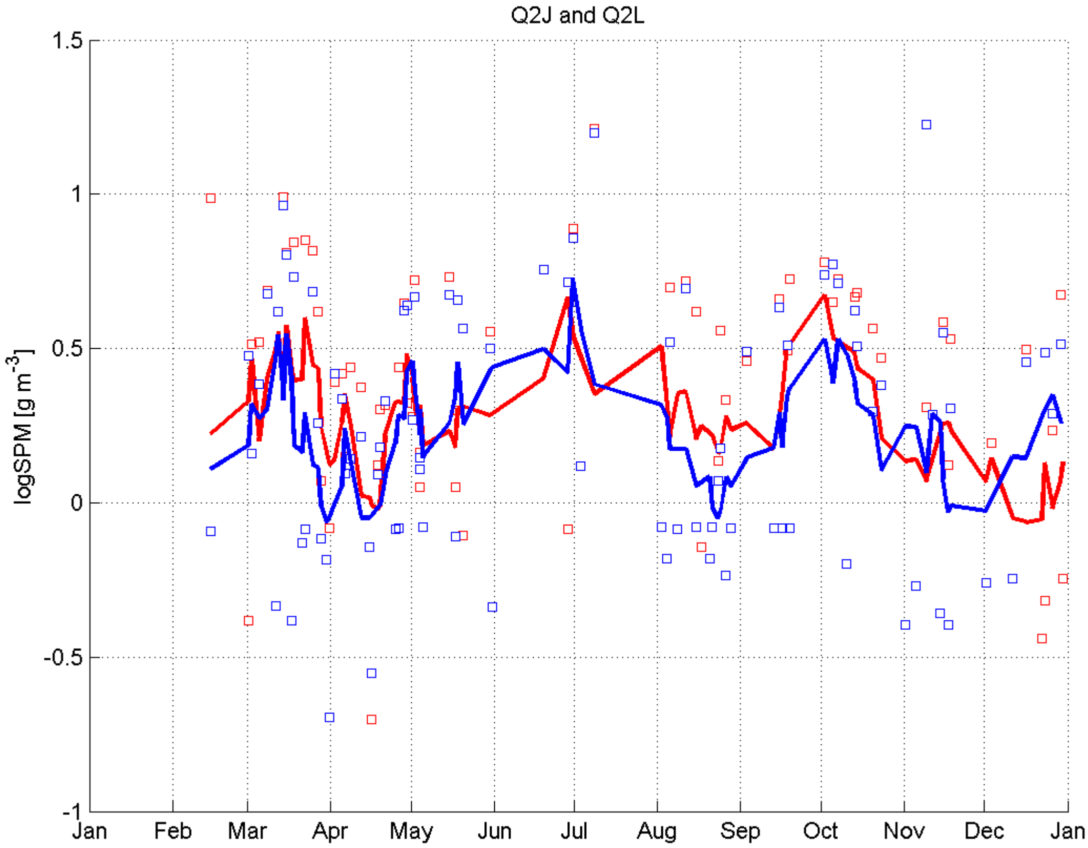

SPM time series at the centre points of the Q2J (red) and Q2L (blue)
In−situ control measurements (T0 conditions) were conducted 22−24 May.
Sand was extracted from 3 Augustus en ca. 23 December 2007.

Alkyon Hydraulic Consultancy & Research	A2273	Fig. 3.47

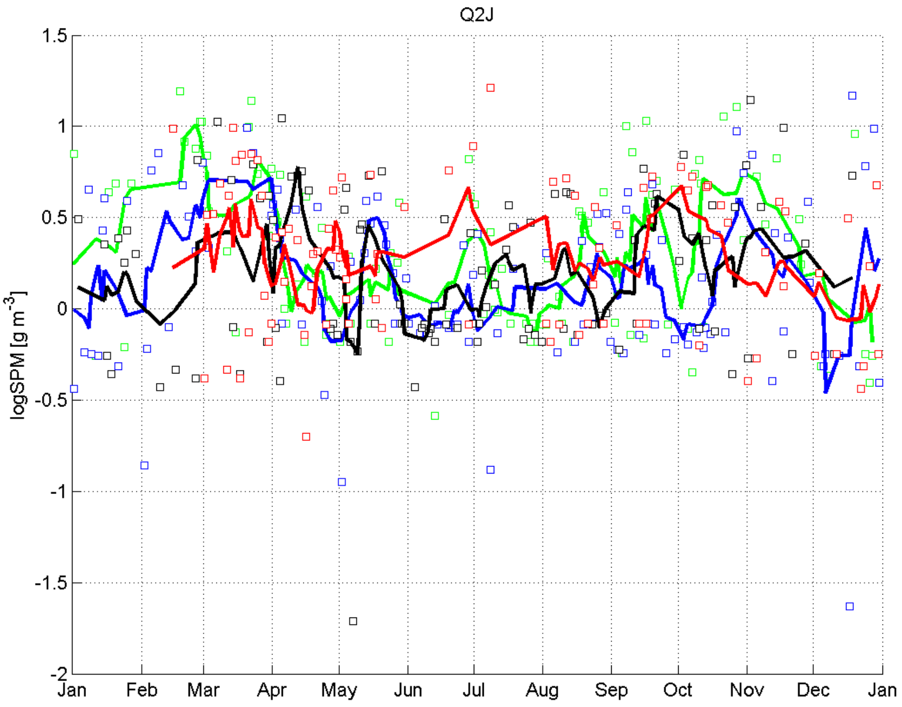

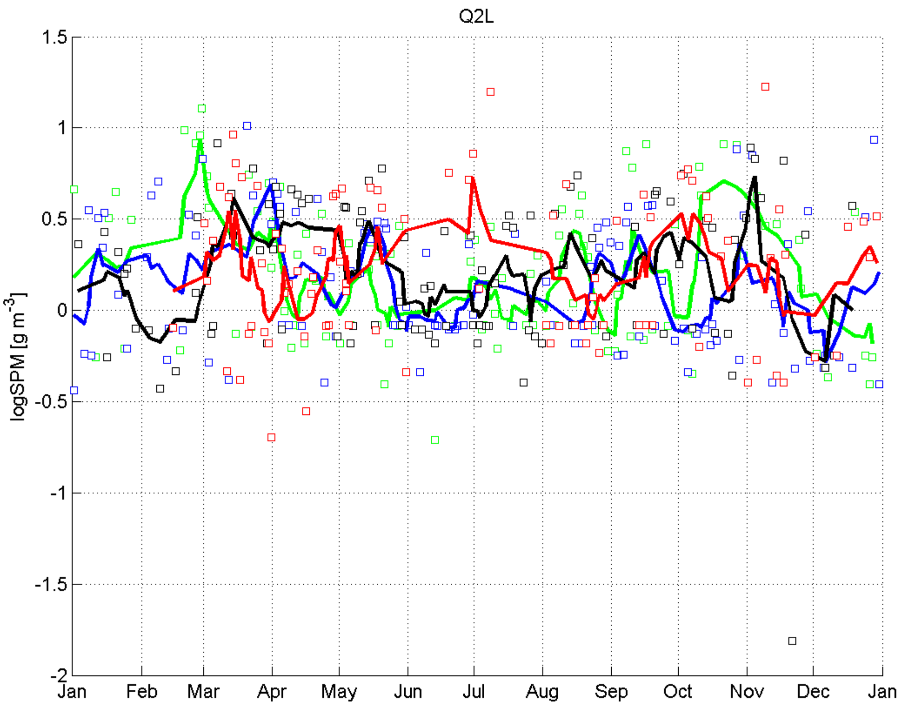

T0 time series (red = 2007 and green =2004, blue = 2005, black = 2006) at the centre points of the Q2J and Q2L Huisduinen sand extraction sites. The (span) moving averages illustrate seasonality and inter−annual variation.

Alkyon Hydraulic Consultancy & Research	A2273	Fig. 3.48

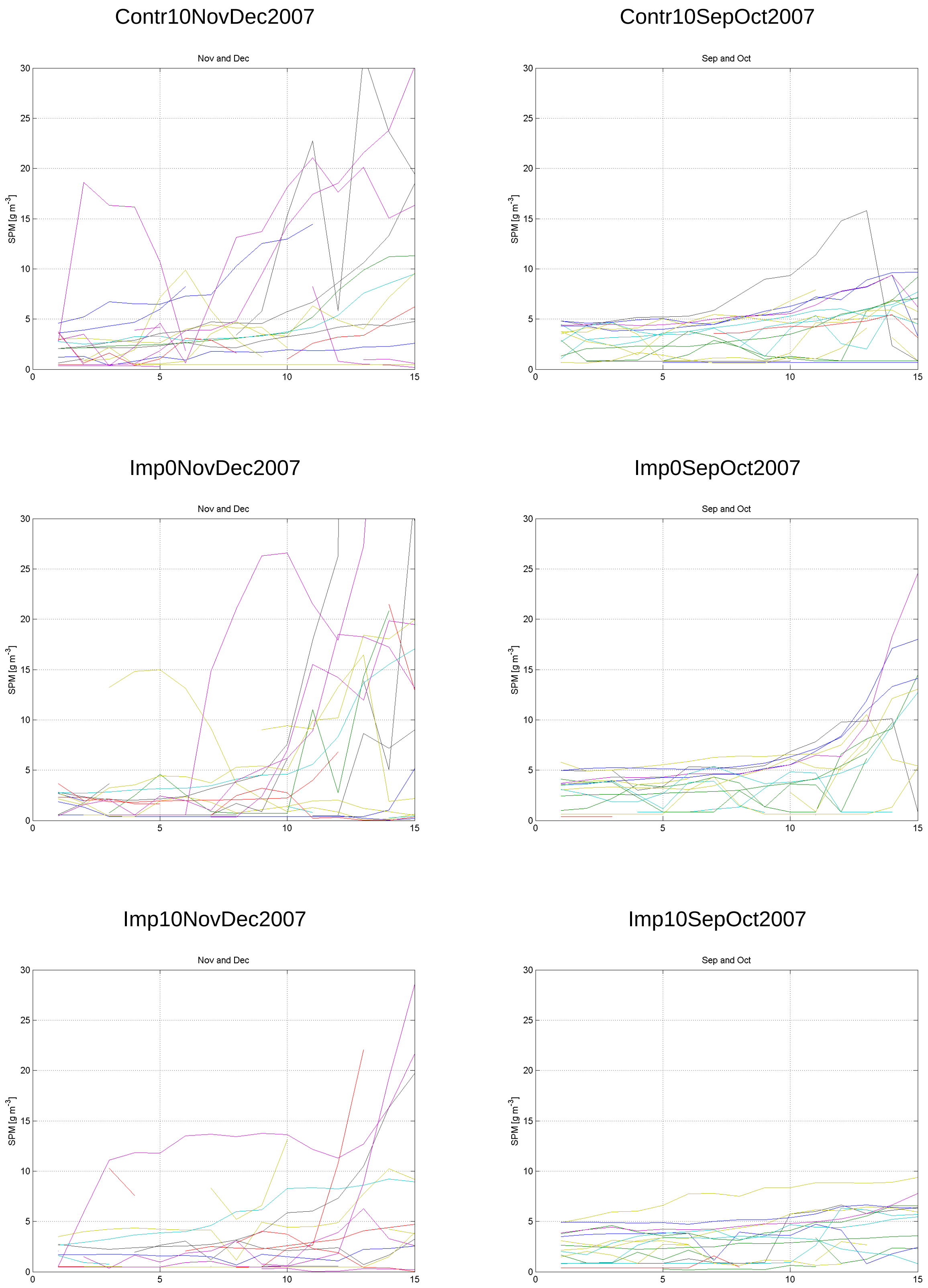

Control (C10) and Impact (I0 and I10) signals.
Higher values occur in Nov.−Dec.

Alkyon Hydraulic Consultancy & Research	A2273	Fig. 3.49

Contr10MayJun2007

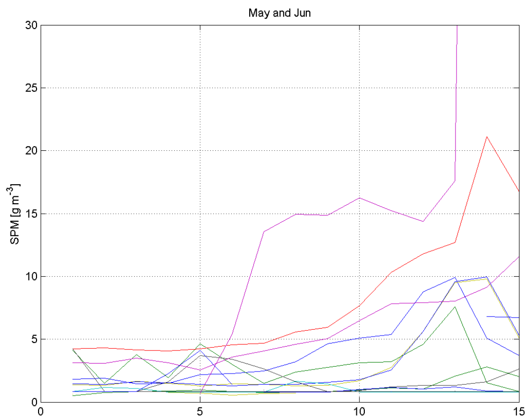

Imp0MayJun2007

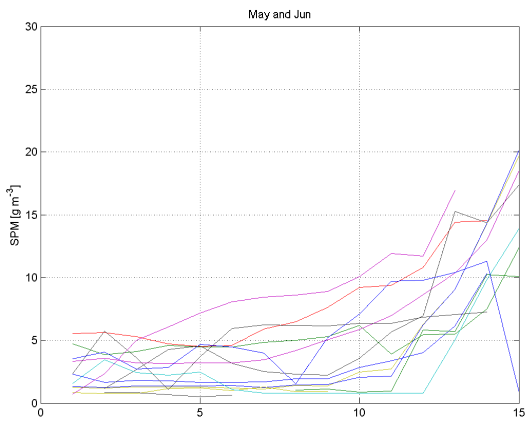

Imp10MayJun2007

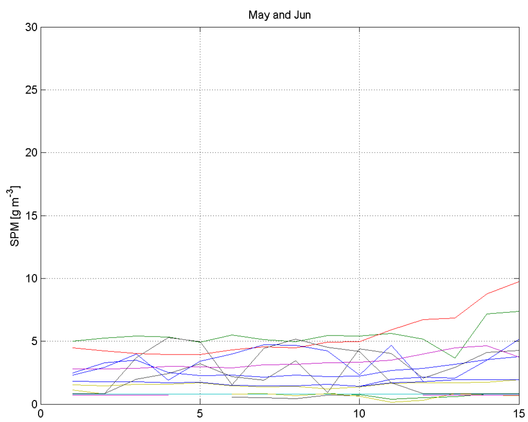

Control (C10) and Impact (I0 and I10) signals. Situation in May−June 2007 before sand extraction	IVM	
Alkyon Hydraulic Consultancy & Research	A2273	Fig. 3.50

01−May−2007

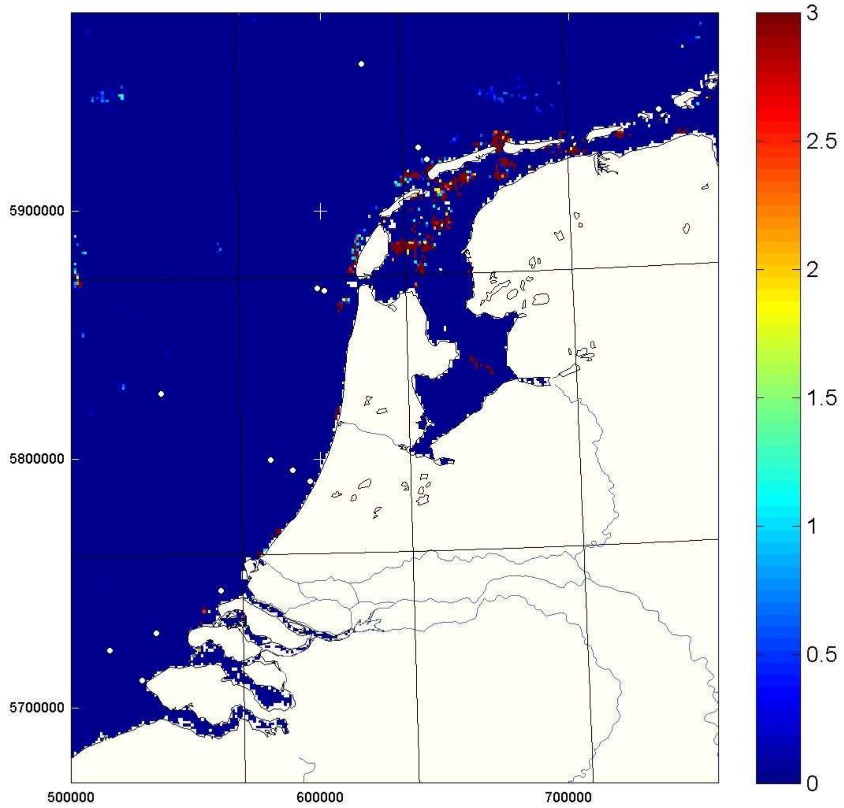

Example of results from Eleveld’s plume detection algorithm
before sand extraction (control)
01−May−2007

IVM

Alkyon Hydraulic Consultancy & Research

A2273

Fig. 3.51

04−May−2007

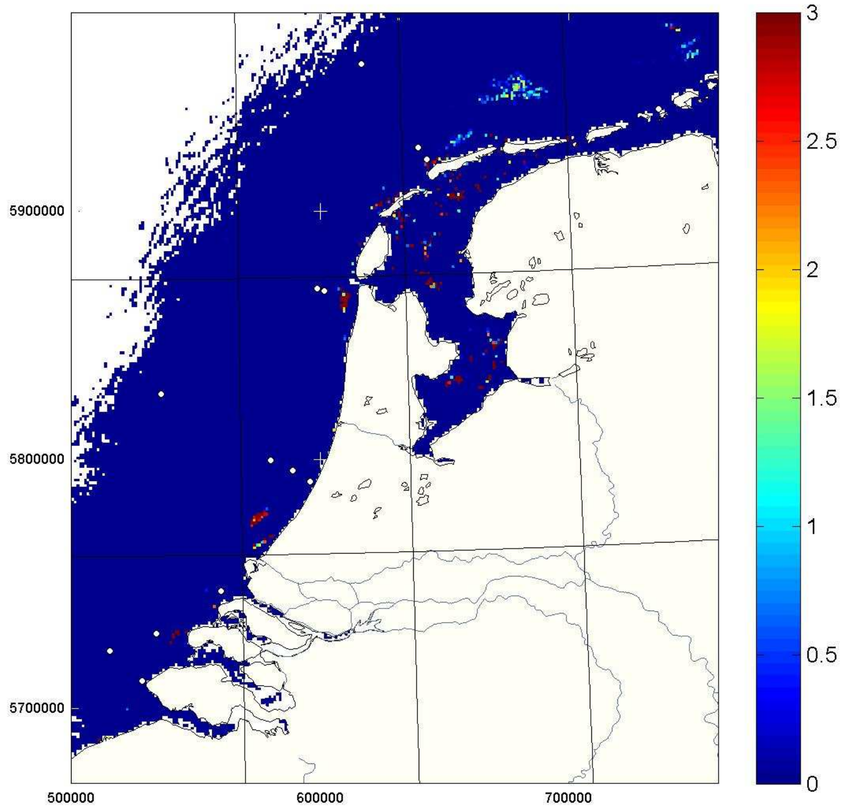

Example of results from Eleveld's plume detection algorithm
before sand extraction (control)
04−May−2007

IVM

Alkyon Hydraulic Consultancy & Research

A2273

Fig. 3.52

15−May−2007

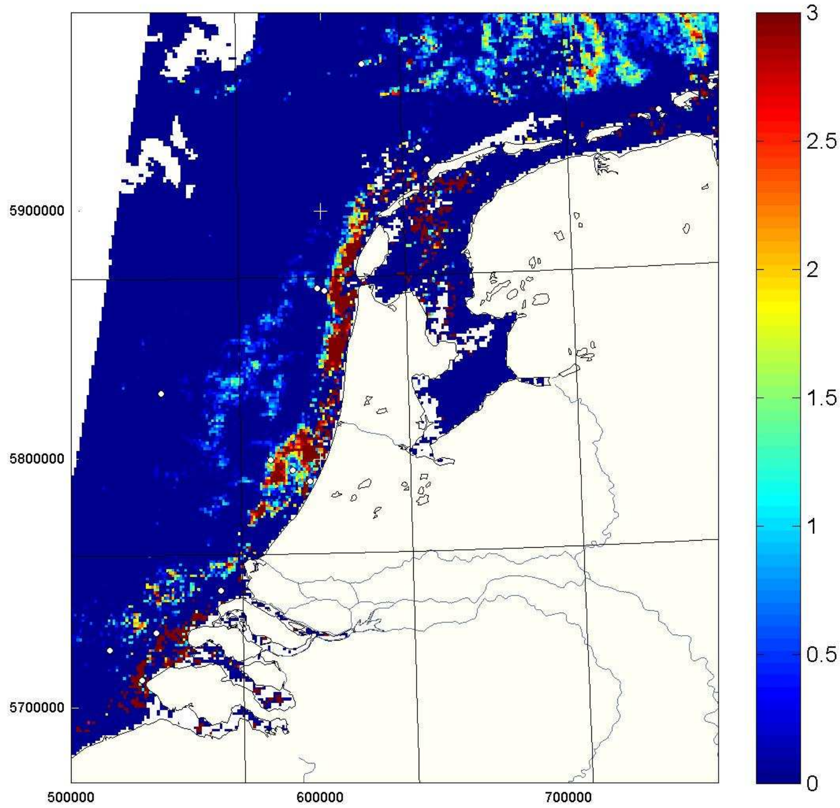

Example of results from Eleveld's plume detection algorithm
before sand extraction (control)
15−May−2007

IVM

Alkyon Hydraulic Consultancy & Research

A2273

Fig. 3.53

30−May−2007

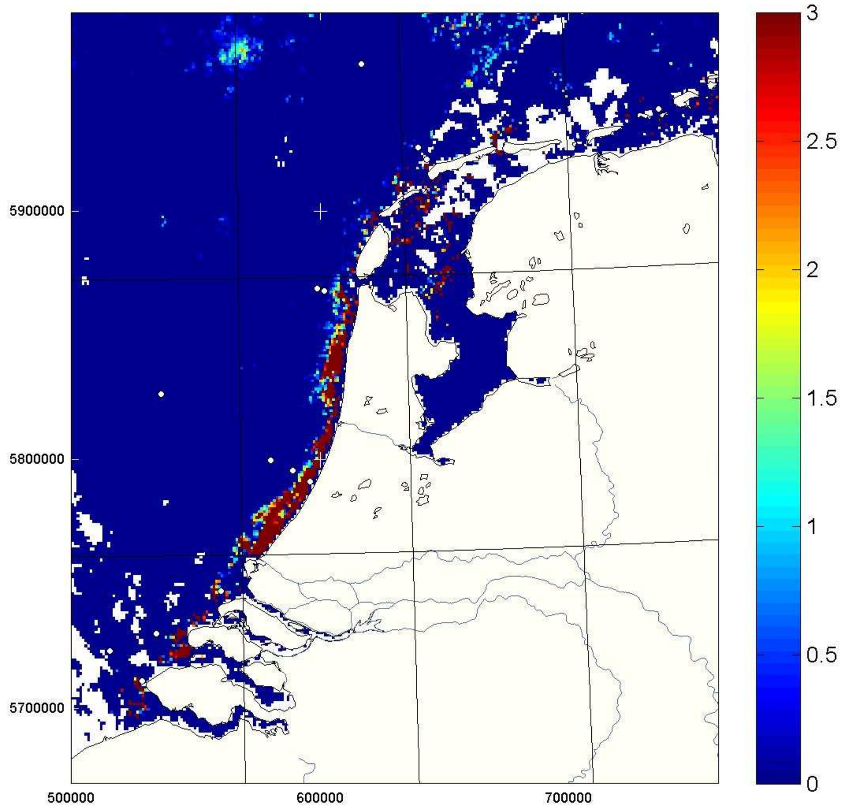

Example of results from Eleveld’s plume detection algorithm
before sand extraction (control)
30−May−2007

IVM

Alkyon Hydraulic Consultancy & Research

A2273

Fig. 3.54

05−Aug−2007

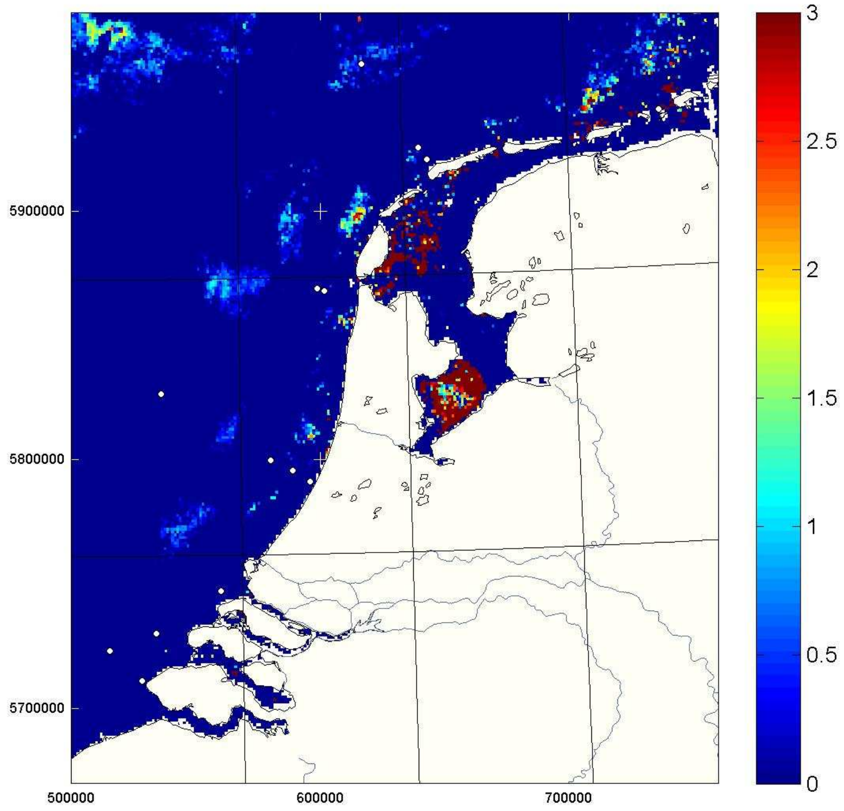

Example of results from Eleveld's plume detection algorithm
during sand extraction (impact)
05−Aug−2007

	IVM	
Alkyon Hydraulic Consultancy & Research	A2273	Fig. 3.55

11−Aug−2007

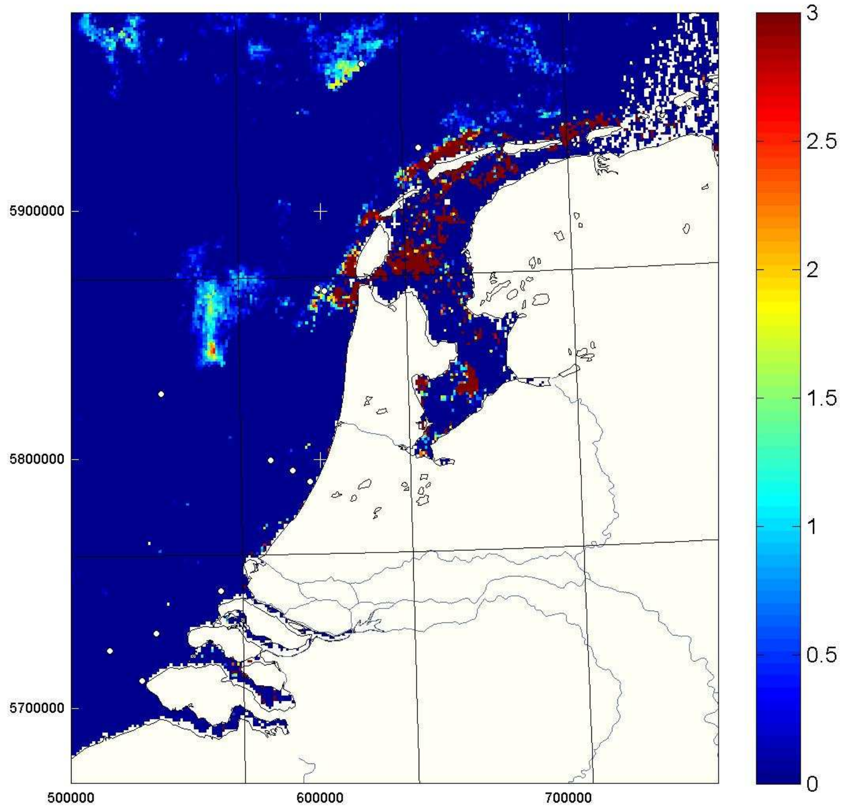

Example of results from Eleveld's plume detection algorithm during sand extraction (impact) 11−Aug−2007	IVM	
Alkyon Hydraulic Consultancy & Research	A2273	Fig. 3.56

17−Aug−2007

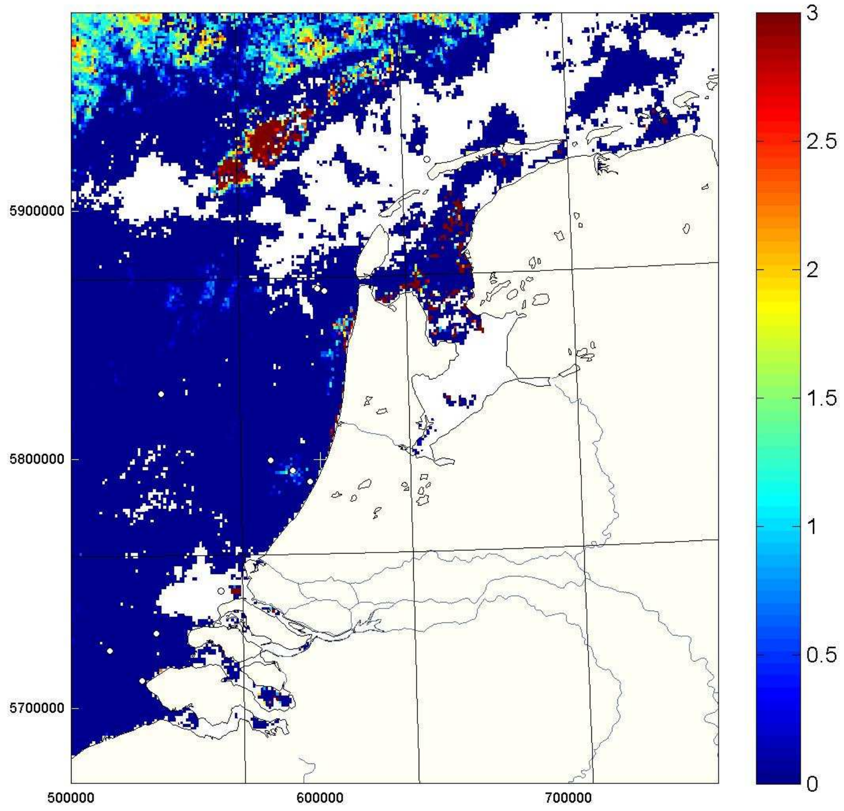

Example of results from Eleveld's plume detection algorithm
during sand extraction (impact)
17−Aug−2007

IVM

Alkyon Hydraulic Consultancy & Research

A2273

Fig. 3.57

15−Sep−2007

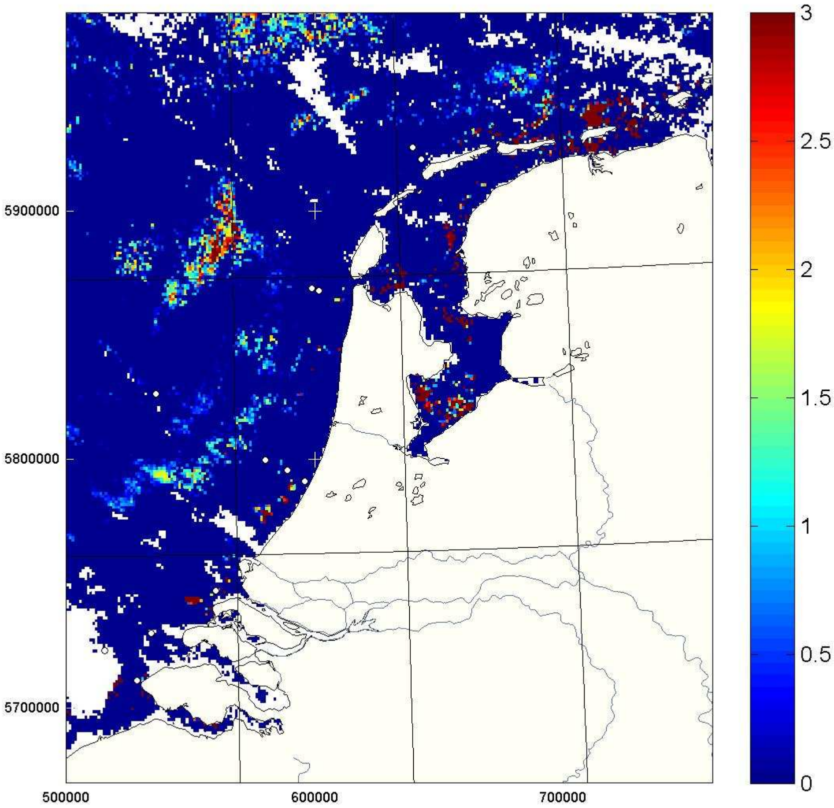

Example of results from Eleveld's plume detection algorithm during sand extraction (impact) 15−Sep−2007	IVM	
Alkyon Hydraulic Consultancy & Research	A2273	Fig. 3.58

16−Sep−2007

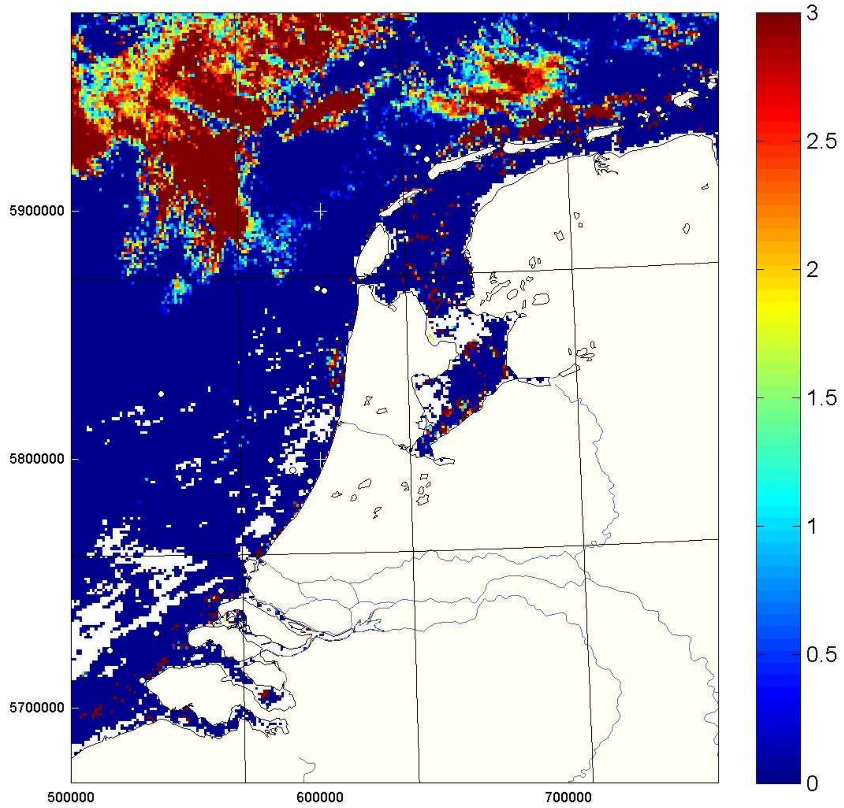

Example of results from Eleveld's plume detection algorithm
during sand extraction (impact)
16−Sep−2007

	IVM	
Alkyon Hydraulic Consultancy & Research	A2273	Fig. 3.59

07−Oct−2007

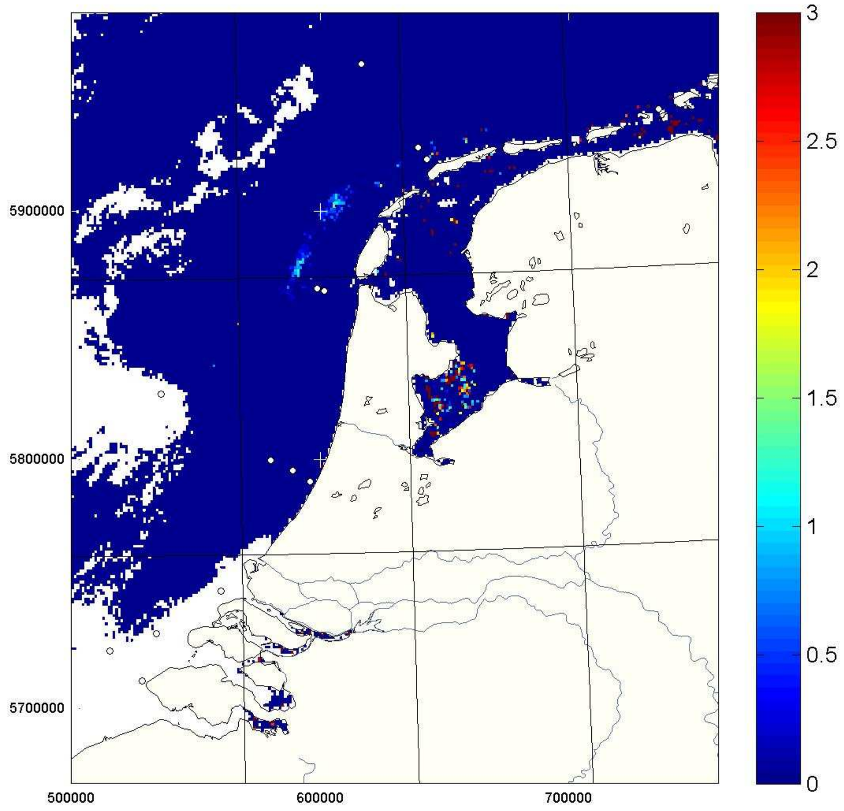

Example of results from Eleveld's plume detection algorithm
during sand extraction (impact)
07−Oct−2007

	IVM	
Alkyon Hydraulic Consultancy & Research	A2273	Fig. 3.60

13−Oct−2007

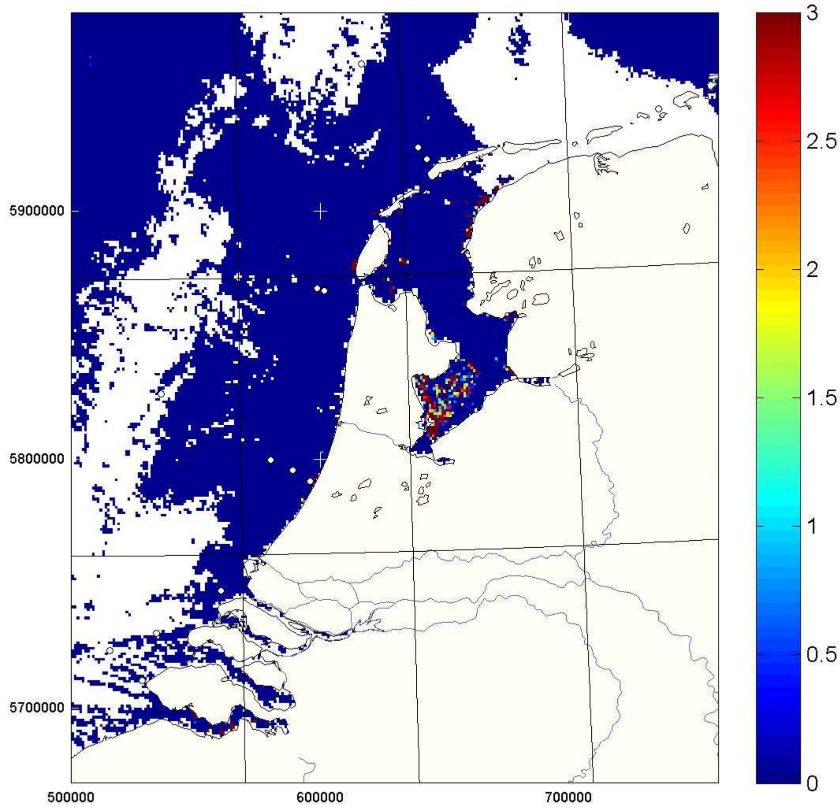

Example of results from Eleveld's plume detection algorithm during sand extraction (impact) 13−Oct−2007	IVM	
Alkyon Hydraulic Consultancy & Research	A2273	Fig. 3.61

14−Oct−2007

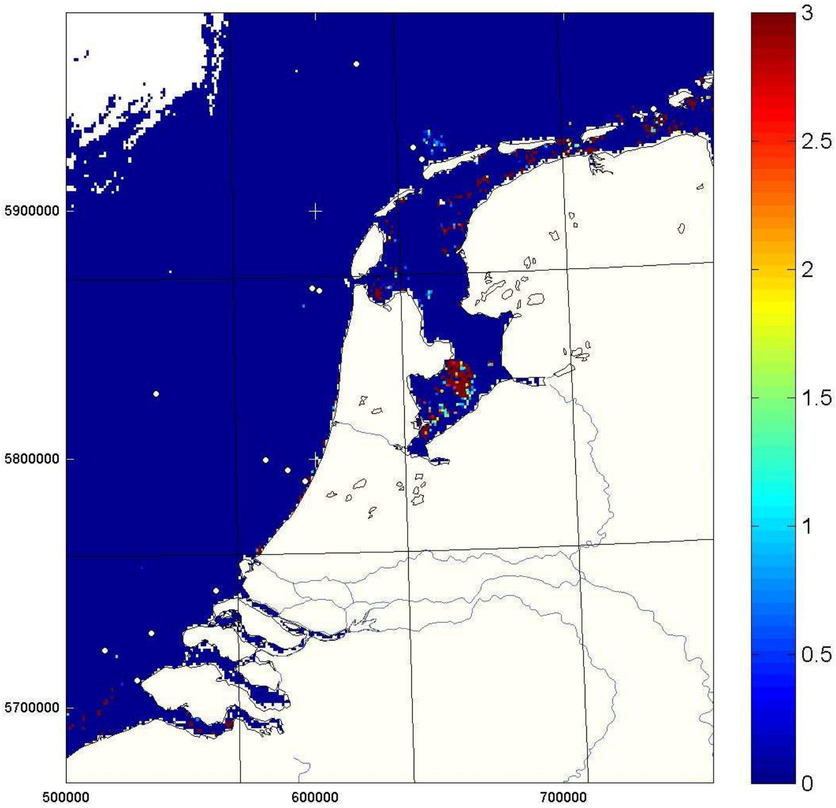

Example of results from Eleveld's plume detection algorithm during sand extraction (impact) 14−Oct−2007	IVM	
Alkyon Hydraulic Consultancy & Research	A2273	Fig. 3.62

20−Oct−2007

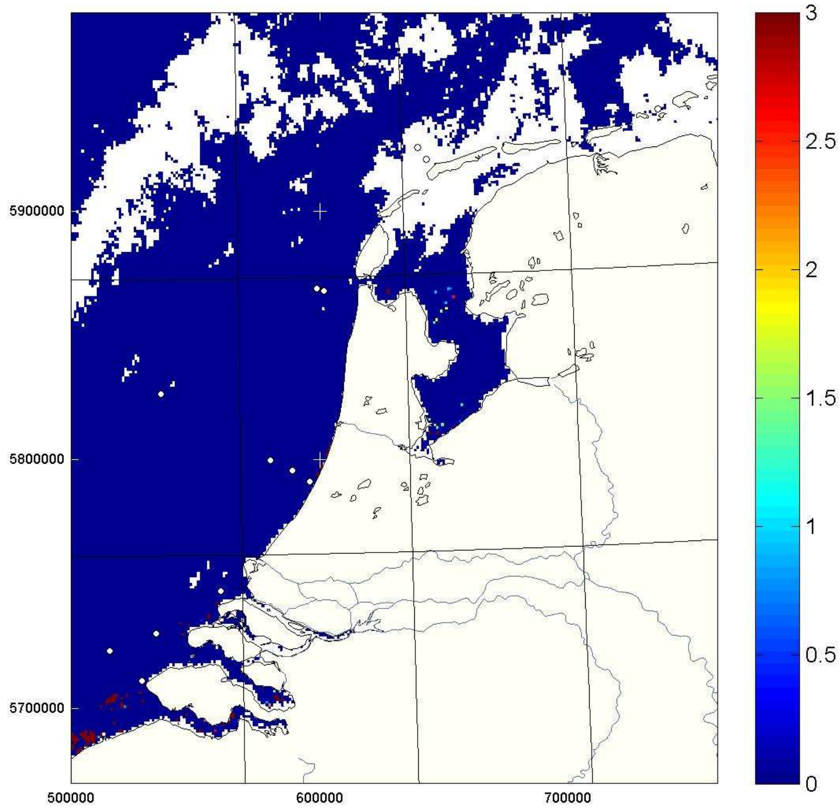

Example of results from Eleveld’s plume detection algorithm
during sand extraction (impact)
20−Oct−2007

	IVM	
Alkyon Hydraulic Consultancy & Research	A2273	Fig. 3.63

23−Oct−2007

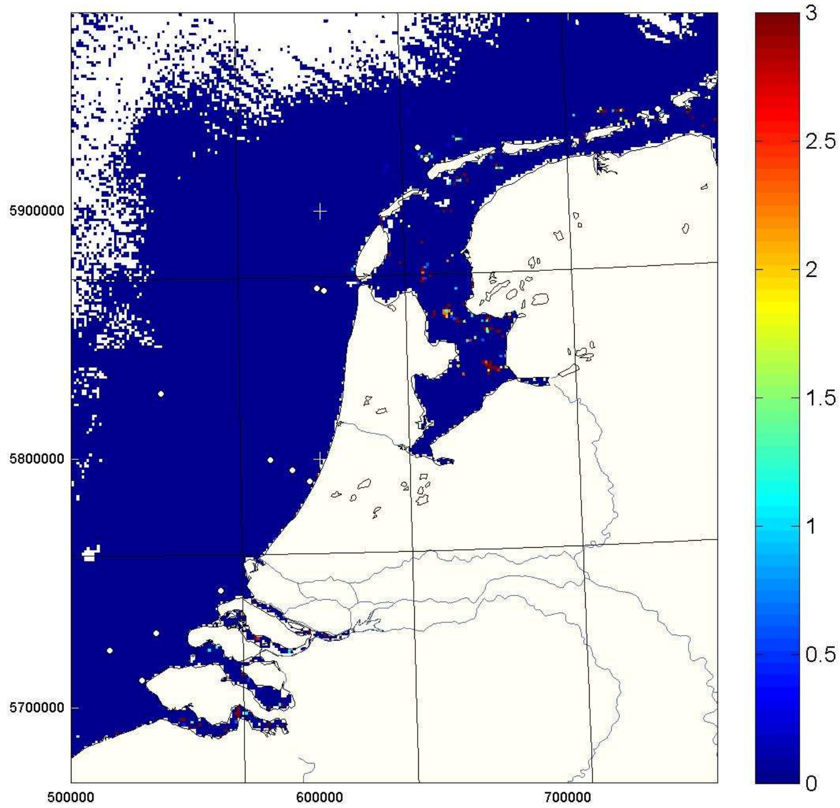

Example of results from Eleveld's plume detection algorithm during sand extraction (impact) 23−Oct−2007		
	IVM	
Alkyon Hydraulic Consultancy & Research	A2273	Fig. 3.64

01−Nov−2007

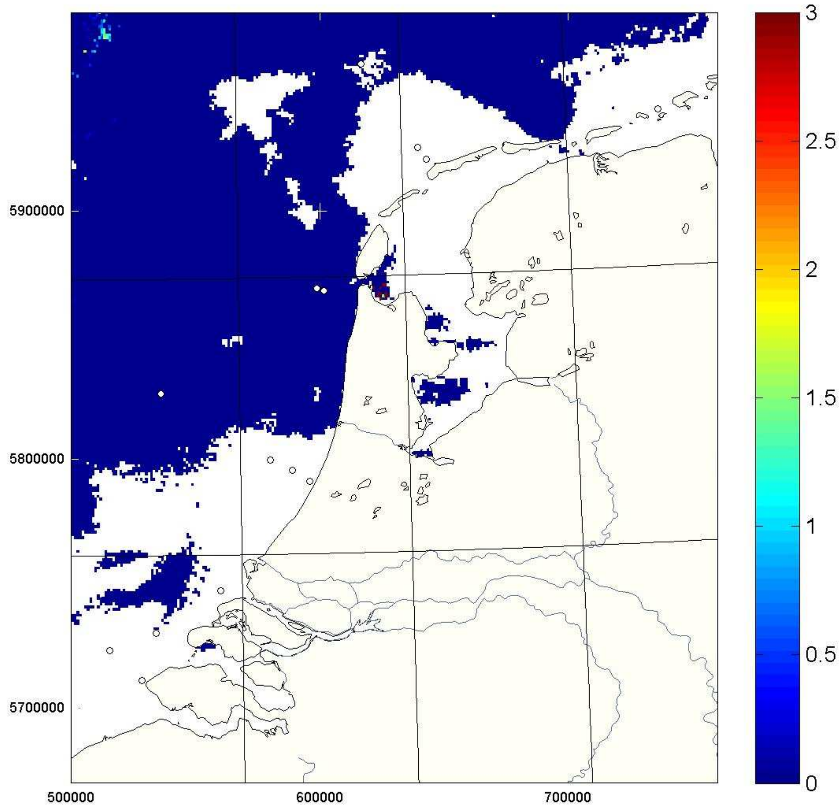

Example of results from Eleveld's plume detection algorithm
during sand extraction (impact)
01−Nov−2007

IVM

Alkyon Hydraulic Consultancy & Research

A2273

Fig. 3.65

15−Nov−2007

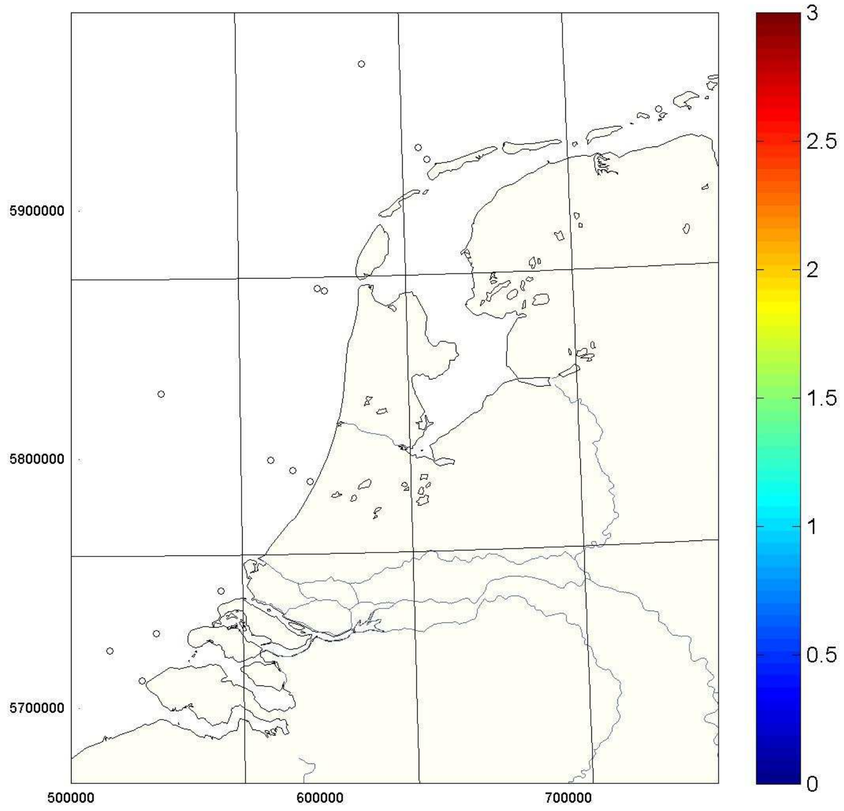

Example of results from Eleveld's plume detection algorithm during sand extraction (impact) 15−Nov−2007		
	IVM	
Alkyon Hydraulic Consultancy & Research	A2273	Fig. 3.66

18−Nov−2007

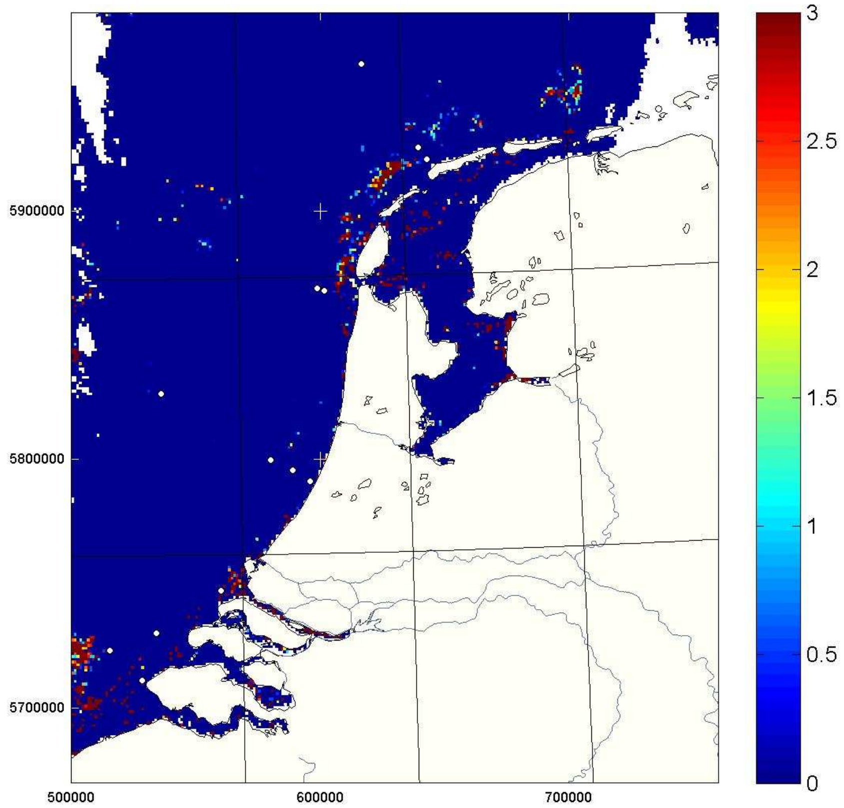

Example of results from Eleveld's plume detection algorithm during sand extraction (impact) 18−Nov−2007		
	IVM	
Alkyon Hydraulic Consultancy & Research	A2273	Fig. 3.67

01−Dec−2007

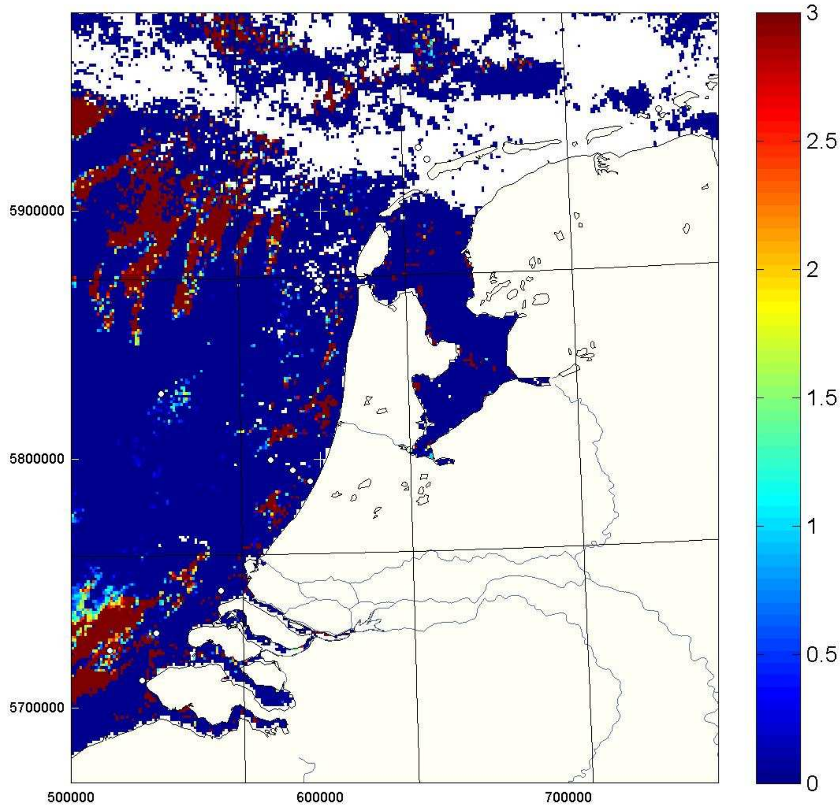

Example of results from Eleveld's plume detection algorithm during sand extraction (impact) 01−Dec−2007		
	IVM	
Alkyon Hydraulic Consultancy & Research	A2273	Fig. 3.68

16−Dec−2007

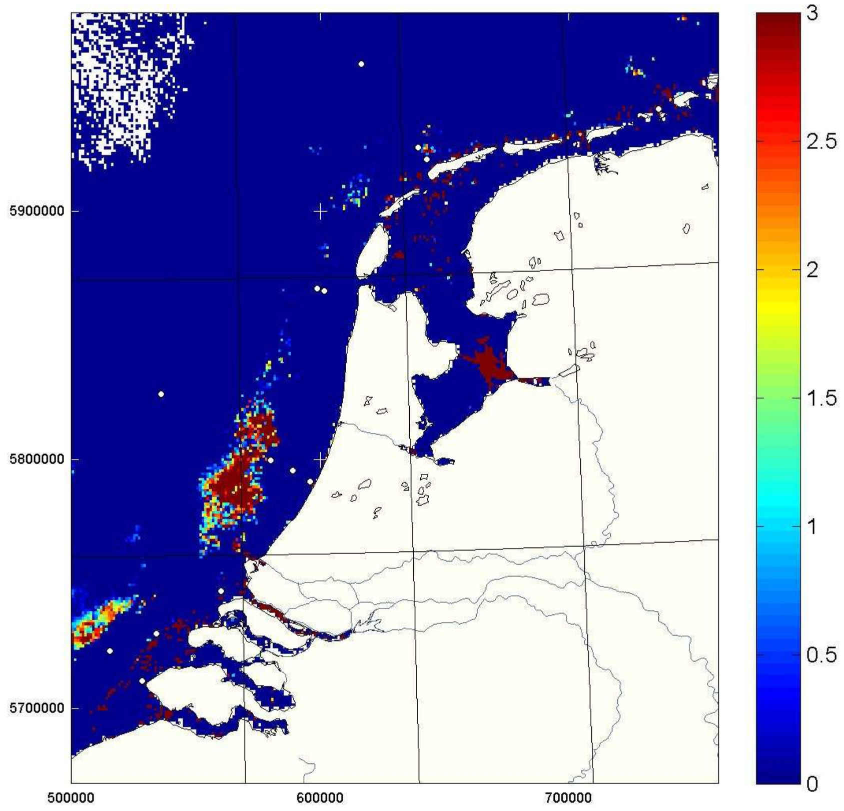

Example of results from Eleveld's plume detection algorithm
during sand extraction (impact)
16−Dec−2007

Example of results from Eleveld's plume detection algorithm during sand extraction (impact) 16−Dec−2007	IVM	
Alkyon Hydraulic Consultancy & Research	A2273	Fig. 3.69

29−Dec−2007

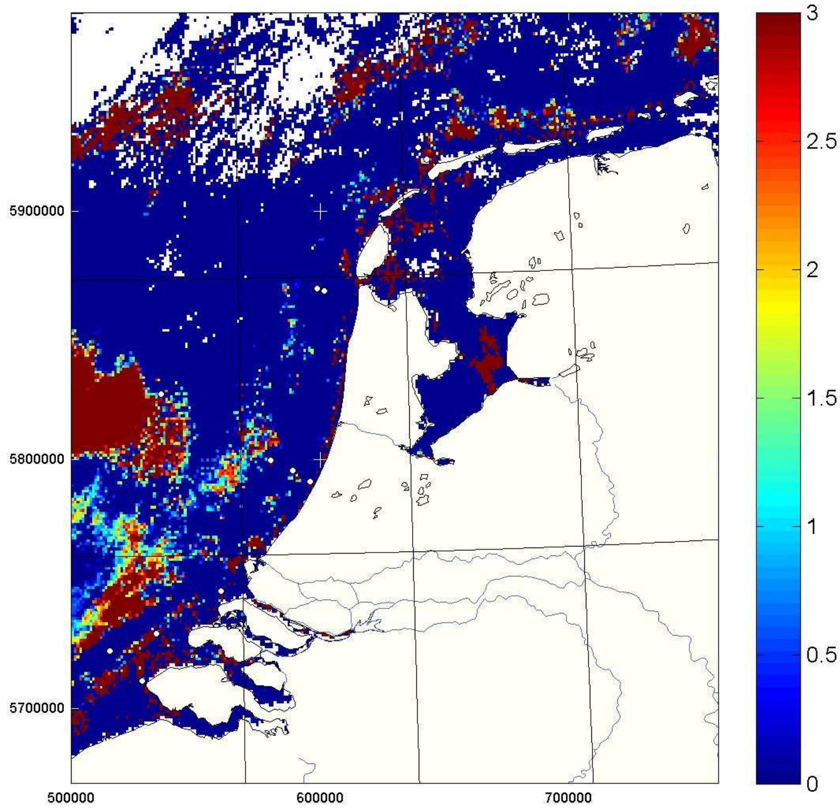

Example of results from Eleveld's plume detection algorithm
during sand extraction (impact)
29−Dec−2007

	IVM	
Alkyon Hydraulic Consultancy & Research	A2273	Fig. 3.70

11−Aug−2007

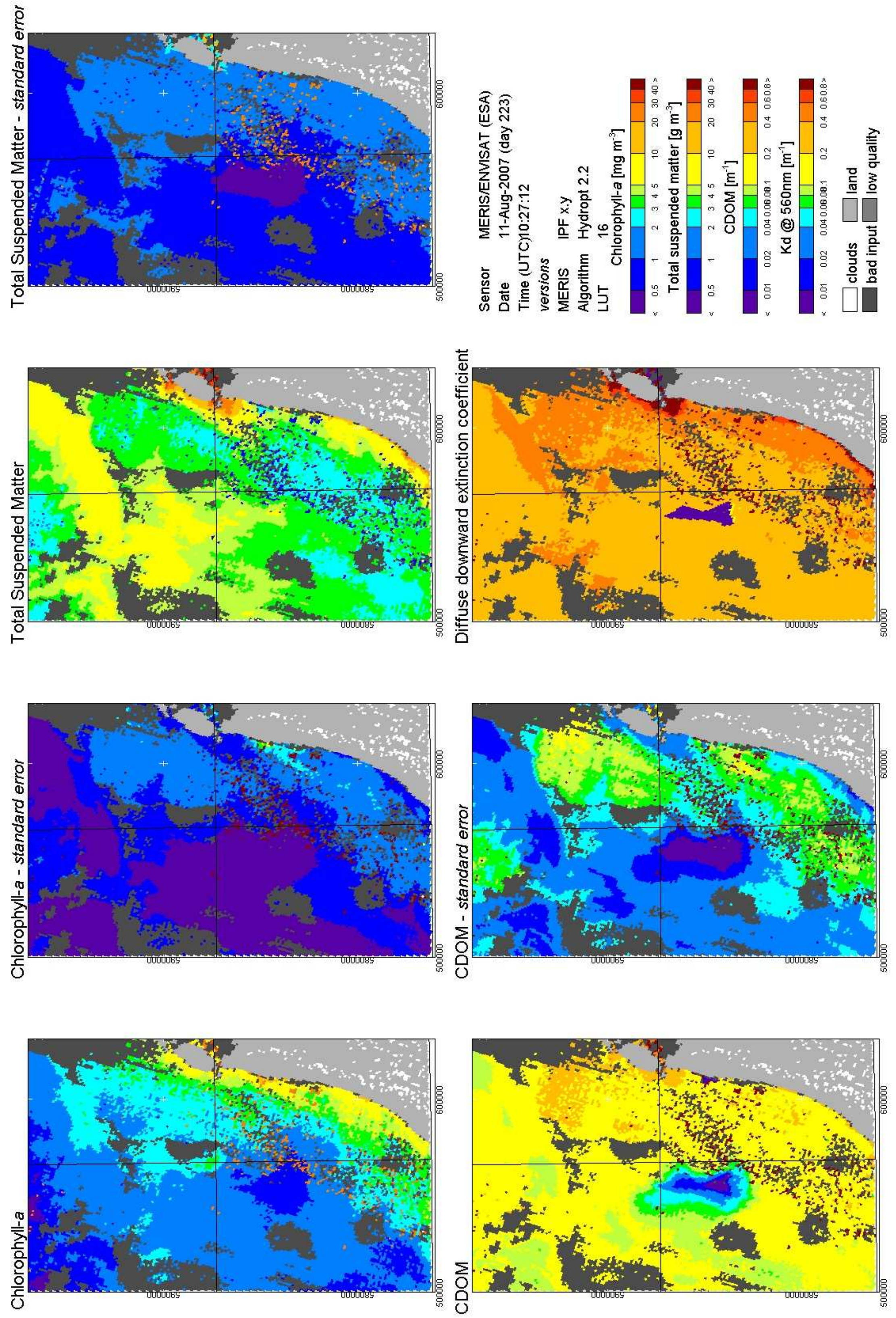

All water quality parameters and products,
which were not masked by confidence flags,
11−Aug−2007

	IVM	
Alkyon Hydraulic Consultancy & Research	A2273	Fig. 3.71

02−Oct−2007

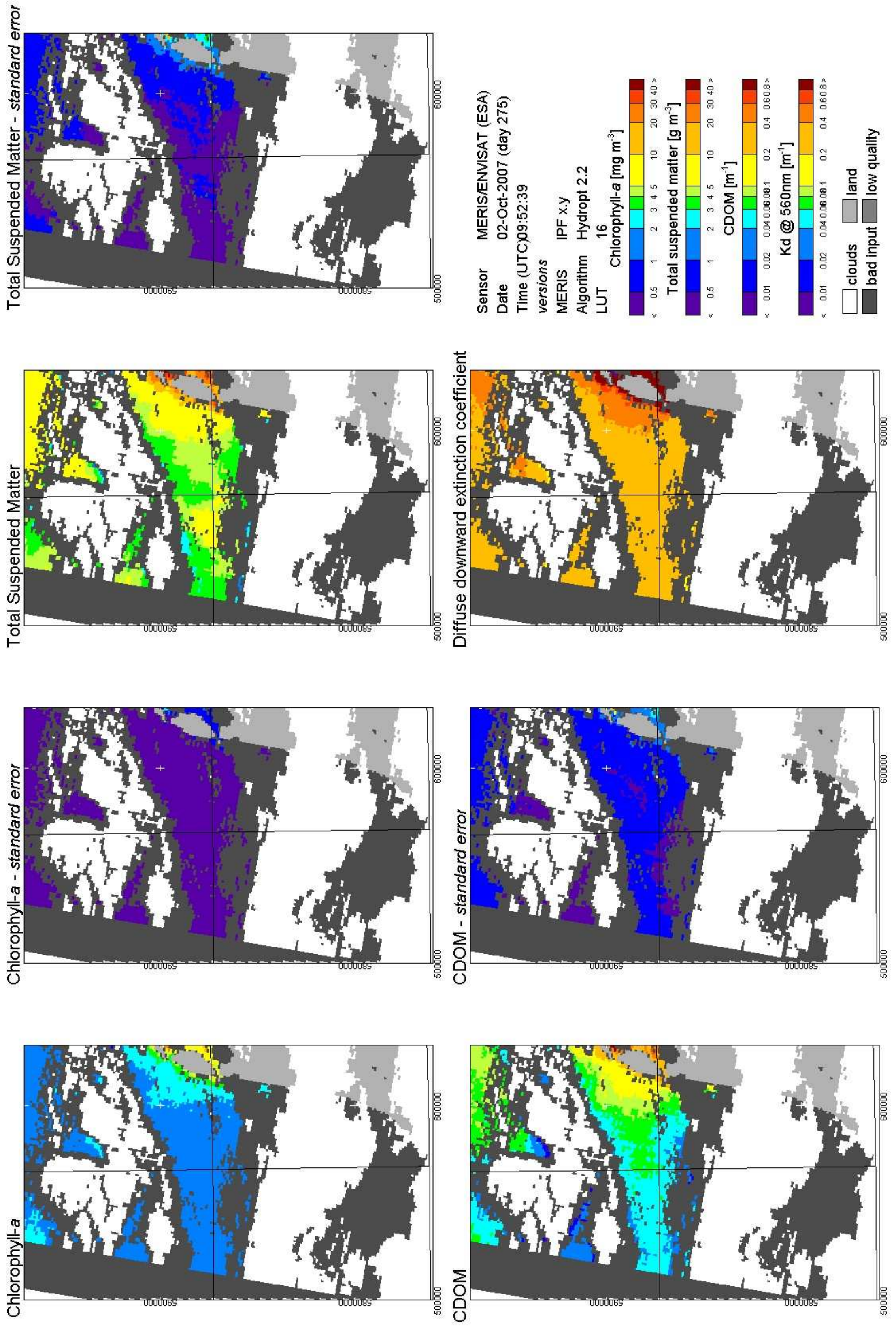

All water quality parameters and products, which were not masked by confidence flags, 02−Oct−2007		
	IVM	
Alkyon Hydraulic Consultancy & Research	A2273	Fig. 3.72

07−Oct−2007

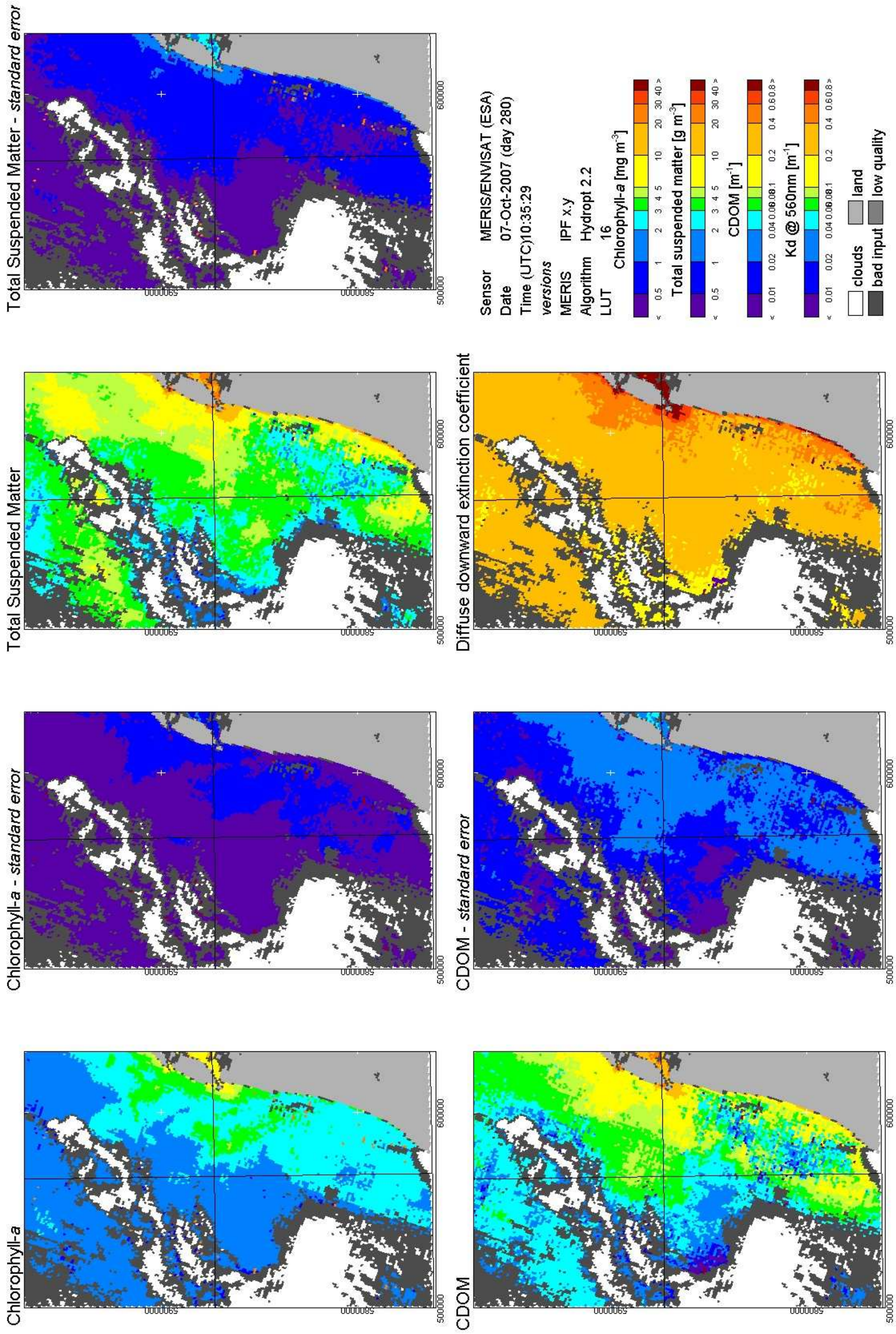

All water quality parameters and products, which were not masked by confidence flags, 07−Oct−2007		
	IVM	
Alkyon Hydraulic Consultancy & Research	A2273	Fig. 3.73

15−Nov−2007

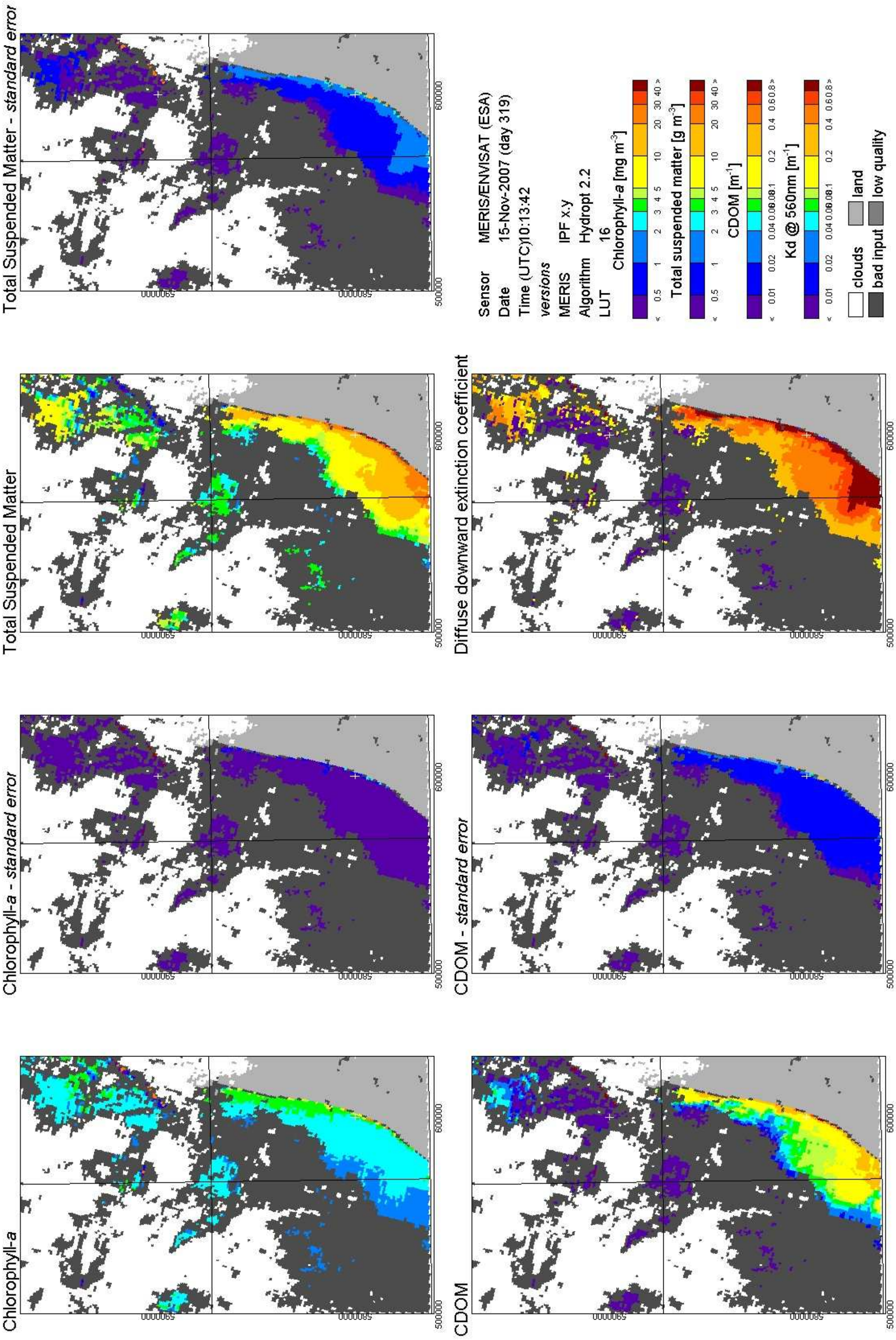

All water quality parameters and products,
which were not masked by confidence flags,
15−Nov−2007

IVM

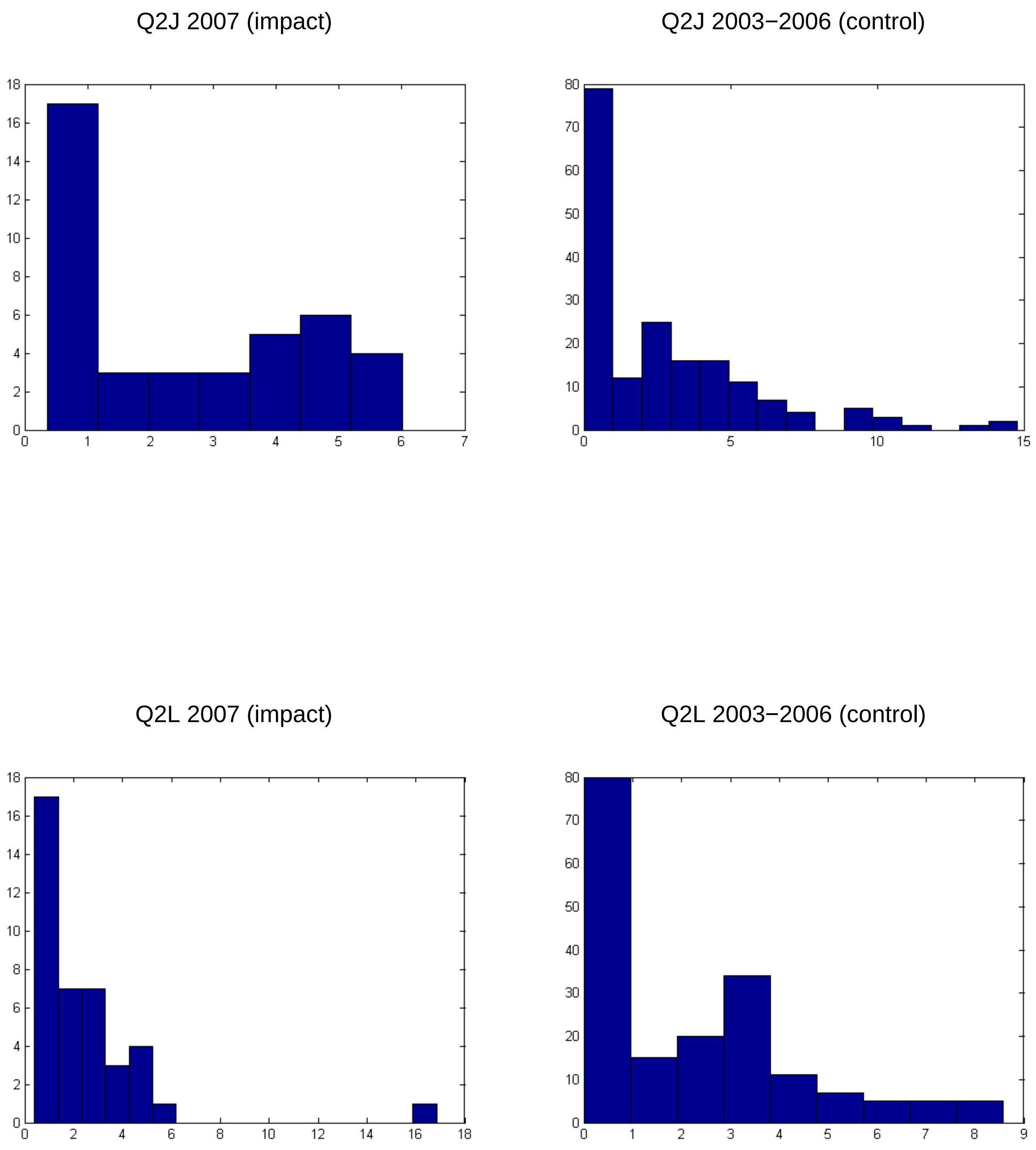

Histograms for Q2J 2007 (upper left), Q2J 2003−2006 (upper right) Q2L 2007 (lower left) and Q2L 2003−2006 (lower right)	IVM	
Alkyon Hydraulic Consultancy & Research	A2273	Fig. 3.75

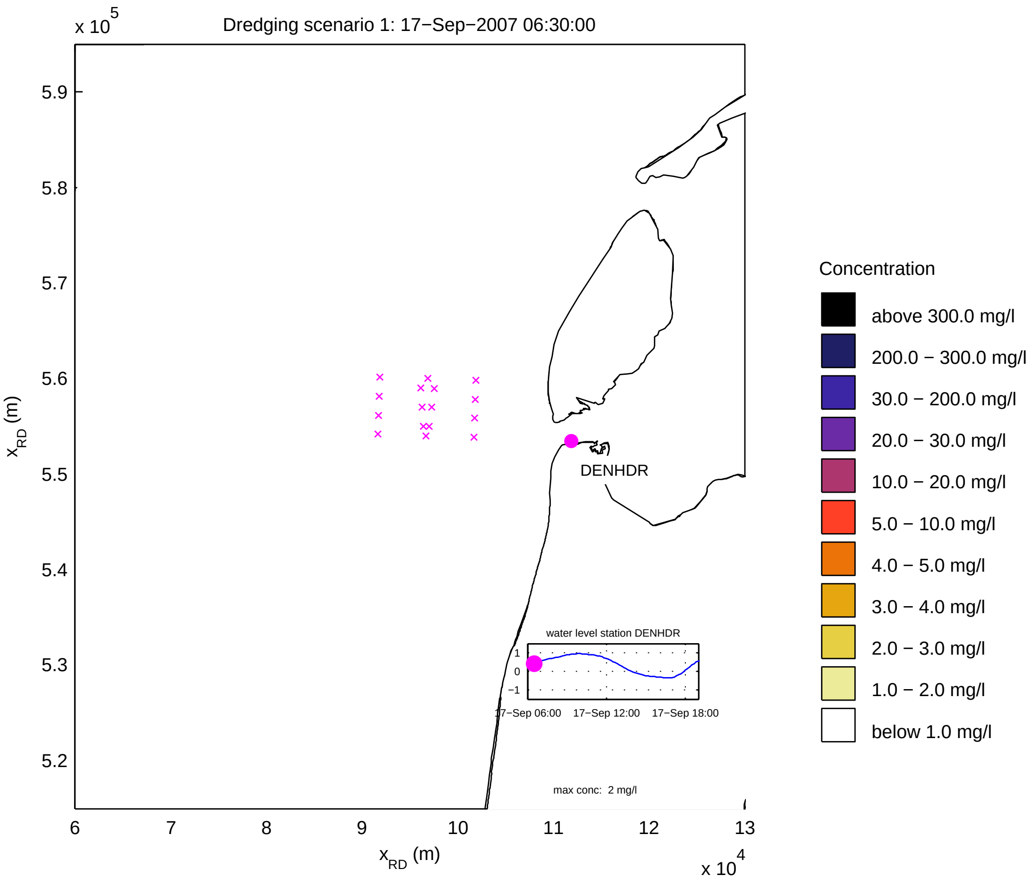

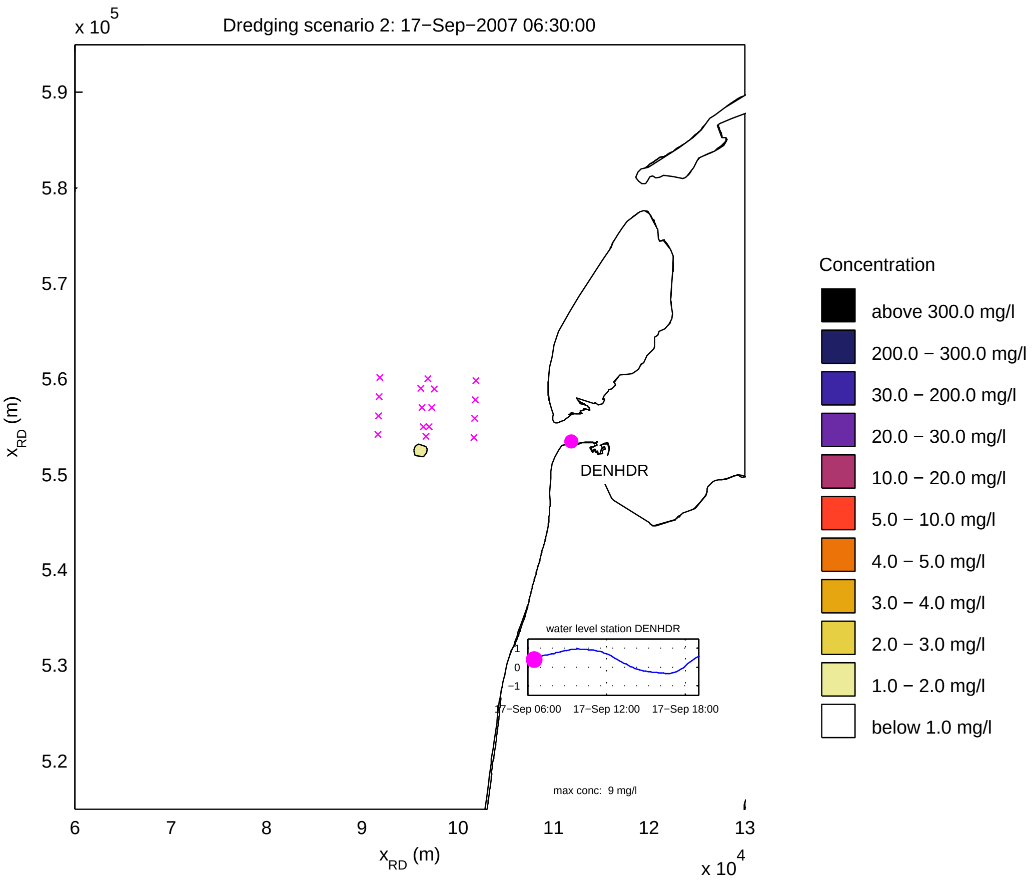

Simulated effect of overflow on silt concentrations (mg/l)
date and time: 17−Sep−2007 06:30:00
x−marks denote locations of T1 observations

Alkyon Hydraulic Consultancy & Research	A2273	Fig. 4.1

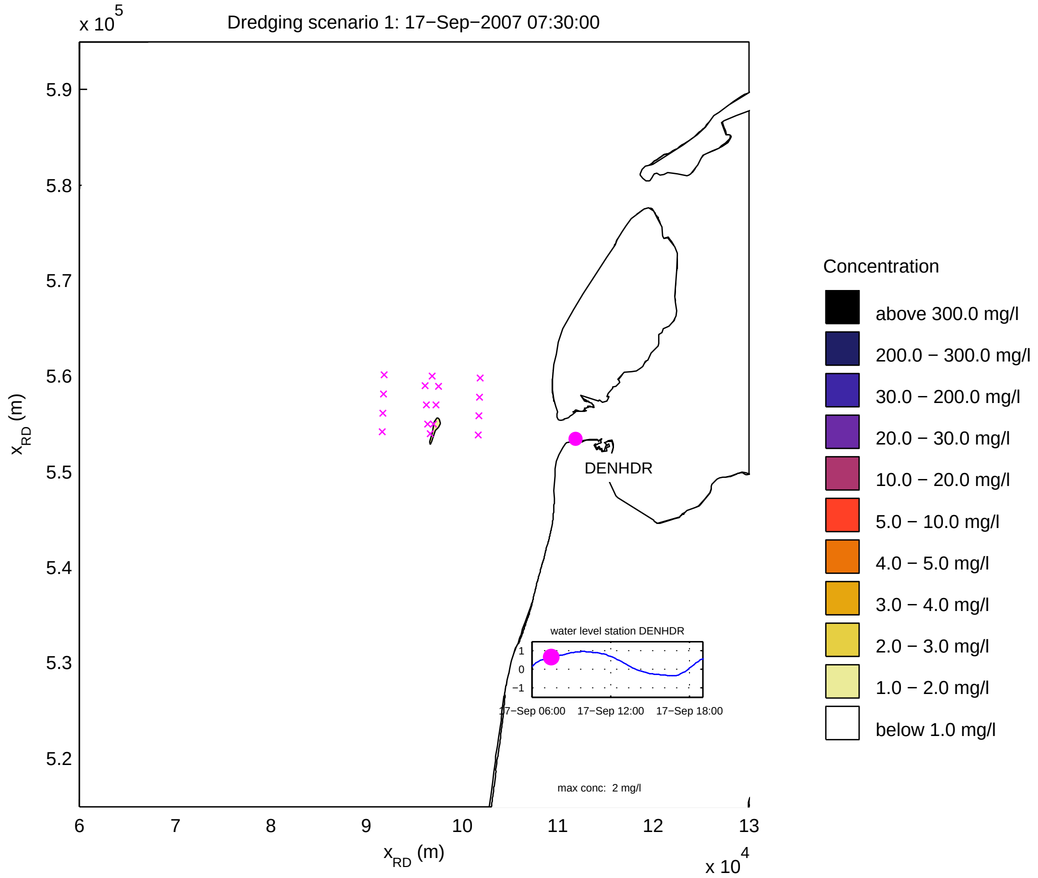

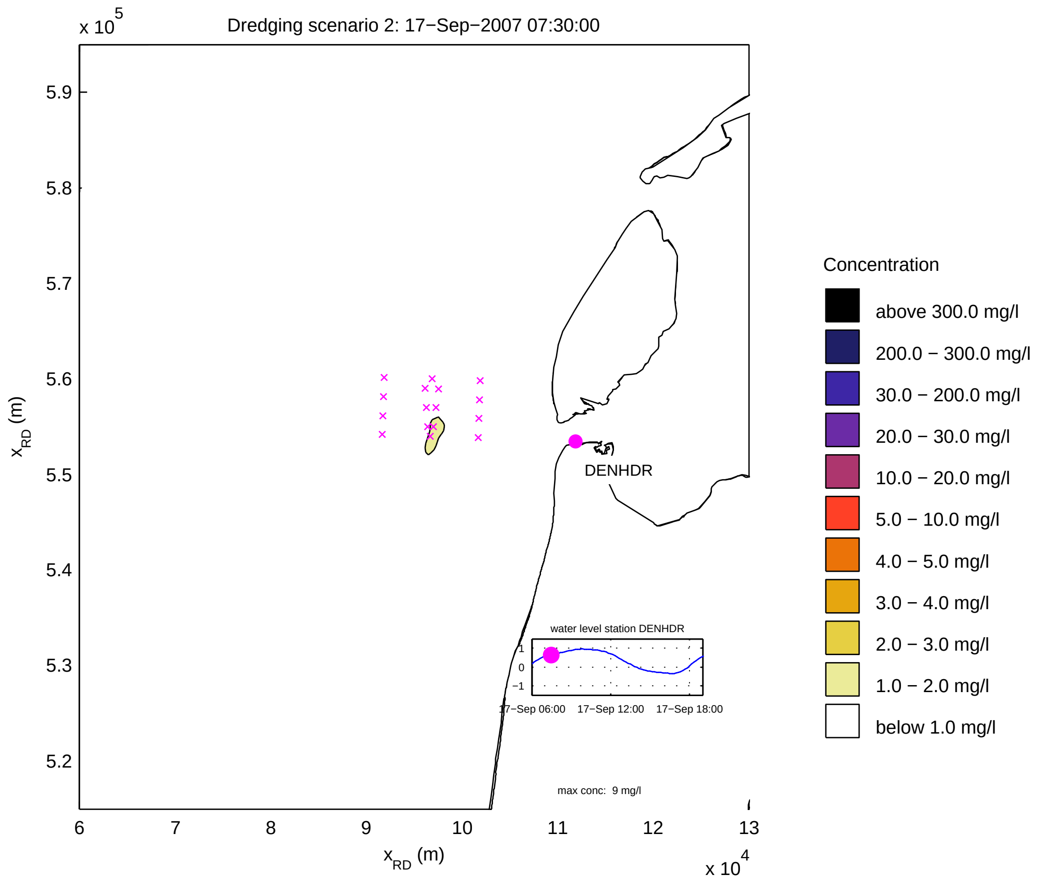

Simulated effect of overflow on silt concentrations (mg/l)
date and time: 17−Sep−2007 07:30:00
x−marks denote locations of T1 observations

Alkyon Hydraulic Consultancy & Research	A2273	Fig. 4.2

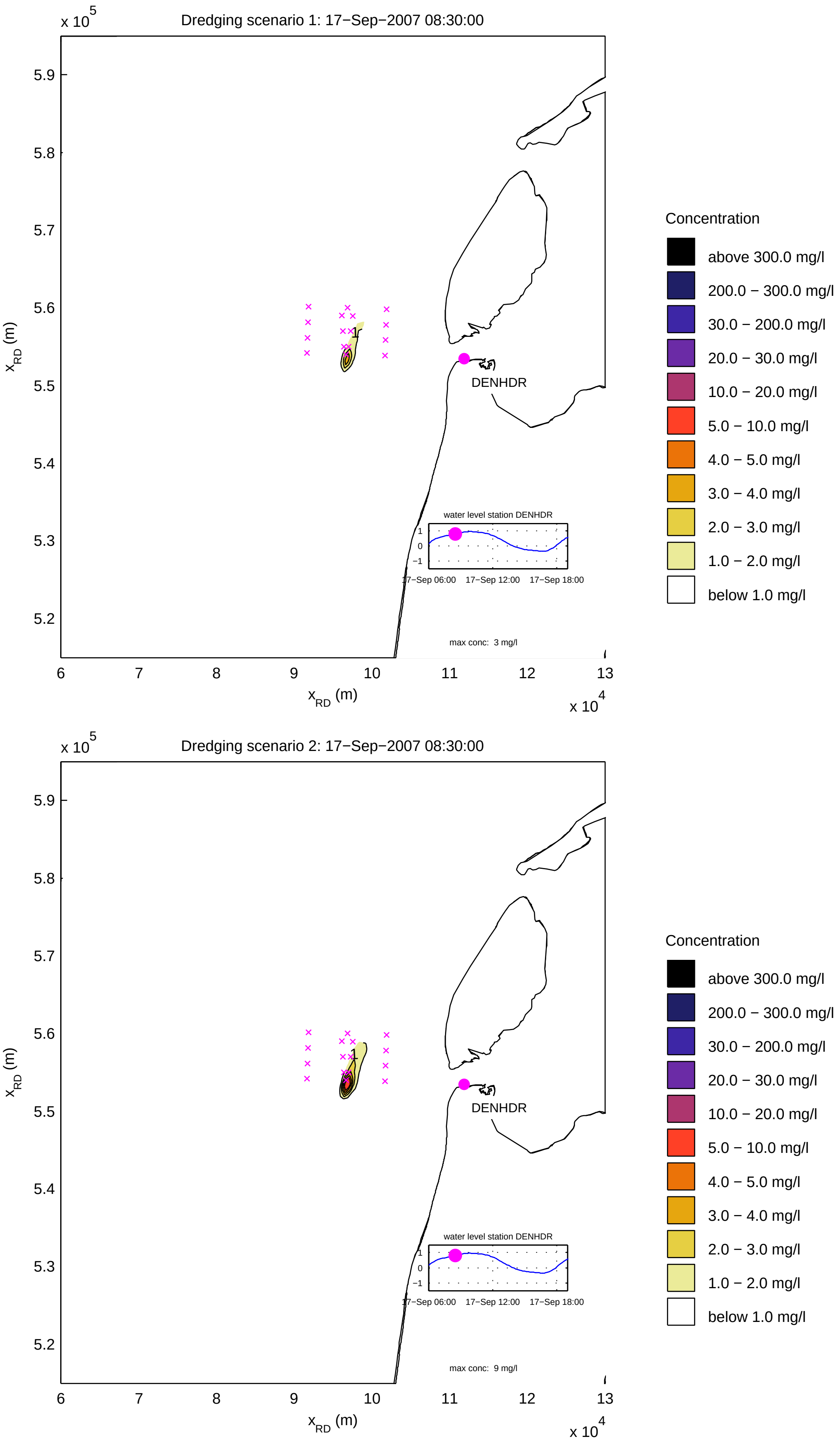

Simulated effect of overflow on silt concentrations (mg/l)
date and time: 17−Sep−2007 08:30:00
x−marks denote locations of T1 observations

Alkyon Hydraulic Consultancy & Research	A2273	Fig. 4.3

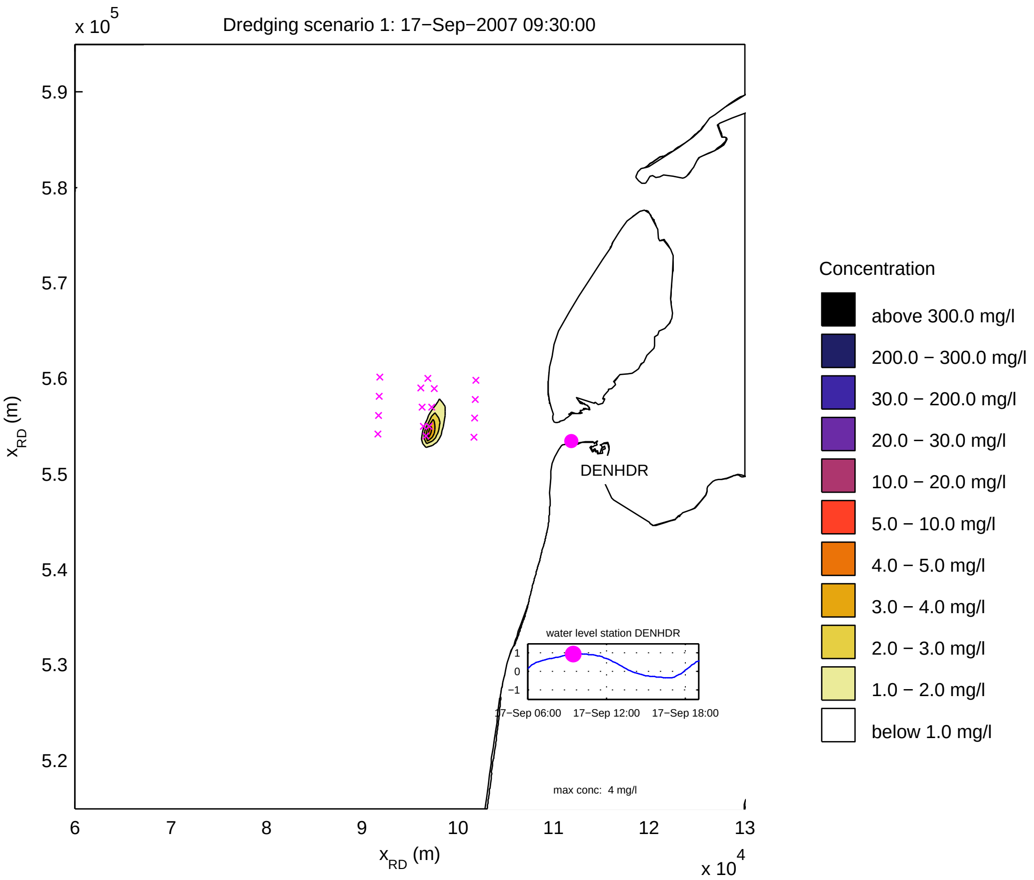

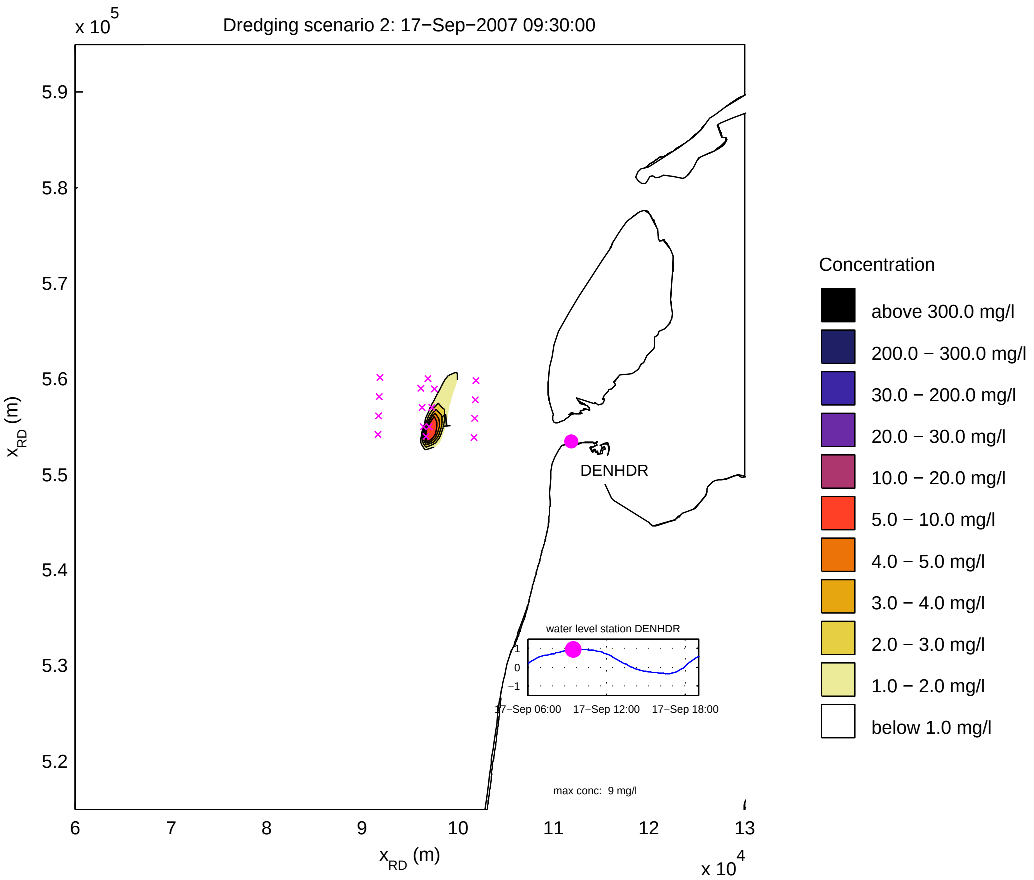

Simulated effect of overflow on silt concentrations (mg/l) date and time: 17−Sep−2007 09:30:00 x−marks denote locations of T1 observations		
Alkyon Hydraulic Consultancy & Research	A2273	Fig. 4.4

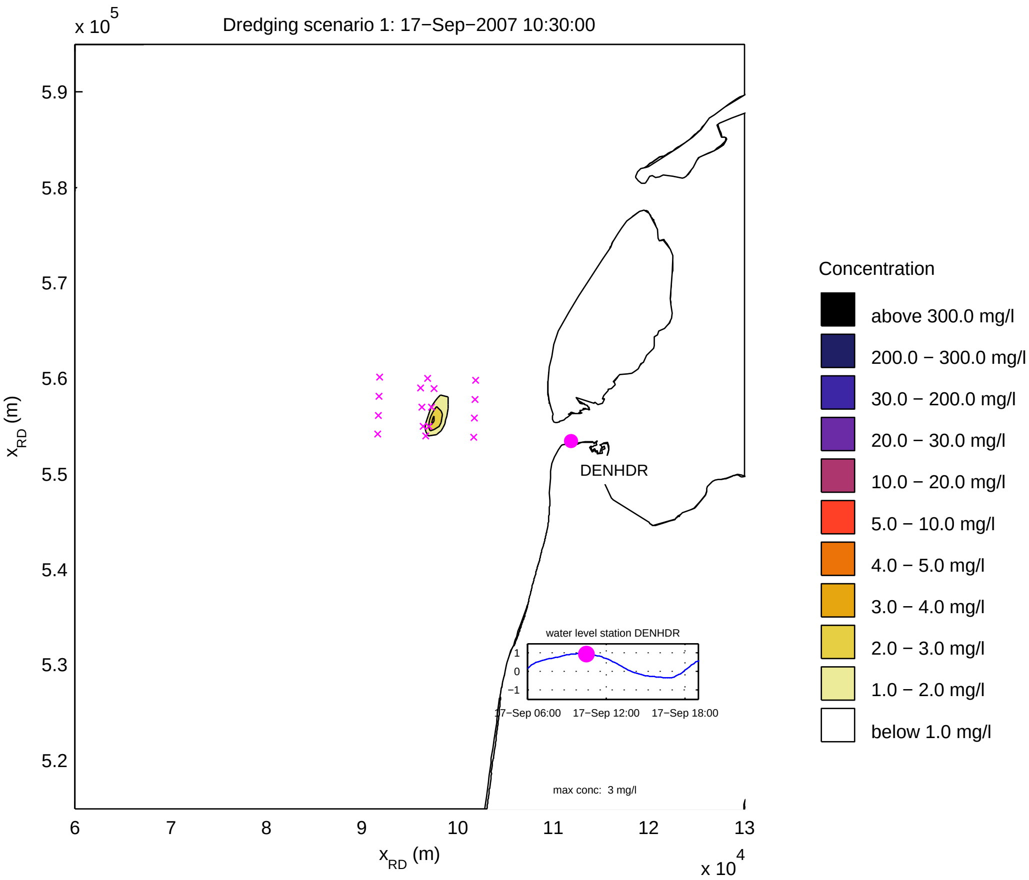

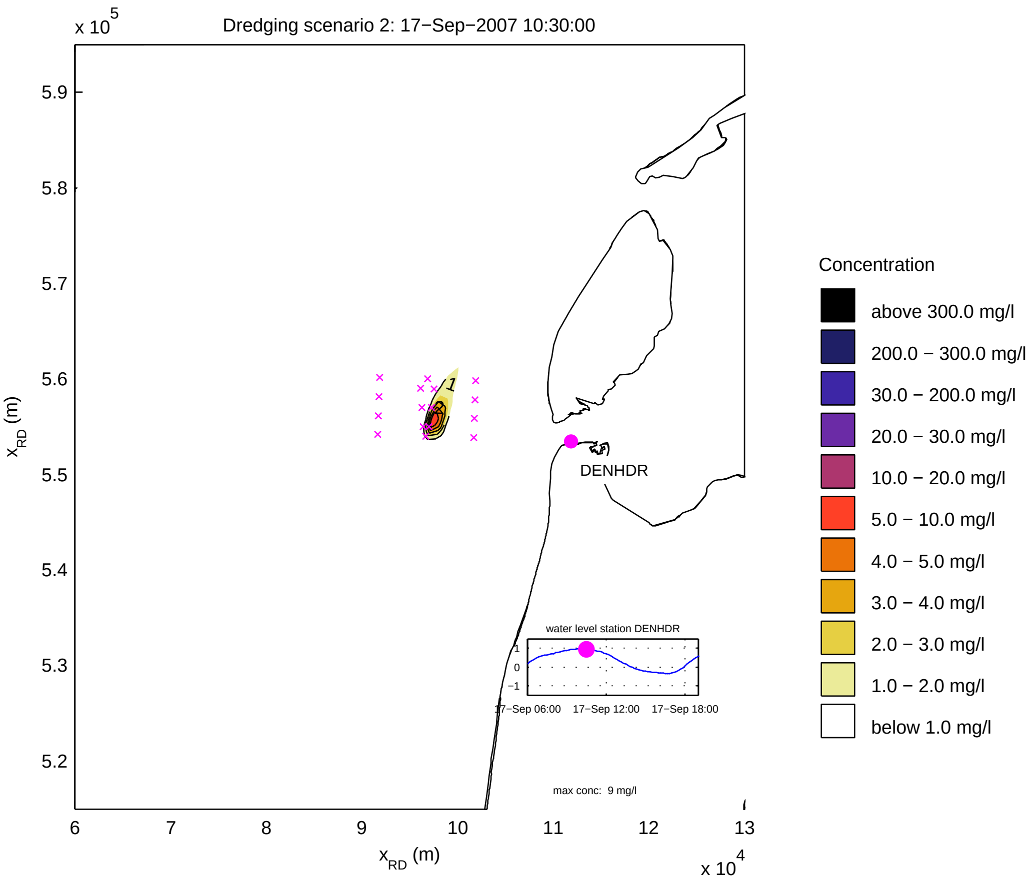

Simulated effect of overflow on silt concentrations (mg/l)
date and time: 17−Sep−2007 10:30:00
x−marks denote locations of T1 observations

Alkyon Hydraulic Consultancy & Research | A2273 | Fig. 4.5

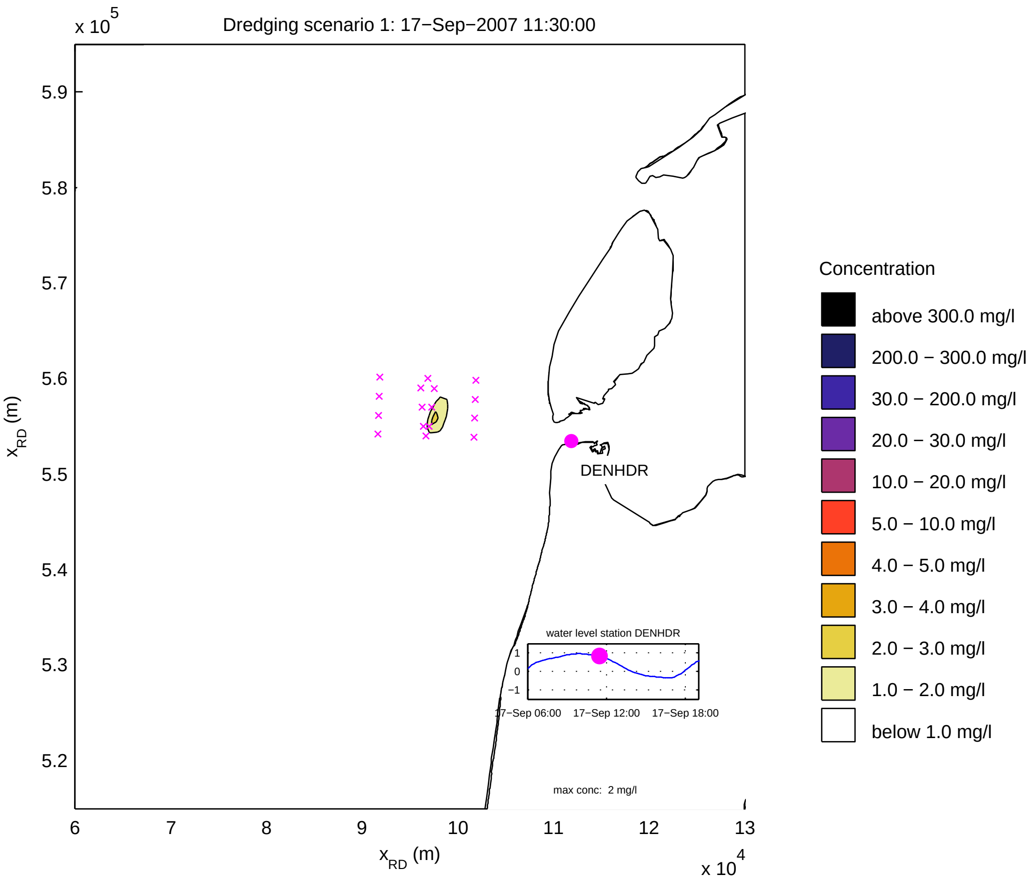

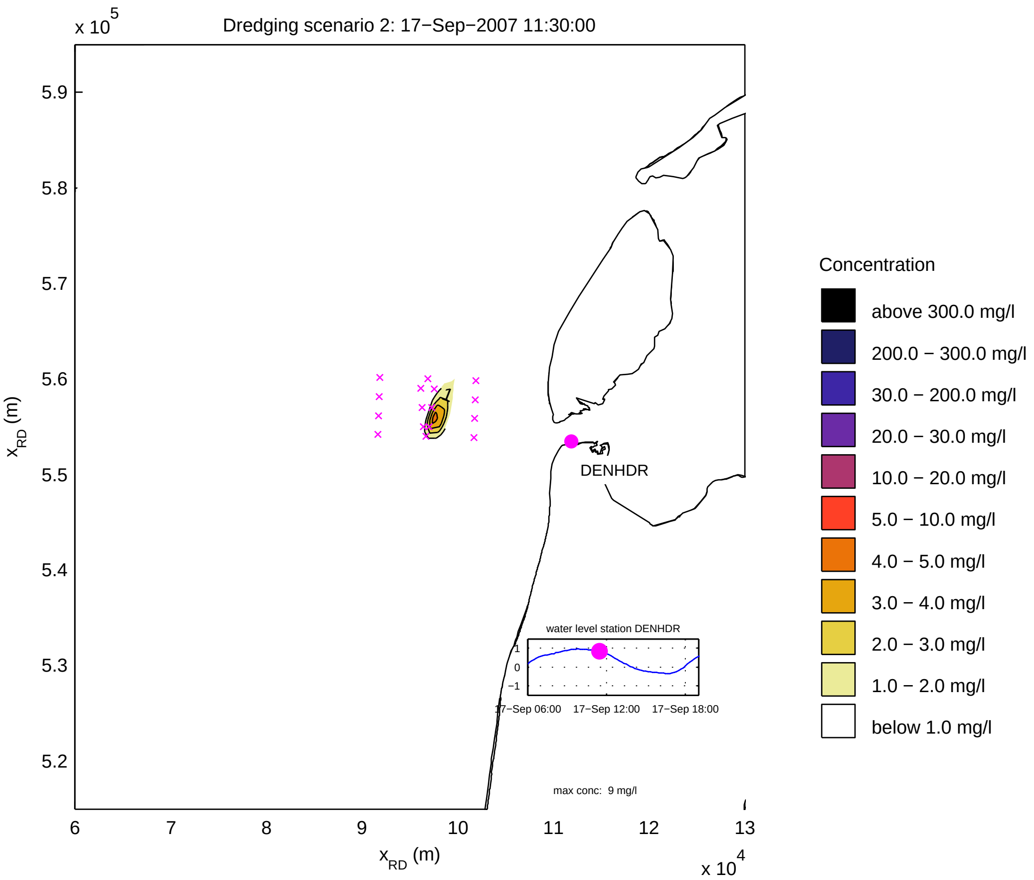

Simulated effect of overflow on silt concentrations (mg/l)
date and time: 17−Sep−2007 11:30:00
x−marks denote locations of T1 observations

Alkyon Hydraulic Consultancy & Research | A2273 | Fig. 4.6

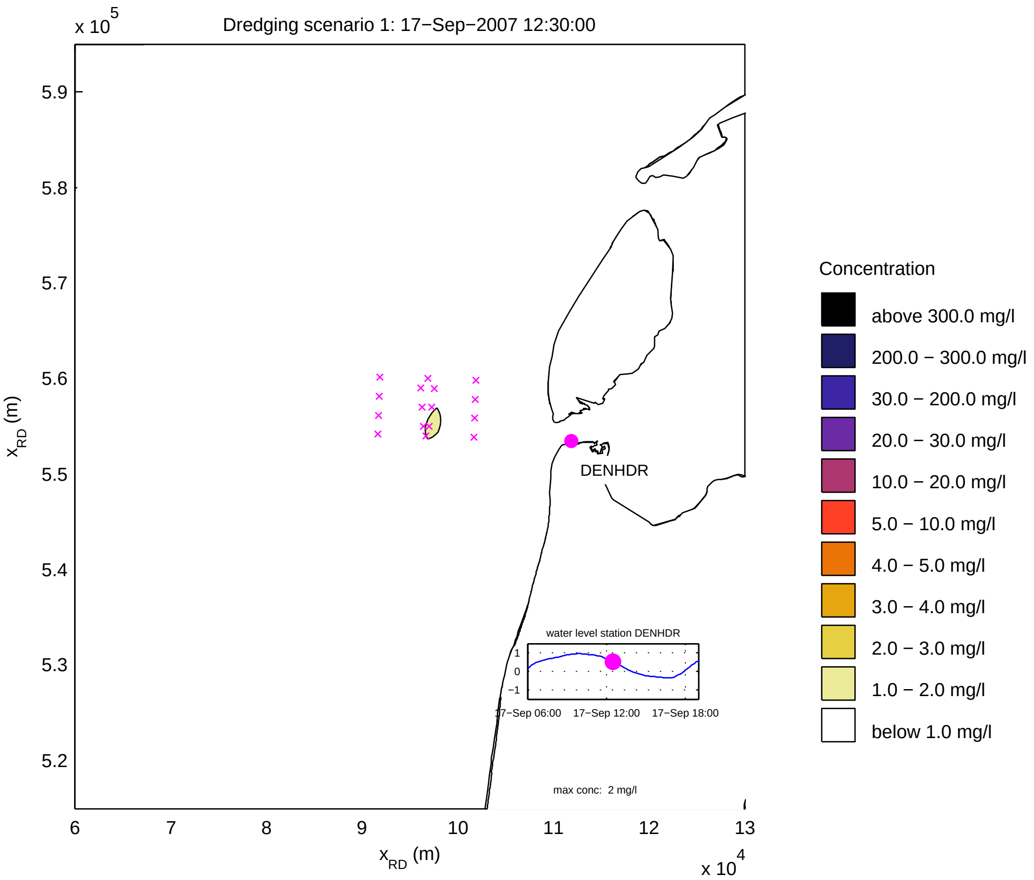

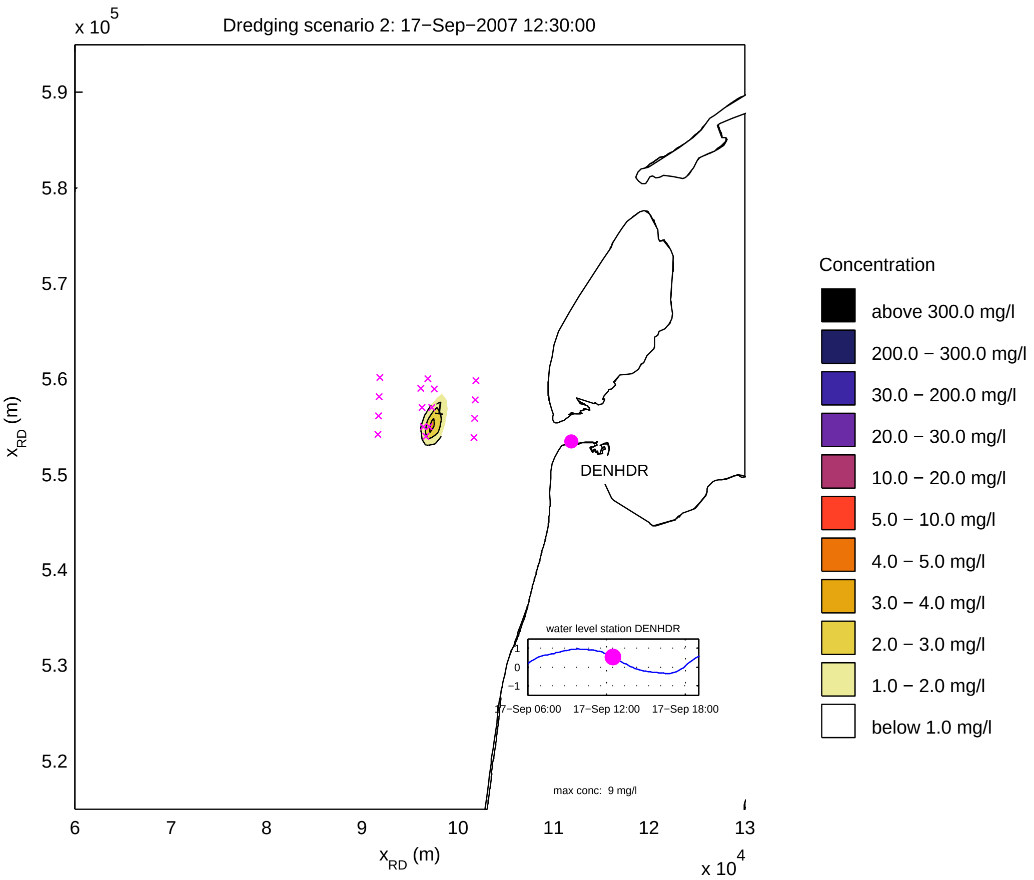

Simulated effect of overflow on silt concentrations (mg/l)
date and time: 17−Sep−2007 12:30:00
x−marks denote locations of T1 observations

Alkyon Hydraulic Consultancy & Research	A2273	Fig. 4.7

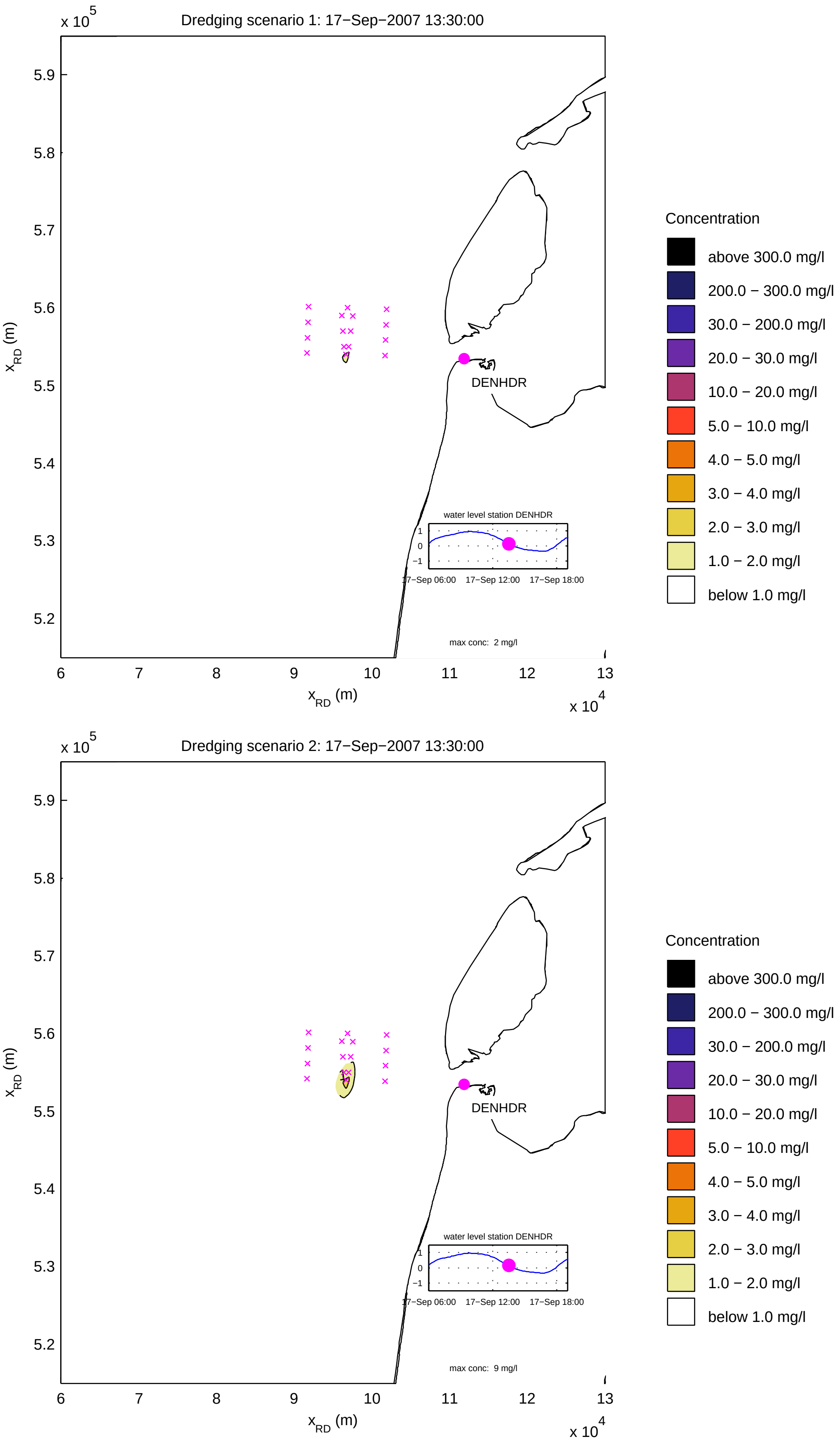

Simulated effect of overflow on silt concentrations (mg/l)
date and time: 17−Sep−2007 13:30:00
x−marks denote locations of T1 observations

Alkyon Hydraulic Consultancy & Research	A2273	Fig. 4.8

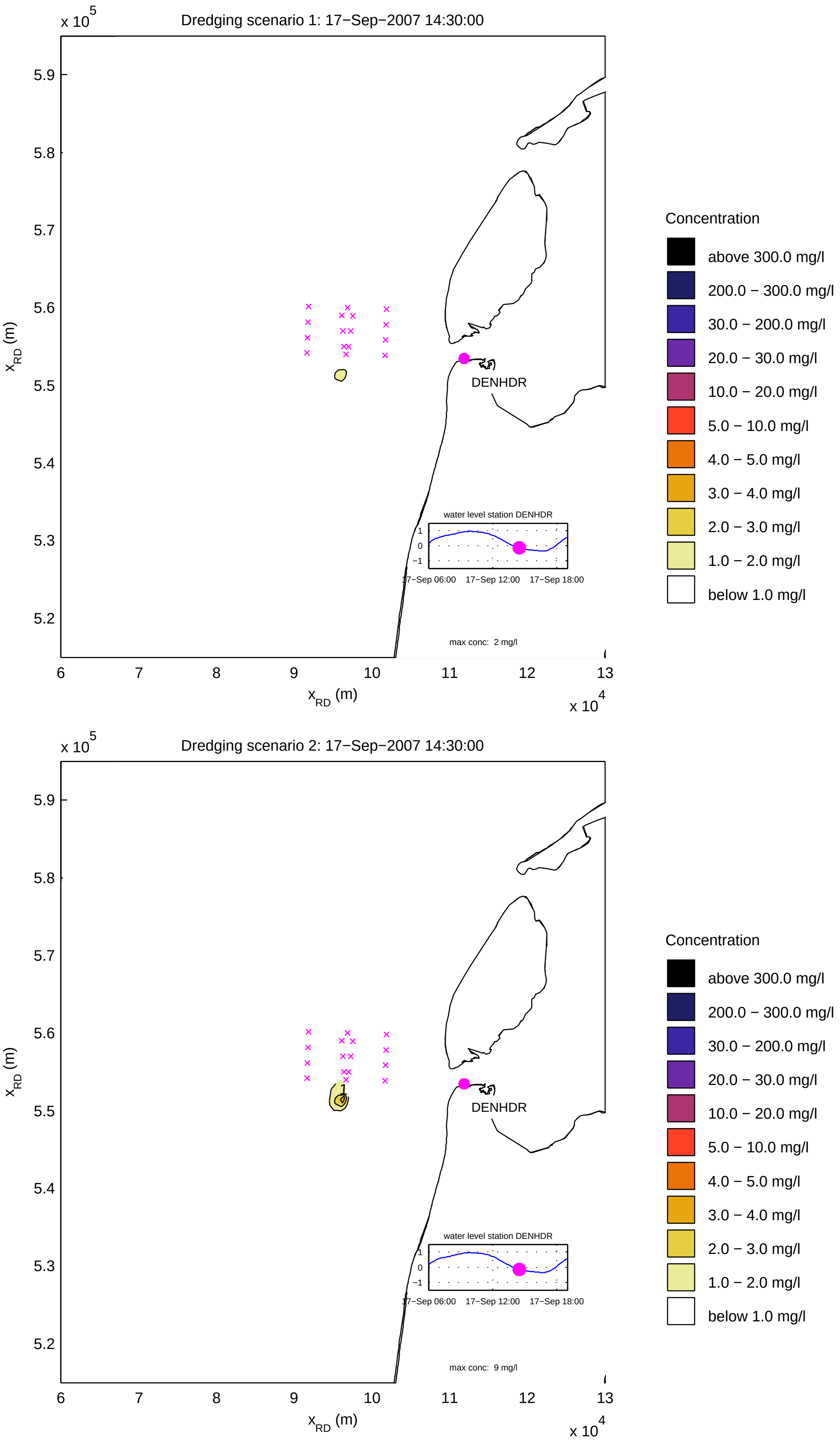

Simulated effect of overflow on silt concentrations (mg/l)
date and time: 17−Sep−2007 14:30:00
x−marks denote locations of T1 observations

Alkyon Hydraulic Consultancy & Research	A2273	Fig. 4.9

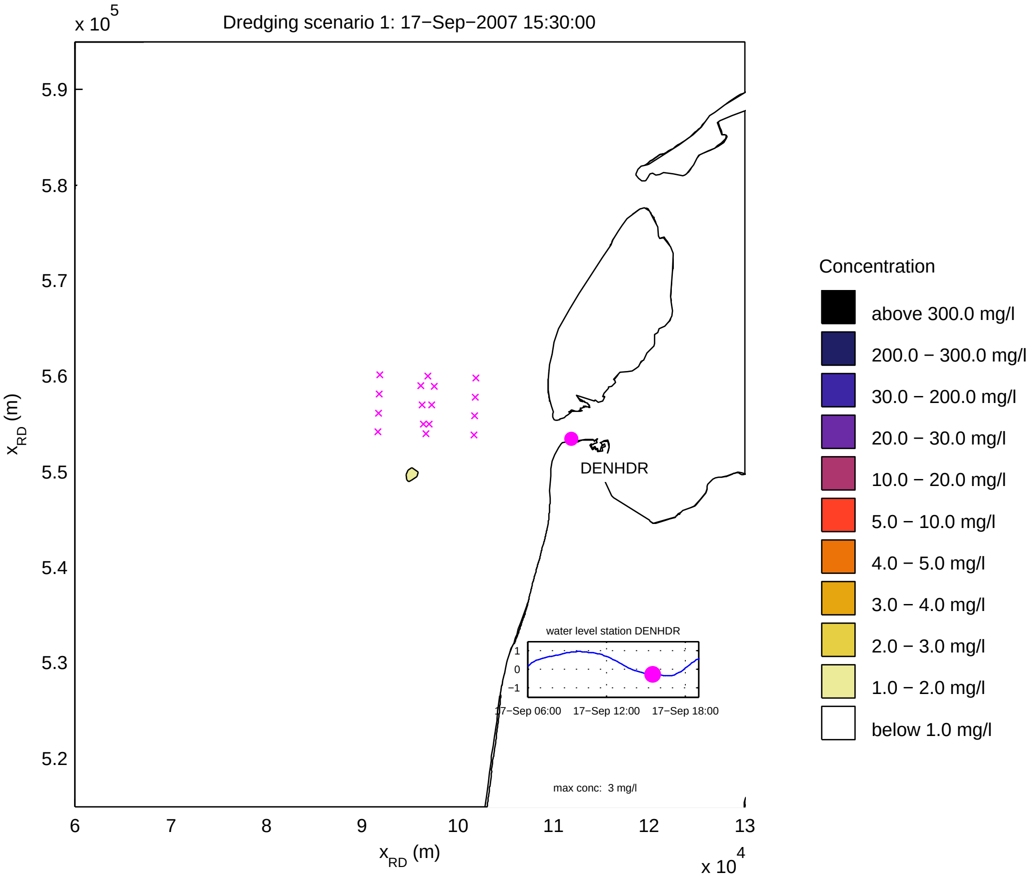

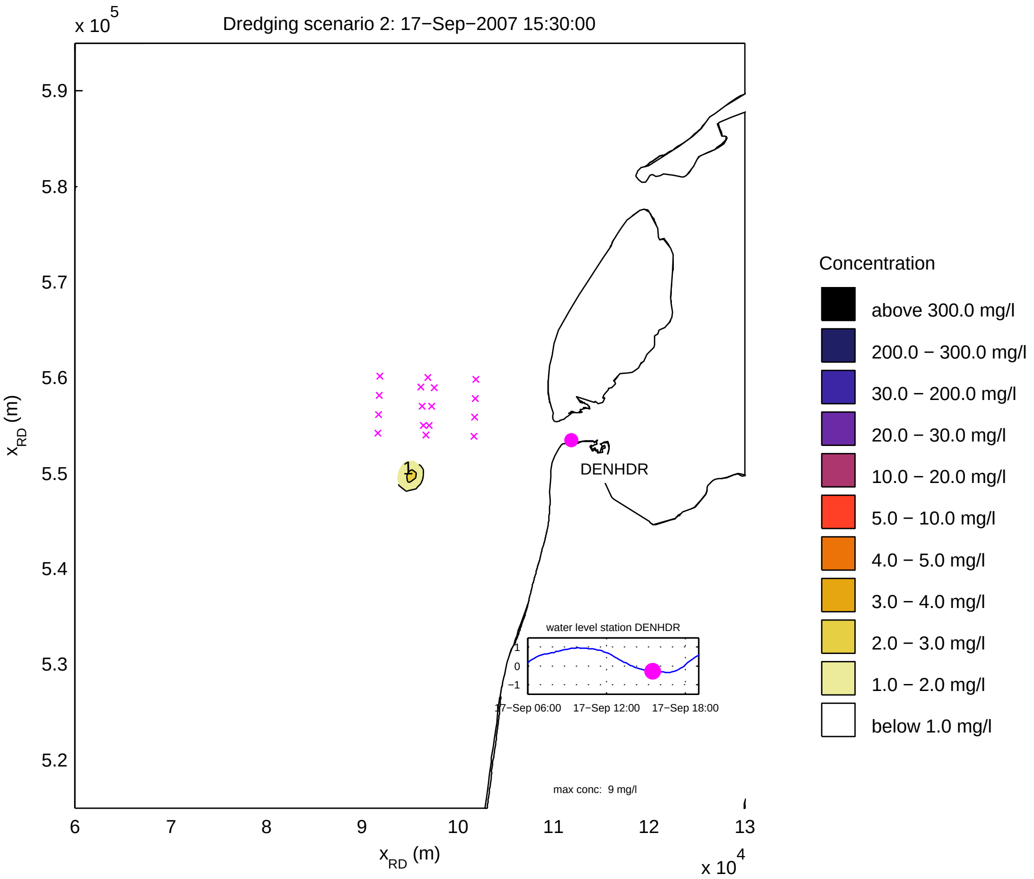

Simulated effect of overflow on silt concentrations (mg/l) date and time: 17−Sep−2007 15:30:00 x−marks denote locations of T1 observations		
Alkyon Hydraulic Consultancy & Research	A2273	Fig. 4.10

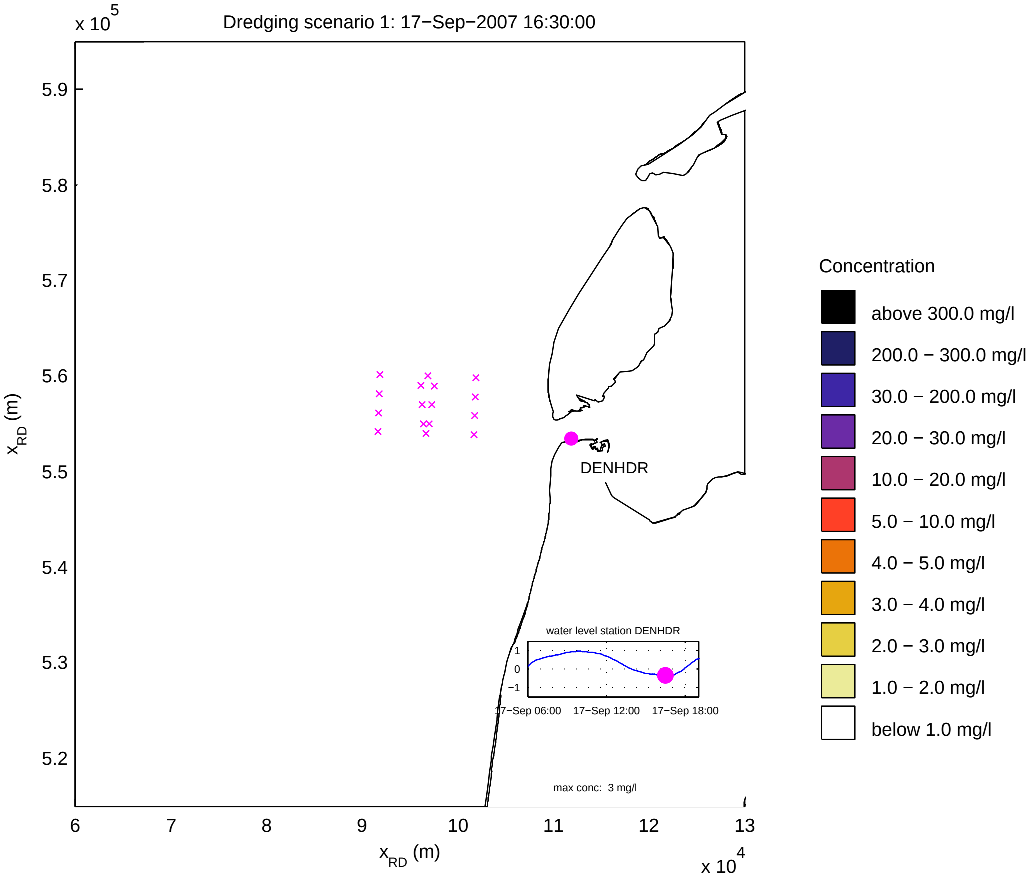

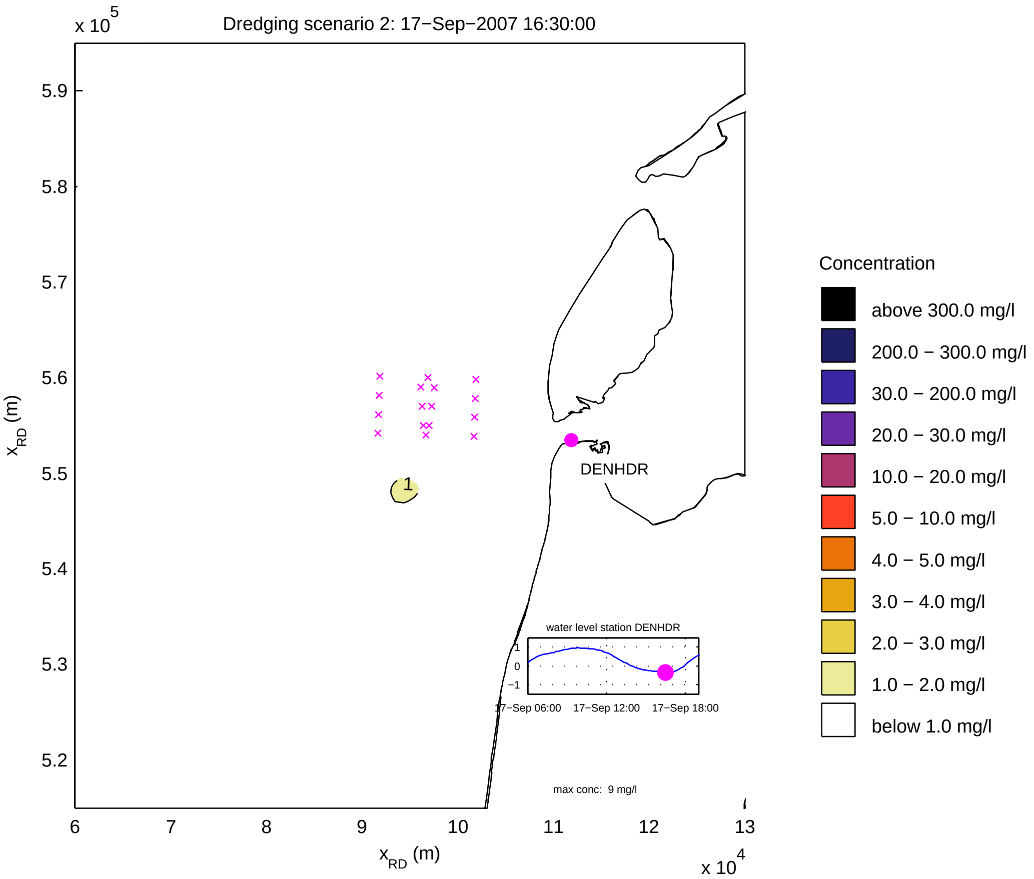

Simulated effect of overflow on silt concentrations (mg/l)
date and time: 17−Sep−2007 16:30:00
x−marks denote locations of T1 observations

Alkyon Hydraulic Consultancy & Research | A2273 | Fig. 4.11

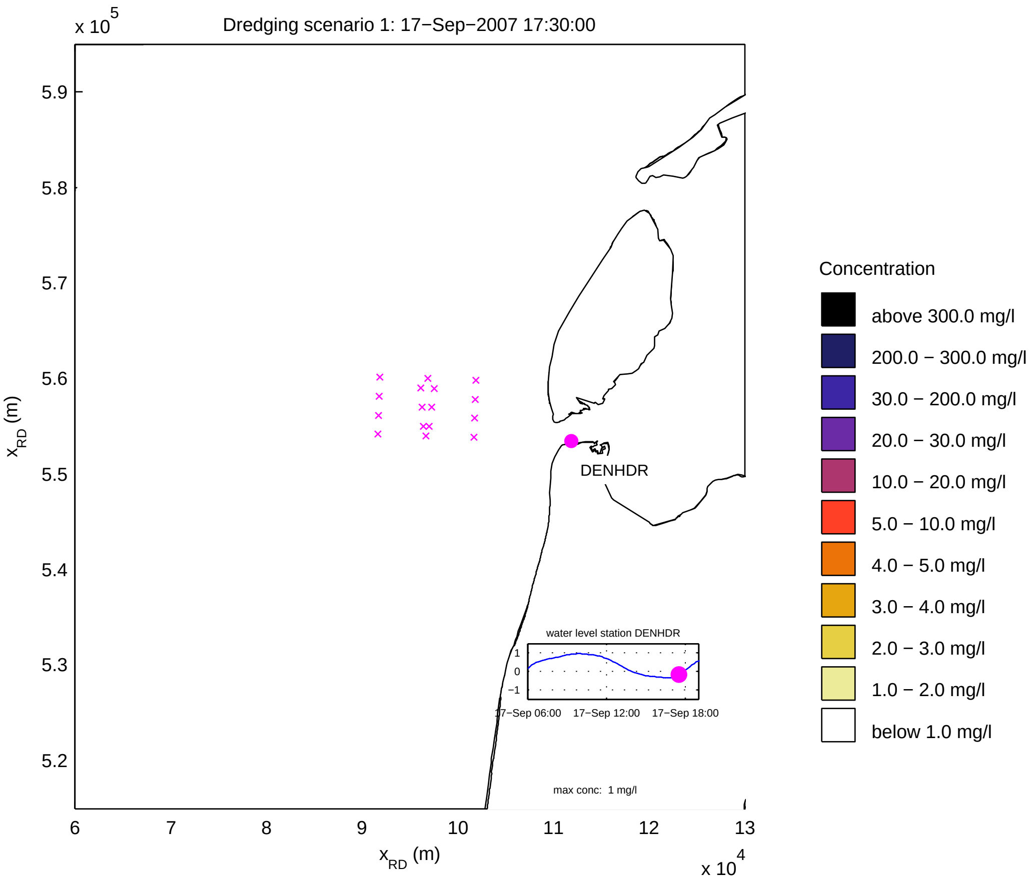

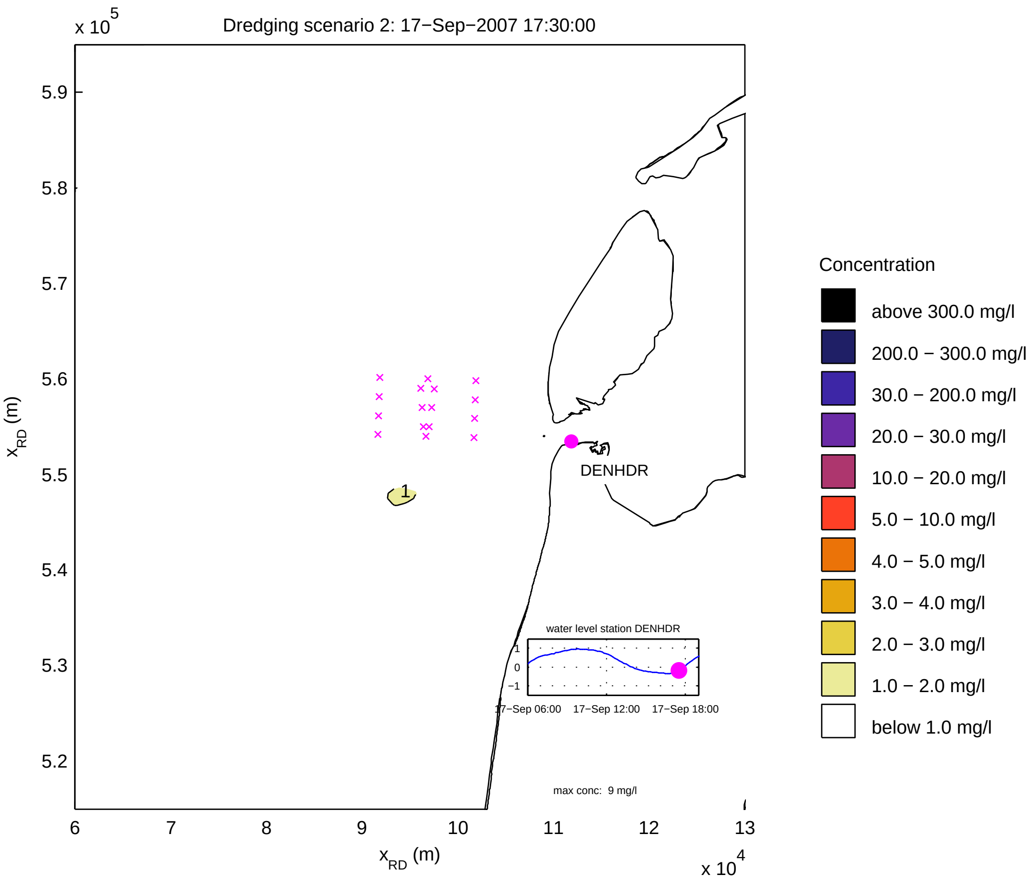

Simulated effect of overflow on silt concentrations (mg/l)
date and time: 17−Sep−2007 17:30:00
x−marks denote locations of T1 observations

Alkyon Hydraulic Consultancy & Research	A2273	Fig. 4.12

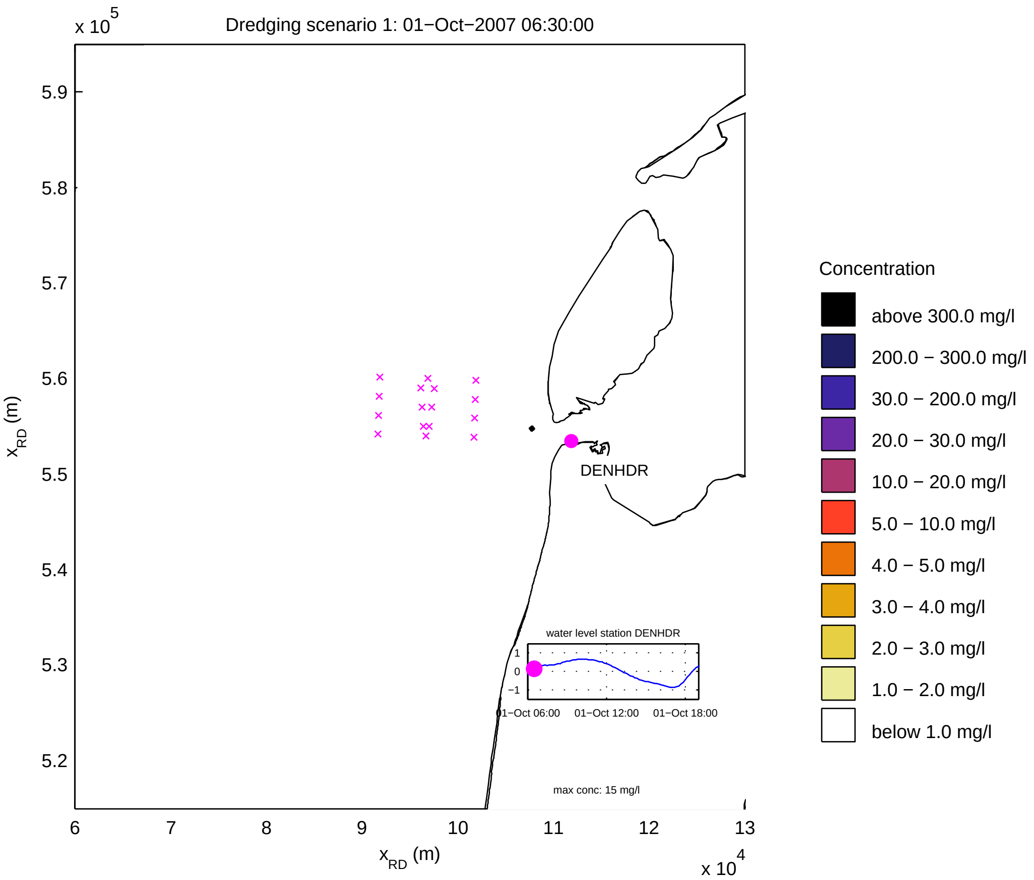

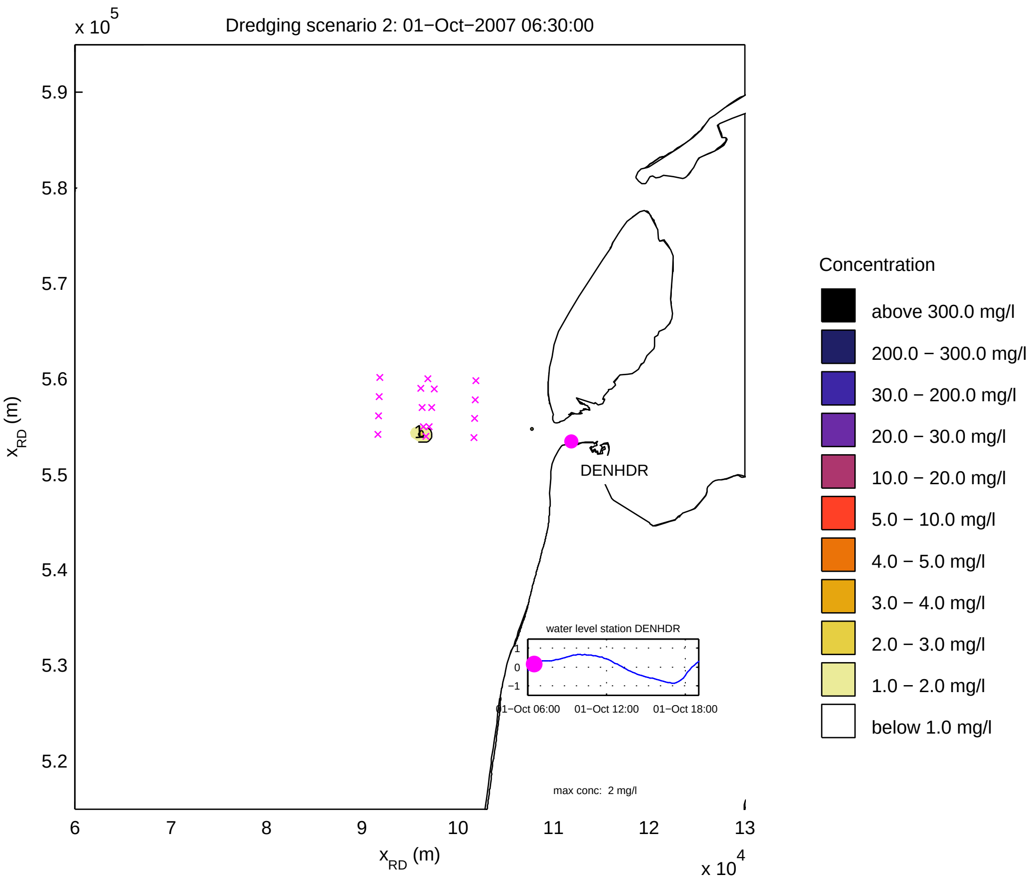

Simulated effect of overflow on silt concentrations (mg/l)
date and time: 01−Oct−2007 06:30:00
x−marks denote locations of T1 observations

Alkyon Hydraulic Consultancy & Research	A2273	Fig. 4.13

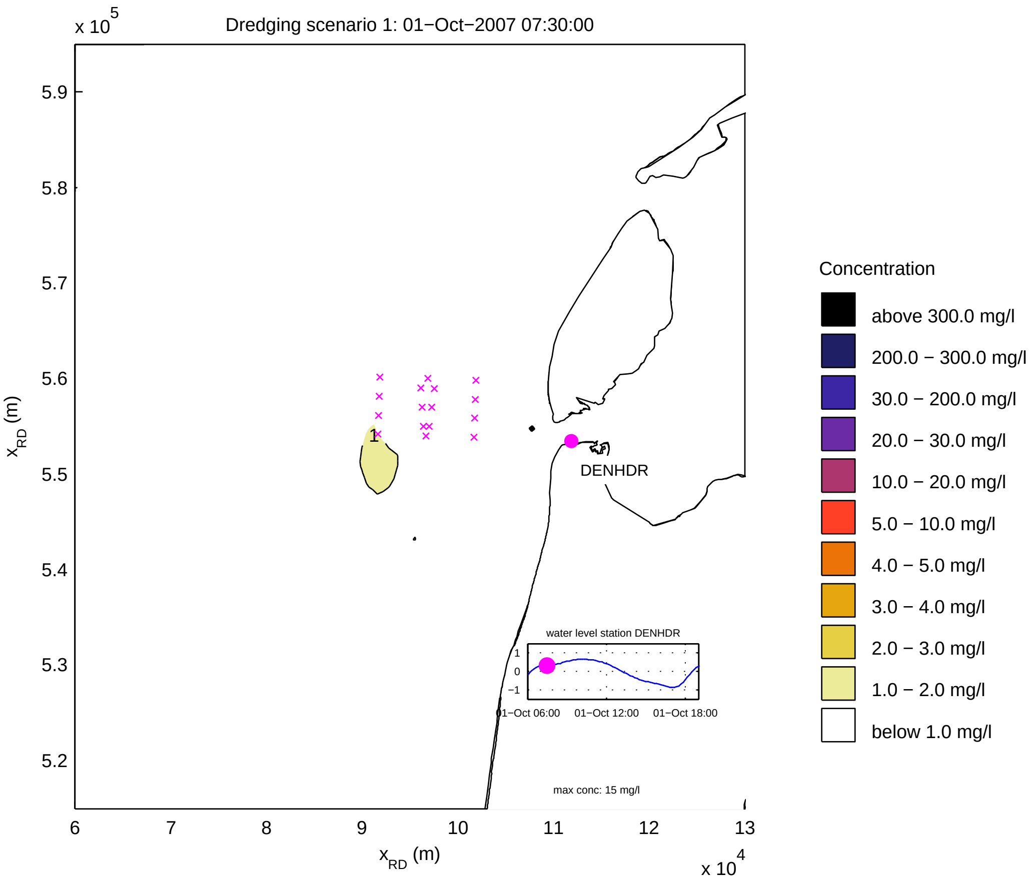

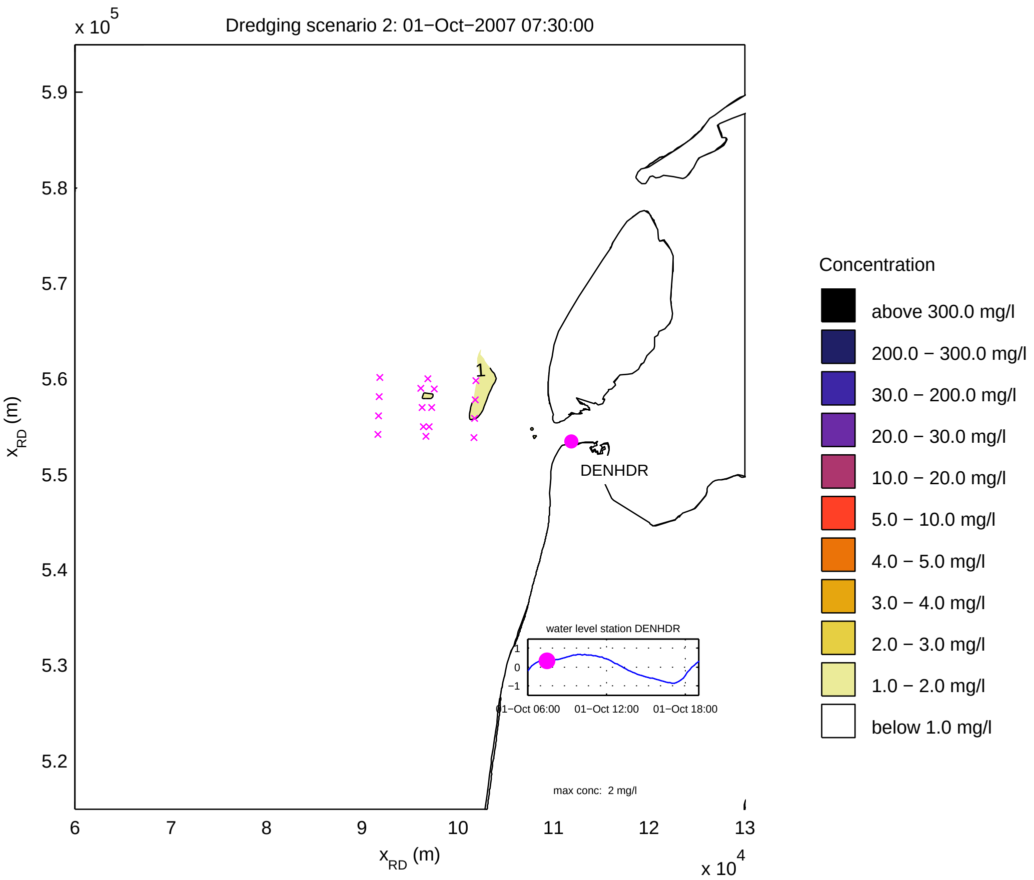

Simulated effect of overflow on silt concentrations (mg/l) date and time: 01−Oct−2007 07:30:00 x−marks denote locations of T1 observations		
Alkyon Hydraulic Consultancy & Research	A2273	Fig. 4.14

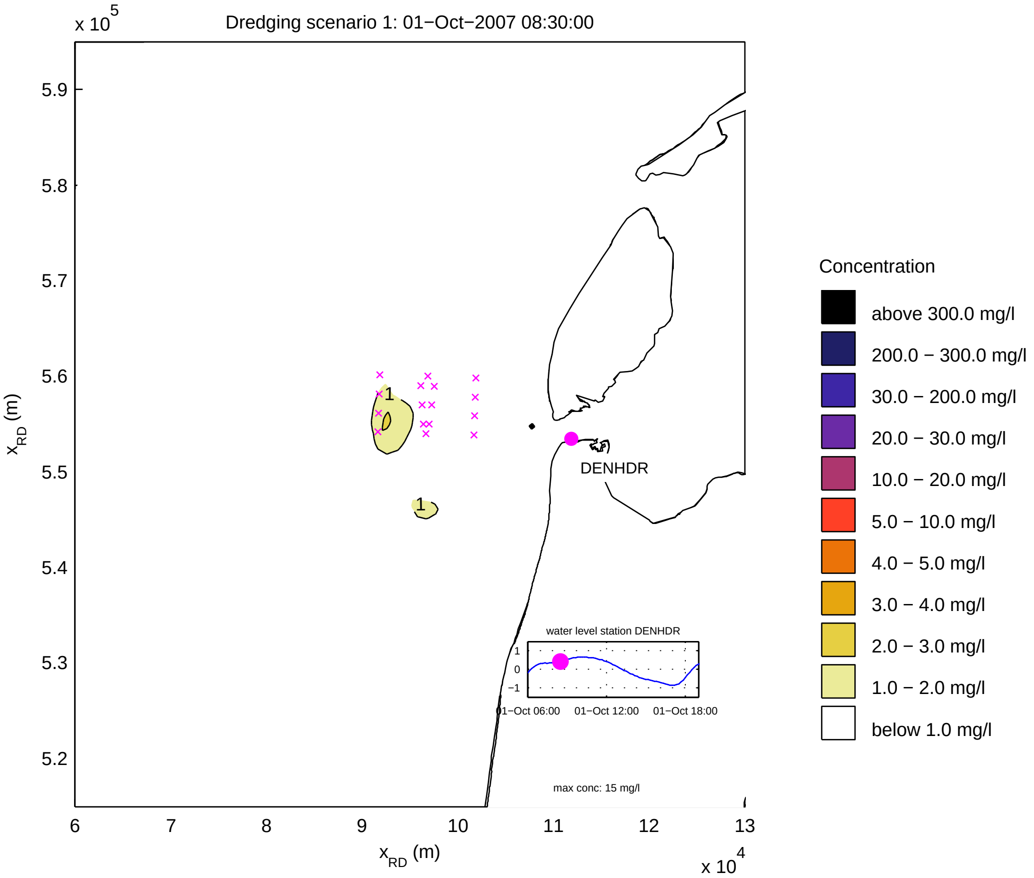

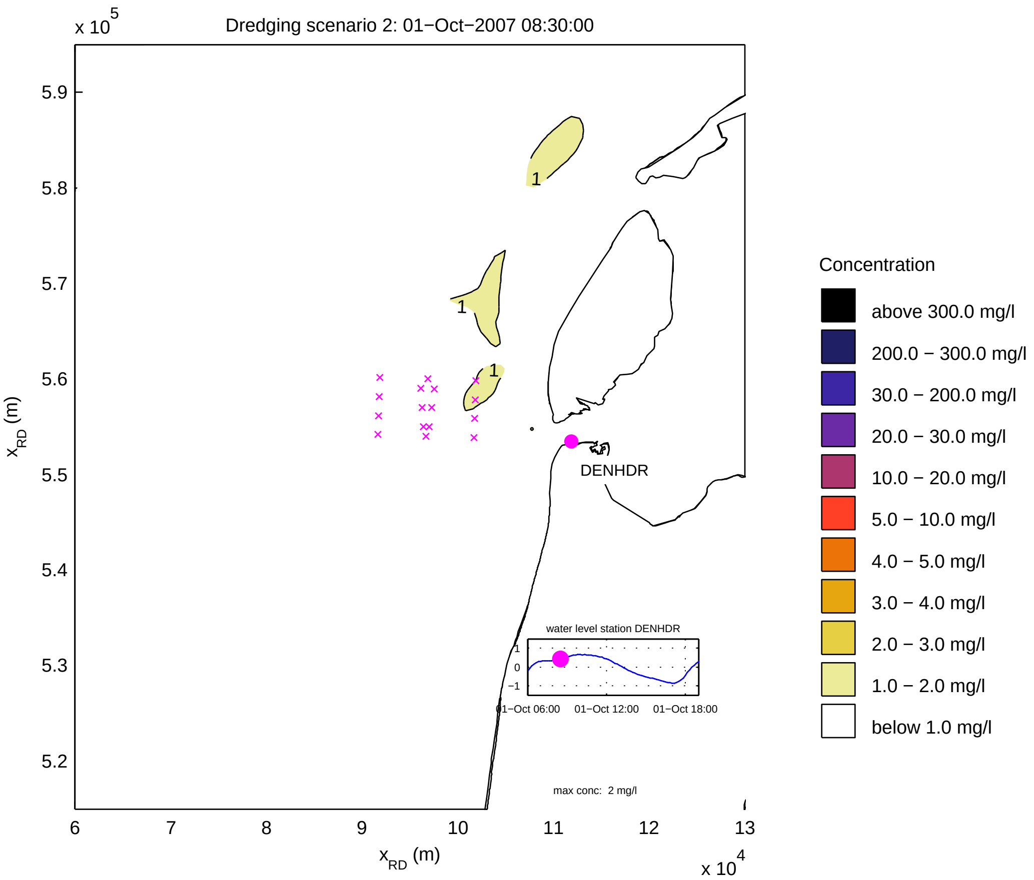

Simulated effect of overflow on silt concentrations (mg/l)
date and time: 01−Oct−2007 08:30:00
x−marks denote locations of T1 observations

Alkyon Hydraulic Consultancy & Research | A2273 | Fig. 4.15

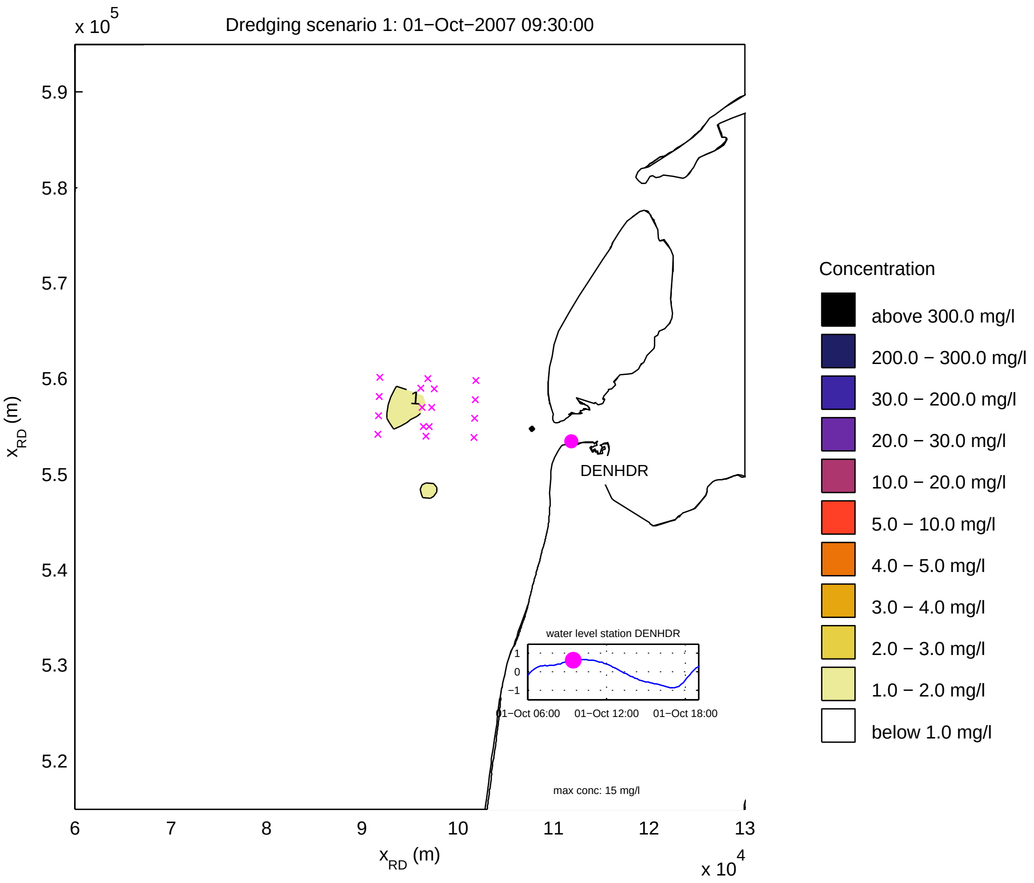

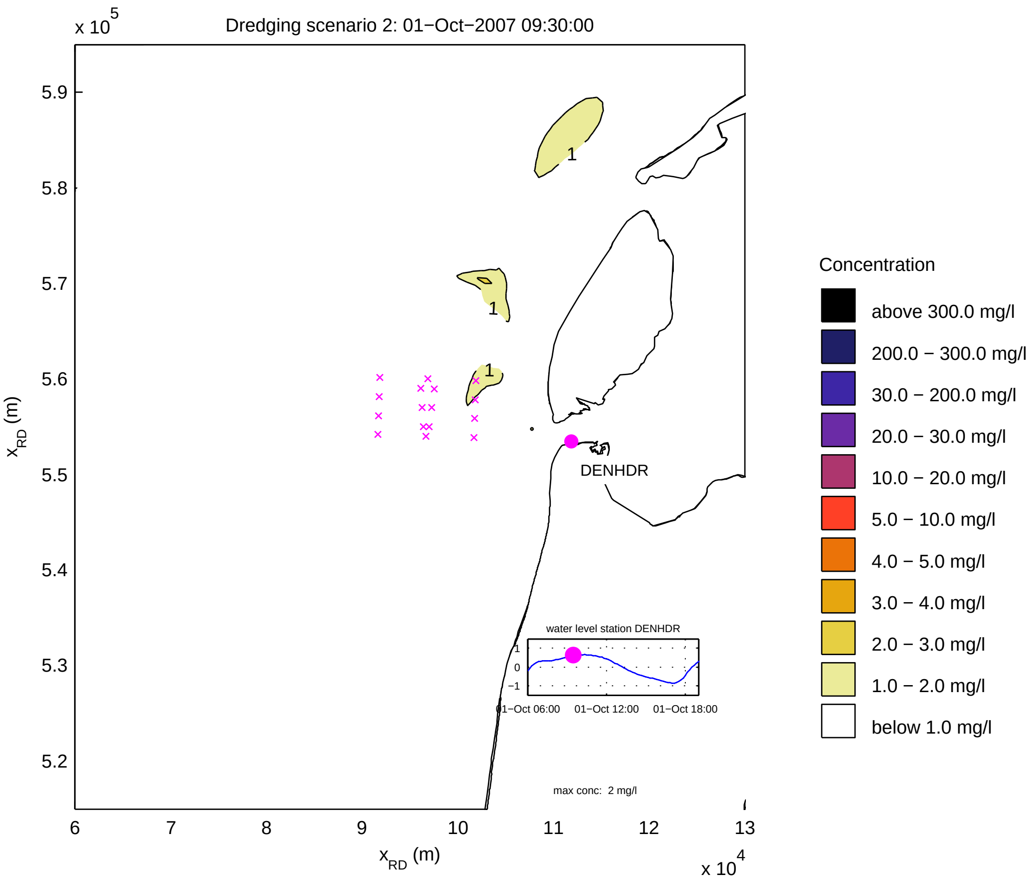

Simulated effect of overflow on silt concentrations (mg/l)
date and time: 01−Oct−2007 09:30:00
x−marks denote locations of T1 observations

Alkyon Hydraulic Consultancy & Research	A2273	Fig. 4.16

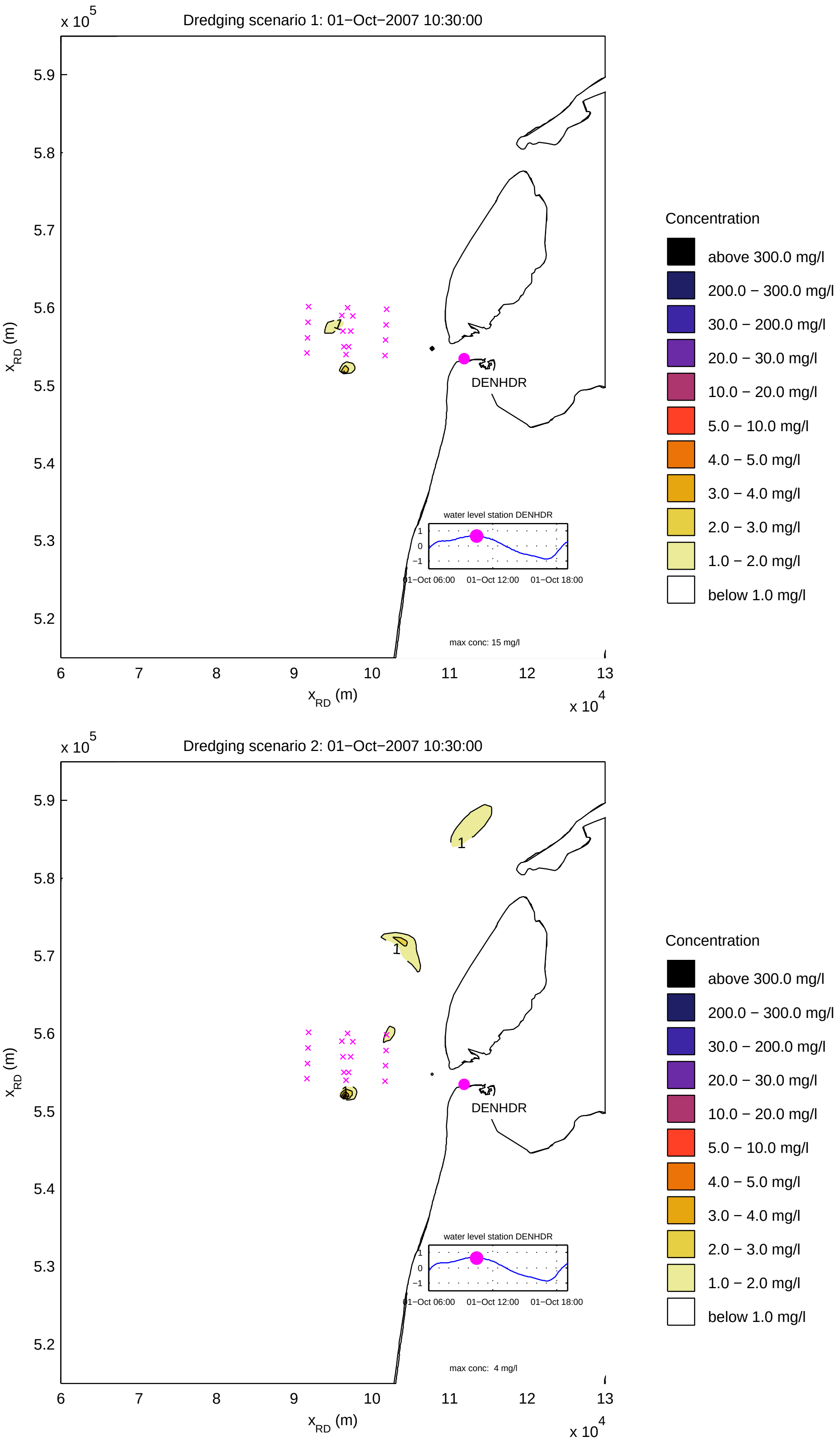

Simulated effect of overflow on silt concentrations (mg/l)
date and time: 01−Oct−2007 10:30:00
x−marks denote locations of T1 observations

Alkyon Hydraulic Consultancy & Research	A2273	Fig. 4.17

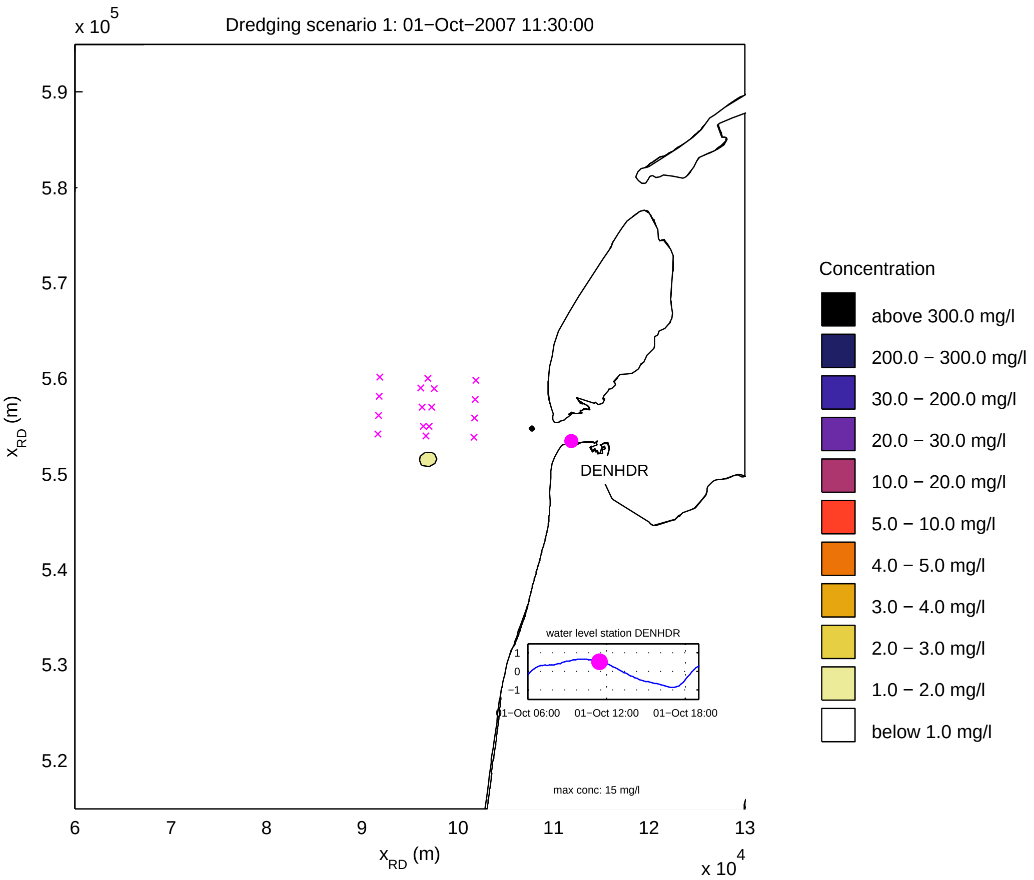

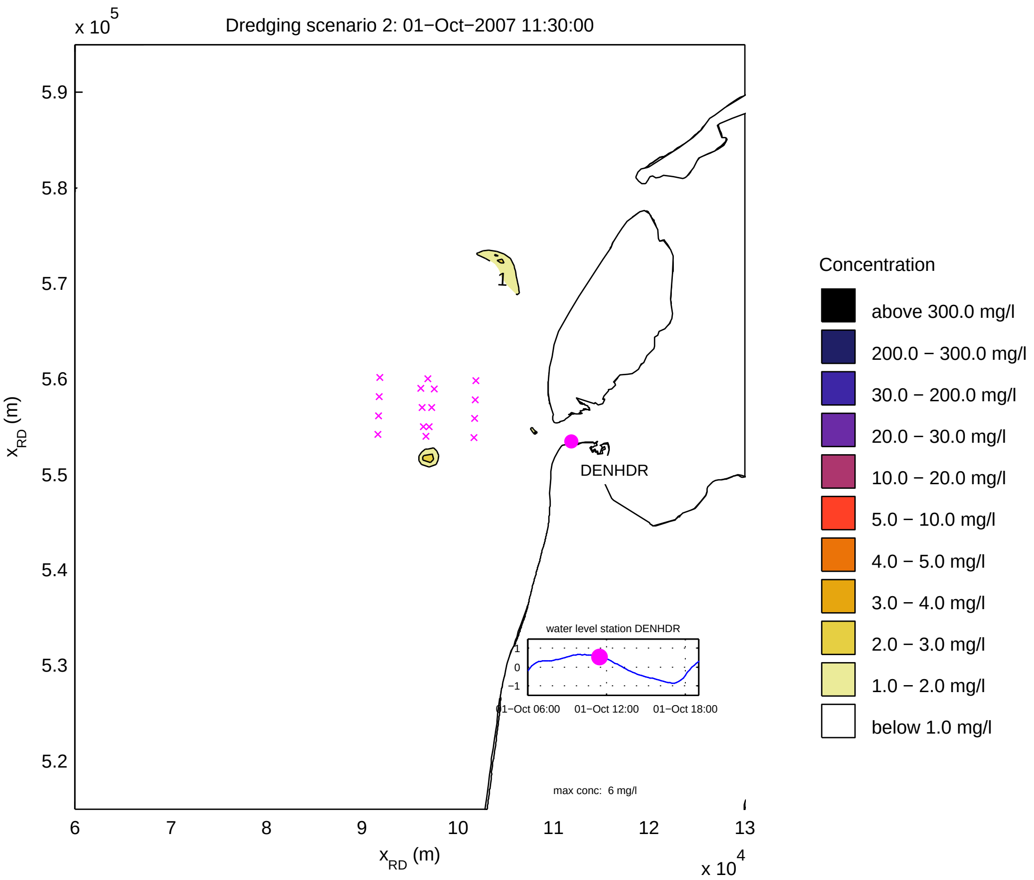

Simulated effect of overflow on silt concentrations (mg/l)
date and time: 01−Oct−2007 11:30:00
x−marks denote locations of T1 observations

Alkyon Hydraulic Consultancy & Research	A2273	Fig. 4.18

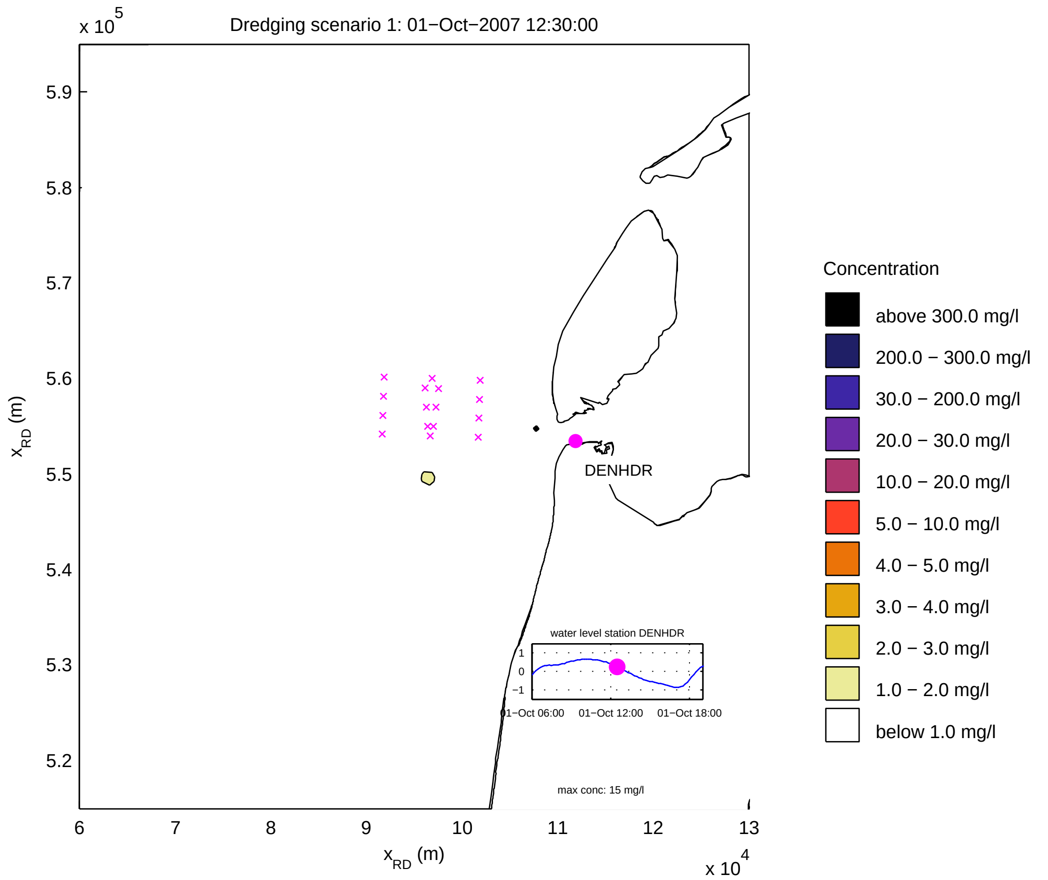

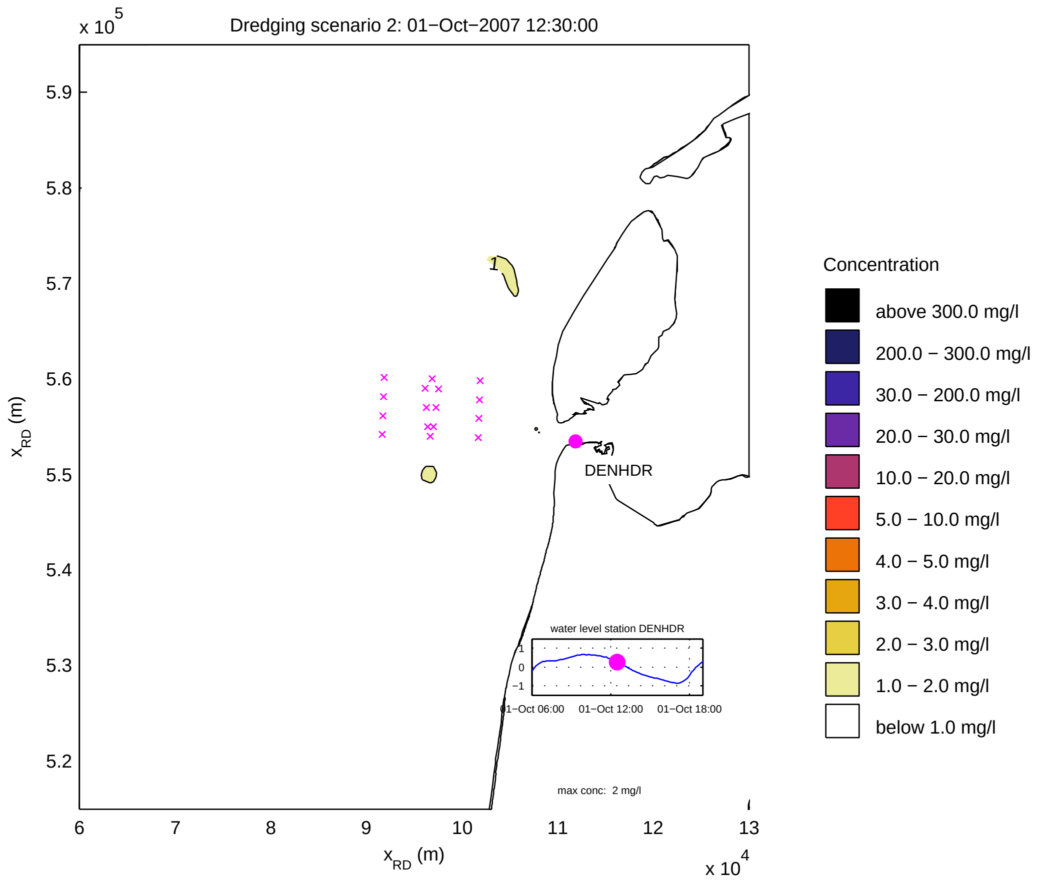

Simulated effect of overflow on silt concentrations (mg/l)
date and time: 01−Oct−2007 12:30:00
x−marks denote locations of T1 observations

Alkyon Hydraulic Consultancy & Research | A2273 | Fig. 4.19

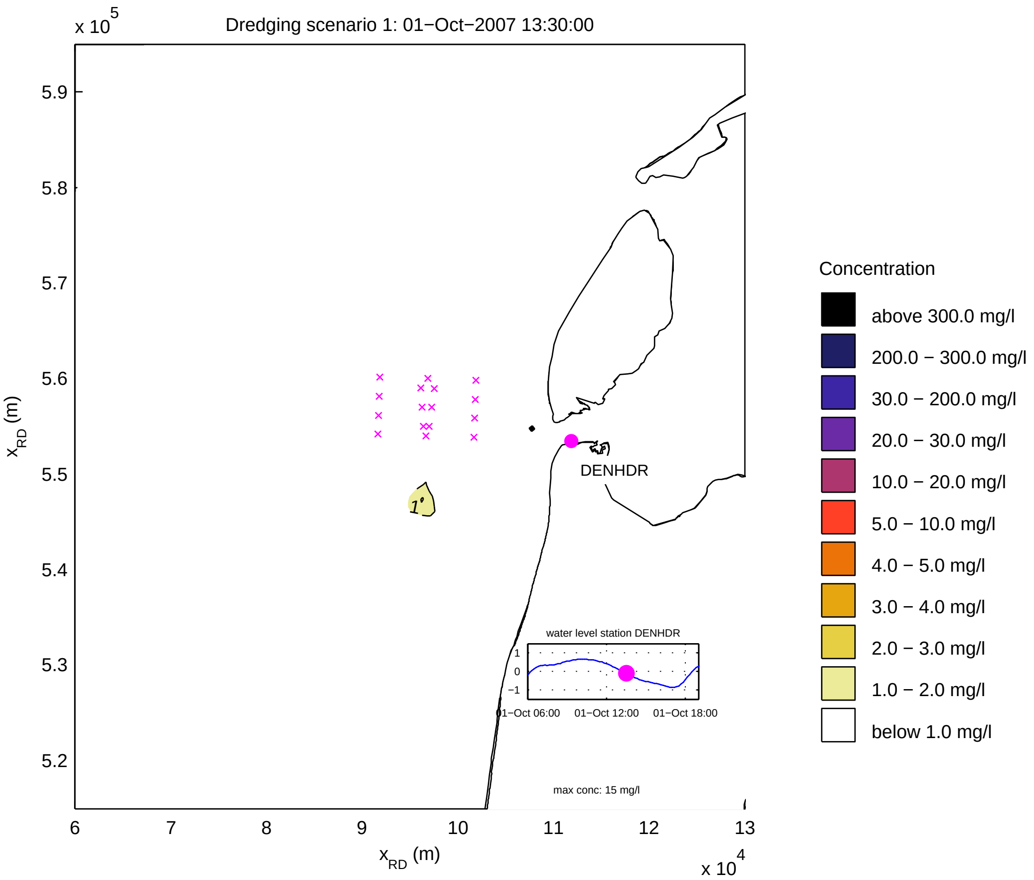

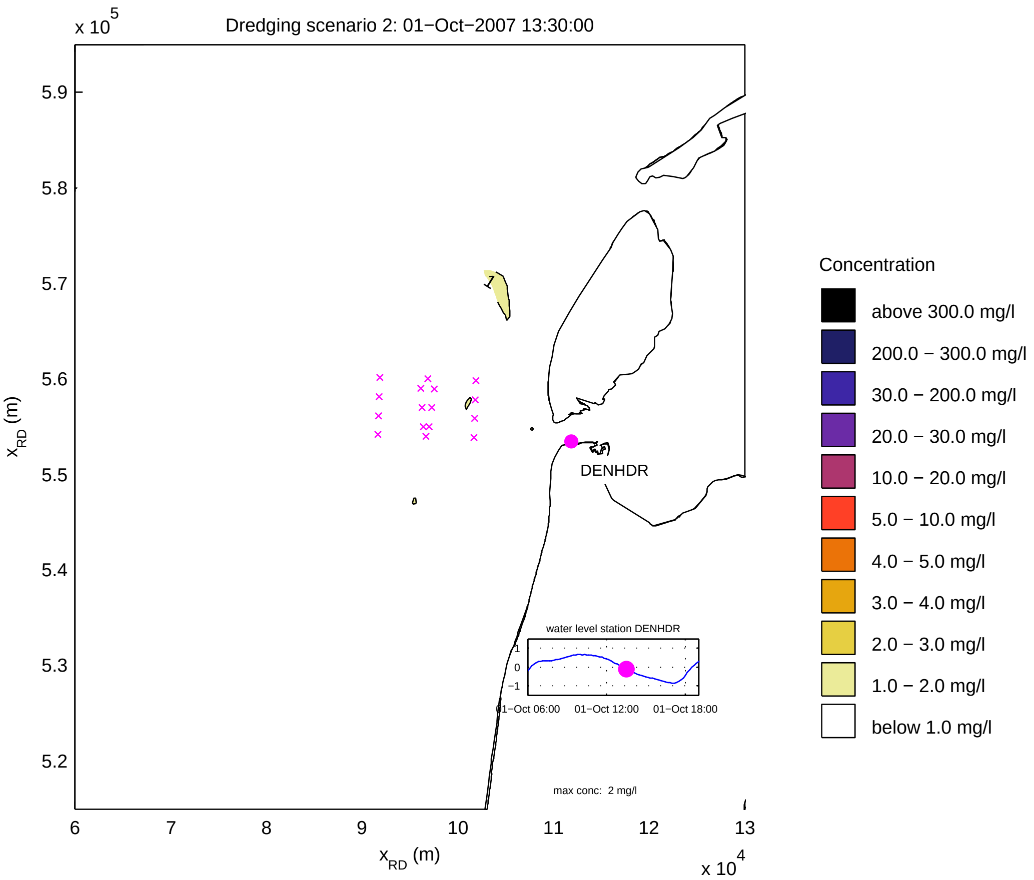

Simulated effect of overflow on silt concentrations (mg/l) date and time: 01−Oct−2007 13:30:00 x−marks denote locations of T1 observations		
Alkyon Hydraulic Consultancy & Research	A2273	Fig. 4.20

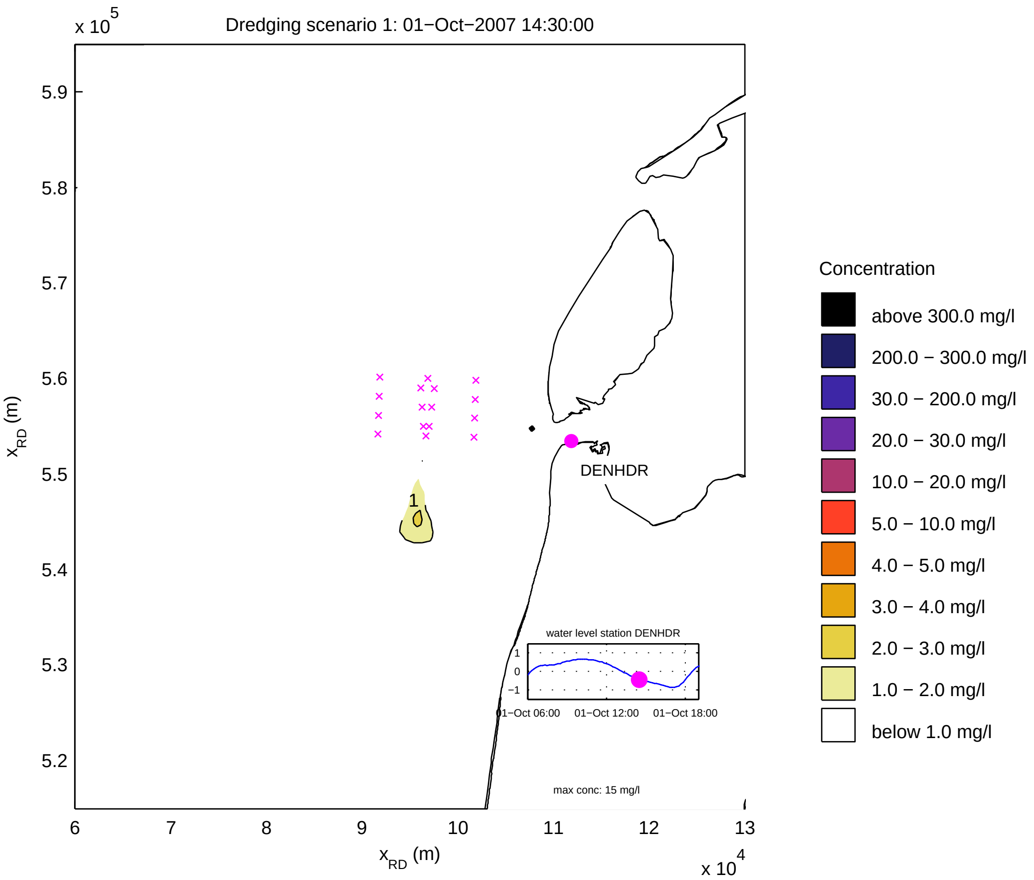

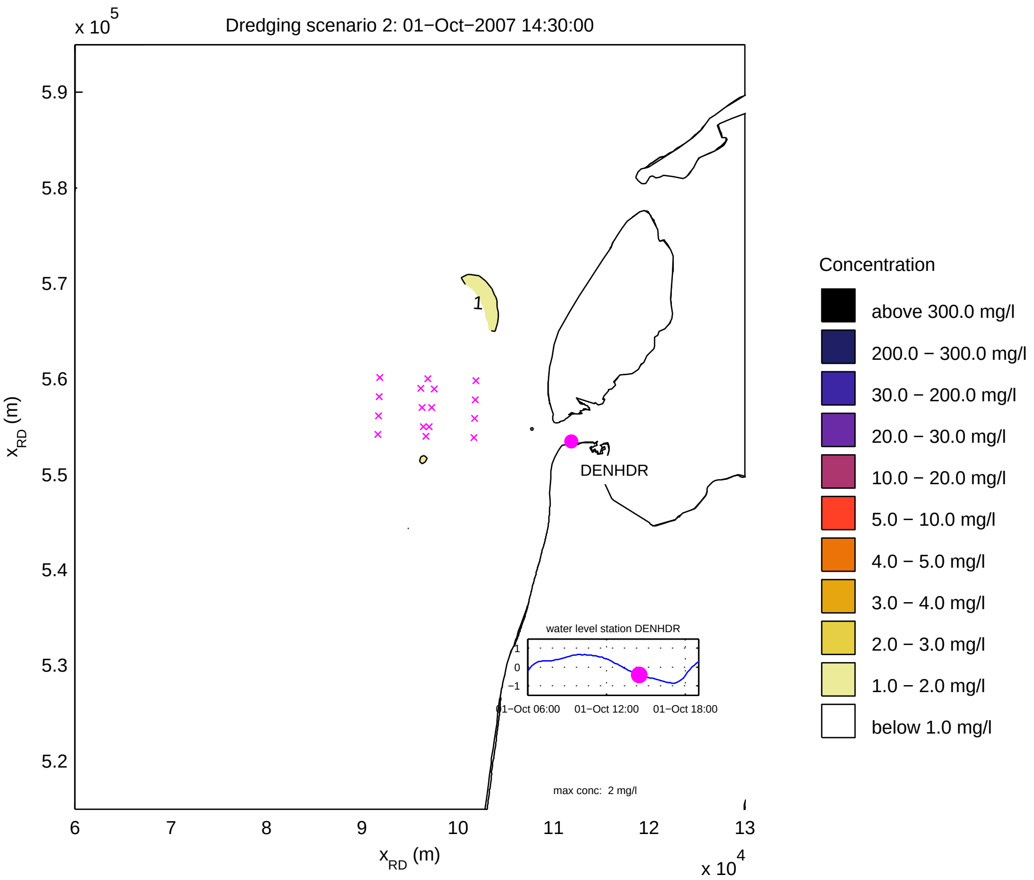

Simulated effect of overflow on silt concentrations (mg/l)
date and time: 01−Oct−2007 14:30:00
x−marks denote locations of T1 observations

Alkyon Hydraulic Consultancy & Research	A2273	Fig. 4.21

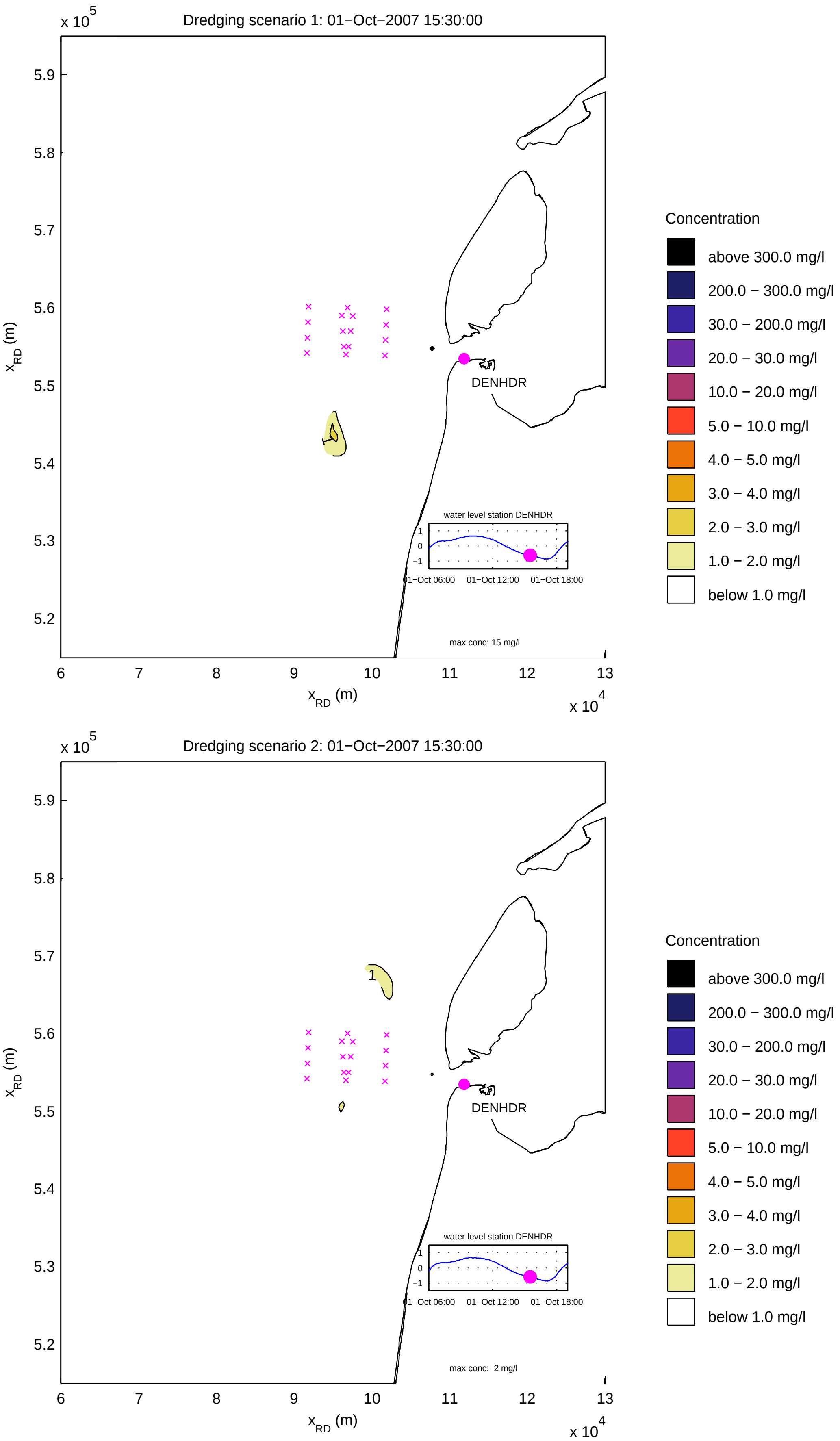

Simulated effect of overflow on silt concentrations (mg/l)
date and time: 01−Oct−2007 15:30:00
x−marks denote locations of T1 observations

Alkyon Hydraulic Consultancy & Research | A2273 | Fig. 4.22

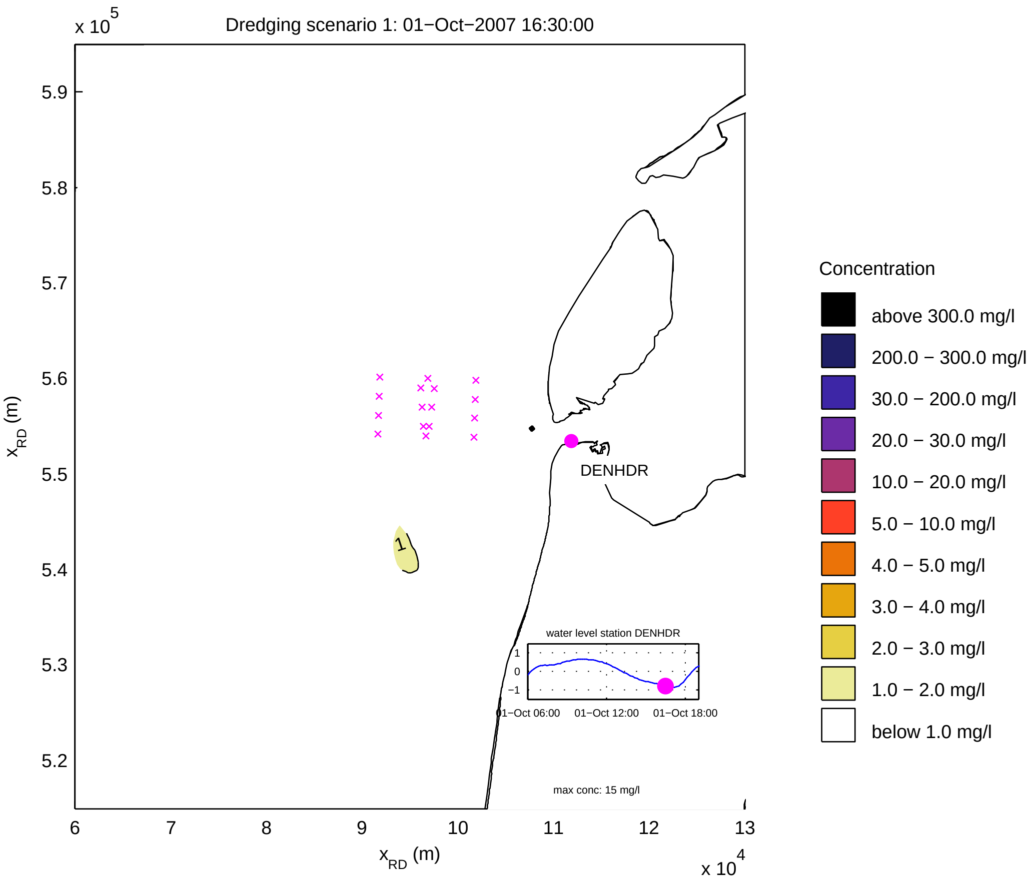

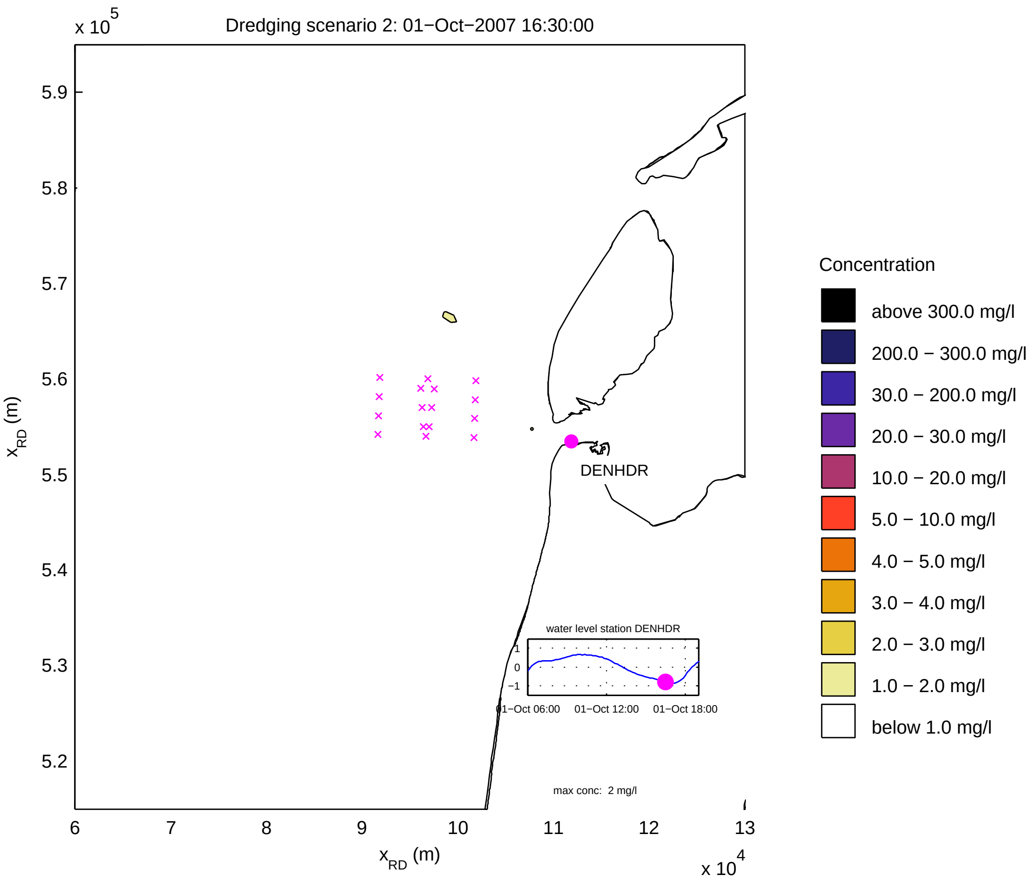

Simulated effect of overflow on silt concentrations (mg/l)
date and time: 01−Oct−2007 16:30:00
x−marks denote locations of T1 observations

Alkyon Hydraulic Consultancy & Research	A2273	Fig. 4.23

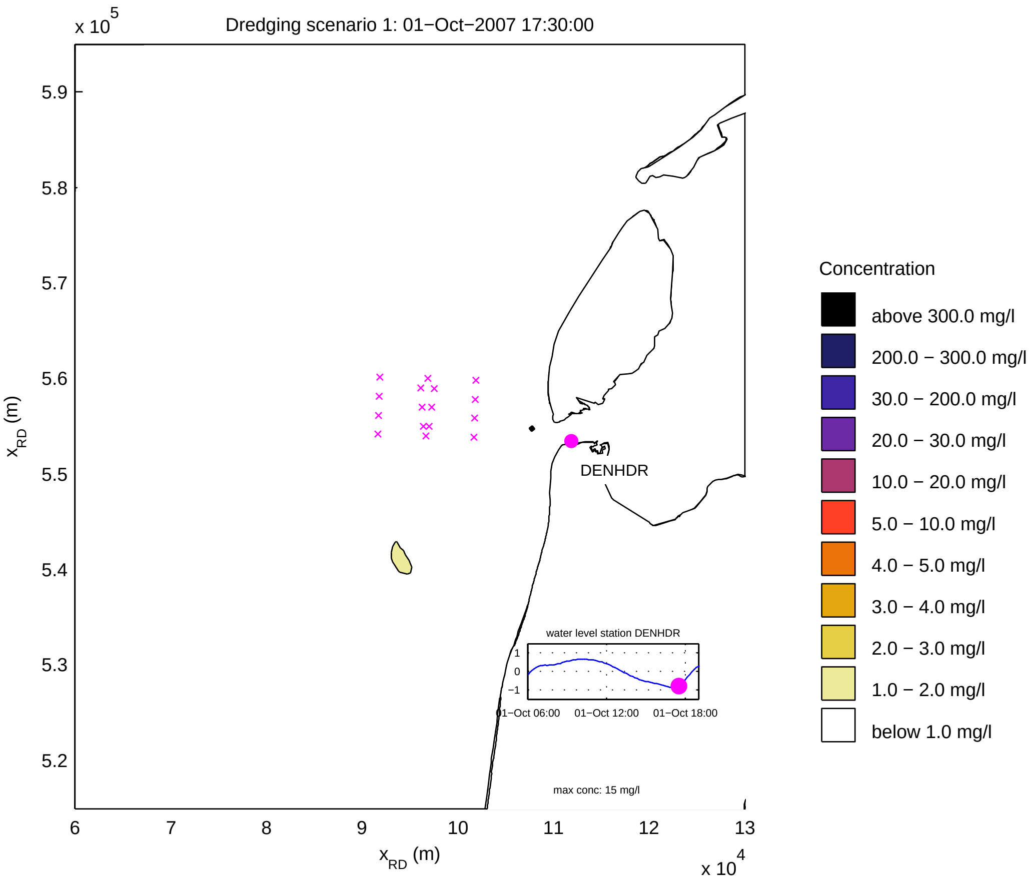

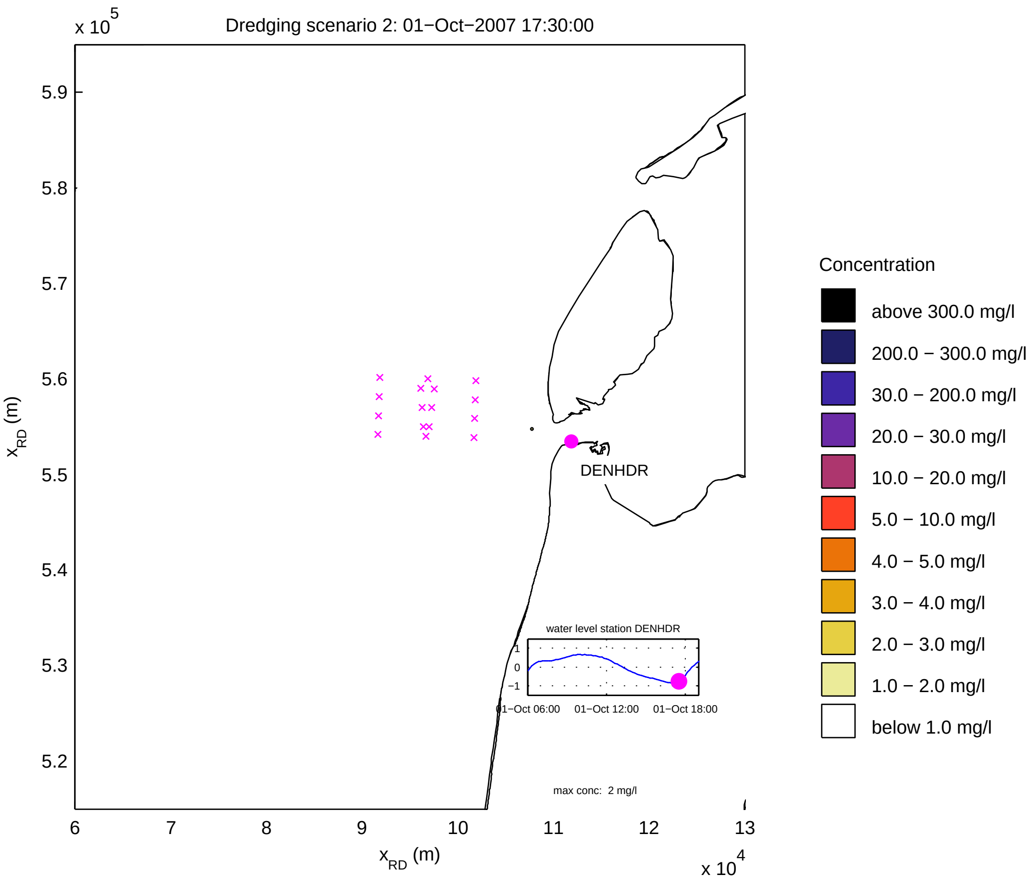

Simulated effect of overflow on silt concentrations (mg/l) date and time: 01−Oct−2007 17:30:00 x−marks denote locations of T1 observations		
Alkyon Hydraulic Consultancy & Research	A2273	Fig. 4.24

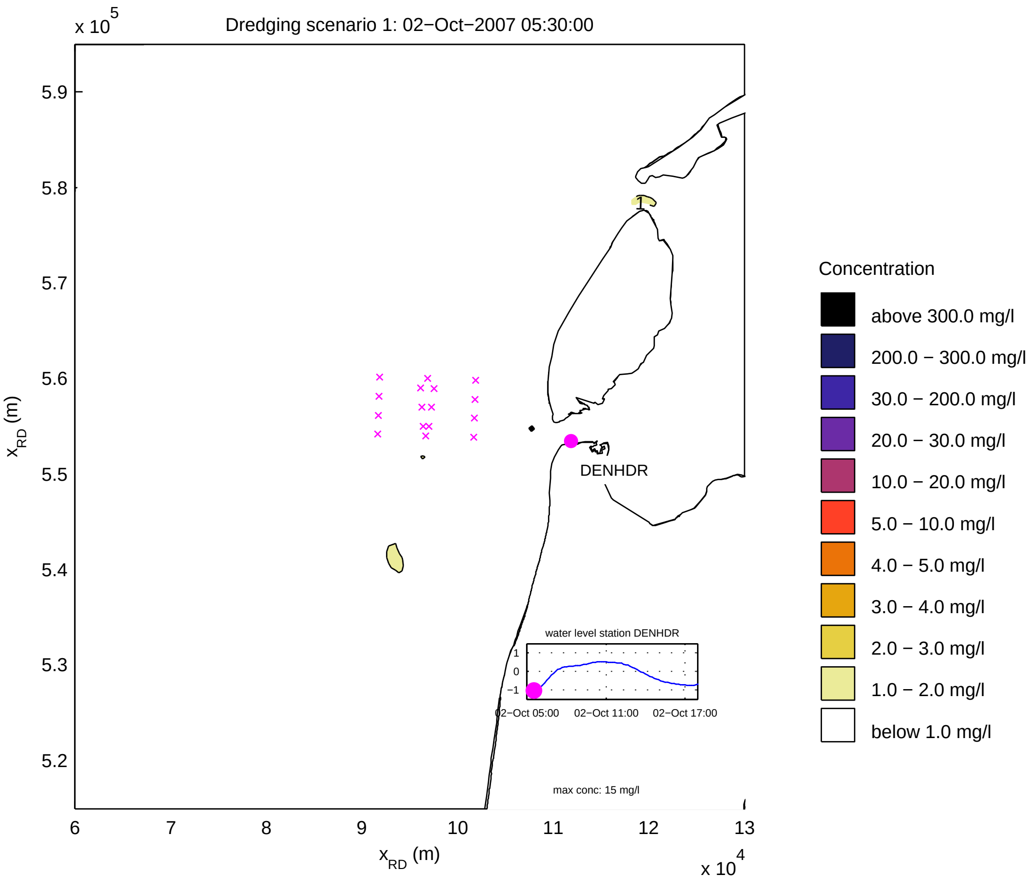

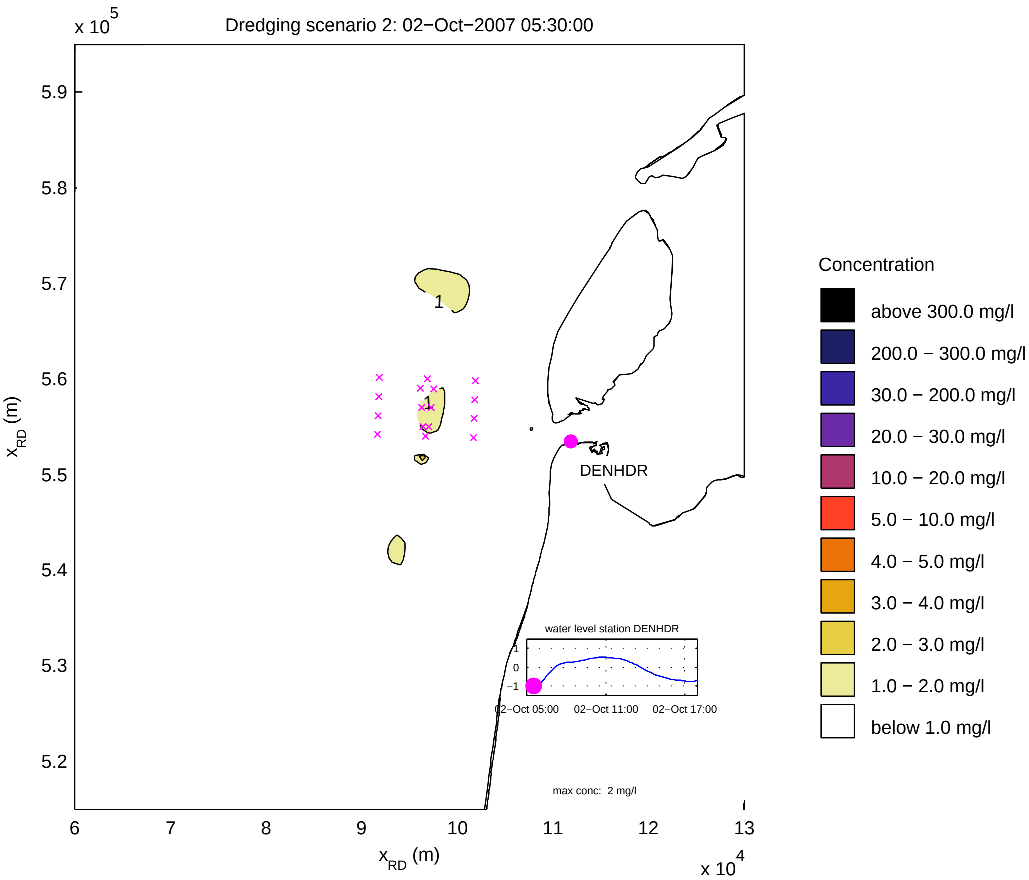

Simulated effect of overflow on silt concentrations (mg/l)
date and time: 02−Oct−2007 05:30:00
x−marks denote locations of T1 observations

Alkyon Hydraulic Consultancy & Research	A2273	Fig. 4.25

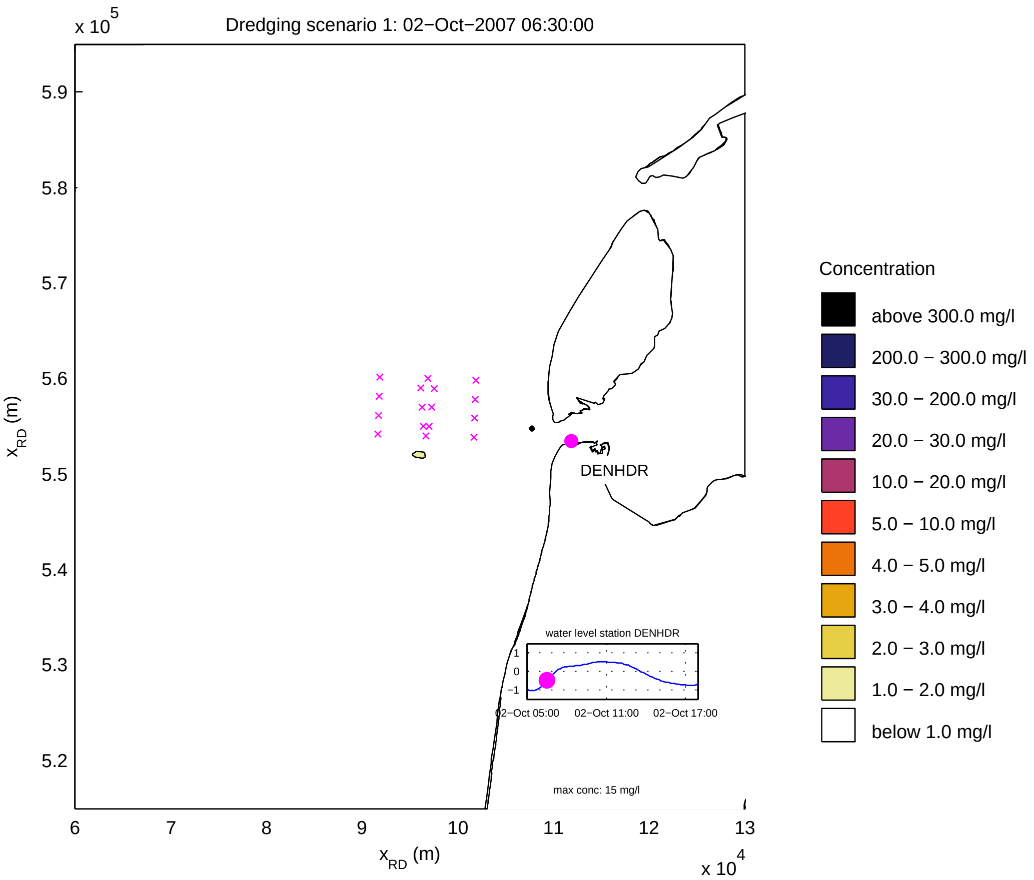

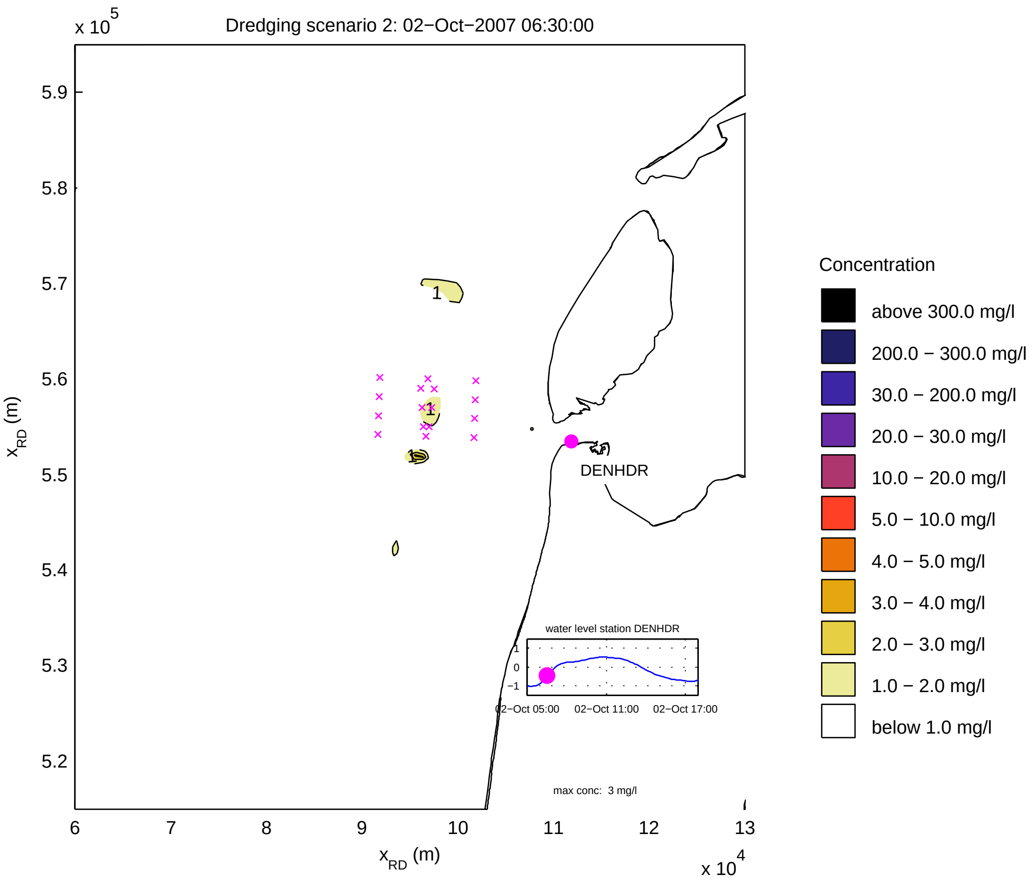

Simulated effect of overflow on silt concentrations (mg/l)
date and time: 02−Oct−2007 06:30:00
x−marks denote locations of T1 observations

Alkyon Hydraulic Consultancy & Research	A2273	Fig. 4.26

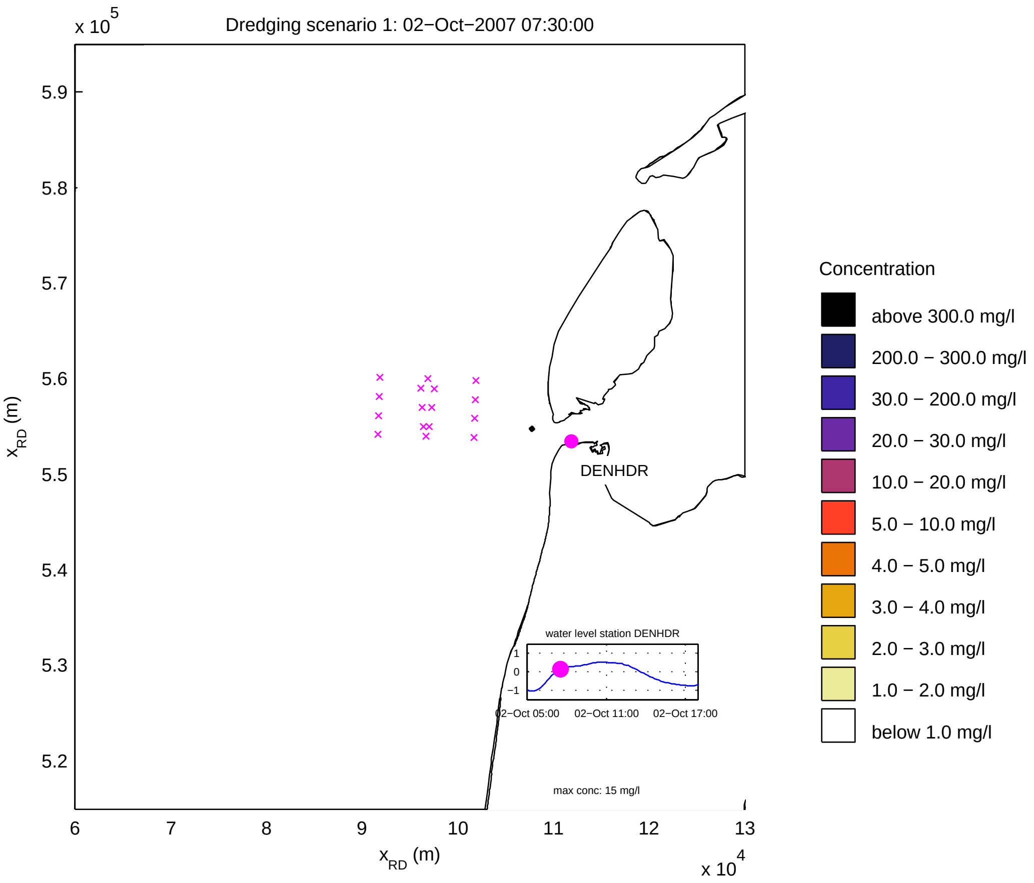

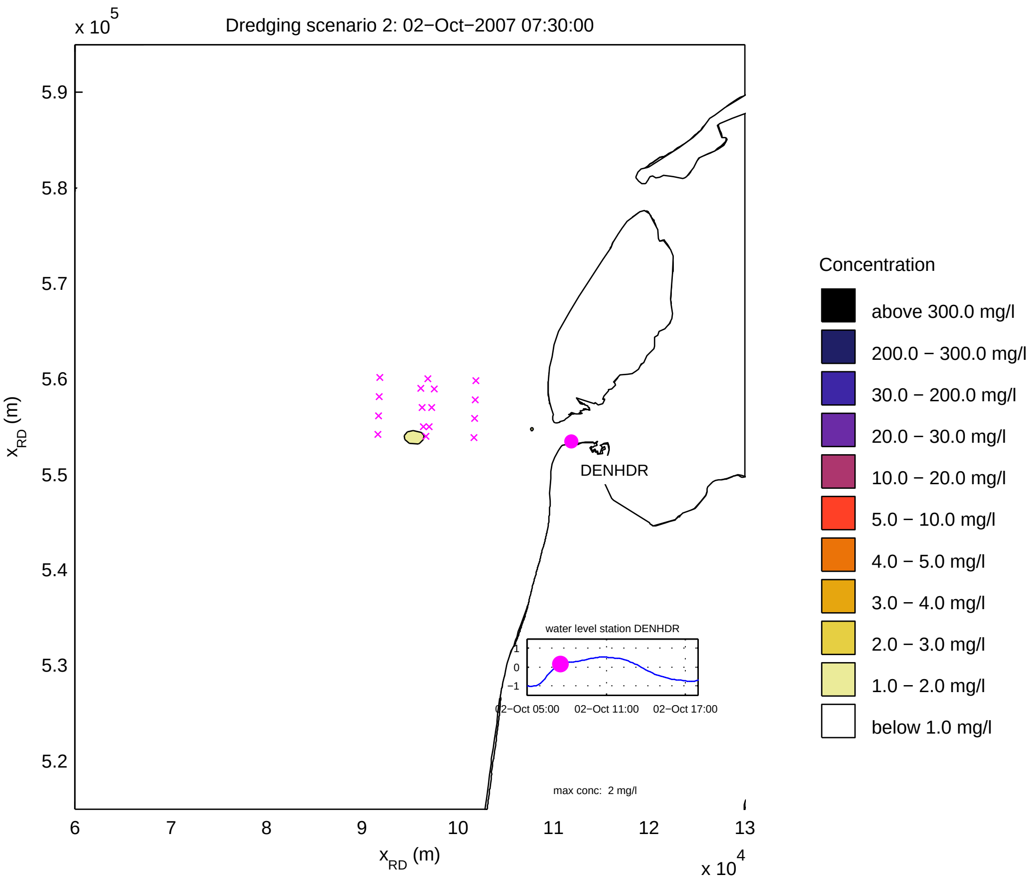

Simulated effect of overflow on silt concentrations (mg/l) date and time: 02−Oct−2007 07:30:00 x−marks denote locations of T1 observations		
Alkyon Hydraulic Consultancy & Research	A2273	Fig. 4.27

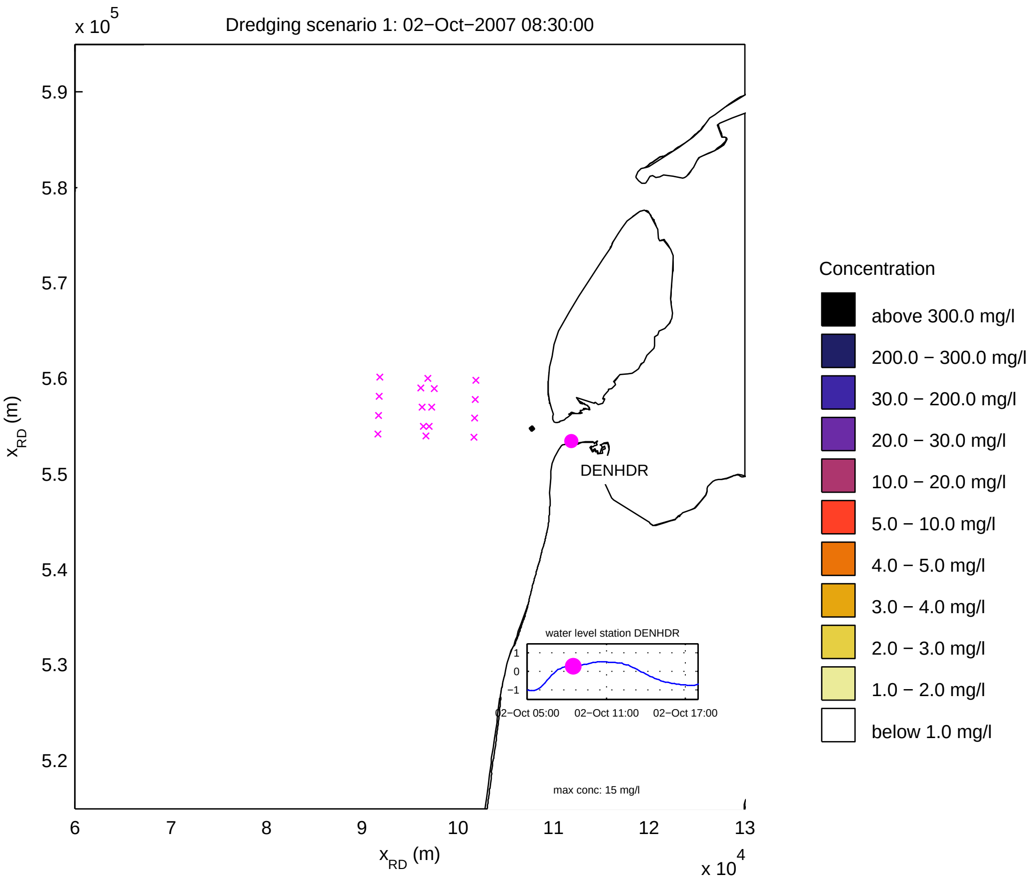

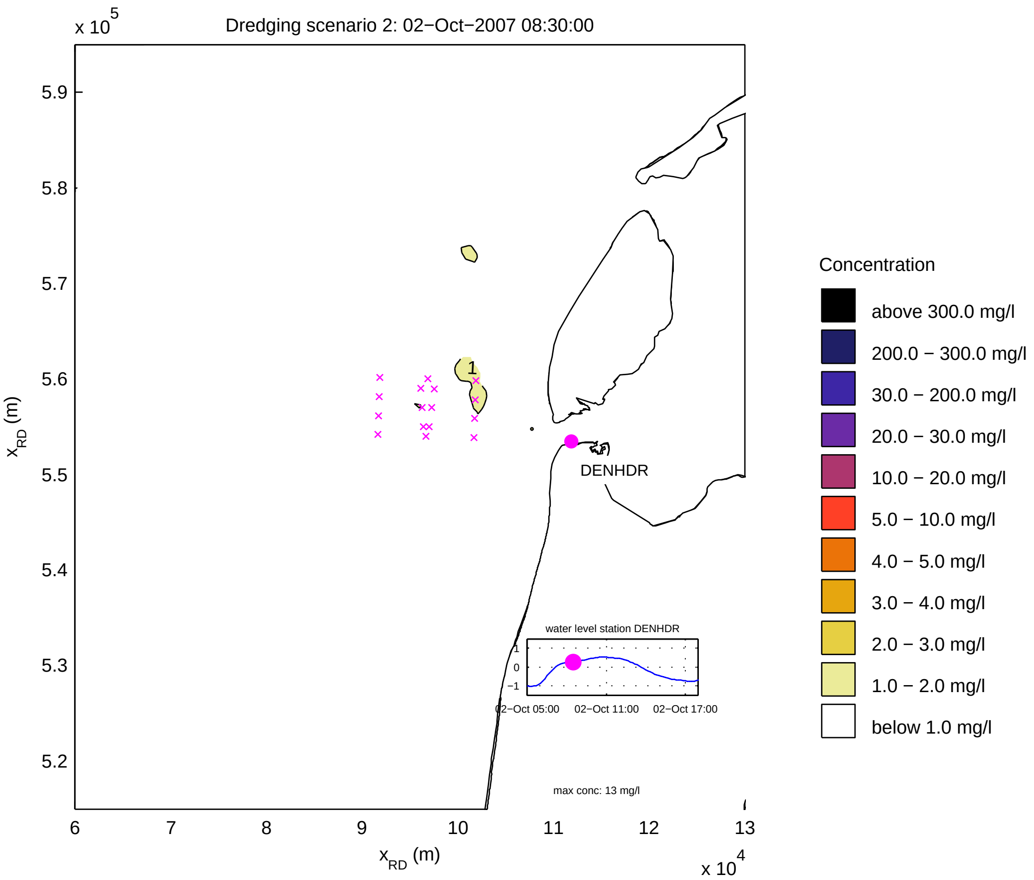

Simulated effect of overflow on silt concentrations (mg/l)
date and time: 02−Oct−2007 08:30:00
x−marks denote locations of T1 observations

Alkyon Hydraulic Consultancy & Research | A2273 | Fig. 4.28

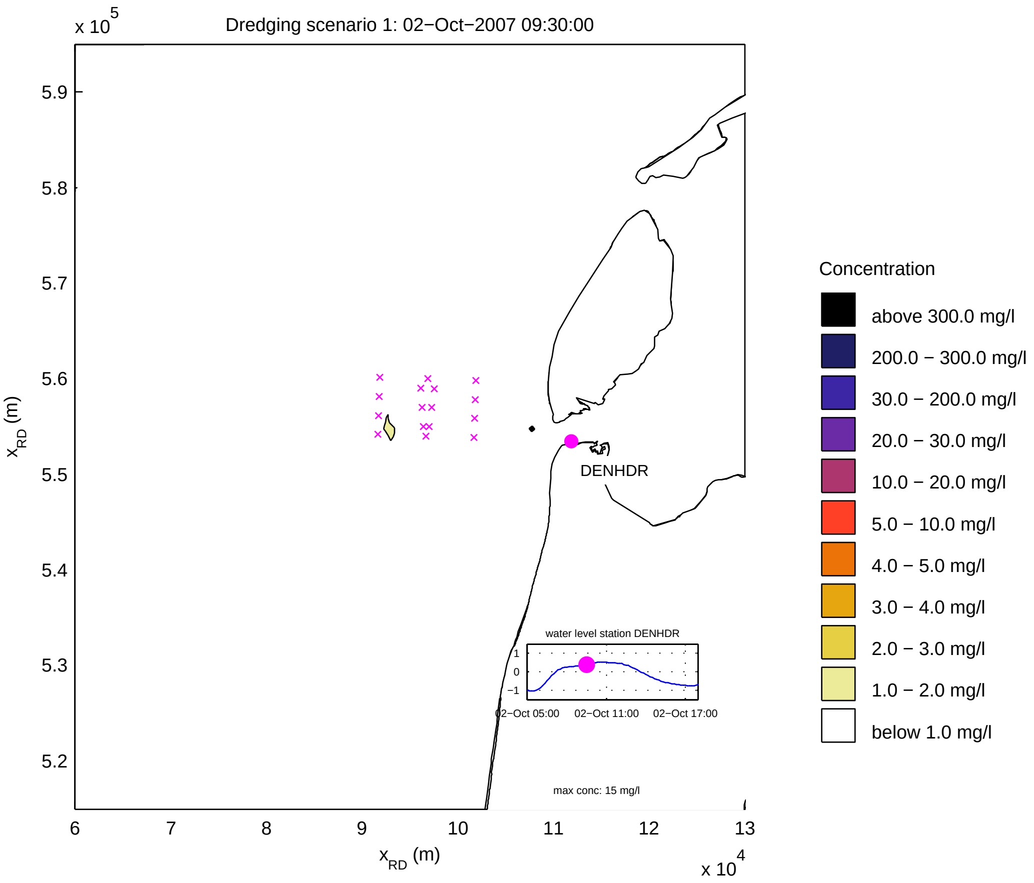

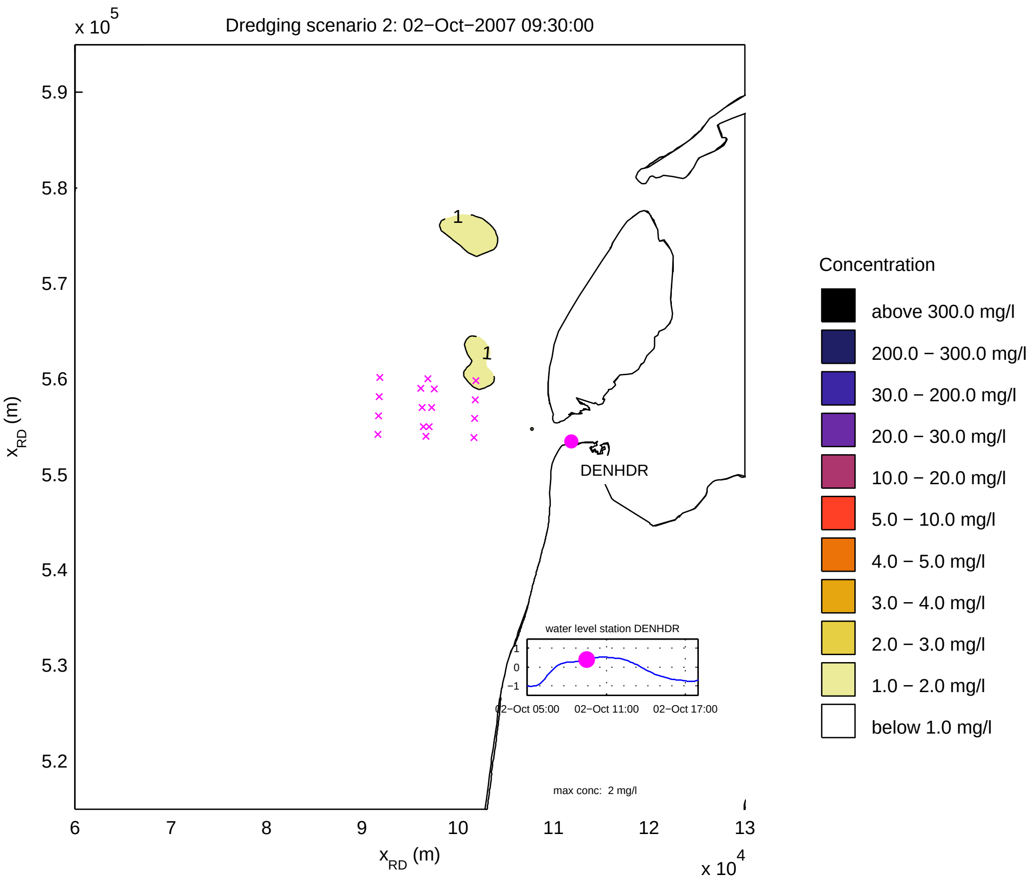

Simulated effect of overflow on silt concentrations (mg/l) date and time: 02−Oct−2007 09:30:00 x−marks denote locations of T1 observations		
Alkyon Hydraulic Consultancy & Research	A2273	Fig. 4.29

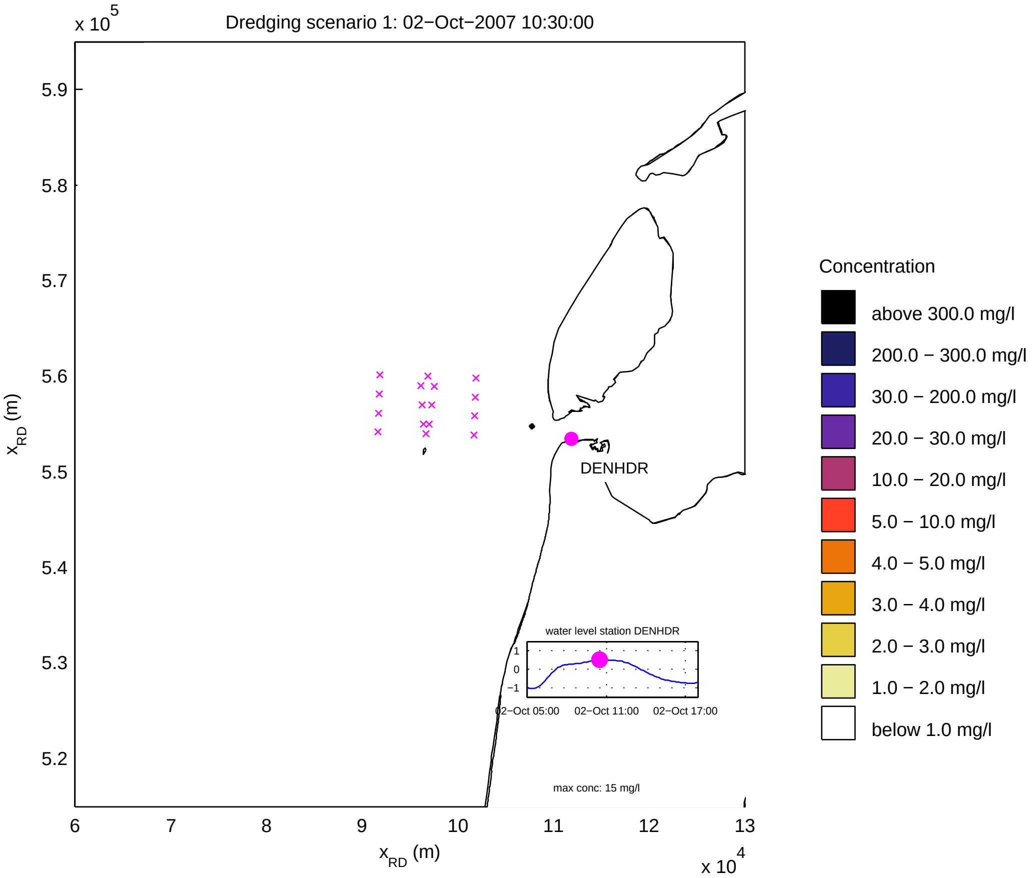

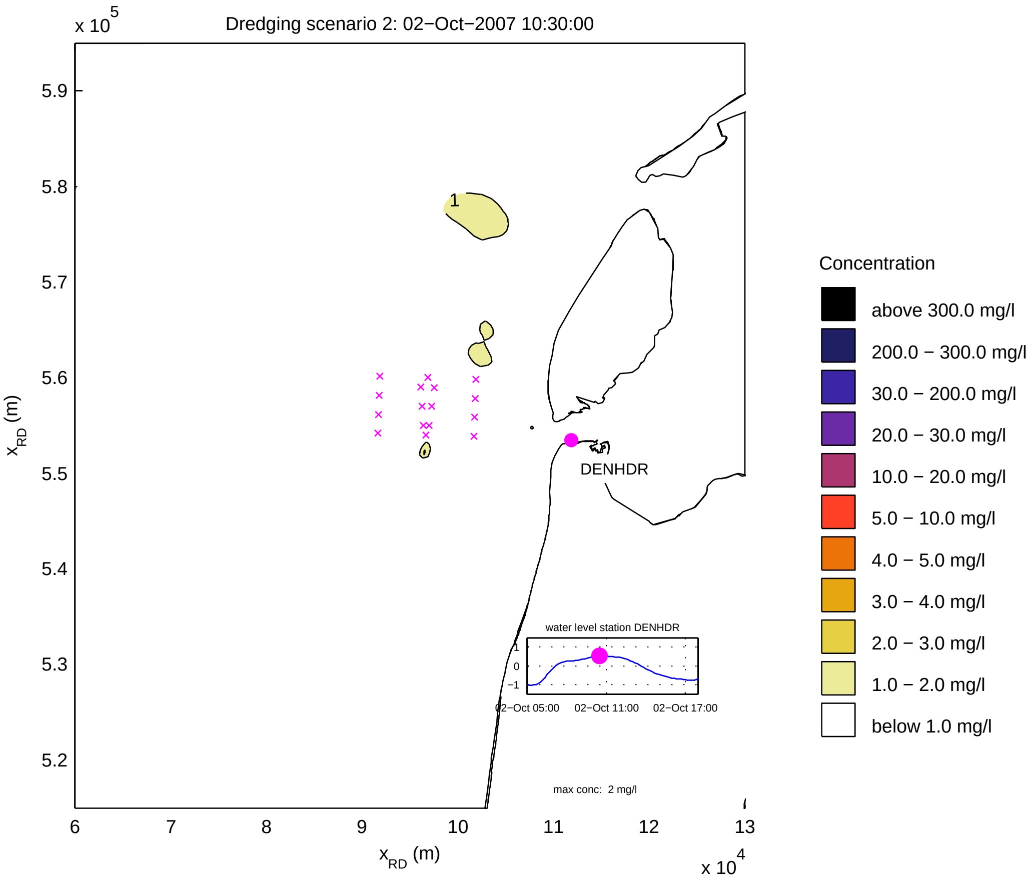

Simulated effect of overflow on silt concentrations (mg/l)
date and time: 02−Oct−2007 10:30:00
x−marks denote locations of T1 observations

Alkyon Hydraulic Consultancy & Research	A2273	Fig. 4.30

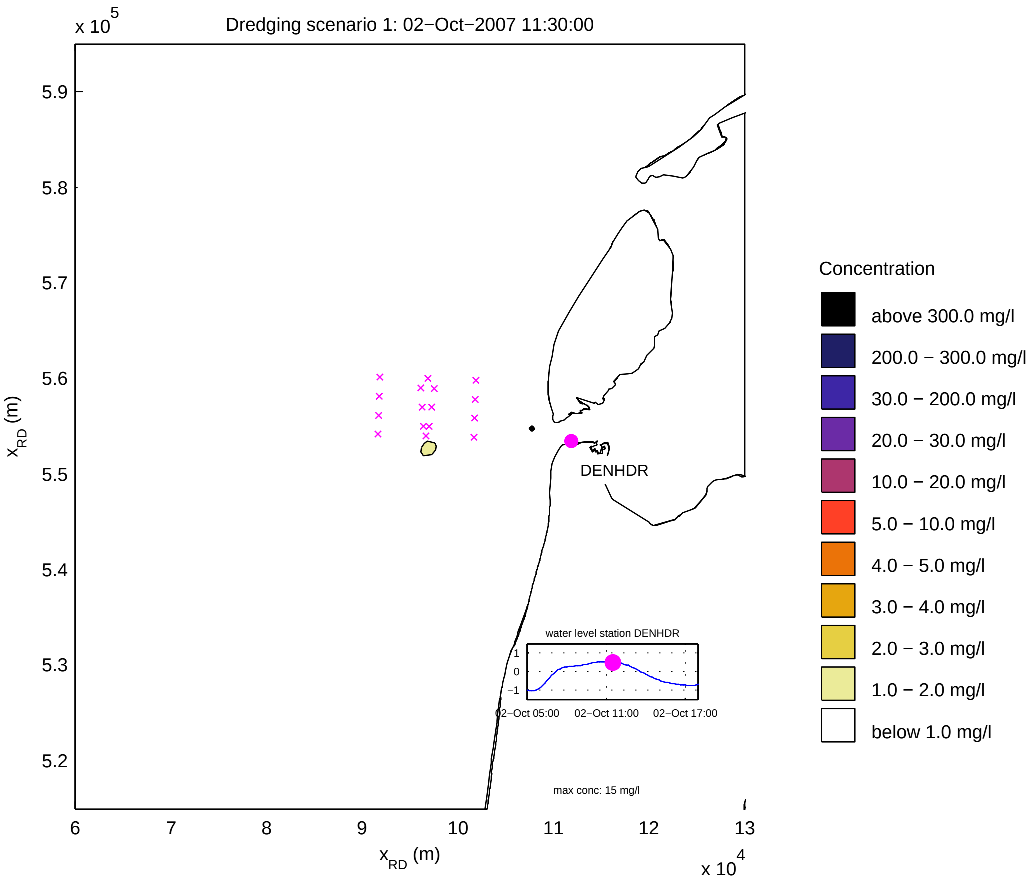

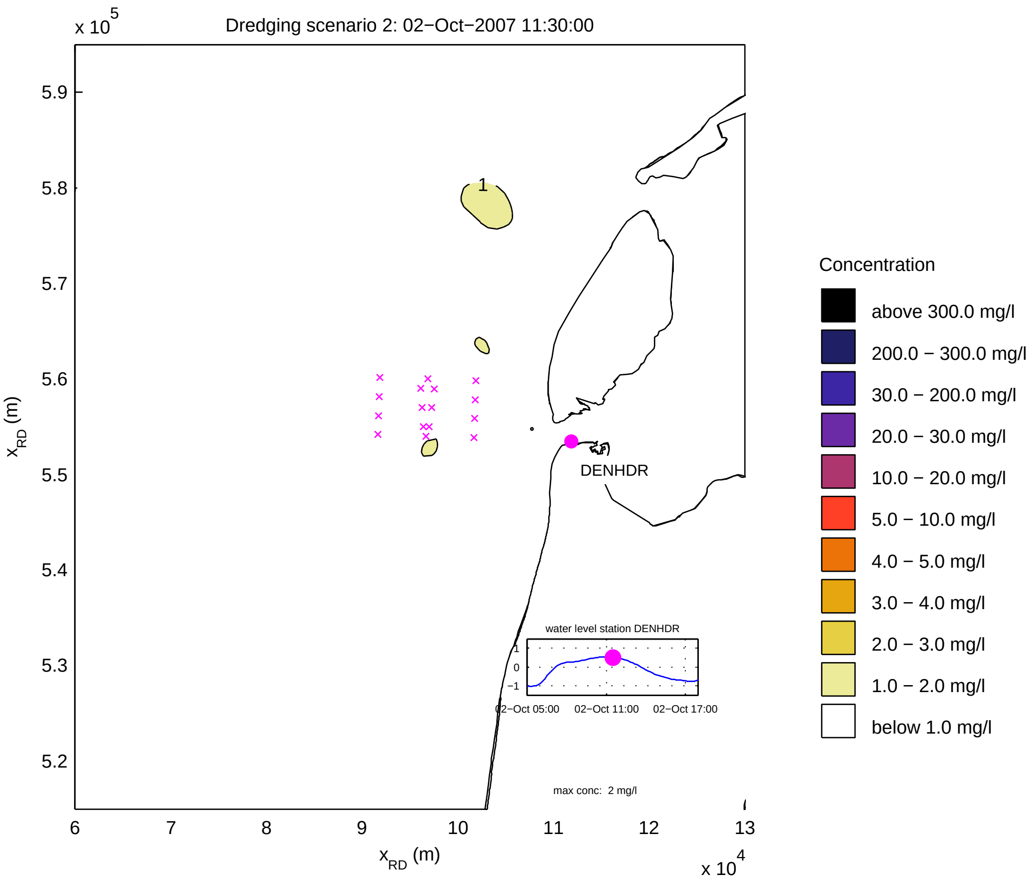

Simulated effect of overflow on silt concentrations (mg/l)
date and time: 02−Oct−2007 11:30:00
x−marks denote locations of T1 observations

Alkyon Hydraulic Consultancy & Research | A2273 | Fig. 4.31

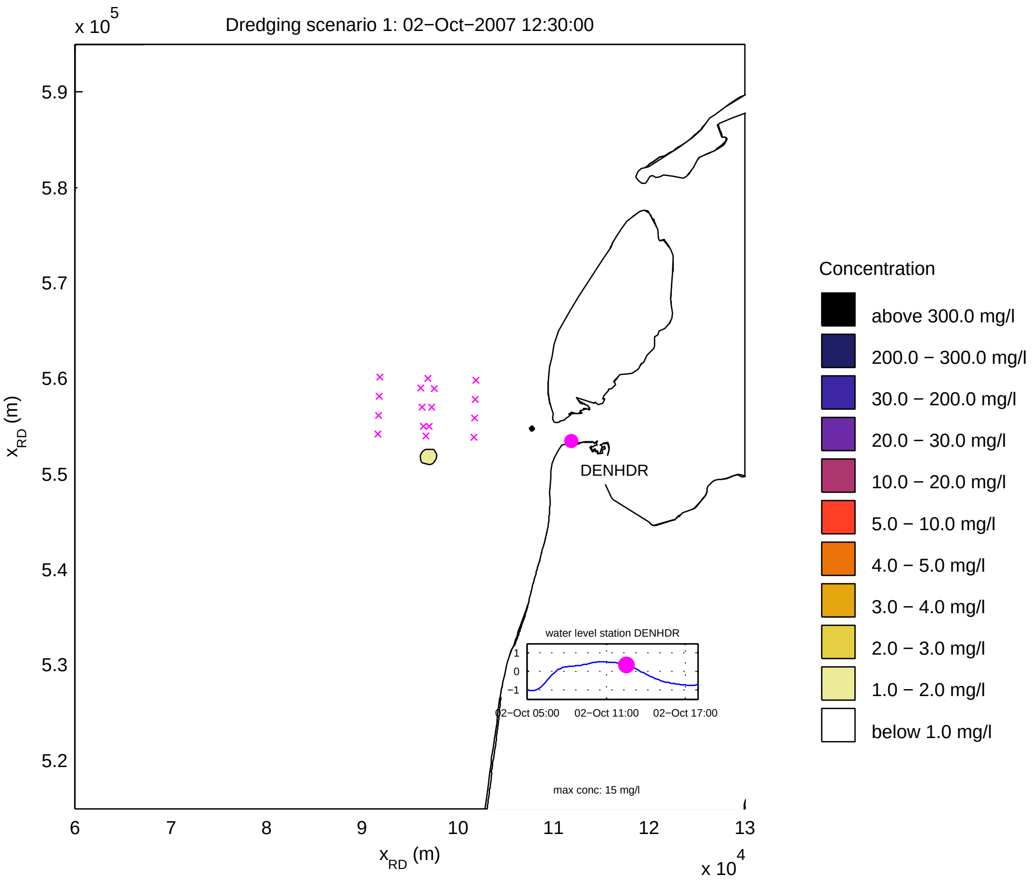

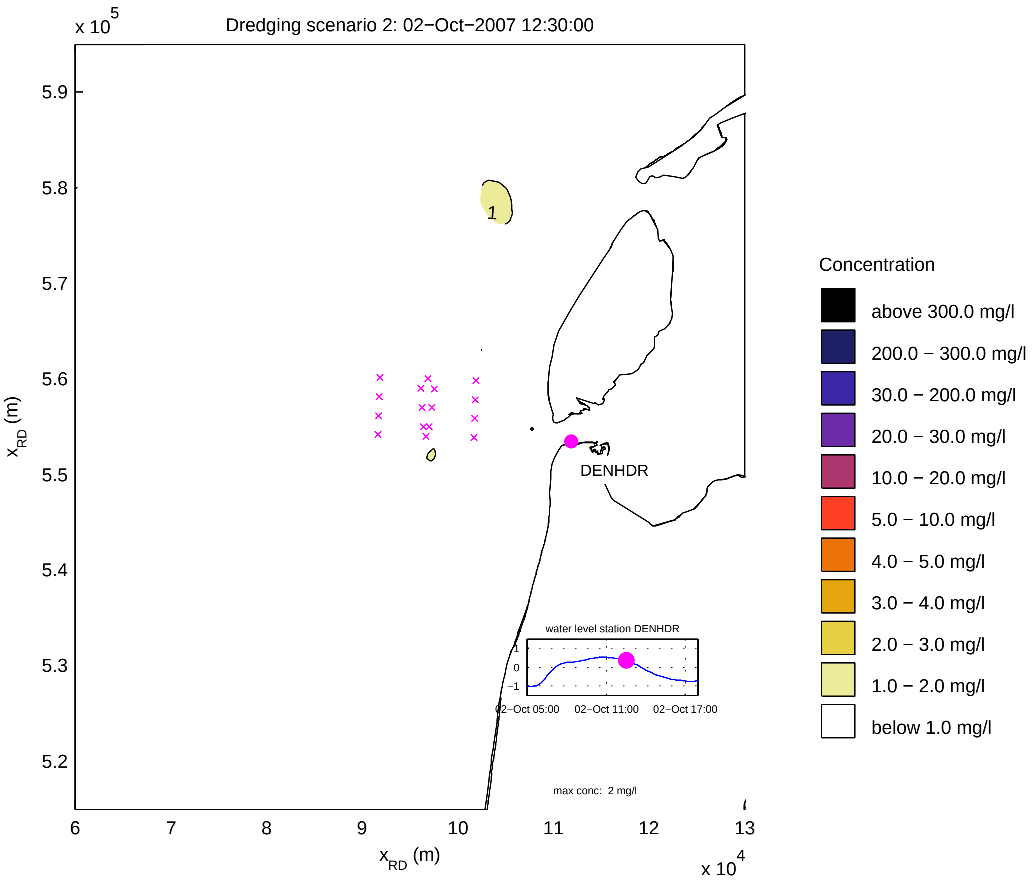

Simulated effect of overflow on silt concentrations (mg/l)
date and time: 02−Oct−2007 12:30:00
x−marks denote locations of T1 observations

Alkyon Hydraulic Consultancy & Research	A2273	Fig. 4.32

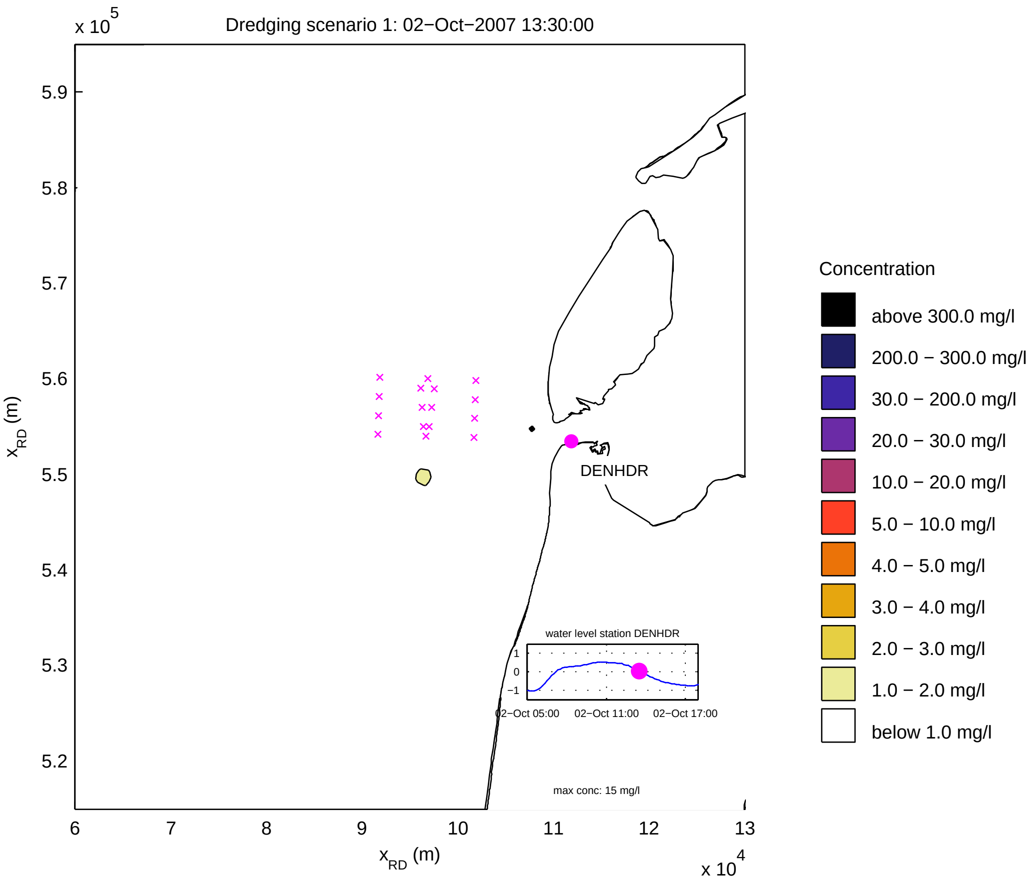

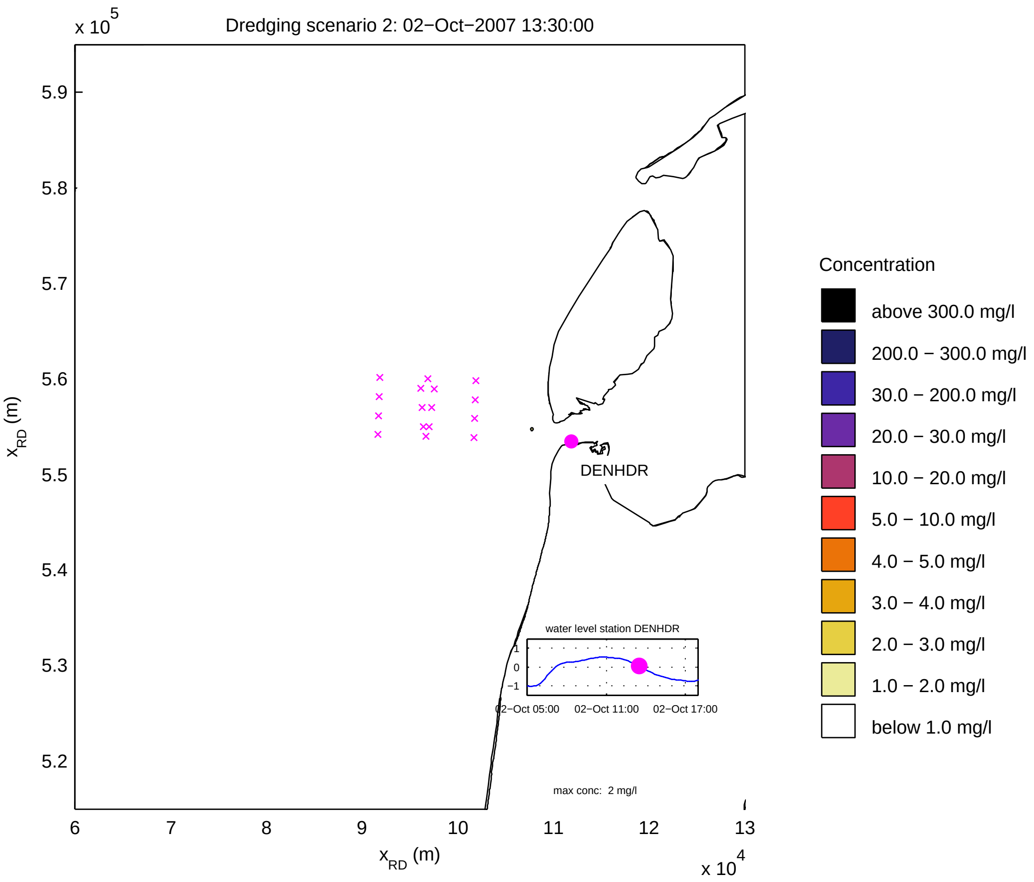

Simulated effect of overflow on silt concentrations (mg/l)
date and time: 02−Oct−2007 13:30:00
x−marks denote locations of T1 observations

Alkyon Hydraulic Consultancy & Research | A2273 | Fig. 4.33

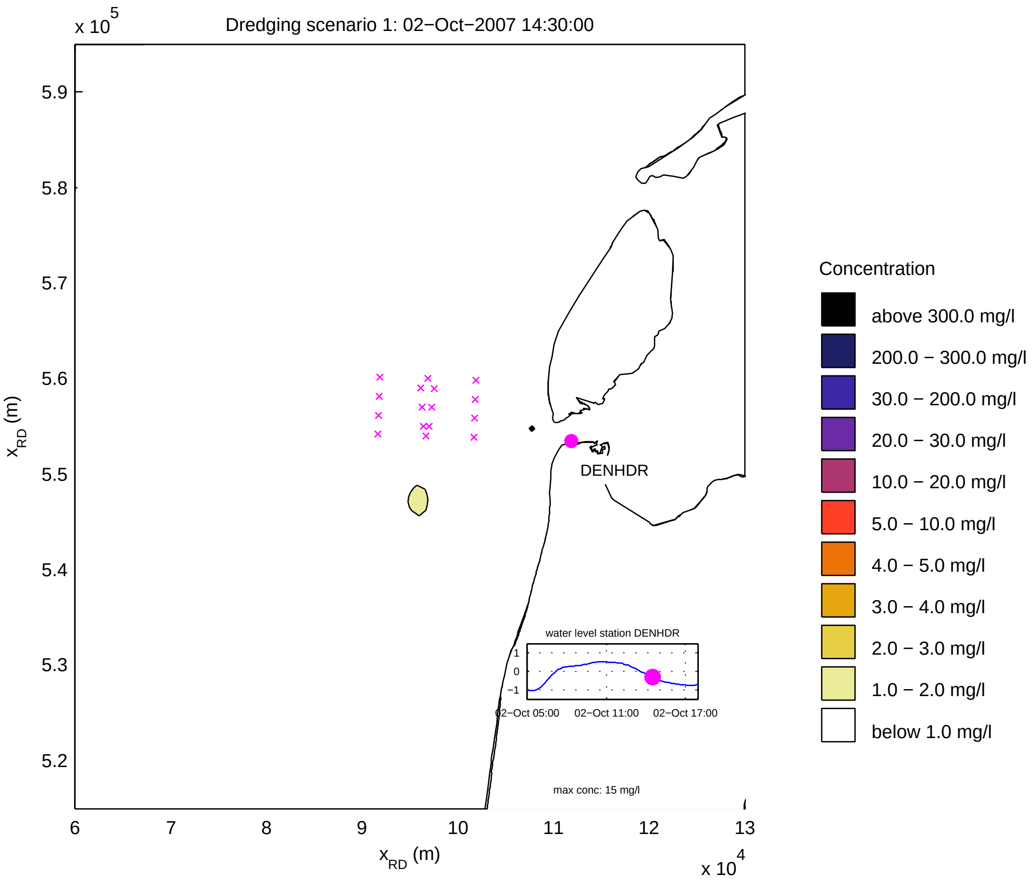

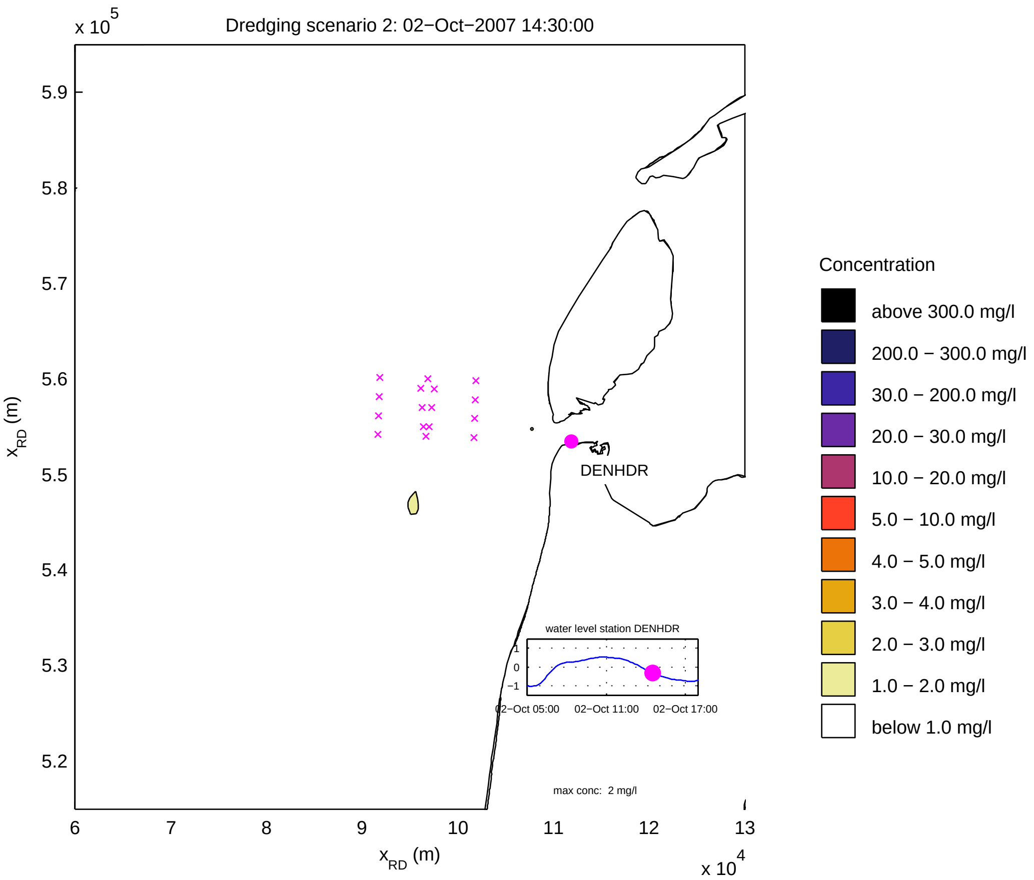

Simulated effect of overflow on silt concentrations (mg/l)
date and time: 02−Oct−2007 14:30:00
x−marks denote locations of T1 observations

Alkyon Hydraulic Consultancy & Research | A2273 | Fig. 4.34

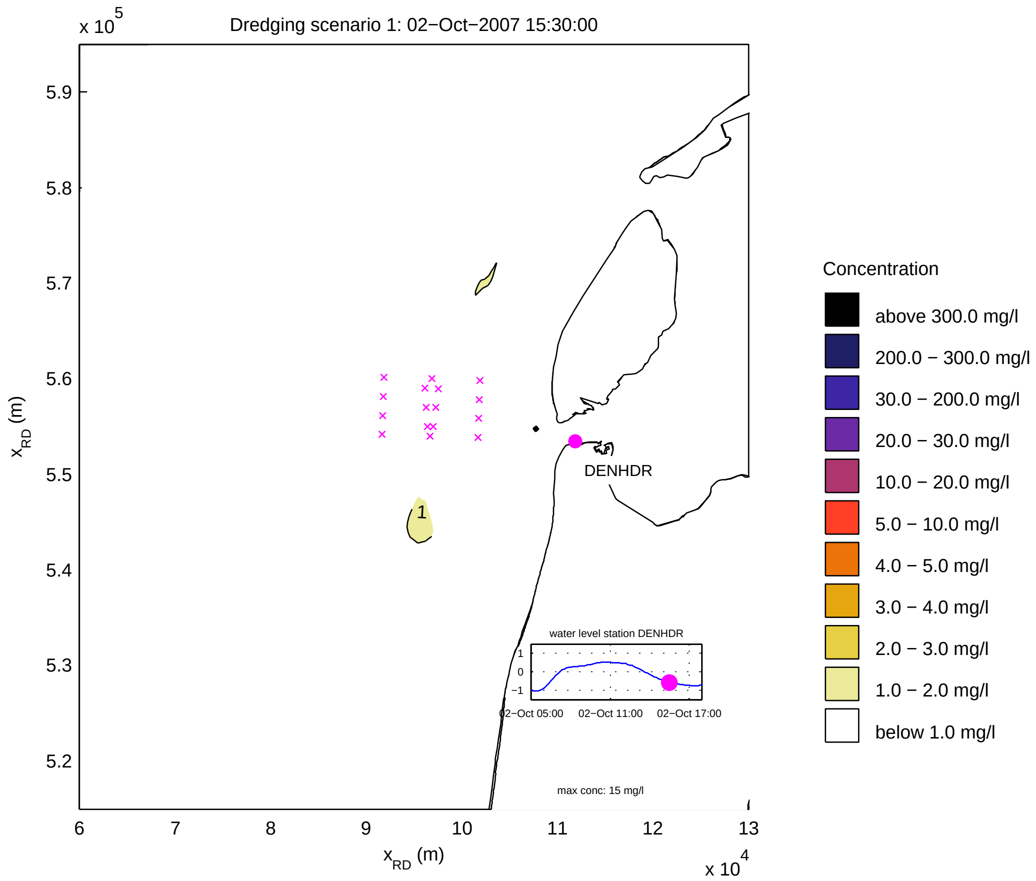

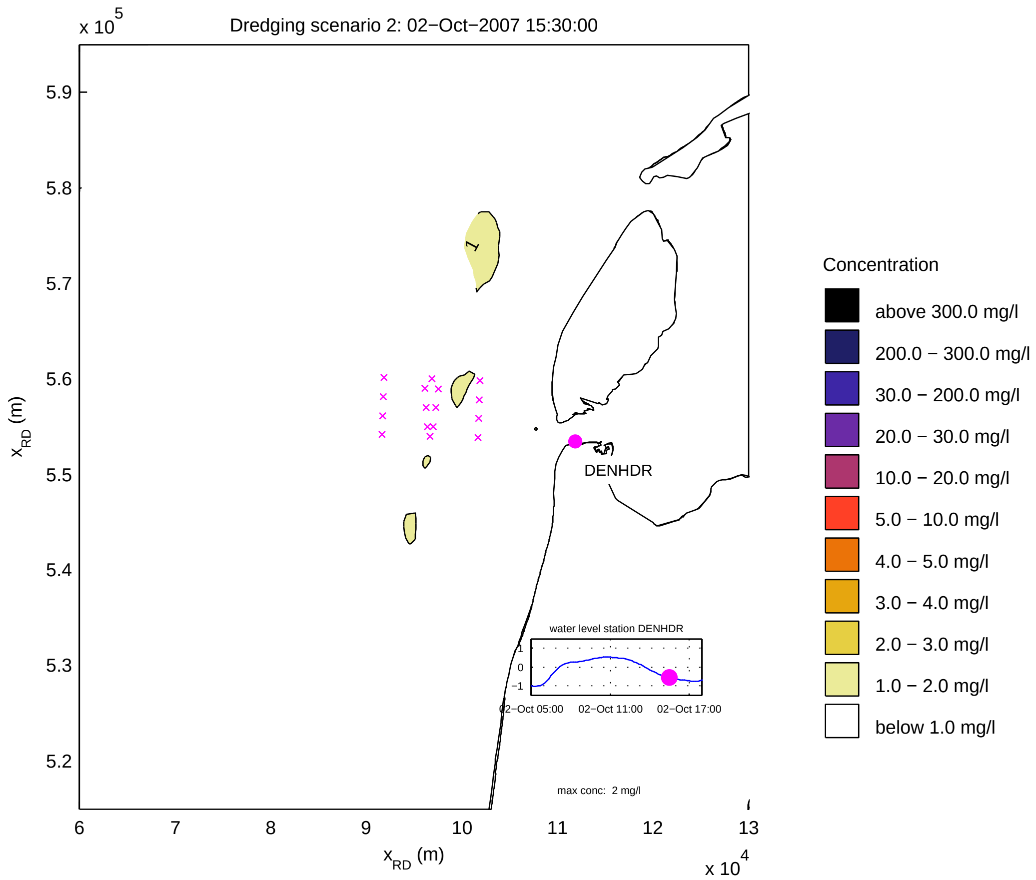

Simulated effect of overflow on silt concentrations (mg/l)
date and time: 02−Oct−2007 15:30:00
x−marks denote locations of T1 observations

Alkyon Hydraulic Consultancy & Research	A2273	Fig. 4.35

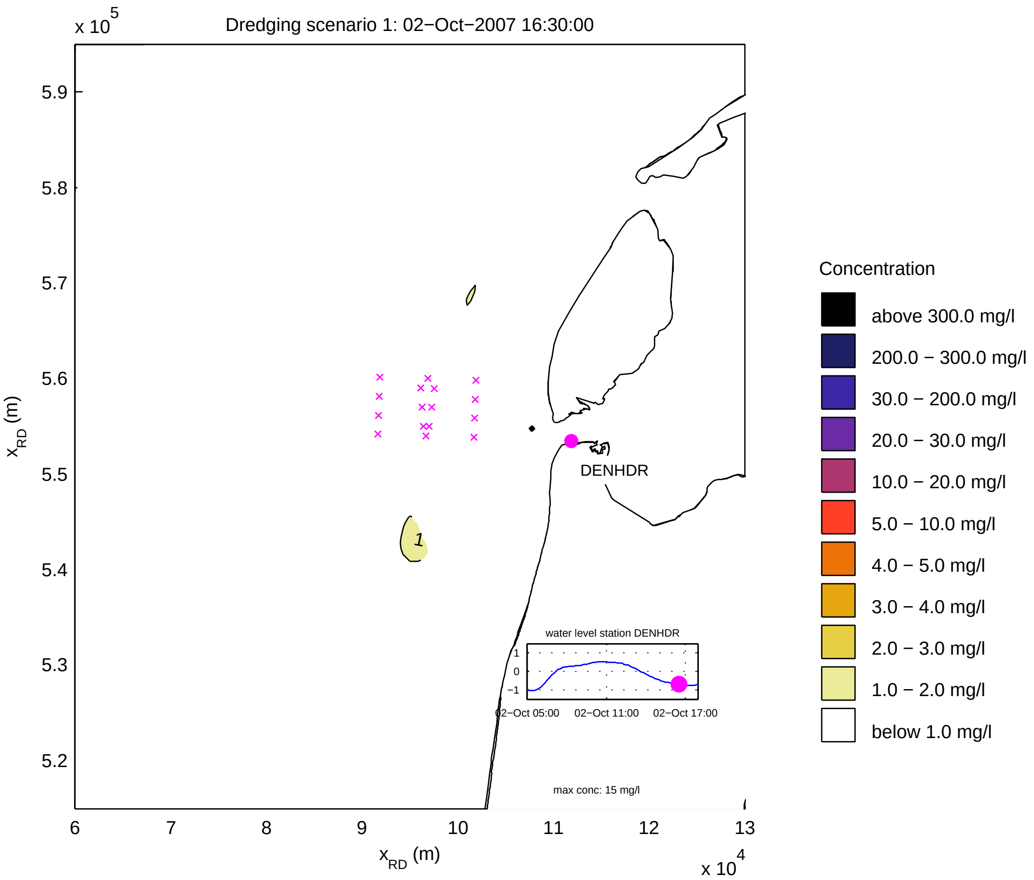

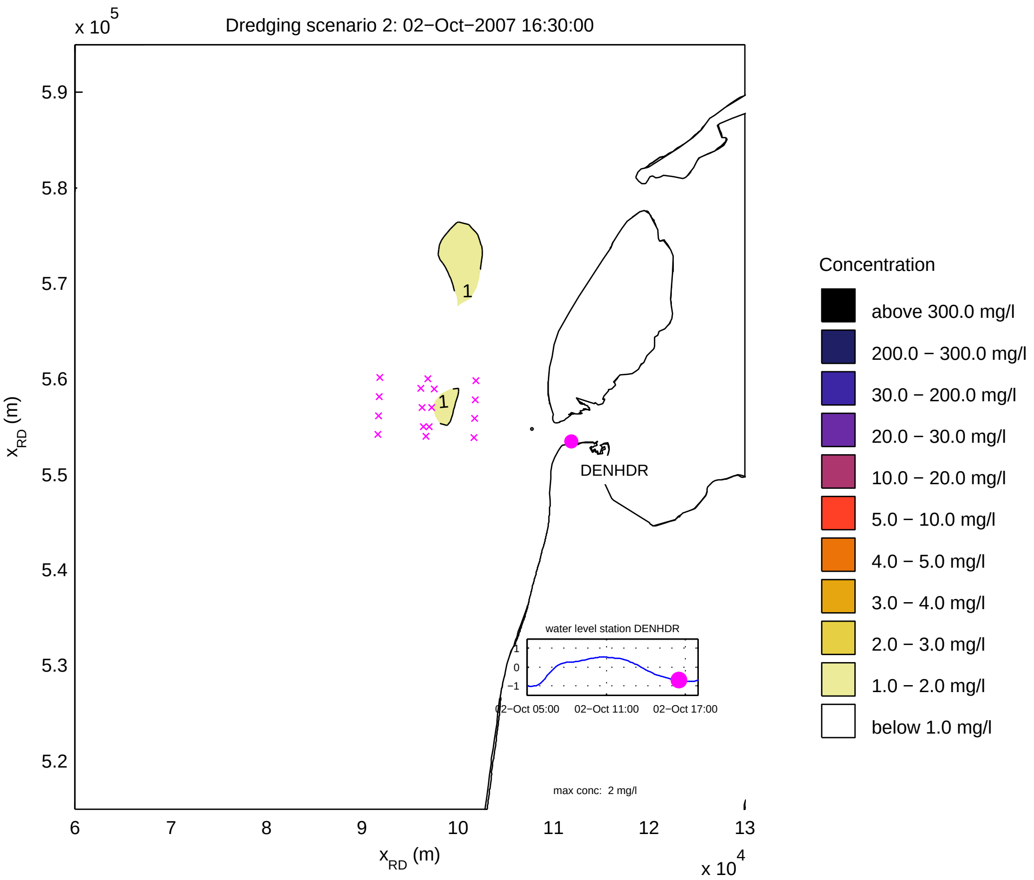

Simulated effect of overflow on silt concentrations (mg/l)
date and time: 02−Oct−2007 16:30:00
x−marks denote locations of T1 observations

Alkyon Hydraulic Consultancy & Research	A2273	Fig. 4.36

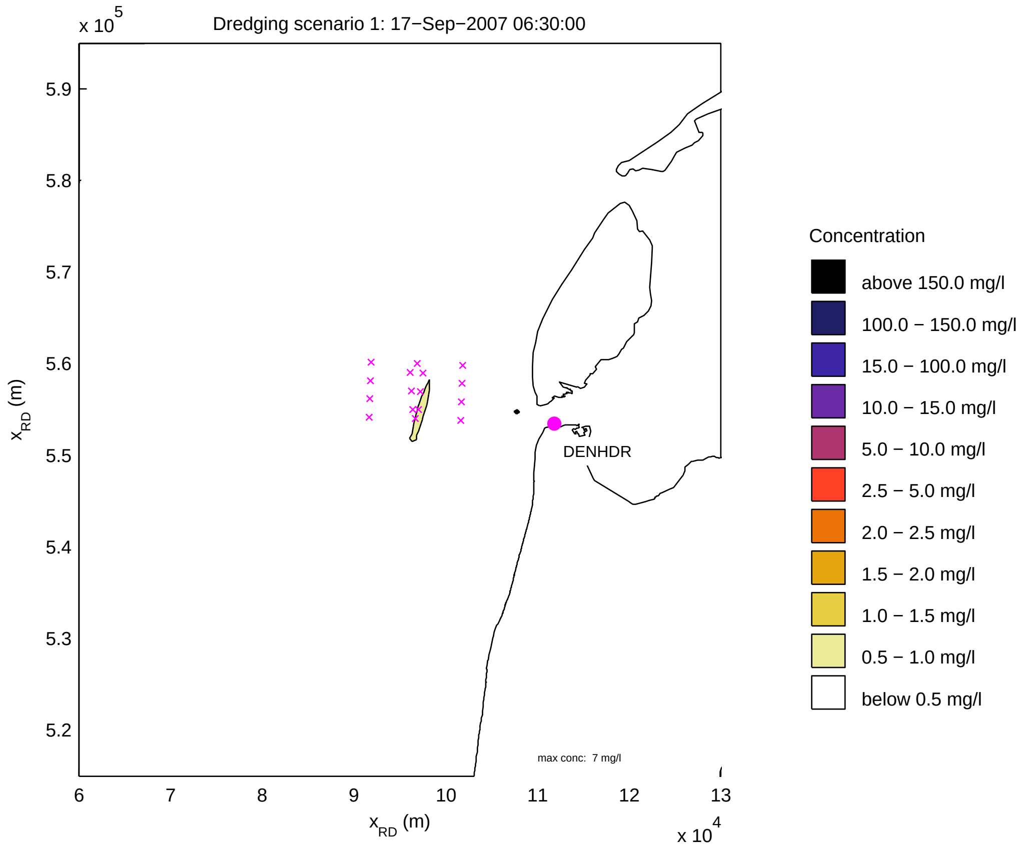

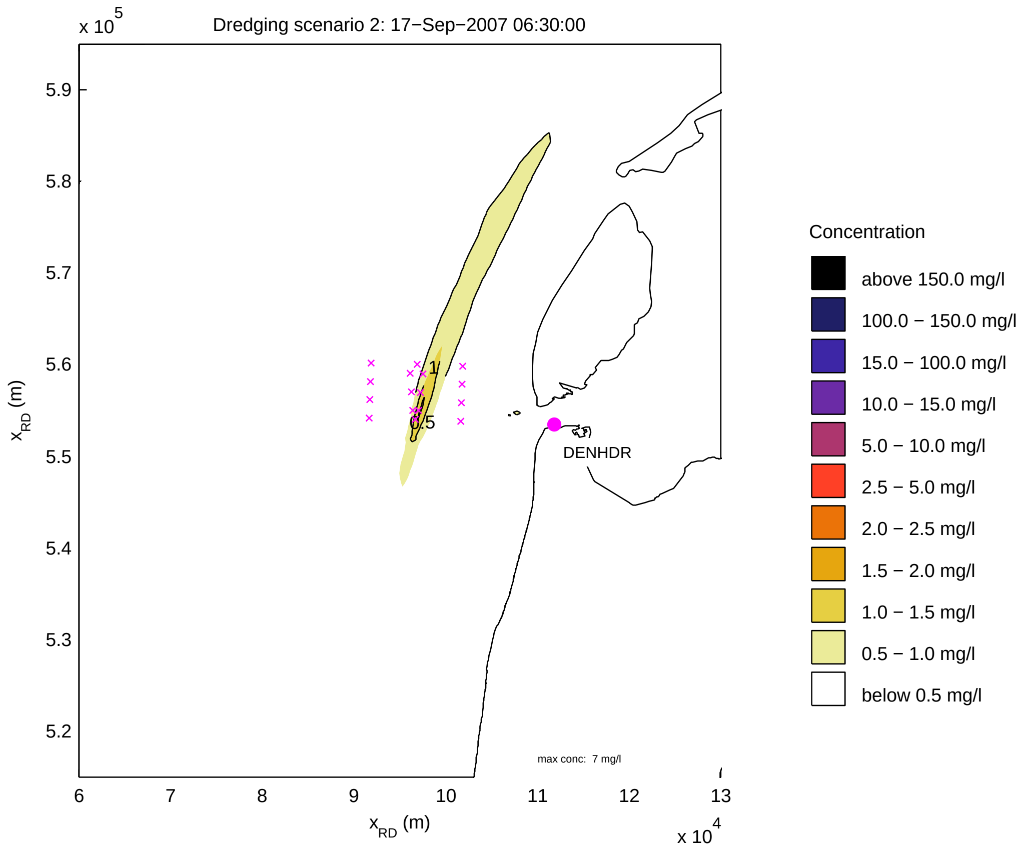

Simulated effect of overflow on mean silt concentrations (mg/l) between 17−Sep−2007 06:00:00 and 02−Oct−2007 18:00:00 x−marks denote locations of T1 observations		
Alkyon Hydraulic Consultancy & Research	A2273	Fig. 4.37